2011

Radiation therapy treatment plan optimization accounting for random and systematic patient setup uncertainties

Joseph Moore
Virginia Commonwealth University

Radiation therapy treatment plan optimization accounting for random and systematic patient setup uncertainties

A thesis dissertation submitted in partial fulfillment of the requirements for the degree of Doctor of Philosophy in Medical Physics at Virginia Commonwealth University.

by

Joseph Andrew Moore
M.S. Applied Physics, Virginia Commonwealth University, 2004
B.S. Physics, Virginia Commonwealth University, 2003
B.S. Computer Science, Virginia Commonwealth University, 2003

Director: Jeffrey V. Siebers, Ph.D.
Professor and Director, Medical Physics Graduate Program
Department of Radiation Oncology

Virginia Commonwealth University
Richmond, Virginia
April, 2011

Acknowledgements

I would like to thank my friends and family for their help and patience throughout the time it has taken to graduate. I would also like to thank my advisor, Jeffrey Siebers for his help in developing the ideas behind this project. For the help to successfully work within the Pinnacle interface, I would like to thank Karl Bzdusek who made implementation substantially easier.

Table of Contents

List of Tables

List of Figures

List of Abbreviations

3DCRT	3D Conformal Radiation Therapy
4DRT	4D Radiation Therapy
c_i	Constant in the objective function for voxel i
CTV	Clinical Target Volume
D_i	Dose in the ith voxel of the ROI
D_{i+s}	Dose in the ith voxel of the ROI shifted by s
D_{Rx}	Prescription dose.
$D_{Rx,o}$	Prescription dose for objective o
$D_{V_{Rx}}$	D at the prescription volume such that $V\left(D_{V_{Rx}}\right) = V_{Rx}$.
$D_{V_{Rx,o}}$	Dose at the prescription volume V_{Rx} for objective o
$D_{V_{Rx,o},s}$	Dose at the prescription volume V_{Rx} for objective o calculated using a dose shift s
DMLC	Dynamic Multi-leaf Collimation
DVCDM	Dose-Volume Coverage Difference Map
DVCM	Dose-Volume Coverage Map
DVH	Dose Volume Histogram
f	Generalized objective function
f_o	Objective function for objective o
F	Pinnacle objective function
F_o	Pinnacle objective function for objective o
$F_{o,s}$	Pinnacle objective function for objective o and shift s
$f^{MaxDose}$	Objective function defined as the dose to an ROI must be less than the prescription dose $$D < D_{Rx}$$
f^{MaxDVH}	Objective function defined as the volume receiving dose D_{Rx} must be less than V_{Rx} $$V(D_{Rx}) < V_{Rx}$$
$f^{MinDose}$	Objective function defined as the dose to an ROI must be greater than the prescription dose $$D > D_{Rx}$$
f^{MinDVH}	Objective function defined as the volume receiving dose D_{Rx} must be greater than V_{Rx} $$V(D_{Rx}) > V_{Rx}$$
$f^{Uniform}$	Objective function defined as the dose to an ROI must be equal to the prescription dose $$D = D_{Rx}$$
G	Pinnacle gradient function

G_i	Pinnacle gradient function for voxel i
$G_{o,i}$	Pinnacle gradient function for objective o and voxel i
$G_{o,s,i}$	Pinnacle gradient function for objective o, shift s and voxel i
GTV	Gross Tumor Volume
$H(x)$	Heaviside function (defined below)
$\mathcal{H}$	Pinnacle diagonal gradient (second derivative of the objective function)
$\mathcal{H}_i$	Pinnacle diagonal gradient for voxel i
$\mathcal{H}_{o,s,i}$	Pinnacle diagonal gradient for objective o, shift s and voxel i
i	Voxel of interest
$i + s$	Voxel of interest offset by a sampled systematic shift s
IGRT	Image Guided Radiation Therapy
IMRT	Intensity Modulated Radiation Therapy
ITV	Internal Target Volume
K_{ij}	Dose contribution of the jth ray to the ith voxel
MLC	Multi-Leaf Collimator
$nObj$	Number of objectives
N_{roi}	Number of voxels in the objective's ROI
NTCP	Normal Tissue Complication Probability
o	Objective of interest
OAR	Organ at Risk
p	Weight of the objective
p_o	Weight of objective o
P+	Probability of Uncomplicated Tumor Control: $P+= TCP(1 - NTCP)$
PDF	Probability Density Function
PDVH	Probabilistic Dose-Volume Histogram
PRV	Planning Risk Volume
PTP	Probabilistic Treatment Planning
PTV	Planning Target Volume
ROI	Region of Interest
TCP	Tumor Control Probability
V_i	Relative volume of voxel i
V_{Rx}	Prescription volume
ω_j	Weight of the jth ray

Abstract

RADIATION THERAPY TREATMENT PLAN OPTIMIZATION ACCOUNTING FOR RANDOM AND SYSTEMATIC PATIENT SETUP UNCERTAINTIES

Joseph A. Moore, Ph.D.

A dissertation submitted in partial fulfillment of the requirements for the degree of Doctor of Philosophy in Medical Physics at Virginia Commonwealth University.

Virginia Commonwealth University, 2010.

Major Director: Jeffrey V. Siebers, Ph.D.
Professor and Director, Medical Physics Graduate Program
Department of Radiation Oncology

External-beam radiotherapy is one of the primary methods for treating cancer. Typically a radiotherapy treatment course consists of radiation delivered to the patient in multiple daily treatment fractions over 6-8 weeks. Each fraction requires the patient to be aligned with the image acquired before the treatment course used in treatment planning. Unfortunately, patient alignment is not perfect and results in residual errors in patient setup. The standard technique for dealing with errors in patient setup is to expand the volume of the target by some margin to ensure the target receives the planned dose in the presence of setup errors.

This work develops an alternative to margins for accommodating setup errors in the treatment planning process by directly including patient setup uncertainty in IMRT plan optimization. This probabilistic treatment planning (PTP) operates directly on the planning structure and develops a dose distribution robust to variations in the patient position. Two methods are presented. The first method includes only random setup uncertainty in the planning

process by convolving the fluence of each beam with a Gaussian model of the distribution of random setup errors. The second method builds upon this by adding systematic uncertainty to optimization by way of a joint optimization over multiple probable patient positions.

To assess the benefit of PTP methods, a PTP plan and a margin-based plan are developed for each of the 28 patients used in this study. Comparisons of plans show that PTP plans generally reduce the dose to normal tissues while maintaining a similar dose to the target structure when compared to margin-based plans. Physician assessment indicates that PTP plans are generally preferred over margin-based plans. PTP methods shows potential for improving patient outcome due to reduced complications associated with treatment.

1 Overview

This chapter serves as an overview of the dissertation.

An introduction into radiation therapy is given in Chapter 2 which describes the history of advances in radiation therapy up to the current methods. Margin formulation and recipes are described along with weaknesses in margin-based approaches. Recent literature on PTP methods is described with the relevance to the work presented in this dissertation.

The mathematical background of objective functions used in IMRT plan optimization is given in Chapter 3. The optimization proposed in this study uses dose-based and dose-volume based objectives and optimizes using Newton's Method. Additionally, specific details of the implementation into the Pinnacle^3 treatment planning are described.

Chapter 4 describes an implementation of random setup uncertainty into treatment planning. This work was published (Moore *et al.*, 2009) in Medical Physics (see Appendix I). Random uncertainty is implemented using fluence convolution and PTP plans are compared to margin-based plans. The validity of fluence convolution as an approximation of random uncertainty is studied for objectives in both PTP and margin-based plans.

Chapter 5 describes an implementation of systematic setup uncertainty into treatment planning. This builds upon the previous chapter by adding systematic uncertainty in addition to random uncertainty in planning. Systematic uncertainty is implemented using a joint optimization over multiple probable patient positions. PTP plans are compared to optimized margin plans using coverage probability, dose-volume coverage maps, dose-volume coverage difference maps, probabilistic dose-volume histograms and physician assessment.

Chapter 6 describes the conclusions and potential future directions. Chapter 7 describes the application of portions of this research to other projects. Components of the fluence convolution approach were used to study the effect of clinical margins on plan quality. Plans developed using margin formulas were tested to determine, in a clinical case, the extent of uncertainty that was covered. In a separate study, additional features were used to incorporate the motion from a Calypso motion track into the dose distribution available in Pinnacle to compare treatments planned using step-and-shoot IMRT and compensator IMRT.

2 Introduction

In 2010, there were an estimated 1.5 million new cases of cancer in the United States (Jemal *et al.*, 2010), of which external beam radiation therapy is recommended for 52% of patients (Delaney *et al.*, 2005). External beam radiotherapy involves delivering a tumoricidal dose of radiation to targeted cancerous tissues while attempting to minimize the dose delivered to normal tissues in order to reduce complications associated with treatment. This goal may be difficult to achieve due to (1) normal tissue located in close proximity to the targeted tissue, (2) inherent limitations in the physics of radiation delivery, and (3) uncertainty in the absolute position of the target and surrounding normal tissues during treatment. Developing methods to reduce the limitations associated with uncertainty in positioning is the focus of this work.

External beam radiotherapy treatment is typically planned on a single image of the patient before therapy and then treatment consists of the delivery of a prescribed dose in multiple fractions delivered on separate days. The fractionation coupled with imperfect daily patient setup leads to small variations in the target position relative to the planned treatment beams. To ensure the target receives the prescription dose when subject to reasonable variations in position, the current standard of practice is to add a geometric margin around the tissues of interest and specify treatment objectives for the expanded volumes. This work develops and quantifies the ability of an alternative method, termed probabilistic treatment planning (PTP), to deliver the prescription dose to target structures in the presence of positional uncertainty. PTP accomplishes this by considering positional uncertainty during the optimization of treatment plans. The overall

hypothesis of this dissertation is that PTP can improve treatment plans by reducing dose to normal structures while maintaining a therapeutic dose to the target as compared to margin-based plans.

The remainder of the introduction describes (1) the evolution of radiation therapy methods, (2) margins and their formulation, (3) prior studies using PTP methods, and (4) novel aspects of this work.

2.1 Evolution of radiation therapy

External beam radiation therapy originally applied rectangular beams to treat the entire target volume to a prescribed dose. Since using the rectangular collimation can only produce a truly conformal distribution on a rectangular target, this delivered a prescription dose to the tumor, but resulted in the irradiation of a large volume of normal tissue near the tumor. Beam shaping consisted of only drawing apertures on 2-D films of the patient. 3-D Conformal Radiation Therapy (3DCRT) improved on this by shaping the beam to the edges of the target, delineated using 3D imaging, while also delivering uniform intensity for each beam resulting in a homogenous dose for the target. 3DCRT uses custom cut blocks or a multi-leaf collimator (MLC) to carefully shape the beam to the target. Blocks are a solid shape cut from a dense material to block radiation while a MLC contains multiple dense leaves that can move independently of each other to produce a shape which blocks radiation. 3DCRT reduces the volume of normal tissue that is exposed to radiation in the beam's eye view.

Intensity Modulated Radiation Therapy (IMRT) improved on 3DCRT by allowing a non-uniform intensity of radiation for each beam. Both 3DCRT and IMRT use an MLC to shape the dose to the patient, however, IMRT uses the MLC to modulate the intensity of radiation delivered to the patient on a per-beam basis. In IMRT, plans are optimized to produce a dose

distribution based on planning objectives which attempt to balance the need for high dose to the target with the need for low doses to normal tissues and/or critical structures. Various types of optimization objectives are used including those based upon dose, dose-volume based, effective uniform dose, and biological indices, with dose-volume objectives being a common method. The objectives used in this study are dose-volume based and are described in Chapter 3.

2.2 Dosimetric effects of uncertainty

Uncertainty in the absolute positions of the target and surrounding normal tissues during treatment with respect to the treatment delivery beams can be split into two components: random and systematic. Since fractionated radiotherapy occurs over a large number (~30) of treatment sessions, random uncertainty – the deviation of patient position from the mean patient position – can be described as a blurring effect on the resultant cumulative dose distribution. Systematic uncertainty – the deviation of the mean patient position from the position used in planning due to setup errors being relative to a single planning image – generally results in a shift of the overall dose distribution from the planned location. Because of the difference in the dosimetric effects from each type of uncertainty, each method must be handled differently in dose evaluation.

The dosimetric effect of random uncertainty has been modeled using convolution (International Commission on Radiation Units and Measurements., 1993, 1999). Two methods of using convolution to model random uncertainty exist: dose convolution and fluence convolution. Dose convolution involves convolving the computed patient dose with the distribution of random uncertainty. One limitation of dose convolution is that it assumes that the dose distribution being convolved is shift-invariant – that is changes in position relative to the beam does not change the shape of the underlying dose distribution (Craig *et al.*, 2003). Shift invariance requires that the underlying patient anatomy be homogenous (McCarter and Beckham, 2000). An alternative to

dose convolution is fluence convolution, which involves convolving the fluence of each beam with the distribution of setup error before dose calculation (Beckham *et al.*, 2002). Fluence convolution does not assume shift invariance due to the convolution occurring before dose is calculated in the patient. Validity of the fluence convolution method for a large number of treatment fractions (30) is shown in Chapter 4. In this work, fluence convolution is used to incorporate random setup uncertainties (random only in Chapter 4 and random + systematic in Chapter 5)

Systematic setup uncertainties manifest themselves as a shift in the total treatment dose (Baum *et al.*, 2004). One method of assessing the dosimetric effects of systematic setup errors is to compute dose for multiple possible systematic shifts of the anatomy and assess dosimetric metrics for each shift (van Herk *et al.*, 2002). Some studies (van Herk *et al.*, 2002; Schwarz *et al.*, 2006) have simulated up to 5000 systematic errors to determine the dosimetric effect of systematic setup error. In this dissertation, systematic errors are randomly sampled and used to simulate the dosimetric effects of systematic uncertainty. This occurs both during the PTP optimization, where up to 128 systematic shifts are simulated, and during the coverage-based plan evaluation where 919 shifts are effectively sampled.

2.3 Margins and formulation

Normally, the detrimental effects of patient setup positioning uncertainties are reduced by adding a geometric safety margin around volumes or structures which are intended to be treated to the prescription dose (the clinical target volume or CTV), and in some cases, margins around volumes or structures where dose delivery is to be avoided (the organs at risk or OARs). ICRU 50 and 62 (International Commission on Radiation Units and Measurements., 1993, 1999) conceptually describes margins and the relationship to tissue structures. Components of the

margin definitions are shown in Figure 1. The tumor contoured by a physician is called the Gross Tumor Volume (GTV), which contains the volume the physician can positively identify in images or feel on the patient. Encapsulating this contour is a Clinical Target Volume (CTV). In the CTV, the regions of suspected subclinical disease are included. To account for the internal motion of the tumor in the patient, a margin surrounding the CTV where the tumor is presumed to move is termed the Internal Target Volume (ITV). Lastly, a volume to account for setup uncertainty of the patient is included by adding a setup margin to the ITV. This setup margin is chosen to be large enough that the prescribed dose will be delivered to the CTV. This final volume is termed the Planning Target Volume (PTV).

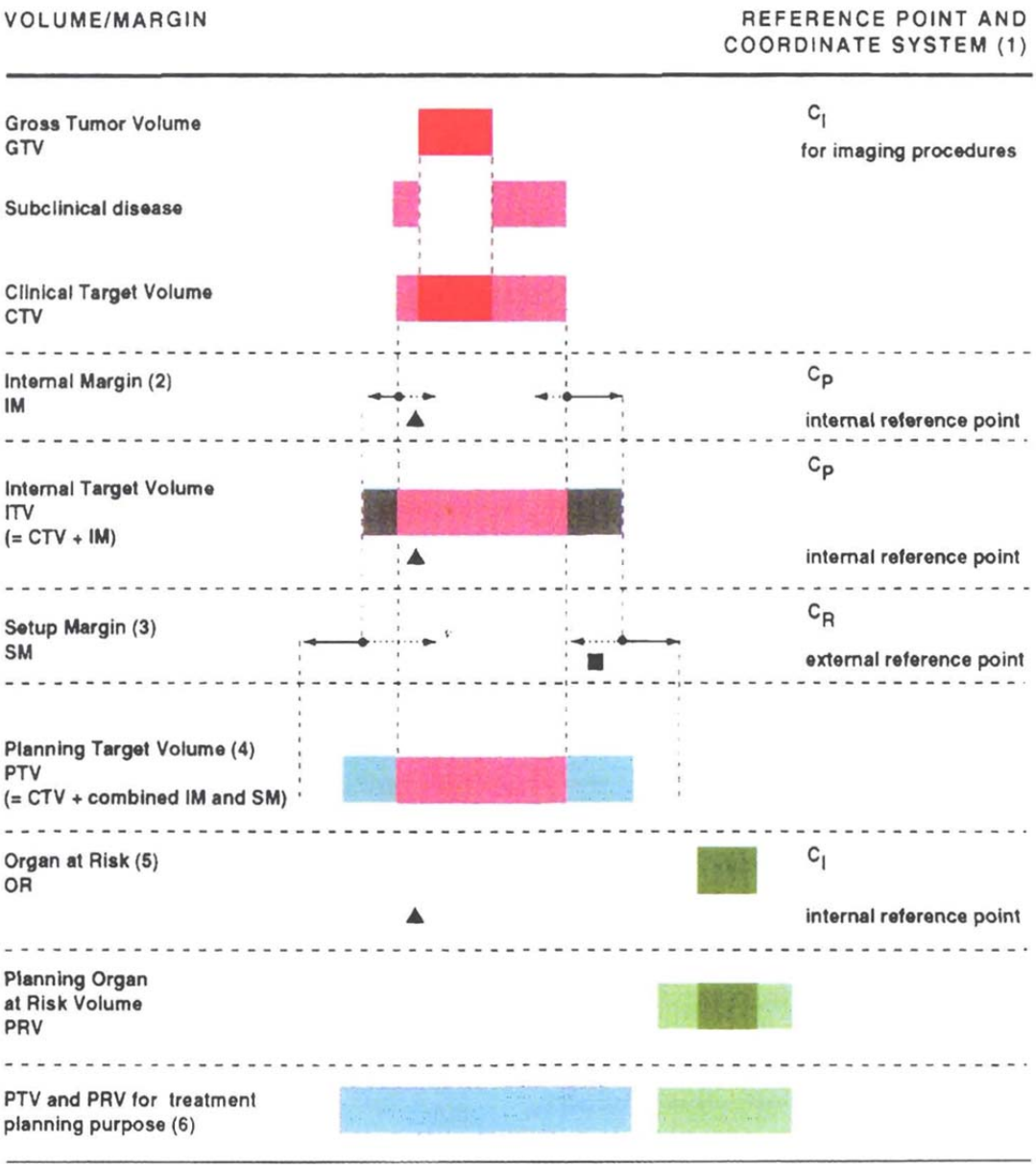

Figure 1: Components of structure definitions and expansions according to ICRU 62. Figure used with permission from ICRU 62, figure 2.14 (International Commission on Radiation Units and Measurements., 1999)

Physicians typically use specific treatment site protocols to specify CTV-to-PTV margins. Studies have been conducted to define formulas with methods for determining the extent of margins that should be added to the target to ensure dosimetric coverage when the effects of target and normal tissue positional uncertainties are considered. Van Herk has proposed a margin

formulation designed to ensure that for 90% of patients at least 95% of the prescription dose is delivered to the CTV (Murshed *et al.*, 2004; Liu *et al.*, 2004). In simplified terms, van Herk's margin formula specifies that the CTV-to-PTV margin should be $M = 2.5\Sigma + 0.7\sigma$ where Σ is the standard deviation of the population systematic uncertainty (the standard deviation of the mean positional setup error) and σ is standard deviation of the population random uncertainty (the standard deviation about the mean for a typical patient in the population). Stroom *et al.* (Stroom *et al.*, 1999) proposed a similar margin formula such that $M = 2.0\Sigma + 0.7\sigma$ to deliver 95% of the prescription dose to 99% of the CTV.

Even margins based upon uncertainty distributions result in the tissue included within the margins receiving a homogenous dose. Additional normal tissue is irradiated due to the fact that in real treatment, the treated volume, which is the volume enclosed by the prescription isodose line, does not strictly conform to the PTV (Murshed *et al.*, 2004; Liu *et al.*, 2004). Often, the treated volume encompasses a volume larger than the PTV resulting in an overly conservative estimate of the target coverage.

As margins are the de-facto standard for accounting for positional uncertainties in external beam radiation therapy treatment planning, this dissertation compares plans developed using the PTP method with margin-based plans. Instead of using margin formulas, which would bias against margins, the margin is adjusted to match the coverage probability of the PTP plan (see Section 5.2.4.).

2.4 Prior studies using PTP methods

Margin-based approaches, particularly those based on margin recipes such as the van Herk margin formula attempt to create a robust plan by including the effects of systematic and random uncertainties before planning by defining the extent of the margin that would be

sufficient to ensure that the delivered dose to the CTV including the effects of positioning errors meets the prescribed treatment dose. PTP incorporates these uncertainties by considering the likelihood that the target will be in a specific location during treatment in the plan optimization process. The CTV-to-PTV expansion is not required. Instead, PTP optimizes the dose to the CTV (and OARs) with knowledge of the estimated setup uncertainty. Several authors (Unkelbach and Oelfke, 2005b, 2004, 2005a; Gordon *et al.*, 2010; Gordon and Siebers, 2009; Moore *et al.*, 2009; McShan *et al.*, 2006; Lof *et al.*, 1998; Witte *et al.*, 2007; Baum *et al.*, 2006; Yang *et al.*, 2005) have reported on the potential for probabilistic methods of treatment planning, generally finding that PTP has the potential to reduce dose to normal structures. Published PTP methods can be classified into three general categories: conceptual models, demonstration studies, and statistical studies.

Conceptual models of PTP mathematically describe proposed methods for including uncertainty in planning (Unkelbach and Oelfke, 2004, 2005a; Lof *et al.*, 1998). In these studies, simplified models of patient anatomy and uncertainty are used to demonstrate the basic mechanics of PTP optimization. Using a 2D circular target surrounded by a normal tissue and simulating a 360^{o} arc delivery, Unkelbach and Oelfke demonstrated the potential for PTP, and showed that PTP can result in non-uniform fluence delivery (Unkelbach and Oelfke, 2004). In another work, they studied the impact of sampling a limited set of images, equal to the number of fractions, from probability distributions (Unkelbach and Oelfke, 2005b) and found that plans based on greater numbers of fractions could utilize sharper delivered dose distributions to obtain target coverage while those based on fewer fractions required a more blurred dose to ensure target coverage. The sharper distribution for greater numbers of fractions leads to higher doses in the target and lower doses in the surrounding tissue as the number of fractions increase. Greater

numbers of fractions also lead to larger standard deviations of dose at a point in the target volume over the 30 fraction treatment of a given patient which can be beneficial in that this indicates sharper dose gradients which spare more normal tissue due to more rapid decrease in dose outside of target structures, however, if the histogram of actual motions differs from that PDF assumed during planning due to the limited number of fractions (samples), dose inhomogeneity of a point in the target between fractions is observed. A variance reduction term in the objective function is required to reduce the dose inhomogeneity due to the motion, which reduces the peaks in the fluence profile generated when delivering an uncertainty optimized plan with a limited number of fractions (Unkelbach and Oelfke, 2004, 2005a). Lof *et al.* (Lof *et al.*, 1998) developed a method for including random and systematic uncertainty into an objective function based upon P+ (the probability of uncomplicated tumor control) which showed the potential to increase P+ compared to margin-based approaches on model geometries.

There have been several demonstration studies which show the potential of PTP to improve plans on a small number of patients (Unkelbach and Oelfke, 2005a; McShan *et al.*, 2006; Baum *et al.*, 2006; Yang *et al.*, 2005). These studies show on example patient cases the benefits of PTP methods, but lack sufficient numbers of patients to draw clinically relevant conclusions. For example, Birkner *et al.* (Birkner *et al.*, 2003) studied re-optimized plans for 3 prostate patients based upon images acquired during the course of treatment. Plans are initially optimized with the expectation value of an EUD-based objective function over all fractions and then re-optimized based on images acquired early in the treatment process to compensate for geometric variation. However, re-optimizing too early will lead to under-dosing of the target, while doing so too late will lead to overdosing of normal tissue due to compensating for early geometric variation. Increased conformality will result from re-optimized plans over margin-based plans

(Birkner *et al.*, 2003). McShan *et al.* (McShan *et al.*, 2006) described a PTP method which uses a weighted sum of dose delivered on multiple anatomical instances during dose optimization to account for the dosimetric effects of random set up errors. Their method, termed Multiple Instance Geometry Approximation (MIGA), uses several (7 in a clinical example) instances of individually shifted anatomies to account for random setup uncertainties. In an idealized geometry and a single clinical head and neck case, decreases in normal structure dose are observed compared to methods using a PTV. Also dealing strictly with random positioning errors, Balter *et al.* (Balter *et al.*, 2005) reports that a plan generated by convolving the dose with a Gaussian representing the random uncertainty and adjusting the fields to maintain coverage can reduce the effective treatment volume by 6-8% as compared to a margin based approach. Yang *et al.* (Yang *et al.*, 2005) reports that incorporating systematic uncertainty around targets and organs at risk by way of a EUD-based objective function composed of scores from a small number of planning scans shifted in one dimension and weighted by their probability resulted in greater sparing of OAR when compared to margin based approaches including methods that incorporate an ICRU 62 PRV (Planning Organ at Risk Volume) margin. Other groups (Gordon *et al.*, 2010; Gordon and Siebers, 2008, 2009; Baum *et al.*, 2006) have incorporated coverage probability calculations into the objective functions.

Statistical studies use large patient populations and can draw statistically valid conclusions of the effectiveness of PTP methods. In a study with 19 prostate patients, Witte *et al.* (Witte *et al.*, 2007) compare PTP using an EUD-based objective function which included the effects of random and systematic uncertainties with margin-based simultaneous integrated boost plans and found a reduction of rectum toxicity by 50%. In two studies on 28 prostate patients, incorporating both random and systematic uncertainty by directly optimizing a plan based upon

coverage probability, Gordon *et al.* (Gordon *et al.*, 2010; Gordon and Siebers, 2009) showed that a ~20% reduction of normal tissue dose could be achieved while maintaining target coverage probability (Gordon and Siebers, 2009) and while maintaining normal tissue dose, the target dose could be increased when compared to margin-based plans (Gordon *et al.*, 2010).

2.5 Novel aspects of the dissertation research

The work presented in this dissertation deviates from most previous work by using a large number (28) of patients. As few studies have used more than 3 patients in demonstrating PTP methods, this work provides a statistically valid conclusion on the benefits of PTP. While previous methods of incorporating random uncertainty have used dose convolution, this work uses fluence convolution to incorporate random uncertainty which does not assume shift invariance. Systematic uncertainty in other methods has been implemented using expectation values in objective functions and grid-based evaluation of systematic shifts, this work uses independent randomly sampled systematic shifts in the analysis of the plan objective function. In many previous PTP studies, EUD-based objectives are used in optimization. While EUD-based objective functions use a biological model to estimate the effect of radiation dose, it is uncommon for EUD objectives to be used clinically. This work uses dose-based and DVH-based objectives in plan optimization which is much more common clinically.

The method of Gordon *et al.* (Gordon *et al.*, 2010)used Dose-Coverage Histograms directly in the objective functions which are generated by accumulating dose-volume histograms sampled from multiple offsets. This work uses coverage probability only in the weight adjustment of the OAR objectives, but not directly during optimization. To date, the published works of Gordon *et al.* have only used the CTV in probabilistic optimization in contrast to this work that uses probabilistic objective for both target and OARs.

In this work, margin-based plans with equivalent coverage probability to the PTP plan are generated by iteratively adjusting the margin. In general, these plans have reduced margins when compared to the van Herk margin formula (Gordon and Siebers, 2009). In most other studies, margin-based plans are developed using a margin formula, thus using coverage adjusted margin-based plans here gives a less biased comparison of margin-based and PTP plans. Despite a more rigorous comparison, this study still establishes a benefit to PTP planning.

Novel tools such as dose-volume coverage maps and dose-volume coverage difference maps aid in visualizing uncertainty in patient dose delivery. This study is the first to use familiar dose-volume plan objectives for accommodating systematic setup uncertainty. This is the first work to compare plans using physician preference.

2.6 Patient alignment techniques, adaptive techniques and error reduction

While PTP methods attempt to reduce the dosimetric consequences of patient setup errors by directly considering their statistical distribution during the treatment plan optimization, an alternative approach is to reduce the errors themselves. This is the role of patient alignment techniques and adaptive radiation therapy techniques which attempt to reduce the daily random and patient specific systematic errors for individual patients. Alignment protocols have been developed to accurately position the patient before treatment. The most basic practice involves marking skin locations to be aligned with the lasers in the room. Other methods improve upon laser alignment by using portal imaging (Bel *et al.*, 1996; de Boer and Heijmen, 2001) to align the patient's bony anatomy with an image generated from the planning system. Modern methods for setup involve using implanted markers (Litzenberg *et al.*, 2002), Calypso, and cone-beam imaging (Jaffray *et al.*, 2002; Lattanzi *et al.*, 1999) to align the patient immediately before treatment. In all of these methods, positioning error is reduced but not completely eliminated.

Improvement of localization and tracking may be realized in Image Guided Radiation Therapy (IGRT) and 4-Dimension Radiation Therapy (4DRT). IGRT involves acquiring images during treatment to determine where the targets are, and adjusting the patient to align the current setup with the planned setup. 4DRT involves tracking motion during treatment which accounts for large motions such as that of the lung. Studies have shown that these methods may reduce the margin requirements in planning (Stroom *et al.*, 2000). These reductions, while significant, still leave residual uncertainty.

Since some level of residual uncertainty seems unavoidable, methods of compensating for uncertainty must still be employed. Reduced margins may be achieved by adaptive planning techniques such as Yan *et al.* (Yan *et al.*, 1998) which uses a small number (~5) daily portal images to adjust the beams which reduces the systematic uncertainty from 4 mm to 0.5 mm. PTP methods including both random and systematic uncertainty (Chapter 5) still have potential to reduce normal tissue doses even when only small residual uncertainties persist. Further, if systematic uncertainty alone can be reduced to negligible values, the remaining random uncertainty can be accommodated using the methods in Chapter 4.

3 Objective Functions

Central to the concept of IMRT plan optimization are the objective functions used to generate the desired dose distribution. An objective function (sometimes termed a "cost function") is a mathematical concept which describes the "costs" associated with the dose distribution of a given plan. Typically, the objective function is used in a minimization problem which aims to reduce the "cost" via modifying plan parameters to reduce the total value of the objective function. For intensity modulated beams, this optimization process is described in detail in the work of Wu and Mohan, 2000. The following description, based on their work and modified to clarify the calculations, is presented as it forms the basis for the optimization objectives described in Chapter 5.

In computer-based optimization, the patient dose is split up into a series of volume elements (voxels) defined by the size of the dose grid. During dose computation, the dose to each volume element is calculated for each voxel. Regions of interest (ROIs) are defined via sets of contours which specify the voxels which are contained the target structures and organs at risk. The CTV, PTV and each OAR is represented by an ROI containing the respective voxels. Each objective function operates on the voxels contained within a single ROI.

3.1 Dose-Based Objective Functions

Dose-based objective functions operate by penalizing dose above (or below) the prescription dose. For a maximum dose objective $f^{MaxDose}$, the goal is to have the dose in each

voxel (D_i) below the prescription dose (D_{Rx}), hence voxels with dose below the prescription dose have no penalty, and voxels with dose above the prescription dose are penalized proportional to the excess squared as:

$$f^{MaxDose} = \frac{1}{N_{roi}} \cdot p \cdot \sum_{i}^{N_{roi}} H(D_i - D_{Rx})(D_i - D_{Rx})^2$$

where N_{roi} is the number of voxels in the objective's ROI, p is the weight of the objective, i is the voxel of interest, H is the Heaviside function defined as

$$H(x) = \begin{cases} 1, x > 0 \\ 0, x \leq 0 \end{cases},$$

D_i is the dose in the ith voxel of the ROI, and D_{Rx} is the prescription dose.

For a minimum dose objective $f^{MinDose}$, the goal is to have the dose in each voxel be above the prescription dose. In this case, the voxels with dose above the prescription dose have no penalty and voxels with dose below the prescription dose are penalized proportional to the deficit squared.

$$f^{MinDose} = \frac{1}{N_{roi}} \cdot p \cdot \sum_{i}^{N_{roi}} H(D_{Rx} - D_i)(D_i - D_{Rx})^2$$

For a uniform dose objective $f^{Uniform}$, the goal is for the dose in each voxel to be a specific dose. In this case, the voxels are penalized proportional to the deviation from the desired uniform dose squared. This is actually equivalent to a combination of minimum and maximum dose objectives.

$$f^{Uniform} = \frac{1}{N_{roi}} \cdot p \cdot \sum_{i}^{N_{roi}} (D_i - D_{Rx})^2 = f^{MaxDose} + f^{MinDose}$$

In Chapter 5, dose-based objectives are used, specifically maximum dose objectives for OAR structures, but primarily, dose-based objectives are the building blocks for dose-volume objectives.

3.2 Dose-Volume based objectives:

Dose-Volume based objectives operate similarly to dose-based objectives by using a dose-volume histogram. A dose-volume histogram displays the percentage of the volume of a given structure which receives greater than a specified dose. In a DVH objective, the proportion of voxels receiving dose above (or below) the prescription dose must be more (or less) than the prescription volume depending upon if it is a maximum or minimum DVH objective function. To accomplish this, an additional Heaviside function is added to the objective function. The Heaviside function uses the term $D_{V_{Rx}}$, that is the dose to the prescription volume, for the current dose distribution, defined as $V\left(D_{V_{Rx}}\right) = V_{Rx}$, and shown visually on a Dose-Volume Histogram (DVH) in Figure 2. In optimization, $D_{V_{Rx}}$ must be recomputed for each iteration.

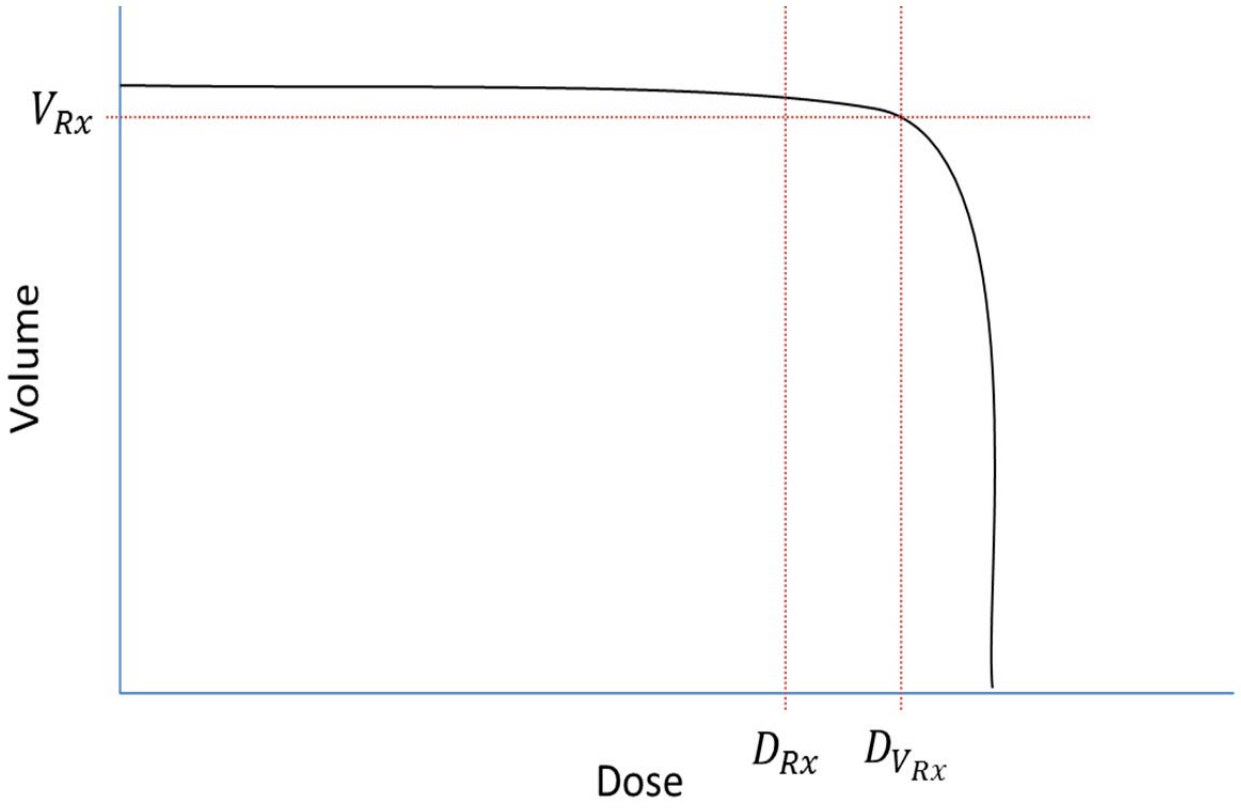

Figure 2: Graphical representation of variables for a maximum DVH objective. The curve represents a DVH line for the ROI specified in the objective. $\boldsymbol{D_{Rx}}$ is the prescription dose for the selected objective. $\boldsymbol{V_{Rx}}$is the prescription volume for the selected objective. $\boldsymbol{D_{V_{Rx}}}$is the dose achieved at the prescription volume, such that $\boldsymbol{V(D_{V_{Rx}}) = V_{Rx}}$. The optimizer operates on voxels with a dose between $\boldsymbol{D_{V_{Rx}}}$ and $\boldsymbol{D_{Rx}}$. Ideally, a completed optimization will result in $\boldsymbol{D_{V_{Rx}} <= D_{Rx}}$completely fulfilling the objective.

For a maximum DVH objective f^{MaxDVH}, the goal is to keep the percentage of the voxels below the prescription dose above the prescription volume. Only voxels with dose below D_{Rx} and above $D_{V_{Rx}}$ are penalized. Voxels with dose below the prescription dose have no penalty, as the dose already remains below the prescription and voxels with dose above $D_{V_{Rx}}$have no penalty as they are in the permitted percentage of the ROI volume allowed to have dose above D_{Rx}. If $D_{V_{Rx}}$is less than or equal to D_{Rx} then the function is zero as the objective has been fully met.

$$f^{MaxDVH} = \frac{1}{N_{roi}}\left(p \sum_{i}^{N_{roi}} H\left(D_{V_{Rx}} - D_i\right) H(D_i - D_{Rx})(D_i - D_{Rx})^2 \right)$$

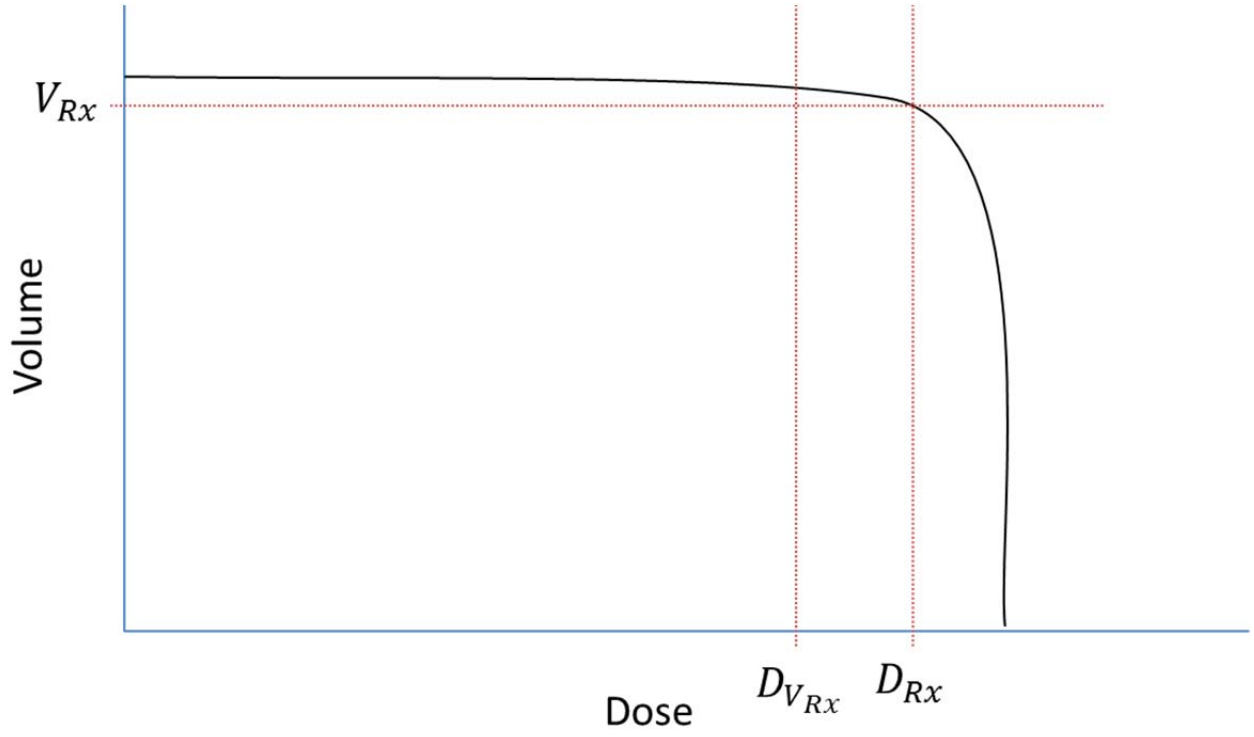

Figure 3: Graphical representation of variables for a minimum DVH objective. The curve represents a DVH line for the ROI specified in the objective. $\boldsymbol{D_{Rx}}$ is the prescription dose for the selected objective. $\boldsymbol{V_{Rx}}$is the prescription volume for the selected objective. $\boldsymbol{D_{V_{Rx}}}$is the dose achieved at the prescription volume, such that $\boldsymbol{V(D_{V_{Rx}}) = V_{Rx}}$. The optimizer operates on voxels with a dose between $\boldsymbol{D_{V_{Rx}}}$ and $\boldsymbol{D_{Rx}}$. Ideally, a completed optimization will result in $\boldsymbol{D_{V_{Rx}} >= D_{Rx}}$completely fulfilling the objective.

For a minimum DVH objective f^{MinDVH}, the goal is to keep the prescribed percentage of the voxels in the ROI volume receiving the prescription dose above the prescription volume. Only voxels with dose above D_{Rx} and below $D_{V_{Rx}}$are penalized. Voxels with dose above the prescription dose have no penalty, as the dose already exceeds the prescription and voxels with dose below $D_{V_{Rx}}$have no penalty as they are in the permitted percentage of the ROI volume

allowed to have dose below D_{Rx}. If $D_{V_{Rx}}$ is greater than or equal to D_{Rx} then the function is zero as the objective has been met.

$$f^{MinDVH} = \frac{1}{N_{roi}}\left(p \sum_{i}^{N_{roi}} H\left(D_i - D_{V_{Rx}}\right) H(D_{Rx} - D_i)(D_i - D_{Rx})^2 \right)$$

3.3 Combination of Objectives

Any combination of the above objectives can be used within an optimization. The composite objective function value is then simply the sum of the individual objectives.

$$f = \sum_{o}^{nObj} f_o$$

where o is the objective of interest, $nObj$ is the number of objectives, and f_o is the objective function for objective o, e.g. f_o^{MinDVH} or f_o^{MaxDVH}.

3.4 Optimization using Newton's Method

To optimize using Newton's method, the objective function is generalized as:

$$f = \sum_{i}^{N_{roi}} c_i (D_i - D_{Rx})^2$$

where c_i is a constant.

The dose D_i at voxel i is given by:

$$D_i = \sum_{j} K_{ij} \omega_j$$

where j is a ray traced from the fluence plane through the patient, K_{ij} is the dose contribution of the jth ray to the ith voxel per unit intensity, and ω_j is the relative weight (or intensity) of the jth ray.

The intent is to optimize the weight of each fluence element, so the process computes the recommended change in weight $\delta\omega_j$ is calculated for each ray. Newton's method defines this change as:

$$\delta\omega_j \approx -\frac{\frac{\partial f}{\partial \omega_j}}{\frac{\partial^2 f}{\partial \omega_j^2}}$$

Using our generalized objective function gives the first derivative:

$$\frac{\partial f}{\partial \omega_j} = 2\sum_i^{N_{roi}} c_i(D_i - D_{Rx})K_{ij}$$

and the second derivative:

$$\frac{\partial^2 f}{\partial \omega_j^2} = 2\sum_i^{N_{roi}} c_i K_{ij} K_{ij}$$

For multiple objectives, the derivatives are the sums of the individual derivatives:

$$\frac{\partial f}{\partial \omega_j} = \sum_o^{nObj} \frac{\partial f_o}{\partial \omega_j}$$

and

$$\frac{\partial^2 f}{\partial \omega_j^2} = \sum_o^{nObj} \frac{\partial^2 f_o}{\partial \omega_j^2}$$

The total weight update for a given ray first and second derivative is then

$$\delta\omega_j \approx -\frac{\sum_o^{nObj}(2\sum_i^{N_{roi}} c_i(D_i - D_{Rx})K_{ij})}{\sum_o^{nObj}(2\sum_i^{N_{roi}} c_i K_{ij} K_{ij})}$$

3.5 Pinnacle Research Objectives

The previous sections describe the theoretical methods for optimizing an IMRT plan. Incorporation of objective functions into a treatment planning system involves minor changes to

the format of objective function equations but produces an equivalent result. In Chapter 5, the basic objective functions presented here are expanded to include the effects of systematic uncertainty.

Objectives in Pinnacle are developed using the Pinnacle Research Interface using Philips Healthcare - Philips Radiation Oncology Systems Pinnacle[3] 8.1y research version. These are compiled codes that are used in the optimization process. The following equations are inferred from the example codes to relate the theoretical equations above to the functions as implemented in the treatment planning system. These are not specifically defined in any Philips documentation, but are derived here for explanatory purposes.

In Pinnacle, each voxel of the ROI has a value V_i representing the relative volume of the voxel that is within the ROI. This allows Pinnacle to have partial voxels within a ROI. The sum of the relative volumes within an ROI is 1:

$$\sum_{i}^{N_{Roi}} V_i = 1$$

This is used to replace the $\frac{1}{N_{Roi}}$ term in the objective function since

$$\frac{1}{N_{Roi}} \cdot \sum_{i}^{N_{Roi}} 1 = \sum_{i}^{N_{Roi}} \frac{1}{N_{Roi}} = 1 = \sum_{i}^{N_{Roi}} V_i$$

which gives a MaxDVH objective function of:

$$f^{MaxDVH} = p \sum_{i}^{N_{Roi}} V_i \cdot H\left(D_{V_{Rx}} - D_i\right) H(D_i - D_{Rx})(D_i - D_{Rx})^2$$

Pinnacle also includes a scaling factor to the objective to normalize scores from different dose levels. This is a multiplicative constant similar to the objective weight:

$$S_{Pinn} = \left(\frac{1}{D_{Rx}}\right)^2$$

This gives the updated Pinnacle objective function F^{MaxDVH}:

$$F^{MaxDVH} = \sum_{i}^{N_{Roi}} p \cdot V_i \cdot S_{Pinn} \cdot H\left(D_{V_{Rx}} - D_i\right) H(D_i - D_{Rx})(D_i - D_{Rx})^2$$

The first derivative of f^{MaxDVH} with respect to beamlet intensity ω_j is:

$$\frac{\partial f}{\partial \omega_j} = \sum_{i}^{N_{Roi}} 2 \cdot p \cdot V_i \cdot S_{Pinn} \cdot H\left(D_{V_{Rx}} - D_i\right) \cdot H(D_i - D_{Rx}) \cdot (D_i - D_{Rx}) \cdot K_{ij}$$

Since K_{ij} is dependent on the beam and anatomy configuration and independent of any objective function, Pinnacle stores it independently of the first derivative matrix. In research objective functions, the independent storage removes the requirement include K_{ij} in computation of the second derivative, thus giving the Pinnacle gradient on a per voxel basis:

$$G_i^{MaxDVH} = 2 \cdot p \cdot V_i \cdot S_{Pinn} \cdot H\left(D_{V_{Rx}} - D_i\right) \cdot H(D_i - D_{Rx}) \cdot (D_i - D_{Rx})$$

where the first derivative can be obtained from

$$\frac{\partial f}{\partial \omega_j} = \sum_{i}^{N_{Roi}} G_i^{MaxDVH} \cdot K_{ij}$$

The second derivative is

$$\frac{\partial^2 f}{\partial \omega_j^2} = \sum_{i}^{N_{Roi}} 2 \cdot p \cdot V_i \cdot S_{Pinn} \cdot H\left(D_{V_{Rx}} - D_i\right) \cdot H(D_i - D_{Rx}) \cdot K_{ij} \cdot K_{ij}$$

Again, Pinnacle computes K_{ij} independently, giving

$$\mathcal{H}_i = 2 \cdot p \cdot V_i \cdot S_{Pinn} \cdot H\left(D_{V_{Rx}} - D_i\right) \cdot H(D_i - D_{Rx})$$

where

$$\frac{\partial^2 f}{\partial \omega_j^2} = \sum_i^{N_{Roi}} \mathcal{H}_i \cdot K_{ij} \cdot K_{ij}$$

Aside from the Heaviside functions, $\mathcal{H}_i$ is a constant for each voxel and is treated by Pinnacle as a scaling value `hDiagScaleFactor_`. The Philips documentation for the Research Interface recommends for the $\mathcal{H}$ computation that "This method *may* be overloaded but it is seldom necessary since the default implementation should suffice for most functions." As this is entirely calculated internally, the second derivative is not modified in the research objective functions described in Chapter 5.

For multiple objectives in Pinnacle, the objective functions are summed, giving:

$$F = \sum_o^{nObj} F_o$$

and the gradient:

$$G_i = \sum_o^{nObj} G_{o,i}$$

$\mathcal{H}$ is neglected here as it is handled internally.

The equations described in this chapter are specifically modified to include systematic uncertainty in Chapter 5, however these equations are still used in Chapter 4 as the basis for IMRT treatment plan optimization using dose-volume based objectives.

4 Probabilistic planning incorporating random uncertainty

Fraction-to-fraction deviations in patient setup positioning from the planning image result in a random uncertainty in patient position relative to the treatment beams. In the case of adaptive planning, the systematic uncertainty in patient setup position may be reduced to a small enough size that it can be safely ignored, leaving only random uncertainty. Since a treatment course typically consists of a large number of treatment fractions (~30), random uncertainty can be approximated as a blurring of the fluence incident upon the patient. A method called fluence convolution, is used to include random uncertainty in the planning process of this study. The purpose of this study is to incorporate random uncertainty into a commercial treatment planning system and compare the results to a margin-based approach. Standard dose-based and DVH-based objectives are used in the optimization process. Comparison metrics include DVH analysis, mean dose, TCP, NTCP, and P+. Additionally, physician assessment of the resulting plans is compared. The concepts of this study have been published in Medical Physics and are included in Appendix I (Moore *et al.*, 2009). In this chapter, the details of the study are described along with the process used to automate implementation.

4.1 Methods

Patient images and contours are acquired from 28 previously treated patients. All patient identifiable information is removed from these plans. Each plan is developed and optimized using Philips Healthcare - Philips Radiation Oncology Systems Pinnacle^3 8.1w research version.

Beams are defined for each patient with angles of 30º, 80 º, 130 º, 180 º, 230 º, 280 º and 330 º. The original IMRT objectives are deleted and new objectives are defined according to the high-dose arm of the RTOG 0126 prostate radiotherapy protocol as shown in Table 7. Direct Machine Parameter Optimization is used for optimization with a dose grid of $2\times2\times2$ mm^3.

For each patient, a PTP and a margin-based plan are generated. This study assumes random uncertainty σ = 3 mm and zero systematic uncertainty ($\Sigma = 0$). Random uncertainty of 3 mm is similar to that used in other studies (van Herk *et al.*, 2002; van Herk *et al.*, 2000; Baum *et al.*, 2004; Birkner *et al.*, 2003; Witte *et al.*, 2007; Craig *et al.*, 2005). For the margin-based plan, the target is defined with a CTV-to-PTV margin of 2.1 mm according to the margin formula of van Herk *et al.* (van Herk, 2004; van Herk *et al.*, 2002; van Herk *et al.*, 2000) which suggests a margin of $M = 2.5\Sigma + 0.7\sigma$. For the PTP plan, the CTV is directly used as the target structure. For other optimization structures, both planning methods use identical optimization objectives. To reduce the dose outside of the target a local normal tissue (LNT) structure is defined as a ring structure expanding 2 cm to 4 cm from the CTV.

During the optimization process for PTP, the fluence is convolved at every dose calculation step. This process is shown in Figure 4. Fluence convolution is made possible by a hook into the dose calculation algorithm in Pinnacle which allows for modification of the fluence prior to dose calculation which is used in a Pinnacle Plugin to convolve the fluence with the PDF of random uncertainty.

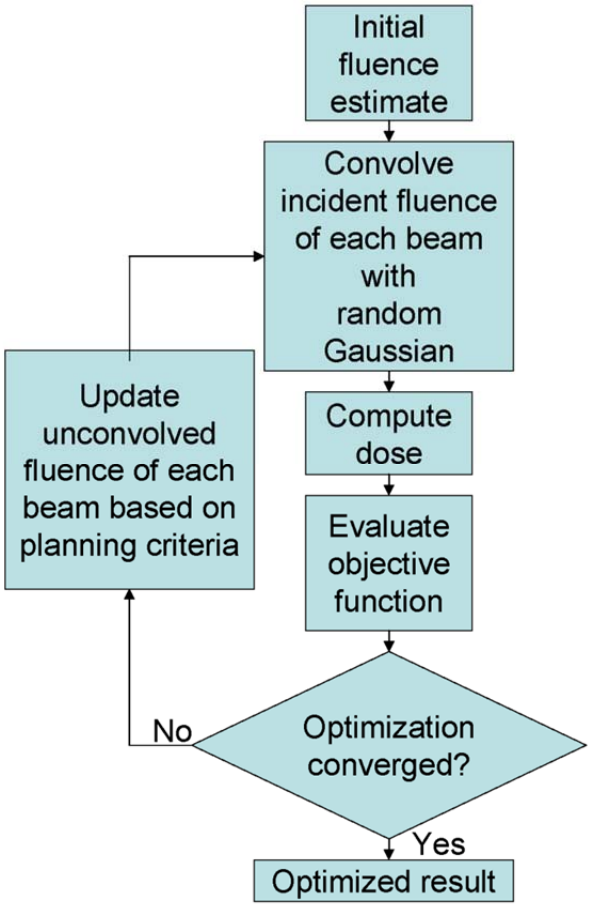

Figure 4: Flowchart of Random PTP. Dose is computed by convolving the fluence with a Gaussian kernel. The objective function is evaluated and convergence is tested. If not converged, fluence is updated based upon the objective function and the process is repeated.

The validity of convolution to approximate random uncertainty on a fixed number of fractions is demonstrated by simulation of multiple 30-fraction treatment courses. A total of 100 treatment simulations are performed. The fluence of each simulated fraction is shifted by a random value sampled from a 3 mm Gaussian distribution. A total treatment course consists of the dose summed over each of the 30 fractions. Each simulated treatment course is compared to a treatment course generated using fluence convolution and DVH metrics are compared for each optimization objective using plans originally optimized with margin-based planning and PTP.

Comparison of each planning method is conducted using the dose-based and DVH-based objectives in planning. For this comparison, the final optimized fluence from both optimized plans is convolved with a 3 mm Gaussian to simulate the effect of random uncertainty. Additionally, TCP, NTCP, and P+ indices are computed for each method.

Using the concept of a Dosimetric Margin Distribution (DMD) developed by Gordon *et al.* (Gordon and Siebers, 2008) the conformity of dose distributions for both methods is computed. DMD is calculated for both the CTV 90% and 50% isodose lines. Sensitivity of the plan to differences in estimated patient uncertainty from the actual distribution of patient setup errors is analyzed by doubling (σ=6 mm) and halving (σ=1.5 mm) the random uncertainty. The previously optimized fluence is convolved with a Gaussian of the modified uncertainty, dose is recomputed (not reoptimized) and DVH indices are compared.

Physician analysis of both methods is conducted. Using the fluence convolved final dose distribution from each patient, DVHs of the CTV, rectum, bladder, left femur and right femur are produced and presented to a physician. The physician indicates which plans are acceptable for treatment and which plan would be preferred for each patient.

4.1.1 Incident Fluence Interface

The Incident Fluence Interface is a plugin into the Pinnacle TPS that allows modification of fluence before dose calculation. This is implemented as a hook – an executable function which intercepts the fluence – into the dose calculation process. If present, every time the dose calculation routines in Pinnacle are executed, the fluence matrix just before dose calculation is passed to the IncidentFluenceInterface plugin. This matrix can then be modified in place and the dose calculation proceeds with the updated values in the array. Pinnacle scripting commands defined the parameters used in the operation of the plugin.

The plugin initially starts in the disabled state. In the disabled state, fluence is passed through the plugin unchanged. In the most basic of functionality, when enabled, the plugin uses the parameter of ConvolutionSigma to generate a 2D kernel with equal width in all dimensions and uses a Fast Fourier Transform to convolve the kernel with the 2D fluence matrix from each beam. Fixed shifts in the fluence can be accomplished by setting the parameters XShift, YShift, and ZShift. In order for these to apply in a 3D patient, projections of the shifts onto the 2D fluence matrix for each beam are calculated and a 2D shift in the fluence matrix is used. Fluence shifts is utilized in the study of the validity of fluence convolution. For debugging purposes, ability of saving and reading the fluence from a file are available and used a comparison study described in Chapter 7.

4.1.2 Automation

The entire process for generating data was implemented in a series of Pinnacle scripts. Pinnacle allows for scripting of most tasks in the system by generating a file with a list of commands to be processed sequentially. For each patient a trial with initial objectives based upon the RTOG-0126 protocol is defined manually (RTOG0126). This is automatically copied to a trial for the margin plan (Margin) and a trial for the PTP plan (PTP). The target structures for both plans are automatically updated. The target structure for the margin plan is PTV_2.1mm which is an ROI generated by expanding the CTV by 2.1 mm. The target structure for the PTP plan is set to the CTV itself. The margin plan is optimized from uniform beams to convergence with fluence convolution disabled. For the PTP plan, fluence convolution is enabled, uses a 3 mm ConvolutionSigma, and is optimized to convergence.

The final dose distribution for the PTP plan is from convolved beams. To compare to the margin-based plan, the margin trial (Margin) is copied to a new trial (Margin-Conv) and dose is

recomputed using fluence convolution and a 3 mm ConvolutionSigma. For both trials (PTP and Margin-Conv), DVHs are plotted and written to file along with the statistics (volume and minimum, maximum, mean and standard deviation of the dose). Biological criteria are computed and TCP for the CTV, and NTCP for the bladder, rectum, left and right femur, as well as P+ are output for the patient. The process for a single patient is entirely contained within the PTP script. A wrapper shell script is written external to Pinnacle which iteratively executes this script on each patient in the database.

Sensitivity analysis is performed by a script which automatically convolves the final optimized fluence distribution with each sigma of random uncertainty (1.5 mm, 3 mm, and 6 mm) for both trials. The DVHs, DVH statistics and biological scores are output for each sigma and method.

Validation of the convolution approximation is accomplished by evaluated the delivered dose by simulating random interfractional motion. Simulations are computed by a plugin which randomly samples a 3D offset from a isotropic 3 mm Gaussian distribution. The IncidentFluenceInterface uses the sampled offset to shift the fluence distribution, simulating a fraction of treatment. The final optimized fluence for the PTP and margin based plans are used in simulation. For both methods, the fluence-convolved dose distribution is stored as the convolved dose. The plugin simulates 30 fractions of treatment, storing the dose distribution from each fraction and the total sum is the final dose distribution for the treatment. DVH curves for the CTV, rectum, bladder, left femur and right femur are output for each simulated treatment course. The plugin repeats this process 100 times for each method with different randomly sampled shifts. A shell script parses the DVH output for the dose and volume parameters of each planning objective. This is output as a comma-delimited file and imported into Excel for analysis.

4.2 Results

Table 1 shows the dose and volume difference between simulated courses and fluence convolution. For margin-based plans, the average deviation of simulated treatments from the fluence convolved dose is less than 0.1% For PTP plans, the average deviation of simulated treatment from the fluence convolved dose is 0.1%. This deviation for both methods is less than the 2-3% variability accepted in beam delivery.

Table 1: Minimum, maximum, range, mean, and standard deviation of DVH criteria observed over the 100 simulated treatment courses for the CTV and LNT structures compared with convolution. Average difference is the absolute value of the convolution value minus the mean of the simulated treatment courses. Simulated treatment course values are the difference from convolution for volumes and the percentage difference relative to convolution for doses.

			Convolution	Simulated Treatment Courses				
				Min	Max	Range	Average	Std Dev
Margin-based	CTV	V7920	98.0%	-0.7%	0.6%	1.3%	0.0%	0.3%
		D98	7920 cGy	-0.2%	0.2%	0.5%	0.0%	0.1%
		V8470	0.4%	-0.4%	0.8%	1.2%	0.1%	0.3%
		D0	8506 cGy	0.0%	0.1%	0.1%	0.0%	0.0%
	LNT	V5000	1.1%	-0.1%	0.1%	0.2%	0.0%	0.0%
PTP-Based	CTV	V7920	97.5%	-2.1%	1.0%	3.0%	-0.1%	0.6%
		D98	7890 cGy	-1.8%	0.7%	2.5%	-0.1%	0.5%
		V8470	0.0%	-1.6%	1.5%	3.1%	0.3%	0.6%
		Max	8470 cGy	-0.2%	0.3%	0.5%	0.1%	0.1%
	LNT	V5000	0.7%	-0.1%	0.1%	0.1%	0.0%	0.0%

Physician review of plans indicates that the PTP-based plan is preferred in 21 out of 28 patients. The physician indicated no preference in one plan, preferred margin in two plans, and rejected both plans for four patients.

Table 2 shows the average difference in dose and volume for each objective. The average CTV D_{98} is 0.5% lower for PTP plans when compared to margin-based plans. The average CTV volume receiving the treatment dose for the PTP method does not differ significantly from margin-based plans. The volume of LNT receiving 5000 cGy is reduced by 48% using the PTP

method when compared to margin-based plans. All other critical structures were below the planning criteria.

Table 2: Mean, maximum, minimum, and p-value for the difference in dose and difference in volume between margin-based and PTP-based plans for the listed objectives averaged over all patients. Plan objectives not listed were met by both methods for all plans. †All plans met objectives except for 2 PTP-based plans and 2 margin-based plans. ‡All plans met criteria except for 1 PTP-based plan. *All plans met criteria except for 1 PTP-based plan and 1 margin-based plan.

Structure	Dose (cGy)	Volume	Δ Dose	Max	Min	p	Δ Volume	Max	Min	P
Target	>7920	98%	-0.5%	0.6%	-2.4%	0.0013	-0.4%	4.7%	-3.0%	0.0916
	<8470	2%	0.1%	1.4%	-0.7%	0.1040	66.6%	780.1%	-86.6%	0.4415
Rectum	<7500	15%	†							
	<8470		‡							
Bladder	<8470		*							
LNT	<5000		-1.9%	4.9%	-10.0%	0.0095	-47.9%	50.2%	-94.4%	<0.0001

Table 3 shows the average difference in mean dose for each structure over all patients. Mean dose of the CTV is increased slightly using PTP when compared to margins. Mean dose to all critical structures is significantly reduced when compared to margin-based plans.

Table 3: Mean, maximum and minimum difference in mean dose between margin-based and PTP-based plans, with associated p-values for objective structures.

Structure	Mean Δ	Max	Min	p
CTV	0.7%	2.0%	-1.2%	<0.0001
Rectum	-8.0%	-1.6%	-15.5%	<0.0001
Bladder	-14.2%	-4.5%	-26.4%	<0.0001
Left Femur	-11.3%	-5.0%	-20.6%	<0.0001
Right Femur	-11.1%	-3.0%	-18.5%	<0.0001
LNT	-12.9%	-9.9%	-18.2%	<0.0001

Table 4 shows the average change in TCP, NTCP, and P+ for each planning method. Compared to margin-based plans, PTP increases P+ by 2.5%, decreases rectum NTCP by 1.9%, decreases bladder NTCP by 0.7%, and decreases LNT NTCP by 0.1%. Left and right femur NTCP for both PTP and margin plans is zero.

Table 4: Mean, maximum, and minimum difference in P+, TCP, and NTCP between margin-based and PTP-based plans with associated p-values for objective structures

Structure	Type	Mean Δ	Max	Min	P
All	P+	2.45%	7.60%	-2.10%	0.0002
CTV	TCP	0.01%	0.30%	0.00%	0.3262
Rectum	NTCP	-1.88%	2.80%	-7.00%	0.0014
Bladder	NTCP	-0.67%	0.00%	-2.60%	<0.0001
Left Femur	NTCP	0.00%	0.00%	0.00%	-
Right Femur	NTCP	0.00%	0.00%	0.00%	-
LNT	NTCP	-0.06%	0.00%	-0.40%	0.0028

The dosimetric margin (Table 5) is smaller for PTP plans in 25 of 28 patients for the 7100cGy isodose line and 27 of 28 for the 3960cGy isodose line, indicating a much more conformal dose distribution.

Table 5: Dosimetric margin distributions. Mean, maximum, and minimum dosimetric margins are presented for margin and PTP plans for both 7100cGy and 3960cGy. A paired t-test indicates the difference between methods is significant.

Dose	7100cGy			3960cGy		
	Mean (cm)	Max (cm)	Min (cm)	Mean (cm)	Max (cm)	Min (cm)
Margin	0.90	1.63	0.37	1.90	4.11	0.92
PTP	0.65	1.47	0.17	1.60	3.67	0.62
P	<0.0001			<0.0001		

Sensitivity analysis of the mean dose (Table 6) shows that for both methods, a decrease in realized uncertainty from the planned uncertainty increases the mean dose for all structures except the LNT which shows a slight decrease. An increase in realized uncertainty from the planned uncertainty decreases mean dose for all structures except the LNT. Analysis of the objectives shows that for a doubling of the planned random uncertainty, no patients meet the CTV minimum dose objective for either method, but, also, none exceed the OAR objectives. For 23 PTP plans and 10 margin plans which did not meet the CTV minimum dose, if the realized random uncertainty is half of the planned random uncertainty, the objective is then met.

Table 6: Differences in mean dose objectives when plans are subject to half (1.5 mm) and double (6 mm) the planned random uncertainty used in optimization.

		Half	Double
Margin	Bladder	0.3%	-1.0%
	CTV	0.2%	-1.6%
	LNT	-0.4%	1.8%
	Left Femur	0.3%	-1.1%
	Right Femur	0.4%	-1.3%
	Rectum	0.3%	-1.0%
PTP	Bladder	0.1%	-0.2%
	CTV	0.4%	-2.6%
	LNT	-0.3%	1.6%
	Left Femur	0.3%	-1.2%
	Right Femur	0.4%	-1.3%
	Rectum	0.3%	-1.0%

4.3 Conclusions

A method of incorporating random setup uncertainty into treatment planning has been developed. Fluence convolution used in the method is shown to be a valid approximation of the total dose of a fractionated radiotherapy plan. PTP-based plans maintain similar target dose to margin-based plans while decreasing dose to normal structures. TCP for both methods remain similar, while a decrease in NTCP is observed. This results in a slight increase in overall P+. Physician assessment of plans generally prefers PTP plans.

PTP Plans are sensitive to inaccuracies in the distributions of random uncertainty, however, this sensitivity is comparable to that of margin-based plans. In either case, due to blurring, a smaller uncertainty than planned results in increased dose to structures in optimization, while a larger uncertainty results in decreased dose to these structures.

The method described in this chapter results in an reduction of normal tissue dose while maintaining a high dose to the target. This method removes the limitation of a CTV-to-PTV margin to account for random uncertainty of patient positioning in the planning process.

5 Probabilistic planning incorporating systematic uncertainty

In the case that adaptive planning methods fail to reduce uncertainty in patient position below the necessary threshold to be ignored, plans can be optimized to reduce dosimetric consequences of both random and systematic patient positional uncertainty. This builds upon the previous chapter which included only random uncertainty. Systematic setup uncertainty is the difference in average patient position from the planned treatment position. Conventionally this is handled by a margin around the target to ensure the target receives a therapeutic dose when subject to an unknown systematic shift.

Unlike random uncertainty, systematic uncertainty cannot be described as a blurring effect. A systematic offset applies throughout the treatment process. The purpose of this work is to explicitly incorporate systematic setup uncertainty into plan optimization. This is achieved by joint optimization of multiple probable systematic shifts. It is hypothesized that directly including systematic uncertainty in planning will reduce dose to critical structures while maintaining a similar target coverage probability. This concepts contained within this chapter are described in the paper submitted to International Journal of Radiation Oncology Biology Physics and also in Appendix II. This chapter contains details of that work with details of the automation and interface developed to aid in the implementation of the proposed methods.

5.1 Planning parameters

For this study, imaging and contour data from 28 previously treated patients are used. Identifying information was removed from each data set. Patients were planned using Philips Healthcare - Philips Radiation Oncology Systems Pinnacle^3 8.1y research version. Each patient has an identical 7-beam setup with beam angles of 30, 80, 130, 180, 230, 280 and 330. The original treatment plan was discarded and new plans were generated. Plans were optimized as Intensity Modulation plans. RTOG-0126 Objectives were added automatically to each plan according to Table 7. For PTP plans custom objective functions were used. For margin-based plans, the built in Pinnacle objectives were used. For all plans, a systematic uncertainty of 3mm was used. Random uncertainty of 3mm was implemented as fluence convolution.

5.2 Optimization process

The novel work of this study is to optimize while incorporating the effects of systematic patient setup uncertainty. The goal is to produce a plan which will deliver the same dose distribution to any systematic shift from the planned position sampled from the systematic uncertainty distribution used in planning. In order to do this, some number of systematic offsets, $nSys$, are sampled from the distribution of systematic uncertainty Σ. The same objectives used in standard optimization are applied to the volume of each shifted anatomy which results in an independent objective for each shifted anatomy and effectively creates a simultaneous optimization over all sampled systematic shifts.

A graphical display of this process is shown in Figure 5. The process is effectively split into three components: create a PTP plan, create a margin-based plan, and compare the two plans. Each of these steps is described below. The process of creating a PTP plan centers around the objective function described below.

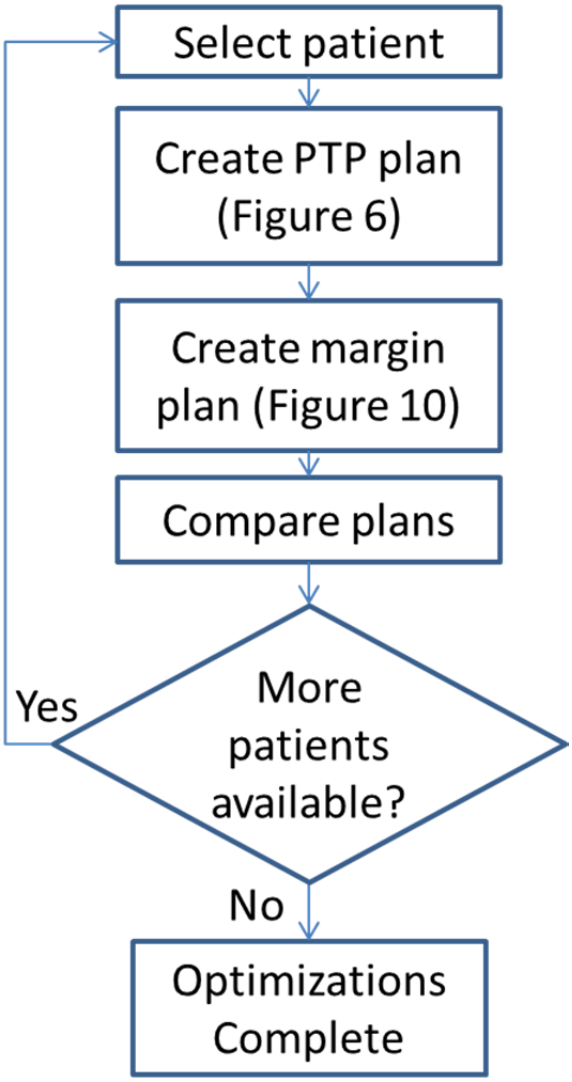

Figure 5: Overall flow of comparison process.

5.2.1 Objective function

The details of a standard objective function are described above and in the work of Wu and Mohan(Wu and Mohan, 2000). This study deviates from the typical objective functions by incorporating systematic uncertainty into the optimization process. This is done by a joint optimization of potential systematic shifts. The objective function is expanded to include an offset to the position of dose used in the function. For a given shift, the objective function score is

$$F_{o,s} = \sum_{i}^{N_{roi}} p_o \cdot V_i \cdot \left(\frac{1}{D_{Rx,o}}\right)^2 \cdot H\left(D_{V_{Rx,o},s} - D_{i+s}\right) H\left(D_{i+s} - D_{Rx,o}\right)\left(D_{i+s} - D_{Rx,o}\right)^2$$

And the gradient for a given shift s and a given voxel i:

$$G_{o,s,i} = 2 \cdot p_o \cdot V_i \cdot \left(\frac{1}{D_{Rx,o}}\right)^2 \cdot H\left(D_{V_{Rx,o},s} - D_{i+s}\right) H\left(D_{i+s} - D_{Rx,o}\right)\left(D_{i+s} - D_{Rx,o}\right)$$

Where $i + s$ represents the position of the voxel offset by the sampled systematic shift s and $D_{V_{Rx,o},s}$is calculated from the DVH generated for each offset and objective. For each systematic shift, $D_{V_{Rx,o},s}$ has to be recomputed.

The systematic objective functions will be computed on multiple systematic shifts. The total objective function for a single objective is given as the sum of the objectives for all shifts:

$$F_o = \sum_{s}^{nSys} F_{o,s}$$

The gradient is similarly defined as:

$$G_{o,i} = \sum_{s}^{nSys} G_{o,s,i}$$

Using the equations inferred from the Pinnacle implementation (Chapter 3), the update to a given intensity element is given by:

$$\delta\omega_j \approx -\frac{\frac{\partial f}{\partial \omega_j}}{\frac{\partial^2 f}{\partial \omega_j^2}} = \frac{\sum_s^{nSys}\sum_o^{nObj}\sum_i^{N_{Roi}} G_{o,s,i} \cdot K_{ij}}{\sum_s^{nSys}\sum_o^{nObj}\sum_i^{N_{Roi}} \mathcal{H}_{o,s,i} \cdot K_{ij} \cdot K_{ij}}$$

Note that in the equations above, a Heaviside function dependent on $D_{V_{Rx,o},s}$ is used such as $H\left(D_{V_{Rx,o},s} - D_{i+s}\right)$. $D_{V_{Rx,o},s}$ is dependent on the dose distribution underlying a specific shift.

Generally, $D_{V_{Rx,o,s}}$ will be different from shift to shift and thus changes the range of voxels affected by the optimizer.

5.2.2 Shift List Manager

Systematic uncertainty is incorporated into the objective function by using a series of multiple systematic shifts. To generate and specify the shifts used during each iteration of optimization, a plugin (ShiftListManager) is written to maintain the list of systematic shifts for optimization. Each shift is generated by randomly sampling each directional component from a 3 mm Gaussian distribution. The number of shifts, size of the Gaussian distribution, and the random seed used to generate the shift are parameters of the ShiftListManager plugin. By specifying a random seed, a reproducible list of shifts can be generated. The same list of shifts is used during each iteration of optimization to ensure that the plan is robust to the list of shifts generated.

5.2.3 PTP plan generation

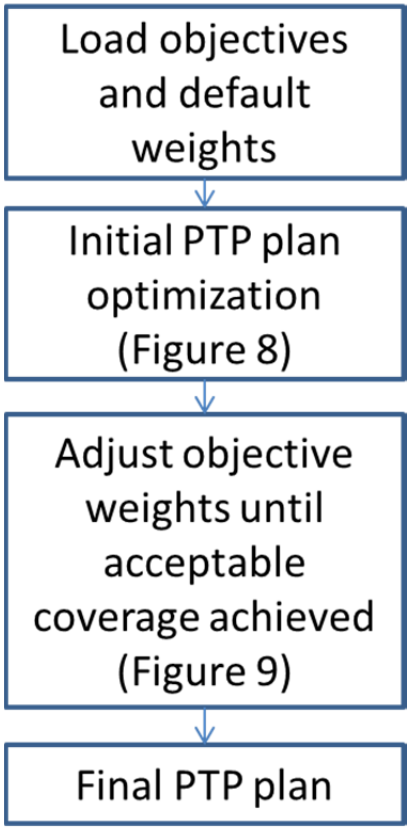

Figure 6: PTP plan generation process. Initial RTOG-0126 objectives are loaded. Then, the initial PTP plan is generated by incrementally doubling the number of systematics used in optimization. Lastly, the weights of the rectum and bladder objectives are adjusted to produce a plan with the desired target coverage probability.

PTP plan generation is split into three main components: define initial parameters, initial plan optimization and coverage-based weight adjustment. The flow of this process is described in Figure 6. The first step specifies the parameters used in optimization. The objectives and weights used here are shown in Table 7. The next step, described in more detail below, generates the initial plan by incrementally doubling the number of systematic shifts used in the optimization process until a large enough number of systematics is used in optimization. The last step, also described in more detail below, adjusts the OAR objective weights to produce an acceptable target coverage probability. The end result of the plan generation is the final PTP plan used for comparisons.

Table 7: RTOG-0126 Optimization Objectives.

Structure	Objective Type	Dose	Volume	Weight
Target	Min DVH	7920	98	100
Target	Max DVH	8470	2	90
Rectum	Max DVH	6000	50	80
Rectum	Max DVH	6500	35	80
Rectum	Max DVH	7000	25	80
Rectum	Max DVH	7500	15	80
Rectum	Max Dose	8470	n/a	80
Bladder	Max DVH	6500	50	80
Bladder	Max DVH	7000	35	80
Bladder	Max DVH	7500	25	80
Bladder	Max DVH	8000	15	80
Bladder	Max Dose	8470	n/a	80
Left Femur	Max DVH	3500	50	20
Left Femur	Max Dose	5000	n/a	20
Right Femur	Max DVH	3500	50	20
Right Femur	Max Dose	5000	n/a	20
Unspecified Tissue	Max Dose	5000	n/a	0

5.2.3.1 PTP Process

The PTP process is the core of the method. This process uses multiple systematic offsets during the optimization process to generate a plan which incorporates systematic patient setup uncertainty into the optimized result. The flow of this process is shown in Figure 7.

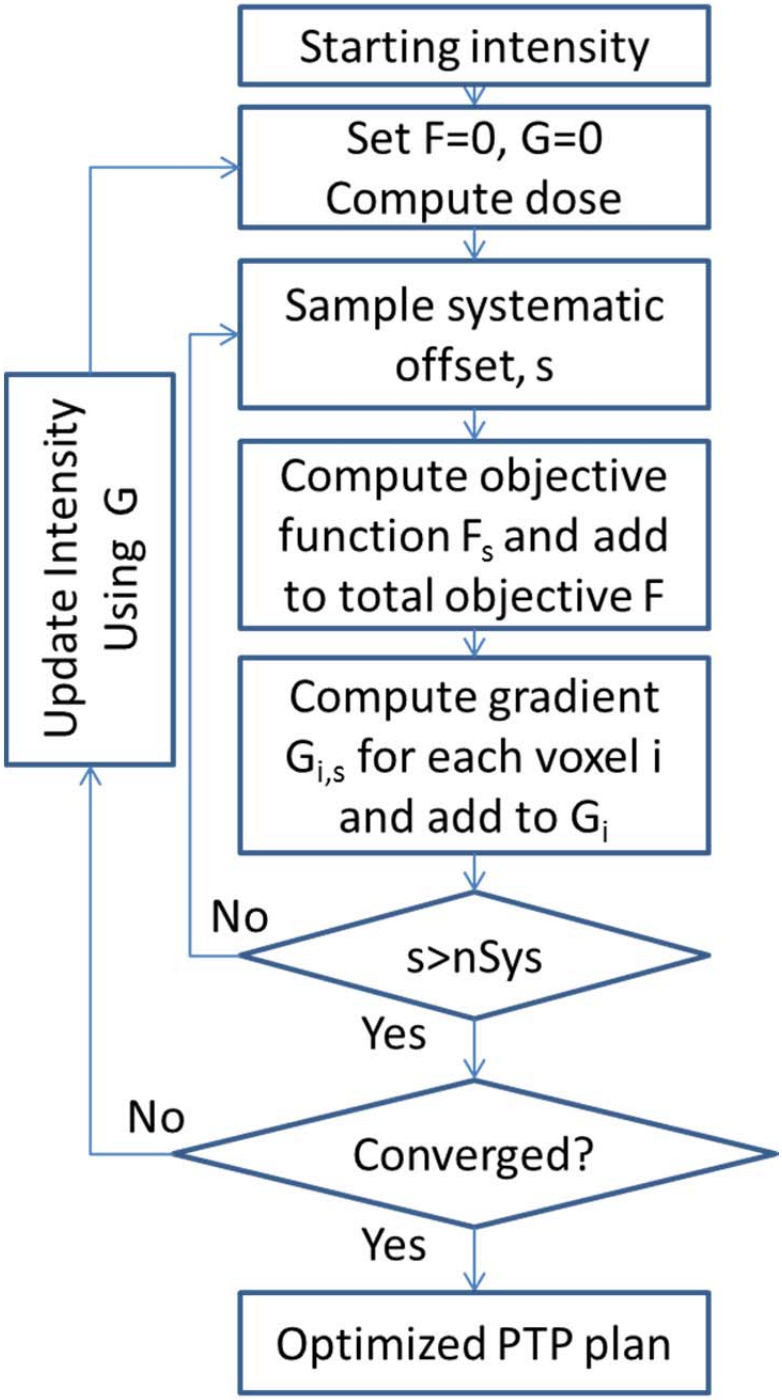

Figure 7: PTP process for incorporating systematic uncertainty into treatment planning

The PTP process starts with an initial intensity. This intensity may be a uniform intensity for new optimizations, or may be a previous "guess" from a previous optimization. A better "guess" for initial intensity will result in a plan that converges more quickly.

The score and gradient array are both zeroed. Dose is calculated using the initial intensity. To incorporate random uncertainty, the initial fluence will be convolved with a Gaussian distribution before dose calculation. This process is described in the previous chapter.

A systematic offset is selected and used to compute the objective function. The objective function for this systematic offset is added to the total objective function. For each voxel in the structure, the gradient is computed and added to the gradient array for that voxel. Afterward, a new systematic offset is selected and the process is repeated until all the objective function has been evaluated on all systematic offsets.

The intensity is then updated using the total objective function and gradient arrays, the arrays are again zeroed, dose is computed and the loop is repeated until convergence. Convergence is defined as a change in score of less than 1E-6 or reaching 500 iterations, whichever occurs first.

5.2.3.2 Initial plan optimization

The initial plan optimization process increases the number of systematic offsets to produce an optimized plan. The flow of this process is shown in Figure 8. Stepping the number of systematic shifts in this way results in a faster optimization as the lesser numbers of systematic shifts produce a good starting point for the next stage of optimization without the time required to optimize all systematic shifts.

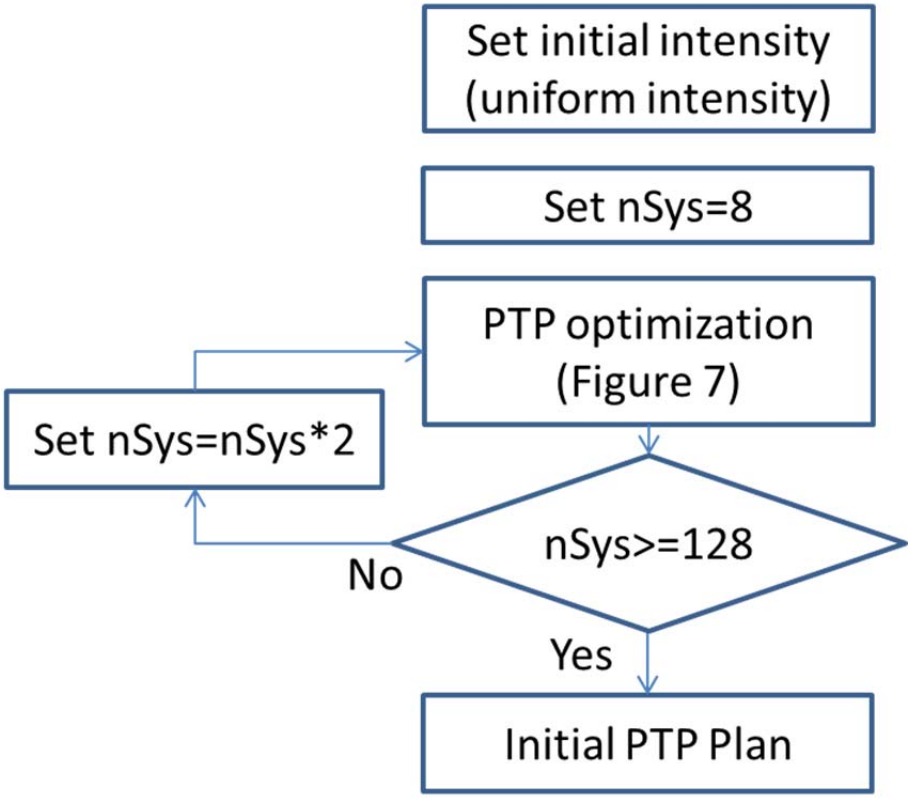

Figure 8: Initial PTP plan creation. An iterative process of increasing the number of systematic shifts is used incrementally doubling from 8 to 128 systematic shifts. For each number of systematic shifts, the PTP method is used to optimize the plan to convergence.

The initial plan optimization starts by defining a uniform intensity over the target structure. Structures are specified as target structures in the initial objectives. Each intensity element that crosses through a voxel contained in a target structure is initially set to a uniform value.

Initially the number of systematics is set to 8. The positions of each of the shifts are randomly generated before PTP optimization and remain fixed throughout the optimization. The PTP process is used to generate an initial intensity using the 8 selected systematic offsets. The optimized result of this is used as the initial intensity into the next step.

After each step, the number of systematic shifts is doubled until it reaches 128. After an optimization using 128 systematic shifts is completed, the initial PTP plan is complete. The number of shifts required was studied (described in Section 5.2.6) and determined to be

approximately 128 shifts. Beyond 128 shifts, little improvement is observed but the time required greatly increases.

5.2.3.3 Weight Adjustment

The coverage probability of the initial PTP plan is variable from patient to patient. To produce a more consistent coverage probability among plans, the weights of the bladder and rectum objectives are adjusted to produce a higher coverage probability. The current standard of practice for treatment planning using margins involves a similar step of adjusting the weights to produce a better trade-off between objectives. In this study, the weight is adjusted automatically to produce a desired coverage probability.

After the optimization is completed for 128 systematic shifts, the objective function weights are adjusted to produce a higher coverage probability of the target. This is done using a binary search algorithm. This process is described in Figure 9. The weights of all rectum and bladder constraints are adjusted with the same value. The weight of the rectum and bladder structures is changed, the fluence distribution from the initial PTP plan with 128 systematic shifts is used as a starting point, and the plan is re-optimized using the PTP method with 128 systematic shifts. For each weight reached in the binary search, coverage probability is computed after optimization converges. The coverage probability calculation method is described below in Section 5.2.5.

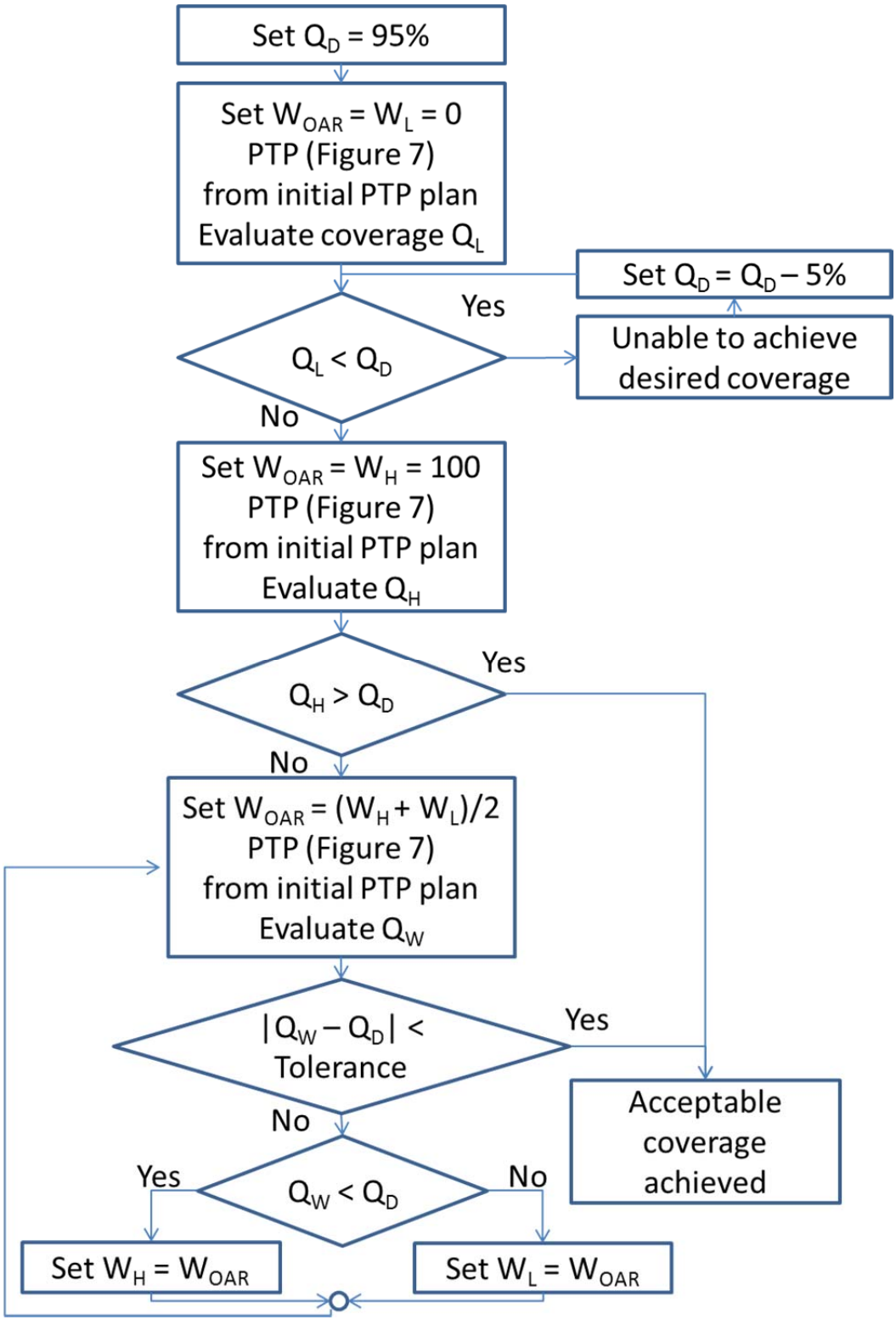

Figure 9: Weight adjustment process for PTP. A binary search method is used to find OAR weights which produce the desired coverage probability.

The allowed range of weights for an objective is integral values from 0 to 100. A weight of zero indicates that the objective will be ignored during optimization. Weights are first be set to 0 and then 100. These check the bounds of the solution space. If the desired coverage probability is higher than the coverage probability produced with a weight of 0, then the adjustment is stopped as the desired coverage probability is higher than what is achievable with this method. Similarly, if the desired coverage probability is less than that produced with a weight of 100, the adjustment is stopped as the achieved coverage probability is higher than the desired coverage probability for any weight specified.

After checking the bounds of the weight adjustment, the weight is set to the middle point of the bounds and coverage probability is calculated. If the desired coverage probability is higher than the achieved coverage probability, the current weight is set to the high weight limit and this step is repeated. Similarly, if the desired coverage probability is lower than the achieved coverage probability, the current weight is set to the low weight limit. This step is repeated until the achieved coverage probability is within a tolerance range of the desired coverage probability, or the step size between weights is below the tolerance limit.

For this study, the desired coverage probability is 95%, the tolerance range for coverage probability is 0.5% and the tolerance range for weight change is 1.

5.2.4 Margin Expansion

After the weight adjustments have been completed, a margin based plan is created. This plan is generated using the RTOG-0126 objectives and weights in Table 7. The CTV-to-PTV margin of this plan is adjusted to produce a plan with the same coverage probability as the weight-adjusted PTP plan. The process is visually shown in Figure 10. This is also accomplished using a binary search method. The target margin is first expanded by the lower bound of the

margin range and optimized to convergence. If the achieved coverage probability is higher than the desired coverage probability, margin adjustment is stopped. The target margin is then expanded by the upper bound of the margin range. If the achieved coverage probability is lower than the desired coverage probability, margin adjustment is stopped as a higher upper bound is required to achieve the desired coverage probability.

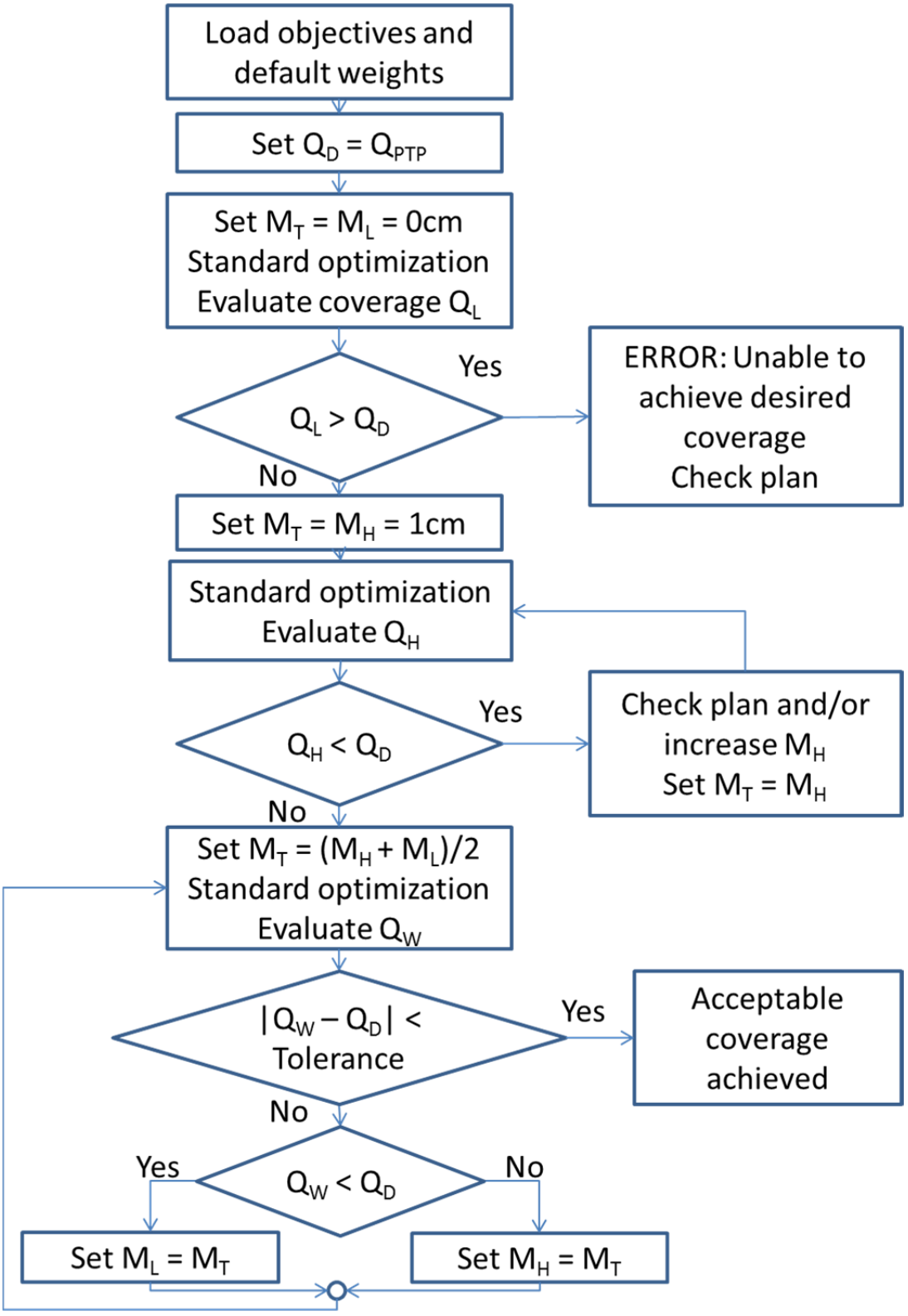

Figure 10: Process for creating optimized margin plans. A binary search algorithm is used to find a margin which gives similar coverage probability to a PTP plan.

The next margin is set to the middle point between the upper and lower bounds. The plan is optimized to convergence. If the achieved coverage probability is lower than the desired coverage probability, the lower margin limit is set to the current margin. If the achieved coverage probability is higher than the desired coverage probability, the higher margin limit is set to the current margin limit. This is repeated until the achieved coverage probability is within the tolerance range of the desired coverage probability or the change in margin is below the margin change threshold.

For this study the desired coverage probability is set to the coverage probability achieved by the PTP plan, the tolerance range for coverage probability is 0.5% and the tolerance range for margin change is 1mm. This optimization is completed with a PRV margin of OAR+1.0cm.

5.2.5 Comparison Metrics

After all optimizations have been completed, coverage probability for all structures is computed along with Probability Dose Volume Histograms (PDVHs) and Dose Volume Coverage Maps (DVCMs). These are then compared for PTP and both margin methods.

Dose volume coverage maps are generated by computing dose-volume histograms for a number of shifts of the dose distribution. These were calculated using a coverage data objective developed by Gordon *et al.* (Gordon *et al.*, 2010) . In the coverage data objective, 919 shifts are used. These shifts are each a multiple of the dose grid resolution. A dose-volume histogram is generated for each shift. The area below the DVH curve is set equal to a value of 1 and the area above the DVH curve is set equal to a value of 0. The DVHs for all shift are then summed together and divided by the number of DVH curves generated and this results in a dose-volume coverage map. DVCMs indicate the probability that the DVH curve will be above any given dose-volume pair. Values of 1 indicate that the dose-volume pair will always have a DVH curve

above the point based upon the given systematic uncertainty. Values of 0 indicate that the dose-volume pair will always be above the curve based upon the given systematic uncertainty. For this study, DVCMs were output as a binary data file with a dose resolution of 5 cGy and a volume resolution of 1%. DVCMs were calculated using a grid method which used steps equal to the size of the dose grid (2mm x 2mm x 2mm) and were imported into Matlab to produce a display and allow an overlay of the planning criteria for each structure.

Dose-Volume Coverage Difference Maps are computed by subtracting one DVCM from another. In this study, the DVCM from the margin-based plan is subtracted from the DVCM from the PTP plan. DVCDMs will range in value from -1 to 1, where values below 0 represent a decrease in coverage probability for a dose-volume pair and values above 0 represent an increase in coverage probability for a dose volume pair. In order to do generate DVCDMs, the DVCMs to be compared are padded to be equal sizes. For padding from zero to the lower dose value on each map, padded values are all 1. For padding from the upper dose value on each map to the desired upper dose line (in this study, this is set to 100Gy) padded values are all 0. The padded array produced from the margin-based plan is subtracted from the padded array produced by the PTP-based plan. The color range is then set to -1 to 1 to ensure that varying arrays can easily be visually compared.

Probability Dose-Volume Histograms represent the expected DVH curve for a given probability. For example, the 95% PDVH indicates that 95% of the time it is expected that the actual DVH curve will lie above the PDVH curve. PDVHs are generated by taking the DVCM described above and tracing a line through the elements of the desired probability. PDVHs is output as a metric using the coverage data objective developed by Gordon *et al.* (Gordon and Siebers, 2009).

Coverage probability is the probability that a given structure will exceed a specified dose-volume level given when subject to uncertainty. Coverage probability is calculated by shifting the dose distribution according to the uncertainty distribution and calculating the percentage of shifts that result in the specified structure exceeding a dose-volume level. Coverage probability values can be taken from the DVCM as a single dose-volume pair in the DVCM. Coverage probabilities are output as a metric using the coverage data objective developed by Gordon *et al.* (Gordon and Siebers, 2009). Coverage probability is output at each planning criteria.

Margin and PTP plans generated in this study are also evaluated by a physician to determine which plans are acceptable and which plan is preferred. For physican evaluation, plans for each patient are randomized and labeled as A or B. PDVH and static DVH plots are presented to the physician to determine if a plan would be acceptable to treat and if both plans are acceptable, which plan would be the preferred plan to treat the patient.

5.2.6 Determining the number of systematics

Prior to optimization, the number of systematic shifts needed to characterize the uncertainty distribution is needed. To determine this value, plans are optimized using different random seeds. The random seed is varied from 0 to 100 in steps of 10, giving 11 different random seeds. Changing the random seed results in a different set of systematic shifts, which if insufficiently sampled will give a different coverage probability. To study the number of systematic shifts, each random seed is used to optimize a plan and coverage probability is calculated. The number of systematic shifts is doubled after each set. The standard deviation in coverage probability is computed for each count of systematic shifts. The process is stopped when the standard deviation of coverage probability for the doubled number of systematic shifts

is no longer significantly different from the standard deviation of coverage probability of the previous number of systematics.

For the entire patient population, plans are first optimized with 16 systematic offsets generated with a random seed of zero (plan 16-0). The final optimized fluence from plan 16-0 is used as the initial fluence for an optimization with 32 systematic offsets generated with a random seed of zero (plan 32-0). The process is repeated for each random seed using the fluence from plan 16-0, and generating plan 32-10 through 32-100. Coverage probability for each of these plans is recorded and the standard deviation of coverage probability is calculated. Starting from plan 32-0, the number of systematics is increased to 64 and the process repeated.

The process for determining the uncertainty in coverage probability for each number of systematics is repeated for the entire patient population and the significance of the difference in uncertainty in coverage probability for each systematic count is computed using a paired t-test.

5.2.7 Automation process

To ensure consistency in the process between patients, the entire study is automated using Pinnacle scripts and Tcl/Tk scripting using PinnComm. PinnComm is a communication system which allows an external application to query and set values within Pinnacle. The PinnComm library is used by a Tcl/Tk application to produce a graphical user interface (GUI) to allow for easily changing variables throughout the process (Figure 11).

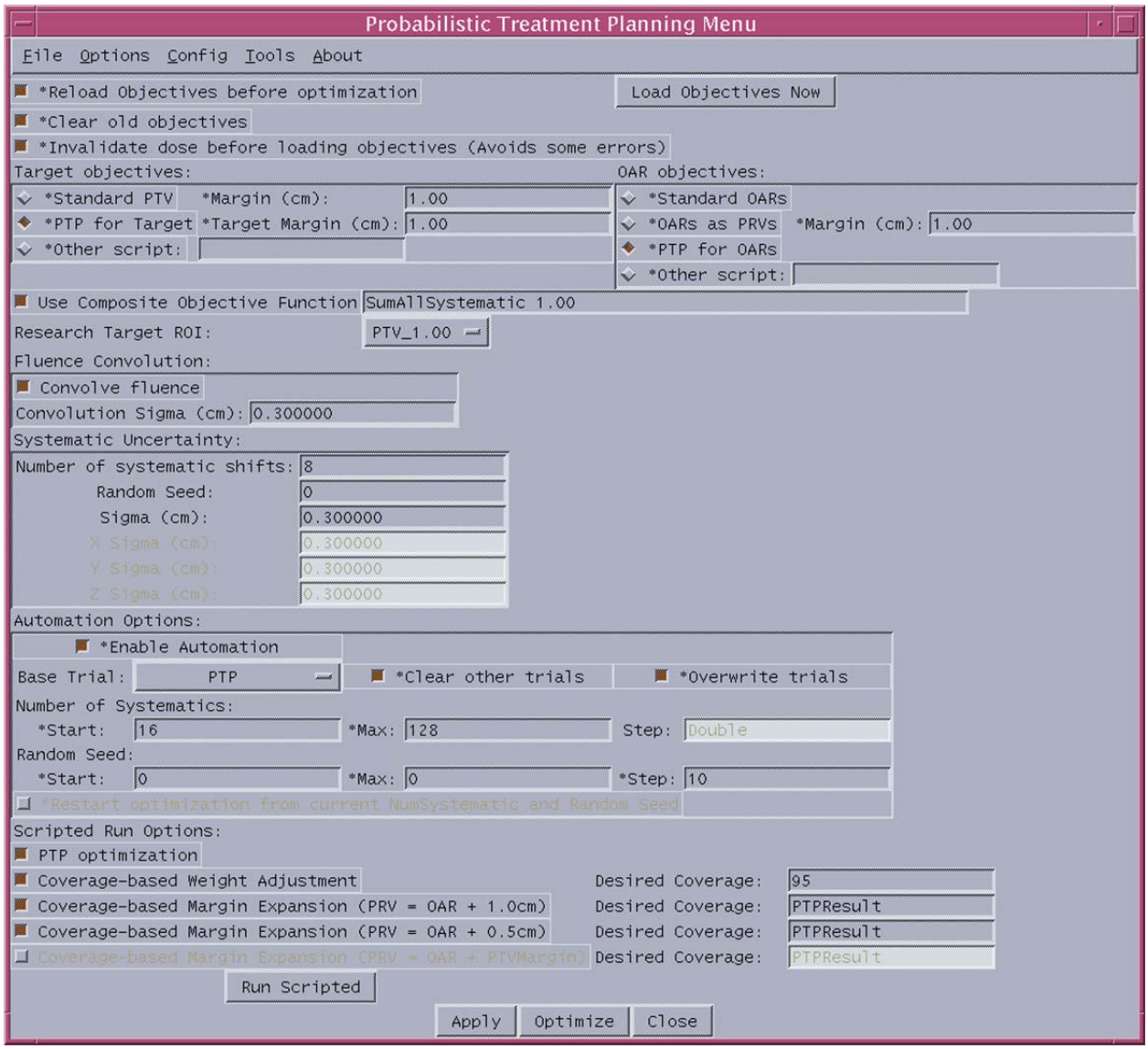

Figure 11: Main GUI window for PTP with random and systematic uncertainty.

At the beginning of the optimization process, all plan objectives are reset to known values. The original plan objectives are removed and the new plan objectives are defined. Each objective is defined for a single ROI. As some of the ROIs used in planning are expansions of the original physician contours, this process discards any expansion contours in the original plan and creates newly expanded contours from the base contours with a user specified expansion which ensures that all contours are expanded in an identical way.

Figure 12 shows the objective definition component of the GUI. Separate options are presented for loading target objectives and OAR objectives. Target objectives may be defined as a 'Standard PTV' or 'PTP for Target'. For 'Standard PTV' the CTV is expanded by a user-specified margin and the newly created PTV is set as a target objective with built-in objective functions. In the case of 'PTP for Target' the CTV is defined as the target objective and custom research objective functions are used. Additionally, for 'PTP for Target', a secondary structure expanded by a user defined margin set as a target objective with zero weight to ensure the intensity matrix will allow variation of intensity outside of the CTV. OAR objectives may be specified as 'Standard OARs', 'OARs as PRVs', or 'PTP for OARs'. If 'Standard OARs' is selected, the OAR objectives are defined using the original physician OAR contours with no expansion and uses built in objective functions. For 'OARs as PRVs' the objectives are defined as the original OAR contours plus a user defined margin expansion and built in objective functions are used. The 'PTP for OARs' option defines the OAR objectives using the original physician OAR contours with no expansion, but uses custom research objective functions.

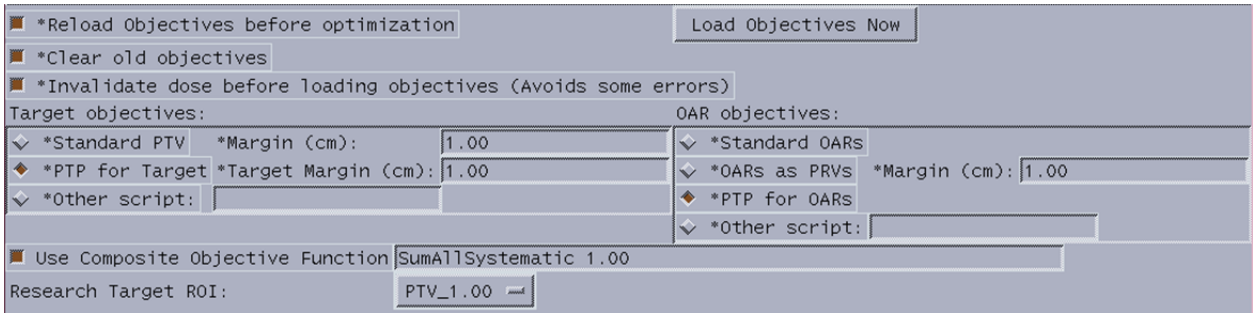

Figure 12: Objective definition GUI. The GUI gives options for selecting the target and OAR objectives to be used during optimization.

As each objective is independent, they must be combined to provide a total composite objective. The most basic composite objective is SumAll which simply sums the scores and gradient matrices for each objective. This is the default built-in composite objective and is used whenever no research objectives are used. Whenever research objective functions are used, a

research composite objective function must be used. This is allowed as a parameter, but in all cases, the research composite objective SumAllSystematic is used.

PTP optimization requires information about the uncertainty distributions to be used in the optimization. For random uncertainty, a toggle option is used to determine if fluence convolution is to be used during optimization as shown in Figure 13. If this toggle option is enabled, the user specifies the sigma of the random uncertainty distribution. For simplicity of this study, the distribution random uncertainty is required to be Gaussian with uncertainty equal in all dimensions. This requirement allows random uncertainty to be implemented by convolving the fluence array with a 2D Gaussian of equal width in all dimensions. This requirement may be relaxed by generating a 2D projection of the 3D probability density function of random uncertainty and convolving each beam's fluence with the resultant kernel.

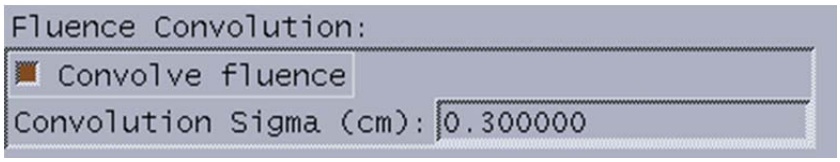

Figure 13: GUI component to specify parameters of random uncertainty. A toggle box to enable convolution and specify the sigma of the random distribution are given.

Systematic PTP requires both the distribution of systematic uncertainty and the number of systematic offsets to be sampled from the distribution. The GUI component shown in Figure 14 allows for the parameters of systematic uncertainty to be specified. The sigma of the systematic uncertainty is required to be uniform in all dimensions, though this too can be relaxed and specified as independent sigmas in each dimension. The functionality to allow this is implemented in the underlying scripting, but is not used for this study. The user specifies a number of systematic offsets as well as a random seed to determine the list of systematic offsets. Systematic offsets are handled by a ShiftListManager plugin for this purpose. These parameters

are passed to the ShiftListManager and a list of shifts is generated. Pseudo-random sampling is used to generate the list of systematic offsets. Pseudo-random sampling uses a mathematical function which generates numbers which appear to be random. This function uses a parameter called a seed which is modified each time a number is sampled. By allowing a user specified random seed, a reproducible set of systematic offsets can be generated, which allows for the entire optimization process to be reproduced. The ShiftListManager generates a list of systematic offsets by setting the random seed, and sampling independently the X, Y, and Z values of each offset. The plugin allows for the research objectives to query the number of offsets and to obtain the value of a selected shift.

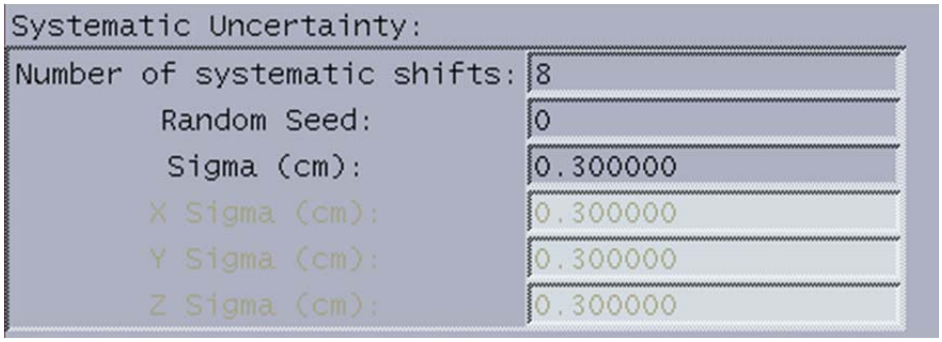

Figure 14: GUI component for systematic uncertainty. The number of shifts, random seed, and systematic sigma may be specified in this component. Future options of independent X,Y and Z sigmas are present but disabled in this version.

Automation of the initial PTP planning (GUI component shown in Figure 15) process allows for varying the number of systematic offsets and random seed. A different random seed produces a different list of systematic shifts. Changing seeds is used to determine the required number of systematics. During the optimization process used elsewhere in this study, the random seed is zero and does not change. The number of systematics is incremented in this automation step by doubling the number of systematics from the starting value (16) to the maximum value (128) and uses the final fluence from the previous optimization as the starting fluence for each

successive optimization. In cases where the random seed changed, the final fluence from the starting random seed (zero) is used as the initial fluence in the next count of systematic offsets.

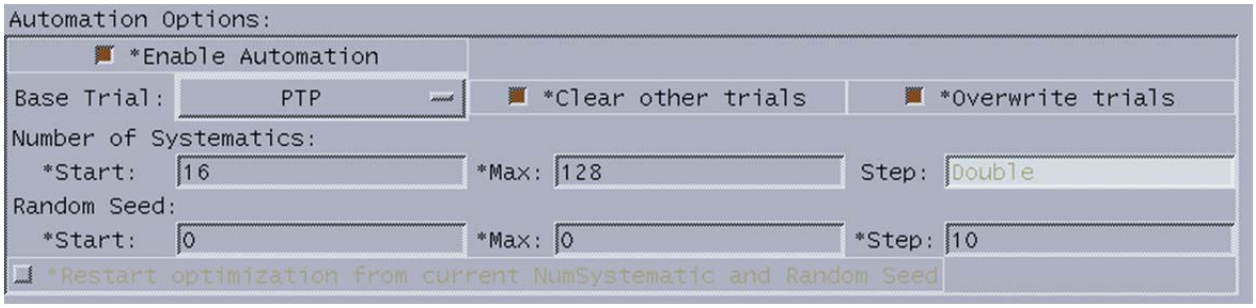

Figure 15: PTP Automation GUI. This component allows for specifying the range of nSys and random seed values.

The subsections of the study are automated (Figure 16) to incrementally follow each other. The optimized fluence from the initial PTP optimization is used as the initial fluence for the weight-adjustment process. The achieved coverage probability from the weight adjustment process is used as a parameter into the margin adjustment process. Each of these processes is implemented as separate GUI components. A separate coverage GUI is designed to calculate the coverage probability and all output metrics. Parameters set in the coverage GUI are used each time coverage probability is calculated.

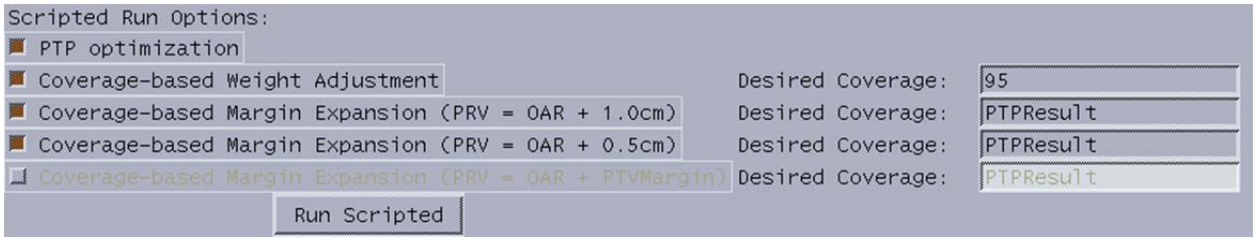

Figure 16: Scripted optimization GUI. Each selection is followed sequentially. The desired coverage probability is specified for the coverage-based weight adjustment process, and the coverage-based margin expansion process uses the final coverage probability from the CBWA plan.

The coverage-based weight adjustment (CBWA) module (Figure 17) accepts parameters for lower and upper weight bounds (default 0-100) and a desired coverage probability (initially 95%). Convergence criteria for the adjustment process are a minimum change in weight

(default=1) and the tolerance of deviation from the desired coverage probability (0.5%). When achieved coverage probability is compared to desired coverage probability during the binary search process, if the difference is less than the tolerance value, an acceptable weight is found. If the change in weight from one iteration to the next is less than the minimum change, the process stops and reports the achieved coverage probability which may have a difference greater than the tolerance range. If the weight used for the final achieved coverage probability is less than 1, the desired coverage probability is reduced by 5% and the coverage-based weight adjustment process is started again. As weights are specified as integral values, a weight less than 1 indicates an objective with zero weight which would be ignored during optimization.

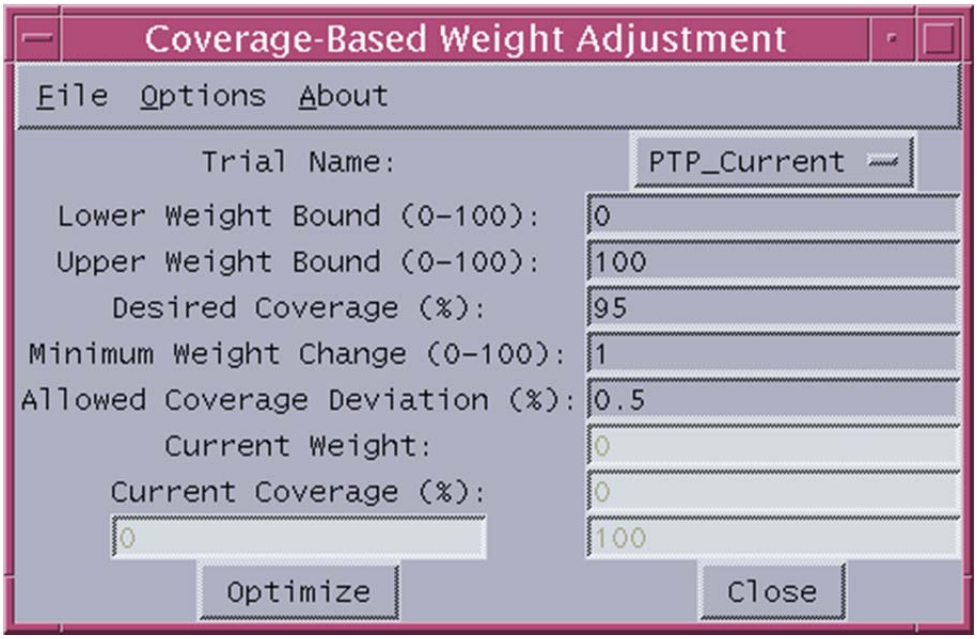

Figure 17: Coverage-based weight adjustment module. This GUI accepts parameters for the weight bounds and desired coverage probability to adjust the PTP rectum and bladder weights to produce the desired coverage probability. Convergence criteria of minimum change in objective weight and allowed deviation from the desired coverage probability are specified.

The coverage-based margin expansion (CBME) module (Figure 18) uses the final achieved coverage probability from the CBWA module as the desired coverage probability during the expansion process. Like the CBWA module, the CBME module requires bounds and

convergence criteria. The initial upper and lower margin bounds are 0 cm to 1 cm. Convergence criteria are a change in margin of less than 0.05 cm or a change in coverage probability of less than 0.5%. The CBME module also requires the name of the ROI to be expanded – for most cases, the CTV – and the name of a new ROI to hold the expanded ROI. The expanded ROI is used as the target structure in the optimization functions.

Figure 18: Coverage-based margin expansion module. This GUI accepts parameters for the CTV-to-PTV margin bounds and desired coverage probability. Convergence criteria of minimum change in objective weight and allowed deviation from the desired coverage probability are specified.

The coverage GUI (Figure 19) specifies the parameters used in coverage probability calculation. The primary coverage probability metric is set which is used in the iterative coverage-based modules. In this study, the primary metric is the coverage probability of the CTV D_{98}>7920cGy objective. Additional options to specify the dose grid size used for coverage probability calculation as well as the option to use fluence convolution are present. Fluence convolution is enabled to include random uncertainty in the coverage probability calculations. In

the coverage data objective developed by Gordon *et al.* (Gordon *et al.*, 2010; Gordon and Siebers, 2009) coverage probability is calculated by shifting the dose grid by integral numbers of voxels. Using the optimization dose grid of 0.4×0.4×0.4 cm^3 results in only 123 offsets in the grid-based coverage probability calculation. A dose grid of 0.2×0.2×0.2 cm^3 is used during coverage probability calculation to increase the number of offsets to 919 in the grid-based calculation. Grid sizes of 0.4×0.4×0.4 cm^3 are supported using the radial-based coverage probability calculation, but the radial-based calculation takes substantially longer to compute (~1 hour) compared to the much faster grid-based calculation (~5 minutes). The additional metrics computed are specified in a list (Figure 20) which allows for coverage probability calculations, DVCMs, and PDVHs for each structure. This list can be saved and loaded to ensure identical metrics are used for all optimizations.

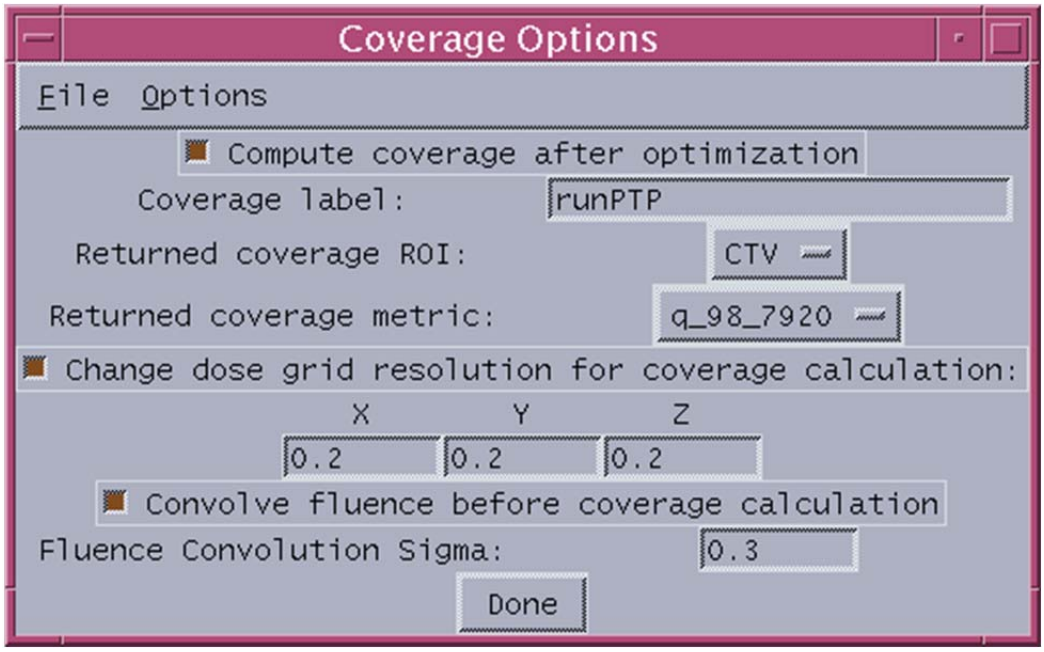

Figure 19: Coverage calculation GUI. The metric used for coverage-based optimization is specified with the size of the dose grid for coverage probability calcuation. To include random uncertainty in coverage probability calculation, fluence is convolved with the specified fluence convolution sigma.

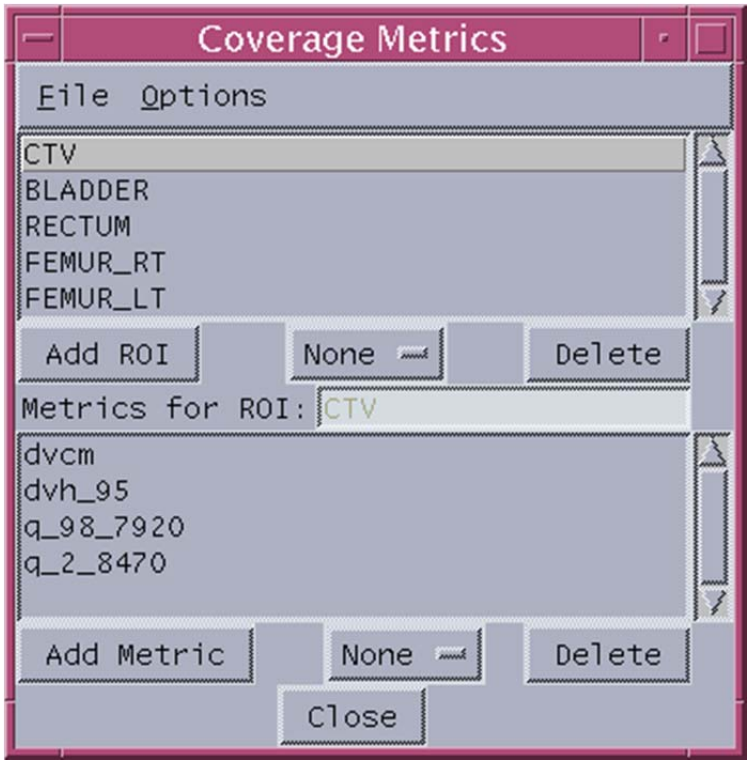

Figure 20: Coverage metric GUI. Structures to compute coverage probability on are specified along with specific metrics to output including dose-volume coverage maps (dvcm), 95% probability dose-volume histogram (dvh_95) and coverage probability (q_98_7920 and q_2_8470).

The GUI allows for saving and loading of a file containing all of the parameters for the entire study. Upon starting the GUI, a default parameter list can be loaded. For this study, the final parameter list is saved as the default parameter list. To reduce time required for computations, multiple patients are analyzed simultaneously. Two x86 Solaris machines with 8 CPUs each are used for computation. Eight patients at a time on each machine are loaded and optimized using the default parameters in the GUI.

After all patients are completed, PDVH curves are combined for all structures and for each planning method. A shell script is used to build the comparison plots for each patient using Xmgrace for visualization. A default parameter file was used for each patient which specifies the data labels, line colors, and plot dimensions. A wrapper around this script allows for the planning

method label to be randomized for each patient. This wrapper randomly assigns the letter A or B to the PTP and margin-based plan. The solid line is always used for plan A and the dashed line is always used for plan B. The script outputs after processing a list indicating which method is represented by plan A or B in order to decode the randomization for final analysis.

DVCM and DVCDM plots are computed using MATLAB. A function is developed to read DVCM data and scale to a common map size. DVCDMs are generated by subtracting the margin-based DVCM from the PTP DVCM. All DVCM plots use a common color axis utilizing the full range of DVCM values (0 to 1) and DVCDM plots use the full range of DVCDM values (-1 to 1). An automated script is used to generate the plots for each patient, structure and method.

5.3 Results

The change in the standard deviation of coverage probability from 32 to 64 systematic offsets is 2.7%, $p<0.0001$. The change in the standard deviation of coverage probability from 64 systematic offsets to 128 systematic offsets is 0.6%, $p=0.16$. Since the difference is no longer statistically significant, 128 systematic offsets is accepted as the minimum number of systematics required and used throughout the rest of this study. The number of systematic shifts may be increased past 128, but will not produce a significantly different coverage probability and will only increase computational time. Optimizations using 128 systematic shifts take approximately 8 hours. Using 256 systematic shifts, the computational time is approximately 16 hours.

5.3.1 Dose-Volume Coverage Maps (DVCM)

DVCMs for all patients are shown in Appendix X. For the target structure, DVCMs were all very similar. This is expected since plans were driven to produce similar target coverage

probability. For all patients and planning methods, the target has 100% coverage probability until very close to the plan objectives and then rapidly falls off above the plan objectives. This is expected due to the plan objectives trying to drive a uniform dose to the target with an upper and lower DVH objective.

Bladder DVCMs showed some difference between methods. PTP-based plans showed a higher coverage probability of the bladder at points below the optimization objectives. In all plans, PTP-based plans have increased coverage probability in the low dose regions. For the dose near the objectives, PTP-based plans show increased coverage probability up to the objective, but show decreased coverage probability once the dose exceeds the objective. For both PTP and margin-based planning, dose approaches the bladder 8470 cGy max dose constraint.

Rectum DVCMs also showed difference between methods. Similar to the bladder, PTP plans showed a higher coverage probability of the rectum in the low dose regions. As the dose approached the objective points, PTP-based plans showed a lower coverage probability. For both PTP and margin-based planning, dose approaches the rectum 8470cGy max dose constraint.

For the left and right femur, the coverage probability is very low for both planning methods. For the 3500cGy to <50% objective, 0% coverage probability was achieved for all patients, plans, and methods. For the 5000cGy max dose objective, a small tail approached the objective on all plans. The size of this tail is generally larger for PTP-based plans than margin-based plans. For the left femur the tail reached the objective on 21 out of 28 plans for PTP-based planning, and 12 out of 28 plans for margin-based planning. For the right femur the tail reached the objective on 22 out of 28 plans for PTP-based planning, and 12 out of 28 plans for margin-based planning.

5.3.2 Dose-Volume Coverage Difference Maps (DVCDMs)

Target DVCDMs show a very small band of coverage change which would be well below the difference caused by any uncertainty in dose. This is expected due to the goal of matching plan coverage.

DVCDMs look significantly different for the OARs. Without any objective to increase dose, the coverage varies below the objectives. For these DVCDMs we define 3 regions as shown in Figure 21: Region A is the region completely below the plan objectives, Region B is the region completely above the plan objectives, and Region C is the region near the plan objectives. Coverage differences in Region A are unimportant as it is below the plan objectives and the optimizer has no objective to drive the dose down in these areas. Coverage differences in Region B are important as this is where the optimizer failed to reduce the dose below the plan objectives. Coverage in Region C shows the objective tradeoff as the optimizer finds a solution.

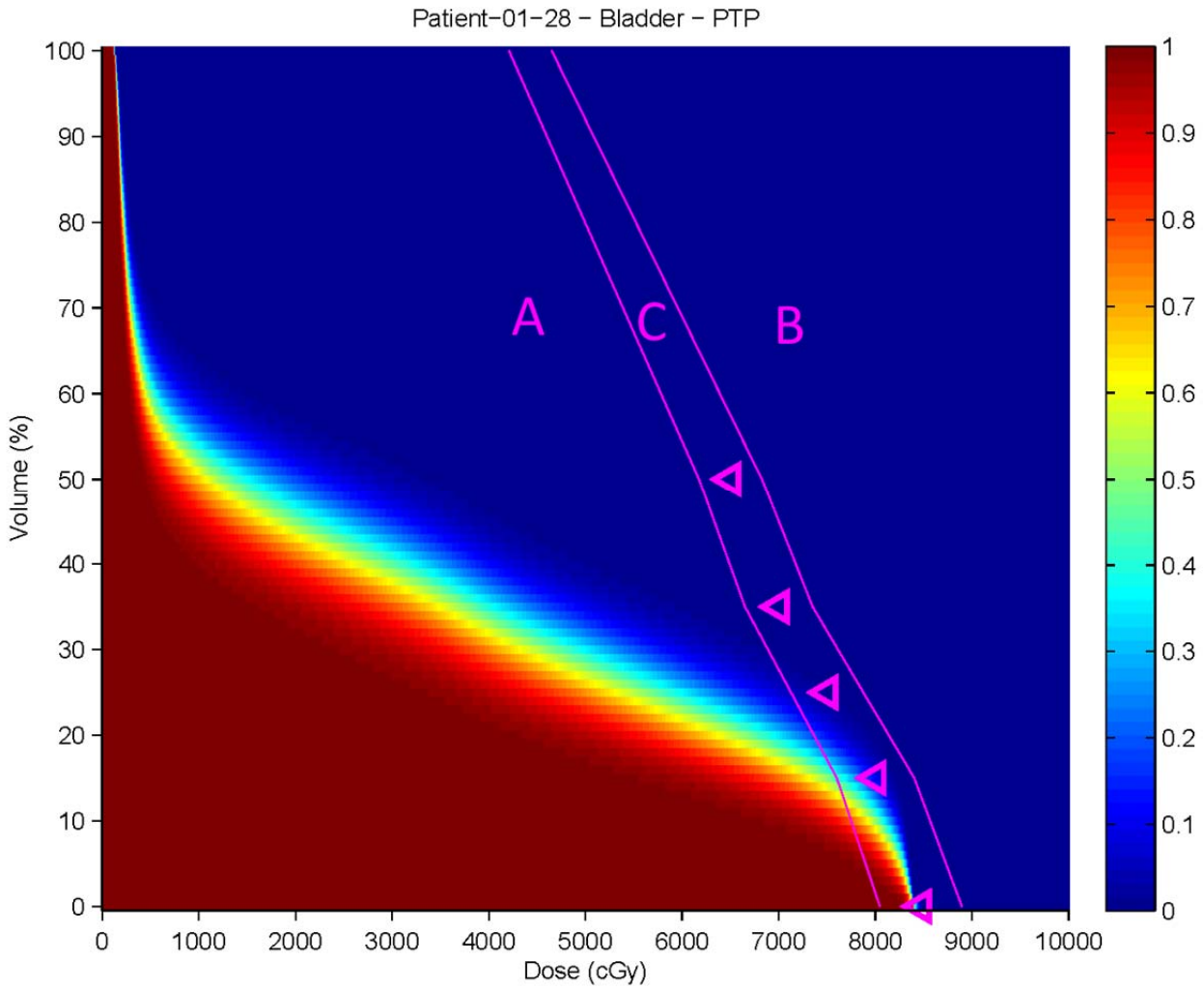

Figure 21: Regions of a DVCM. Region A is below plan objectives, Region B is above plan objectives and Region C is near plan objectives.

For the bladder DVCDM, PTP-based plans show an increased coverage in Region A. For Region B, some plans show a slight reduction in coverage, but generally both plans have no coverage in this region. For region C, there is no noticeable trend in coverage change. Some PTP-based plans have higher and others have lower coverage.

For the rectum DVCMs, PTP-based plans show an increased coverage in Region A. For Region B, PTP-based plans generally show a reduction in coverage, though for some patients, both plans are below criteria. For Region C, PTP-based plans generally show a reduction in coverage, though for some patients some slight increases occur.

For the left and right femur, all PTP-based plans show an increase in coverage. This is predominantly in Region A where both plans are substantially below the plan criteria. Some increase in coverage is noted in Region C as a tradeoff for lower dose in other structures. Neither plan has coverage in Region B.

5.3.3 Coverage Probability

Target coverage probability is generally the same for each patient due to the design of the study. On average the coverage probability achieved by PTP-based plans is 90% +/- 5% and the average coverage probability for margin-based plans is 91% +/- 5%. A paired t-test indicates that this is not significant (p=0.1697). For the margin-based plan, the average margin required to match the PTP plan is 0.6 cm.

When compared to margin-based plans, PTP plans reduced the average coverage probability for the rectum D_{35}=65Gy objective by 17% (p=0.010), 23% for the D_{25}=70Gy (p=0.0001), and 27% for the D_{15}=75Gy objective (p<0.0001). The average coverage probability of the bladder increased 2% for the D_{50}=65Gy objective (p=0.0005), increased 3% for the D_{35}=70Gy objective (p=0.0157), decreased 6% for the D_{15}=80Gy objective (p=0.0146). Left femur coverage probability increased 4% for the D_{max}=50Gy objective (p=0.0078) and the right femur increased 6% for the D_{max}=50Gy objective (p=0.0024). None of the other objectives showed significant changes.

5.3.4 Probability Dose-Volume Histograms (PDVH)

Target PDVH curves were very similar between both methods. Again, this is expected since the both plans were driven to produce the same target coverage probability. PDVHs for all

patients are shown in Appendix X. For both methods, the PDVH curve is 100% until nearly the D98 objective after which the dose drops off sharply to D2 objective.

For OAR structures, PDVHs tend to show that PTP plans have higher volumes receiving dose below the plan objectives and lower volumes receiving dose above the plan objectives. The rectum specifically shows a noticeable decrease in volume near the planning objectives for the PTP plans. The bladder shows a higher overall volume receiving dose but is generally below the objectives for both plans. PTP shows higher volumes receiving dose for both left and right femur, but this is well below the plan objectives for both methods.

5.3.5 Physician Assessment

Plots were generated to be presented for physician assessment. The process of generated these plots involved the output of Probability Dose-Volume Histograms and static Dose-Volume Histograms from the treatment planning system. Before presenting these to the physician, the plans are randomized to remove any bias from the assessment. Randomly, plans for each patient were assigned a letter of A or B. On the plots, curves from plan A are displayed as a solid line while curves from plan B are displayed as a dashed line. Curves were generated and displayed for the CTV, bladder, rectum, left femur and right femur structures. Additionally, markers were placed on the graph to indicate the planning objectives used during optimization. A single plot was produced for each patient for both PDVHs and static DVHs.

Initially, Probability Dose-Volume Histograms (PDVHs) were presented to a physician. The initial response was that none of the plans from either method was acceptable. After further discussion with the physician, it was determined that plans were deemed unsatisfactory due to a high rectal dose on the majority of plans. The RTOG-0126 protocol allows for rectal dose to reach these limits, but this conflicted with the physician's personal protocol for prostate

radiotherapy. Additionally, since PDVHs show a greater dose to critical structures, the plan was further from acceptable limits. The physician was then asked to choose which plan would be preferred if a choice had to be made. Using the PDVHs, the physician would choose the PTP plan over the margin plan for 21 patients and would prefer the margin plan for 7 patients.

The physician was then presented with static DVH plots. For these plots, it was assumed that there was no margin on the critical structures (PRV = OAR) and the PTV expansion was CTV+0.3 cm posteriorly and CTV+0.7 cm in all other directions. These values match the prostate IMRT protocol used by the protocol typically used by that physician. Static DVHs were generated using these structures, but planning and optimization was not repeated. Using these definitions, the physician again found the majority of plans to be unacceptable. After discussions, the physician selected the preferred plan even if neither was acceptable. The PTP plan was chosen for 25 patients while the margin plan was chosen for 3 patients.

An additional physician was sought that uses the RTOG-0126 protocol on a regular basis. This physician reviewed the plans using the same static DVHs presented to the first physician and reported that the PTP plan is preferred for 24 patients while the margin is preferred for 4 patients. For 23 patients, both physicians preferred the PTP plan. For 2 patients, both physicians preferred the margin-based plan. For 3 patients, there was not a consensus on the preferred plan.

5.4 Discussion

In the plan assessment stage, both static DVHs and PDVHs were used. It is believed that PDVHs present a more realistic view of plan quality. In a static DVH, the curves indicate the dose delivered in a single idealized patient setup. To incorporate uncertainty into the static DVHs, the physician looks at a curve representing the PTV as representative of the CTV under uncertainty while the critical structures are only displayed in a purely static idealized case. In a

PDVH, the curves represent the expected DVH for a specified coverage probability. For the curves demonstrated in this work, the probability of CTV doses exceeding the PDVH is 95% and the probability of the dose to the critical structures being lower than the PDVH is 95%. Therefore, it is expected that in 95% of cases, the plan will perform better than the displayed curves.

Use of PDVHs in physician approval of plans will incorporate uncertainty into the decision making process. This may initially raise concerns as the dose displayed for critical structures is typically much greater than displayed on a static DVH, however, these curves are generated from the same underlying dose distribution.

For two patients (Patients 13 & 15) visual artifacts were observed in the DVCMs. These visual artifacts appeared as “squiggles” in the data as shown in Figure 22. This was determined to be a result of low resolution calculation of the DVCMs. The original DVCM data for this study was computed using a grid method which used rigid shifts in the dose grid to compute coverage probability. This produced a very fast calculation (~5 min) but sampling was restricted to the size and dimensions of the dose grid. An alternate method of calculating this is radial mode. In this mode, samples are chosen radially (In this study, at 10 degree increments) and at a given step along each ray (0.5mm). This method takes much longer (~2 hours) but produces a much smoother result similar to Figure 23. Graphically these results appear fairly different, however, when looking at the difference between the two shown in Figure 24, the differences are relatively small.

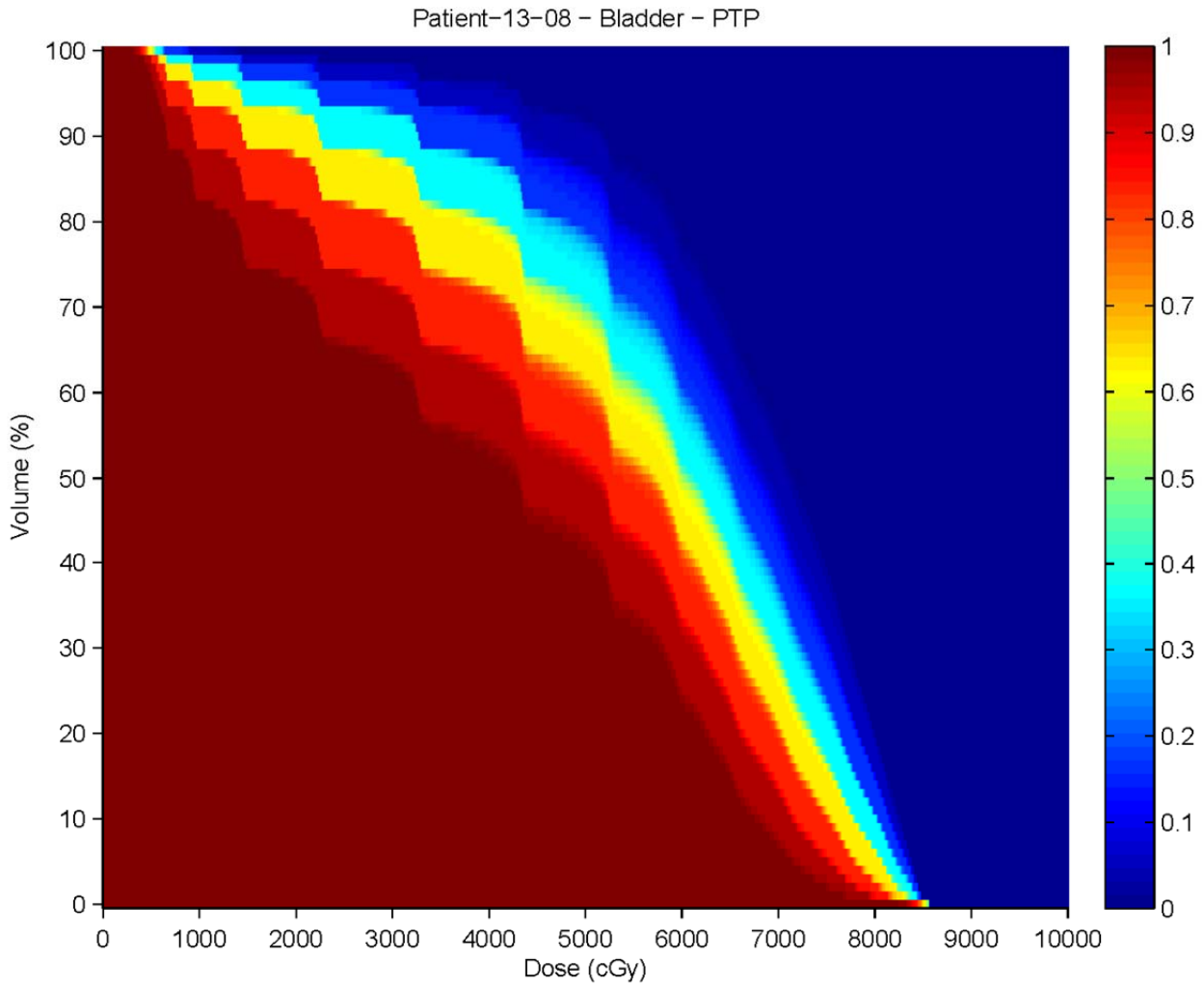

Figure 22: DVCM "Squiggles". These are produced due to the size of the dose grid used to calculate coverage probability in grid mode.

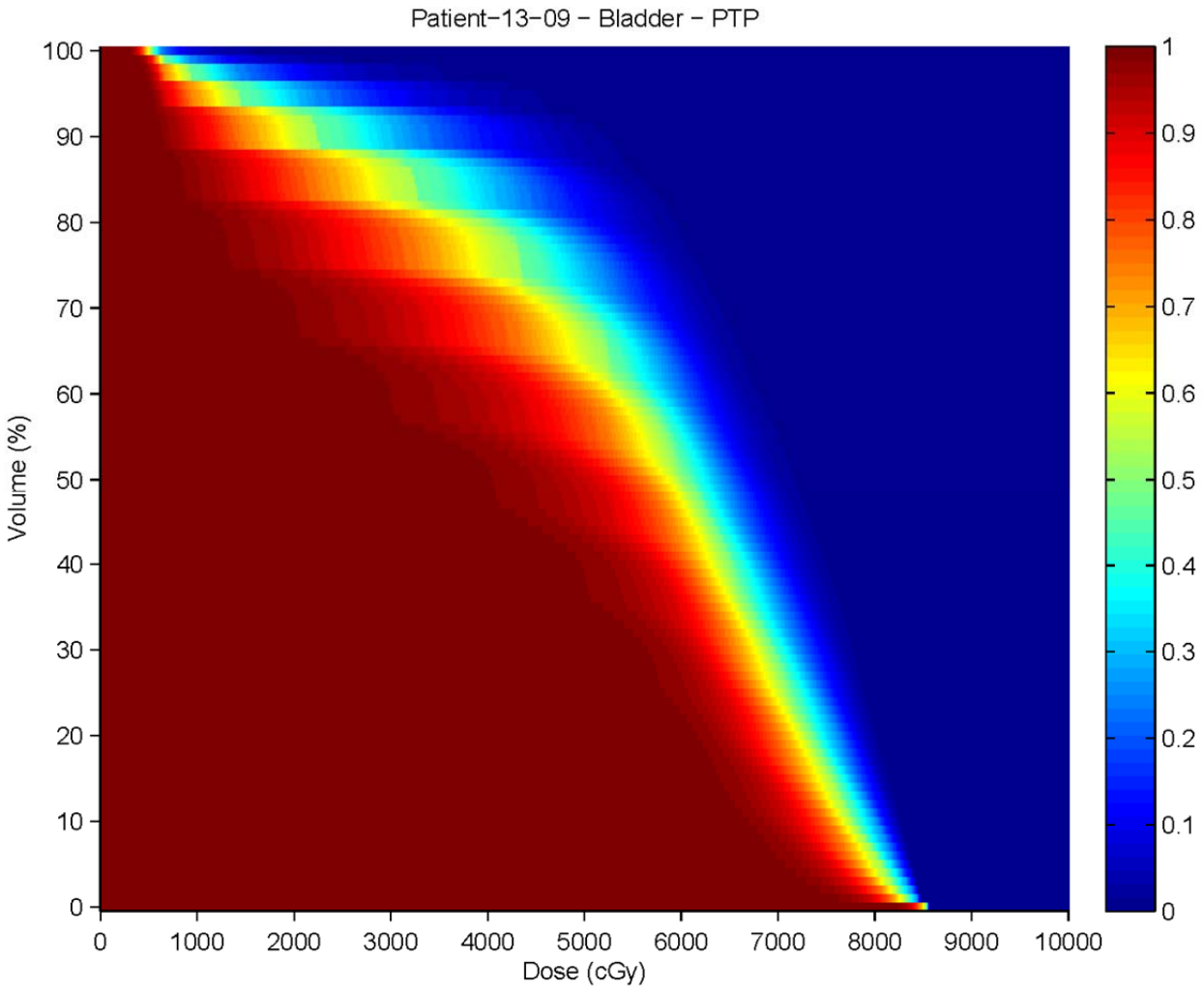

Figure 23: Smoothed DVCM using radial mode. In radial mode, the distribution of coverage probability values is sampled more accurately at the cost of significant computational time. The smoothed DVCM shows an image with less stepped transitions between coverage levels.

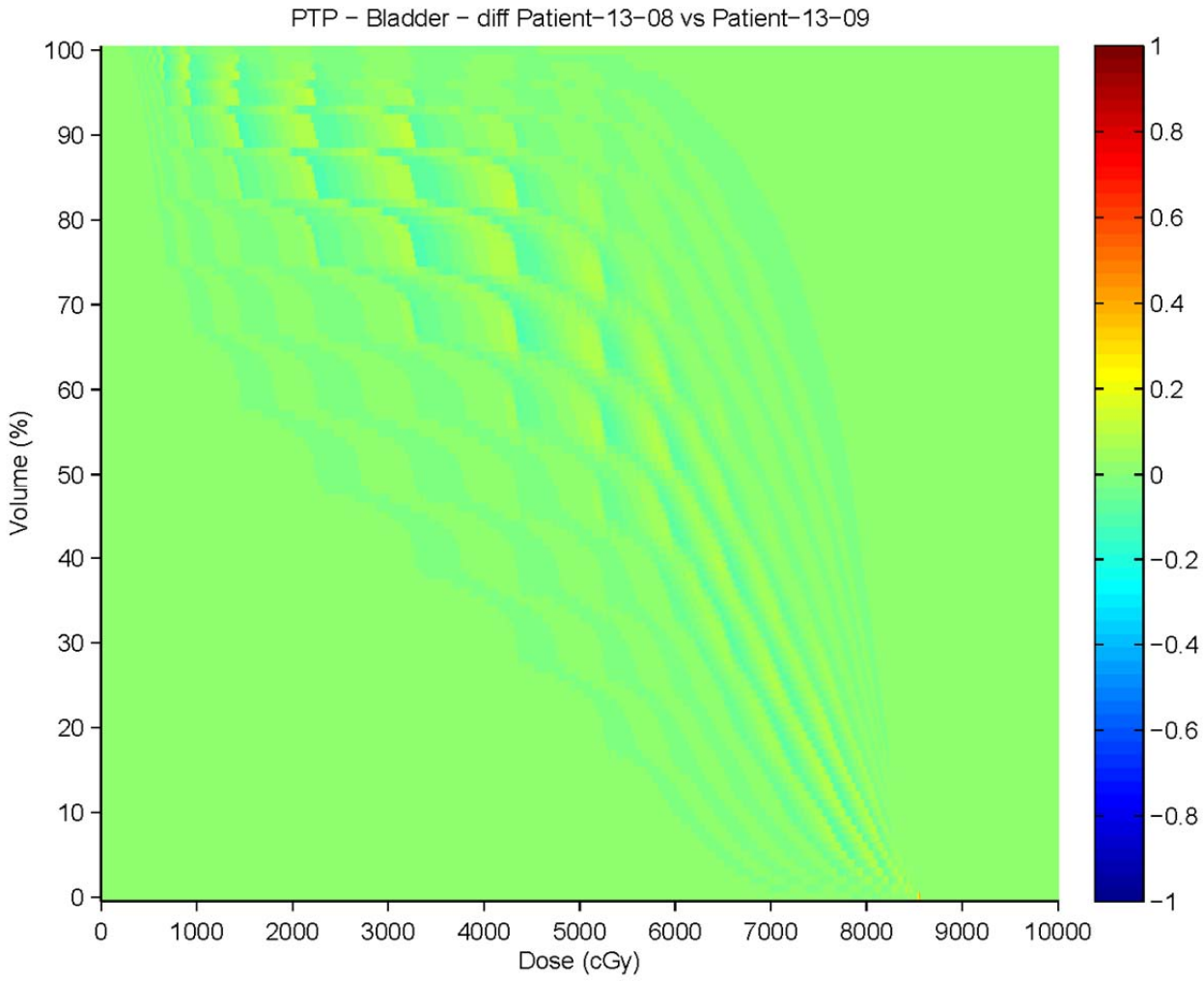

Figure 24: Difference between DVCM computation modes

Pinnacle loads every trial into memory when the plan is loaded. These trials stay loaded in memory until Pinnacle is closed. This is normally not of any concern, however, when a large number of trials are maintained in a Pinnacle session, the memory overhead becomes very large. A single trial loaded into Pinnacle may only require on the order of 300MB, but when more than 10 trials are kept in memory, the 32-bit memory limit of approximately 4GB is exceeded.

In this study, random sampling from a Gaussian PDF is used. It is assumed that with a sufficient number of samples, the distribution will be well characterized. In the case of large numbers, each random sample has equal weight as less likely samples should occur less

frequently. Alternatives to this are quasi-random sampling and weighted sampling. Quasi-random sampling attempts to more uniformly sample the distribution to better characterize it with fewer samples. Quasi-random samples, like random samples, have equal weight. Weighted sampling (similar to MIGA) chooses a number of fixed offsets and assigns a weight to each based upon their likelihood. In weighted sampling, samples close to the expected value will have higher weights, while samples further from the expected value will have reduced weights.

In several cases, it was noted that the ROIs for the OARs overlapped the CTV ROI. In these cases, a conflict for objectives was observed. To resolve objective conflicts, the OARs were redefined as the original OAR with the target volume excluded. This was achieved in Pinnacle by expanding by a zero margin an ROI with the OAR as the source and excluding the interior of the target.

5.4.1 Other Attempted Methods

The original attempt at implementing systematic uncertainty into treatment planning involved using an external application linked to Pinnacle via scripting. This external application used scripts to obtain the patient anatomy, compensator matrix, and beam configuration. Using this information, objectives were defined for optimization. These objectives were limited to dose-based and dose-volume based objectives.

The method used for optimization in the external application involved directly modifying the fluence matrix. A flow chart describing this method is shown in Figure 25. For each sampled offset, the plan was optimized for a single iteration. After all offsets are optimized, the fluence was averaged to produce the updated fluence. This fluence was again optimized for a single iteration for each offset, and the process was repeated until convergence. The basic function of this is

$$\omega_j = \frac{1}{nSys} \sum_{s}^{nSys} \omega_{j,s}$$

This method was eventually abandoned due to difficulties in modification of the original external IMRT optimizer. The most prevalent of issues being that the state of the intensity and dose matrices were not consistently maintained throughout code execution. While for a static optimization, this had no effect, when attempting to update the intensity, the incorrect matrices led to incorrect updates to the fluence. Additionally, this external code was originally written before plugins had been developed for Pinnacle. Directly interfacing with a clinically approved treatment planning system allows for a more reliable solution without recreating an existing implementation.

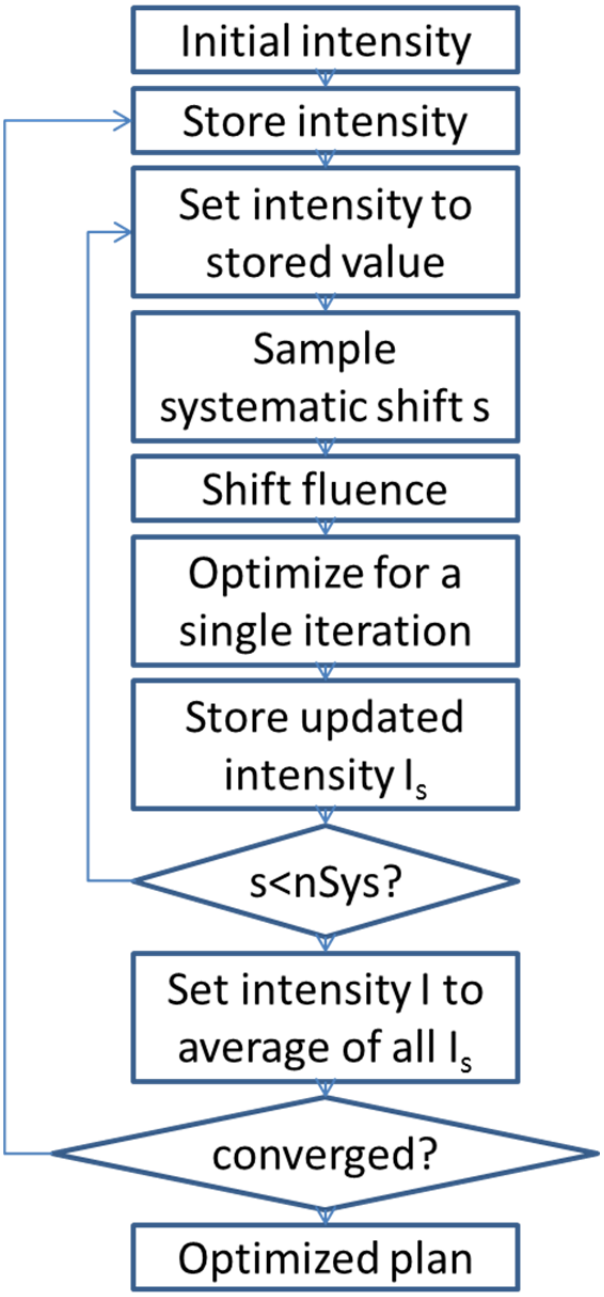

Figure 25: Direct fluence PTP

Later, this method was incorporated into a Pinnacle plugin. Unfortunately, due to the intense computational requirements (approximately 2 weeks per patient), this too was abandoned in search of a less time consuming method.

5.5 Conclusions

This chapter describes the implementation a method for including random and systematic patient setup uncertainty into the treatment planning process. Generally, PTP results in a decrease in dose to normal tissues (especially the rectum) while maintaining the same coverage probability for the target when compared to margin-based plans. Physician assessment indicates preference of PTP plans due to the ability to reduce rectal dose. PTP may result in the ability to remove CTV-to-PTV margins and optimize directly on the CTV.

New methods of plan analysis are presented in this study. The use of DVCMs and DVCDMs as an assessment and comparison metric allows for visual display of the effects of uncertainty on a treatment plan. Physician assessment of plans allows for demonstration of clinical feasibility of treatment plans generated using PTP.

6 Conclusions and future directions

Methods for incorporating random and systematic uncertainty into treatment planning using PTP have been implemented and tested using a commercial treatment planning system. Each method presented in this dissertation shows the ability to reduce normal tissue dose while maintaining a therapeutic dose of radiation to the target. For both methods, plans producing similar target coverage probability have been developed using a margin-based approach for comparison. These methods have potential to remove the need for a CTV-to-PTV margin in treatment planning.

For random only PTP plans, PTP and margin plans both show similar dose to the target structure, though PTP plans tend to have a slightly lower dose to the target structure. Compared to margin-based plans, PTP plans show a significant decrease in dose to the local normal tissue structure. Mean dose for OARs is decreased using PTP methods. Compared to margin-based plans, PTP plans have similar TCP but a lower NTCP for critical structures resulting in an overall increase in P+.

Physician assessment of margin-based and random-only PTP plans shows that for 75% of patients, PTP plans are preferred over margin-based plans. For 7% of the patients, the margin-based plan is preferred and no plan is preferred for 18% of patients.

For PTP including both random and systematic uncertainty, PTP and optimized margin plans produce similar target coverage probability. PTP plans can be generated which meet a specified coverage probability goal and margin-based plans can be optimized to meet similar

achieved coverage probability. Compared to margin-based plans, PTP plans reduce the coverage probability of high dose rectal objectives. PTP plans generally show a decrease in coverage probability near the plan objectives while increasing dose in unconstrained regions.

Physician assessment of PTP plans generated using random and systematic uncertainty indicates that PTP plans are generally preferred. For 71% of patients, PTP plans are preferred over margin-based plans. Margin-based plans are preferred for 7% of patients, while physicians indicate mixed preference for 21% of patients.

The work presented here approximates both random and systematic uncertainty distributions as isotropic Gaussian distributions. The framework is largely in place to relax this restriction. Random uncertainty is implemented via convolution of a 2D Gaussian kernel with the 2D fluence matrix of each beam. An arbitrary 3D distribution of uncertainty may be used by generating a 3D kernel from the distribution and projecting it on the 2D plane of the fluence matrix. Systematic uncertainties are handled by generating a list of shifts. These shifts are currently generated by sampling a shift in each dimension from a 1D Gaussian distribution of equal width for each dimension. This can be trivially relaxed by allowing a different width of the Gaussian distribution for each dimension. A process for doing this is already implemented in the ShiftListManager but isotropic Gaussian distributions are used here for simplicity. This can be further relaxed by allowing sampling from any specified distribution. Rigid shifts in patient setup position are used in this study, but future studies may extend this to the use of deformed anatomy. In the case of deformed anatomy, multiple patient images can be used instead of rigid systematic shifts.

In the current implementation, optimization incorporating systematic uncertainty requires substantial computational time. Fortunately, the optimization method here is easily parallelized.

If multiple computers (or CPUs) are available, the processing of systematic shifts can be split such that a portion of the processing is done on several independent CPUs. Splitting of the calculations is possible since the computation of each individual systematic shift is independent of other systematic shifts. In theory, using twice as many CPUs should result in half the computational time (ignoring overhead). Allowing the process to use as many CPUs as the number of systematic shifts used in optimization should result in the optimization requiring the same amount of time as a standard optimization.

7 Extensions to other projects

Many software modules have been described in this dissertation. Each of these software modules were developed to further the study described. Fortunately, these modules also have use in other studies conducted at this university. This chapter briefly describes two specific projects which used components of the software developed for this work.

A plugin which modifies the fluence during dose calculation is used in the studies described in the chapters above. The primary use in the chapters above is to convolve the fluence with the random uncertainty distribution during IMRT optimization. A similar implementation, prior to the Pinnacle hook to modify the fluence distribution, is to convolve the intensity matrix with a Gaussian distribution. Unfortunately, the intensity convolution method requires slight adjustments to the width of the jaws to account for the widening of the fluence distribution. The intensity convolution method is used in Gordon *et al.* (Gordon *et al.*, 2007) to simulate the effect of random and systematic setup errors on the dose distribution and compare to margin formulas. Gordon's study of 27 patients convolved the intensity matrix to include random uncertainty in simulation and used 50 simulated systematic shifts to include systematic uncertainty. The results generally show that margin formulas are pessimistic and smaller margins can be used (Gordon *et al.*, 2007).

The IncidentFluenceInterface can additionally be used to input arbitrary fluence matrices into the dose calculation process. The ability to save and load fluences in the plugin allows for modification of the fluence outside of Pinnacle. In the study by Waghorn *et al.* (Waghorn *et al.*,

2010) the IncidentFluenceInterface plugin is used to export the fluence for each beam to a file. The file is used as a parameter into Matlab code executed on a different computer which adapts the fluence to the motion tracks generated by Calypso – an implanted seed-based localization system. The adapted fluence is then loaded into Pinnacle for dose calculation. The study shows with a Gamma pass rate of 98.3% +/- 0.7% that the motion-encoded fluence maps agree well with film measurement of the Calypso tracks.

References

Balter J M, Brock K K, Lam K L, Tatro D, Dawson L A, McShan D L and Ten Haken R K 2005 Evaluating the influence of setup uncertainties on treatment planning for focal liver tumors *Int J Radiat Oncol Biol Phys* **63** 610-4

Baum C, Alber M, Birkner M and Nusslin F 2004 Treatment simulation approaches for the estimation of the distributions of treatment quality parameters generated by geometrical uncertainties *Phys Med Biol* **49** 5475-88

Baum C, Alber M, Birkner M and Nusslin F 2006 Robust treatment planning for intensity modulated radiotherapy of prostate cancer based on coverage probabilities *Radiother Oncol* **78** 27-35

Beckham W A, Keall P J and Siebers J V 2002 A fluence-convolution method to calculate radiation therapy dose distributions that incorporate random set-up error *Phys Med Biol* **47** 3465-73

Bel A, Vos P H, Rodrigus P T, Creutzberg C L, Visser A G, Stroom J C and Lebesque J V 1996 High-precision prostate cancer irradiation by clinical application of an offline patient setup verification procedure, using portal imaging *Int J Radiat Oncol Biol Phys* **35** 321-32

Birkner M, Yan D, Alber M, Liang J and Nusslin F 2003 Adapting inverse planning to patient and organ geometrical variation: algorithm and implementation *Med Phys* **30** 2822-31

Craig T, Battista J and Van Dyk J 2003 Limitations of a convolution method for modeling geometric uncertainties in radiation therapy. II. The effect of a finite number of fractions *Med Phys* **30** 2012-20

Craig T, Wong E, Bauman G, Battista J and Van Dyk J 2005 Impact of geometric uncertainties on evaluation of treatment techniques for prostate cancer *Int J Radiat Oncol Biol Phys* **62** 426-36

de Boer H C and Heijmen B J 2001 A protocol for the reduction of systematic patient setup errors with minimal portal imaging workload *Int J Radiat Oncol Biol Phys* **50** 1350-65

Delaney G, Jacob S, Featherstone C and Barton M 2005 The role of radiotherapy in cancer treatment: estimating optimal utilization from a review of evidence-based clinical guidelines *Cancer* **104** 1129-37

Gordon J J, Crimaldi A J, Hagan M, Moore J and Siebers J V 2007 Evaluation of clinical margins via simulation of patient setup errors in prostate IMRT treatment plans *Med Phys* **34** 202-14

Gordon J J, Sayah N, Weiss E and Siebers J V 2010 Coverage optimized planning: probabilistic treatment planning based on dose coverage histogram criteria *Med Phys* **37** 550-63

Gordon J J and Siebers J V 2008 Evaluation of dosimetric margins in prostate IMRT treatment plans *Med Phys* **35** 569-75

Gordon J J and Siebers J V 2009 Coverage-based treatment planning: optimizing the IMRT PTV to meet a CTV coverage criterion *Med Phys* **36** 961-73

International Commission on Radiation Units and Measurements. 1993 *Prescribing, recording, and reporting photon beam therapy* (Bethesda, MD: International Commission on Radiation Units and Measurements)

International Commission on Radiation Units and Measurements. 1999 *Prescribing, recording, and reporting photon beam therapy* (Bethesda, Md.: International Commission on Radiation Units and Measurements)

Jaffray D A, Siewerdsen J H, Wong J W and Martinez A A 2002 Flat-panel cone-beam computed tomography for image-guided radiation therapy *Int J Radiat Oncol Biol Phys* **53** 1337-49

Jemal A, Siegel R, Xu J and Ward E 2010 Cancer statistics, 2010 *CA Cancer J Clin* **60** 277-300

Lattanzi J, McNeeley S, Pinover W, Horwitz E, Das I, Schultheiss T E and Hanks G E 1999 A comparison of daily CT localization to a daily ultrasound-based system in prostate cancer *Int J Radiat Oncol Biol Phys* **43** 719-25

Litzenberg D, Dawson L A, Sandler H, Sanda M G, McShan D L, Ten Haken R K, Lam K L, Brock K K and Balter J M 2002 Daily prostate targeting using implanted radiopaque markers *Int J Radiat Oncol Biol Phys* **52** 699-703

Liu H H, Wang X, Dong L, Wu Q, Liao Z, Stevens C W, Guerrero T M, Komaki R, Cox J D and Mohan R 2004 Feasibility of sparing lung and other thoracic structures with intensity-modulated radiotherapy for non-small-cell lung cancer *Int J Radiat Oncol Biol Phys* **58** 1268-79

Lof J, Lind B K and Brahme A 1998 An adaptive control algorithm for optimization of intensity modulated radiotherapy considering uncertainties in beam profiles, patient set-up and internal organ motion *Phys Med Biol* **43** 1605-28

McCarter S D and Beckham W A 2000 Evaluation of the validity of a convolution method for incorporating tumour movement and set-up variations into the radiotherapy treatment planning system *Phys Med Biol* **45** 923-31

McShan D L, Kessler M L, Vineberg K and Fraass B A 2006 Inverse plan optimization accounting for random geometric uncertainties with a multiple instance geometry approximation (MIGA) *Med Phys* **33** 1510-21

Moore J A, Gordon J J, Anscher M S and Siebers J V 2009 Comparisons of treatment optimization directly incorporating random patient setup uncertainty with a margin-based approach *Med Phys* **36** 3880-90

Murshed H, Liu H H, Liao Z, Barker J L, Wang X, Tucker S L, Chandra A, Guerrero T, Stevens C, Chang J Y, Jeter M, Cox J D, Komaki R and Mohan R 2004 Dose and volume reduction for normal lung using intensity-modulated radiotherapy for advanced-stage non-small-cell lung cancer *Int J Radiat Oncol Biol Phys* **58** 1258-67

Schwarz M, Van der Geer J, Van Herk M, Lebesque J V, Mijnheer B J and Damen E M 2006 Impact of geometrical uncertainties on 3D CRT and IMRT dose distributions for lung cancer treatment *Int J Radiat Oncol Biol Phys* **65** 1260-9

Stroom J C, de Boer H C, Huizenga H and Visser A G 1999 Inclusion of geometrical uncertainties in radiotherapy treatment planning by means of coverage probability *Int J Radiat Oncol Biol Phys* **43** 905-19

Stroom J C, Olofsen-van Acht M J, Quint S, Seven M, de Hoog M, Creutzberg C L, de Boer H C and Visser A G 2000 On-line set-up corrections during radiotherapy of patients with gynecologic tumors *Int J Radiat Oncol Biol Phys* **46** 499-506

Unkelbach J and Oelfke U 2004 Inclusion of organ movements in IMRT treatment planning via inverse planning based on probability distributions *Phys Med Biol* **49** 4005-29

Unkelbach J and Oelfke U 2005a Incorporating organ movements in IMRT treatment planning for prostate cancer: minimizing uncertainties in the inverse planning process *Med Phys* **32** 2471-83

Unkelbach J and Oelfke U 2005b Incorporating organ movements in inverse planning: assessing dose uncertainties by Bayesian inference *Phys Med Biol* **50** 121-39

van Herk M 2004 Errors and margins in radiotherapy *Semin Radiat Oncol* **14** 52-64

van Herk M, Remeijer P and Lebesque J V 2002 Inclusion of geometric uncertainties in treatment plan evaluation *Int J Radiat Oncol Biol Phys* **52** 1407-22

van Herk M, Remeijer P, Rasch C and Lebesque J V 2000 The probability of correct target dosage: dose-population histograms for deriving treatment margins in radiotherapy *Int J Radiat Oncol Biol Phys* **47** 1121-35

Waghorn B J, Shah A P, Ngwa W, Meeks S L, Moore J A, Siebers J V and Langen K M 2010 A computational method for estimating the dosimetric effect of intra-fraction motion on step-and-shoot IMRT and compensator plans *Phys Med Biol* **55** 4187-202

Witte M G, van der Geer J, Schneider C, Lebesque J V, Alber M and van Herk M 2007 IMRT optimization including random and systematic geometric errors based on the expectation of TCP and NTCP *Med Phys* **34** 3544-55

Wu Q and Mohan R 2000 Algorithms and functionality of an intensity modulated radiotherapy optimization system *Med Phys* **27** 701-11

Yan D, Ziaja E, Jaffray D, Wong J, Brabbins D, Vicini F and Martinez A 1998 The use of adaptive radiation therapy to reduce setup error: a prospective clinical study *Int J Radiat Oncol Biol Phys* **41** 715-20

Yang J, Mageras G S, Spirou S V, Jackson A, Yorke E, Ling C C and Chui C S 2005 A new method of incorporating systematic uncertainties in intensity-modulated radiotherapy optimization *Med Phys* **32** 2567-79

Appendix I

Comparisons of Treatment Optimization Directly Incorporating Random Patient Setup Uncertainty with a Margin-based Approach

Joseph A. Moore

J. J. Gordon

Mitchell Anscher

Jeffrey V Siebers

Medical Physics 36(9), 2009

Comparisons of treatment optimization directly incorporating random patient setup uncertainty with a margin-based approach

Joseph A. Moore,[a] John J. Gordon, Mitchell S. Anscher, and Jeffrey V. Siebers
Department of Radiation Oncology, Virginia Commonwealth University, Richmond, Virginia 23298

(Received 27 December 2008; revised 17 June 2009; accepted for publication 22 June 2009; published 11 August 2009)

The purpose of this study is to incorporate the dosimetric effect of random patient positioning uncertainties directly into a commercial treatment planning system's IMRT plan optimization algorithm through probabilistic treatment planning (PTP) and compare coverage of this method with margin-based planning. In this work, PTP eliminates explicit margins and optimizes directly on the estimated integral treatment dose to determine optimal patient dose in the presence of setup uncertainties. Twenty-eight prostate patient plans adhering to the RTOG-0126 criteria are optimized using both margin-based and PTP methods. Only random errors are considered. For margin-based plans, the planning target volume is created by expanding the clinical target volume (CTV) by 2.1 mm to accommodate the simulated 3 mm random setup uncertainty. Random setup uncertainties are incorporated into IMRT dose evaluation by convolving each beam's incident fluence with a $\sigma=3$ mm Gaussian prior to dose calculation. PTP optimization uses the convolved fluence to estimate dose to ensure CTV coverage during plan optimization. PTP-based plans are compared to margin-based plans with equal CTV coverage in the presence of setup errors based on dose-volume metrics. The sensitivity of the optimized plans to patient-specific setup uncertainty variations is assessed by evaluating dose metrics for dose distributions corresponding to halving and doubling of the random setup uncertainty used in the optimization. Margin-based and PTP-based plans show similar target coverage. A physician review shows that PTP is preferred for 21 patients, margin-based plans are preferred in 2 patients, no preference is expressed for 1 patient, and both autogenerated plans are rejected for 4 patients. For the PTP-based plans, the average CTV receiving the prescription dose decreases by 0.5%, while the mean dose to the CTV increases by 0.7%. The CTV tumor control probability (TCP) is the same for both methods with the exception of one case in which PTP gave a slightly higher TCP. For critical structures that do not meet the optimization criteria, PTP shows a decrease in the volume receiving the maximum specified dose. PTP reduces local normal tissue volumes receiving the maximum dose on average by 48%. PTP results in lower mean dose to all critical structures for all plans. PTP results in a 2.5% increase in the probability of uncomplicated control ($P+$), along with a 1.9% reduction in rectum normal tissue complication probability (NTCP), and a 0.7% reduction in bladder NTCP. PTP-based plans show improved conformality as compared with margin-based plans with an average PTP-based dosimetric margin at 7100 cGy of 0.65 cm compared with the margin-based 0.90 cm and a PTP-based dosimetric margin at 3960 cGy of 1.60 cm compared with the margin-based 1.90 cm. PTP-based plans show similar sensitivity to variations of the uncertainty during treatment from the uncertainty used in planning as compared to margin-based plans. For equal target coverage, when compared to margin-based plans, PTP results in equal or lower doses to normal structures. PTP results in more conformal plans than margin-based plans and shows similar sensitivity to variations in uncertainty. [DOI: 10.1118/1.3176940]

Key words: IMRT, probabilistic planning, robust treatment, uncertainty

I. INTRODUCTION

In external beam radiation therapy, the current method of compensating for patient positioning uncertainties is to apply margins around the contoured patient structures.[1,2] Treatment dose levels are planned to be delivered to the margin-expanded region around the target while doses are limited within the margin-expanded regions around critical structures. Margins are intended to ensure that the target is covered when subject to "reasonable" random and systematic patient position variations and that critical structures are similarly spared when subject to such variations. If the clinical target volume (CTV) margin is insufficient, the CTV can move outside of the expected treatment region resulting in underdosing of the target and poor tumor control. Similarly, if a planning organ at risk volume (PRV) margin is insufficient, normal tissue and critical structures can move into regions receiving treatment dose levels resulting in unnecessarily high doses to these structures, which may result in greater complications. The addition of a margin reduces the likelihood of the target being outside of the treatment region; however, this also increases the likelihood that normal tissue

or critical structures will fall within the treatment dose region. In order to meet the goals of margin-based planning, formulas have been created to determine the size of suitable margins.[3,4] An example is the margin formula of van Herk *et al.*,[4–6] which specifically aims for 90% of patients to receive 95% of the prescribed treatment dose.

Patient treatment involves many sources of positioning uncertainty. Random uncertainty stems from daily changes in patient positioning and patient anatomy. Systematic uncertainty represents a shift from the mean of the expected patient position. Random uncertainty results in a blurring of the dose distribution. Systematic uncertainty results in an unknown shift in the dose distribution. Given these differences, the methods of including the effects of these uncertainties into the dose distribution differ. Random uncertainties can be compensated for by multiple sampling of the patient position or by convolution. Systematic uncertainties do not lend themselves to convolution-based solutions. Fortunately, modern advances in image guidance have decreased the systematic and random uncertainties present in radiation therapy. Implanted markers, portal image-based setup, and cone-beam CT are just a few of the methods that show potential to decrease setup errors.[7–12] Systematic uncertainties can be significantly reduced using repeated imaging adaptive setup protocols such as those used by Yan *et al.* and Hoogeman *et al.* that indicate that use of four to six initial portal or CT images can estimate and effectively reduce systematic setup errors.[13,14] While adaptive setup protocols can significantly decrease systematic uncertainty, random uncertainties are less effectively reduced using these methods.[14]

In IMRT planning, the margin-expanded planning target volume (PTV) acts as a surrogate for the CTV, the actual position of which varies from fraction to fraction. With the patient setup uncertainty added over several treatment fractions, ensuring coverage or sparing of the margin-expanded volume should ensure coverage or sparing of the underlying structure of interest. In margin-based planning, the dose distribution of the expanded structure is intended to be representative of the underlying structure when expected setup uncertainties are considered.[4] However, with knowledge of the setup uncertainty and tissue motion distributions, the PTV surrogate can be removed and planning can be done directly on the CTV. Probabilistic treatment planning (PTP) attempts to ensure coverage of the target without addition of explicit margins by incorporating an uncertainty model directly into the plan optimization process. Several authors have studied PTP.[15–31] The general finding of these studies is that PTP reduces normal tissue and organ at risk (OAR) doses while maintaining the same target coverage as margin-based plans.

The purpose of this study is to implement a method of incorporating random uncertainty into treatment planning and to compare this method with margin-based planning. Plans are generated using standard dose-volume histogram (DVH)-based criteria for prostate planning on a large population of patients including many structures with criteria defined in RTOG0126. The simplicity of the proposed method allows for arbitrary optimization objective functions to be defined in the treatment planning system (TPS). Comparison metrics include DVH analysis, mean dose, tumor control probability (TCP), normal tissue complication probability (NTCP), and coverage probability. Systematic errors are not considered within this optimization. It is assumed that systematic errors are substantially reduced by application of an adaptive therapy protocol,[14] and any remaining systematic uncertainty in a structure's position is incorporated into the structure contours. Fluence convolution is used to approximate the effects of random patient setup errors over multiple fractions of dose delivery. The validity of the fluence convolution assumption is tested by sampling different possible treatment scenarios. The sensitivity of the optimized result to changes in the patient's random setup uncertainty from that applied within the optimization is also studied.

This paper deviates from previous PTP work in that it uses existing objective functions directly within the commercial TPS. Additionally, fluence convolution is used to simulate the effect of random errors instead of dose convolution during the plan optimization, typical DVH-based objective functions are used instead of custom TCP-based objective functions, and a large patient population is used to demonstrate statistical significance of the similarity in dose coverage for the CTV and the dose reduction to normal tissues for PTP. This study compares PTP to margin-based planning, showing differences using the DVH metrics used in optimization. Models for $P+$, TCP, and NTCP are used to compare plan quality. Dosimetric margins are computed for both methods to evaluate conformality changes between methods. Finally, sensitivity analysis is conducted to verify that PTP is not highly sensitive to inaccuracies in the patient uncertainty distribution estimate.

II. MATERIALS AND METHODS

Patient imaging data and structure contours used in this study are derived from 28 in-house prostate patients. In accordance with our institutional review board protocol, all patient identifiable information is stripped from each data set prior to use in the study. Since this study employs a paired comparison between two planning methods that are unrelated to the treatment plans used for the actual patient treatments, the plans that were used for patient treatment are deleted. Additional structure contours are added as needed.

For each patient image set, IMRT treatment plans are developed using Philips Medical Systems Pinnacle[3] 8.1w research version (Philips Medical Systems, Fitchburg, WI). The research version allows for the in-house code to be incorporated into the planning system by way of plugins. Dose is calculated using the adaptive convolution algorithm with a dose grid of $2\times2\times2$ mm^3. The IMRT plans are optimized with direct machine parameter optimization (DMPO). Each patient is planned with seven beam angles of 30°, 80°, 130°, 180°, 230°, 280°, and 330° in IEC coordinates. Patients are each planned according to criteria specified by RTOG0126, an external beam radiation therapy prostate carcinoma dose

TABLE I. Optimization criteria used for generating patient plans, based on RTOG0126. Values of "Max." for the volume indicate that the specified dose should not be exceeded anywhere within the volume.

Structure	Dose (cGy)	Volume
Target	>7920	98%
	<8470	2%
Rectum	<6000	50%
	<6500	35%
	<7000	25%
	<7500	15%
	<8470	Max.
Bladder	<6500	50%
	<7000	35%
	<7500	25%
	<8000	15%
	<8470	Max.
Left femur	<3500	50%
	<5000	Max.
Right femur	<3500	50%
	<5000	Max.
LNT	<5000	Max.

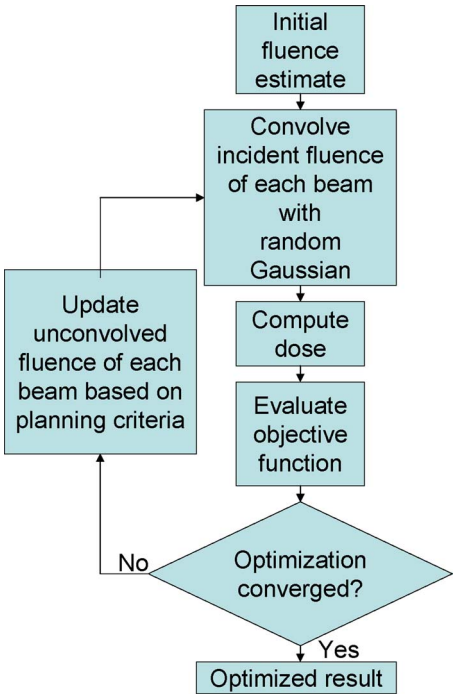

FIG. 1. PTP optimization flow using fluence convolution used in this study.

escalation protocol. The plan optimization criteria are shown in Table I. Each virtual patient is planned to be delivered over a course of 30 treatment fractions.

Two planning approaches are used, traditional margin-based planning and PTP. For margin-based planning, a PTV is created using a 2.1 mm margin around the CTV. This is in accordance with the margin formula of van Herk *et al.*[4–6] which recommends a margin of $M=2.5\Sigma+0.7\sigma$. With an assumed random uncertainty of $\sigma=3$ mm and no systematic uncertainty ($\Sigma=0$), the recommended margin is $M=2.5(0)+0.7(3)=2.1$ mm.

The 3 mm random setup uncertainty is representative of those used in related literature[4,6,15,17,30,32] and is consistent with, though somewhat larger than, what is observed in in-house internal marker-based daily alignment protocol. Reported random setup uncertainty values have significant variation, ranging from 0.9 to 5.1 mm. We believe that the exact value for the assumed random uncertainty is not required for the comparisons performed in this study. The simulations assume that the value of the uncertainty is known and plan according to this known value. Afterwards, the final dose for the treatment course is computed with the same uncertainty as in planning. Both arms of the study use the same random uncertainty assumption. This eliminates the need for knowledge of the exact value of real patient uncertainty. In actual clinical application of the proposed methods, in-house measurements of setup uncertainty would be required.

Standard margin-based plans are optimized using the criteria specified above. In margin-based planning, the target is the PTV. A pseudovolume termed local normal tissue (LNT), which is a ring extending from 2 cm outside of the CTV to 4 cm outside of the CTV, is used by the optimization process to attempt to reduce dose outside of the target. After optimization is completed, dose for the margin-based plan is recalculated using fluence convolution, as discussed below, to generate the dose distribution representative of the patient subject to random setup uncertainties over the 30-fraction treatment.

PTP-based plans are optimized using the same criteria as the margin-based plans with the exception of the target structure criterion. For PTP, the CTV is used as the target structure in planning rather than the PTV. A flow chart describing the PTP optimization process is shown in Fig. 1. During each iteration of the optimization, an in-house written plugin is used to convolve each beam's incident fluence with a $\sigma=3$ mm Gaussian during the dose computation process. The dose resultant of the convolved fluence is then used by the optimizer to determine the next update to the fluence matrix. Fluence updates are performed on an unconvolved representation of each beam's fluence matrix. After optimization is completed, the dose distribution is representative of the dose distribution of a patient subject to random uncertainty.

The convolution plugin operates by intercepting the intensity-modulated fluence before casting the fluence through the patient geometry. The plugin convolves the fluence with a kernel representing the probability density function (PDF) of the random patient positioning uncertainty, assumed to be a Gaussian kernel for this study. This efficiently simulates the effect of uncertainty over an entire fractionated treatment course, with an infinite number of fractions. The convolved fluence is then passed back to the dose calculation engine. The resultant dose distribution is the result of a con-

TABLE II. Parameters used in TCP and NTCP evaluations. Values are equivalent to the default values given by the Pinnacle TPS (Refs. 40–42).

Type	ROI	Organ/tumor	End point/stage	D_{50}	Gamma	Alpha/beta	Seriality
TCP	CTV	Prostate	Stage B	5270	4.2	10	
NTCP	Bladder	Bladder	Contracture	8000	3	3	0.18
NTCP	Rectum	Rectum	Necrosis/stenos	8000	2.2	3	1.5
NTCP	Left femur	Femur	Necrosis	6500	2.7	3	1
NTCP	Right femur	Femur	Necrosis	6500	2.7	3	1
NTCP	LNT	Normal tissue	Necrosis	6500	2.8	3	1

volved fluence. Fluence convolution-based dose calculations are used in the PTP optimization process and in the comparative analysis for margin-based plans.

Fluence convolution is technically only valid for an infinite number of fractions. Unkelbach and Oelfke[27] demonstrated that PTP methods that optimize the expectation value of the dose can yield undesirable dose undulations when delivered in a finite number of fractions. Therefore, they required a variance reduction term in the objective function to minimize these undulations.

To determine if our optimization results show such undulations, we perform postoptimization treatment delivery simulations to simulate multiple 30-fraction treatment courses for a single patient. This is similar to the stochastic method used by Craig *et al.* to validate dose convolution.[33] A single treatment course is simulated by computing the total dose for 30 fractions, where each fraction is simulated by shifting the fluence by a random value sampled from a $\sigma=3$ mm Gaussian and computing the dose. The dose from each fraction is summed to produce a distribution representative of the dose accumulated over an entire treatment course. This process is repeated 100 times to produce a total of 3000 fractions representing 100 treatment courses. The results of these treatment courses are then compared to a treatment course computed using fluence convolution. For each total treatment dose, the difference in DVH results from the convolution method is computed. Validation of convolution is shown on both PTP-based and margin-based optimized fluences.

For evaluation of the clinical acceptability of the automatically generated treatment plans, both PTP-based and margin-based plans are reviewed by a physician. The physician determines if each plan is clinically acceptable and chooses the preferred plan for treatment.

Comparisons between plans are conducted based on the dose that incorporates the expected random daily setup errors. For each structure, plans are compared based upon the dose-volume criteria specified during optimization. The volume receiving the prescription dose and the dose received by the prescription volume are computed at each point specified in the plan criteria. Plan criteria that are completely satisfied by the optimized dose distribution are excluded from the analysis as the optimizer does not attempt to improve the plan beyond the defined criteria. For example, given the objectives used in this study, if the dose to the bladder is below 65 Gy the planning objective would be met; therefore, this criterion would not be reported. Since the dose distributions used in this evaluation include the effects of random errors, both margin-based and PTP methods use the CTV in the DVH analysis. The PTV is only used in the optimization process for margin-based planning as it is only a surrogate for the complete treatment dose on a static plan. In addition to dose-volume metrics used as optimization objectives, the mean dose to each structure is computed.

For each of the structures specified in the plan criteria, TCP and NTCP indices are computed. These are computed using the Biology tool available under the Plan Evaluation menu in Pinnacle. Parameters for TCP/NTCP indices are equal to the defaults for each given organ in the Biology tool. Table II displays these values. TCP is computed for the target structure and NTCP is computed for normal tissue structures. Additionally $P+$ is computed for each plan. $P+$ is a composite measure incorporating all TCP and NTCP indices from the plan into a single metric which represents the probability of uncomplicated tumor control. For these metrics, an increase in TCP or $P+$ is considered beneficial while a decrease in NTCP is preferred.

The conformity of the plans is quantified by computing the dosimetric margin distribution (DMD).[34] The DMD is a generalization of the ICRU conformity index[2] that measures the distance a structure can move before crossing a given isodose line in different directions. DMD evaluations are performed on the fluence-convolved dose distributions for the CTV to both the 90% prescription line (7100 cGy) and the 50% prescription dose line (3960 cGy). The DMD is obtained from 146 equispaced directions around the CTV. The 50% isodose line is evaluated since it corresponds to the irradiated volume[2] and conventionally indicates the location of the edge of the treated volume.

Clinically, the random component of the setup uncertainty varies from patient to patient and is unknown at the time of planning. The sensitivity of the plans generated assuming a $\sigma=3$ mm random uncertainty to deviations in patient-specific random uncertainty value σ_T is studied by evaluating the dose distributions corresponding to halving ($\sigma_T=1.5$ mm) and doubling ($\sigma_T=6$ mm) the uncertainty used during the plan optimization. DVH indices are compared and the number of plan objectives met by each is scored.

TABLE III. Minimum, maximum, range, mean, and standard deviation of DVH criteria observed over the 100 simulated treatment courses for the CTV and LNT structures compared with convolution. Average difference is the convolution value minus the mean of the simulated treatment courses. RMS value is the sum of the squared differences of each simulated course from the convolution value. Simulated treatment course values are the difference from convolution for volumes and the percentage difference relative to convolution for doses.

				Simulated treatment courses					
			Convolution	Min. (%)	Max. (%)	Range (%)	Average (%)	RMS (%)	Standard deviation (%)
Margin based	CTV	V_{7920}	98.0%	−0.7	0.6	1.3	0.0	0.3	0.3
		D_{98}	7920 cGy	−0.2	0.2	0.5	0.0	0.1	0.1
		V_{8470}	0.4%	−0.4	0.8	1.2	0.1	0.3	0.3
		Max.	8506 cGy	0.0	0.1	0.1	0.0	0.0	0.0
	LNT	V_{5000}	1.1%	−0.1	0.1	0.2	0.0	0.0	0.0
PTP based	CTV	V_{7920}	97.5%	−2.1	1.0	3.0	−0.1	0.6	0.6
		D_{98}	7890 cGy	−1.8	0.7	2.5	−0.1	0.5	0.5
		V_{8470}	0.0%	−1.6	1.5	3.1	0.3	0.6	0.6
		Max.	8470 cGy	−0.2	0.3	0.5	0.1	0.1	0.1
	LNT	V_{5000}	0.7%	−0.1	0.1	0.1	0.0	0.0	0.0

III. RESULTS

The suitability of using fluence convolution to simulate the 30-fraction treatment delivery for plan evaluation and plan optimization is shown in Table III. The variability of margin-based and PTP-based plans for one hundred 30-fraction delivery simulations and deviations from convolution are evaluated using the planning DVH criteria. For margin-based plans, the convolved dose differs by $<0.1\%$ from the average dose from treatment simulations. The volume receiving the prescription dose after convolution differs by 0.02% from the volume receiving the prescription dose from treatment simulations. The $<0.1\%$ variability in dose observed is much smaller than the 2%–3% accepted variability in beam delivery[35,36] and is therefore considered clinically acceptable. The maximum and minimum doses deviations are also well within a 2% tolerance. For PTP-based plans, the difference between the convolution and the average of the treatment simulations is with 0.1% in dose and 0.3% in volume. The 0.5% variability of the PTP-based plans for the treatment simulations is larger than the 0.1% observed for the margin-based plans but still well within a 2% tolerance. The maximum deviation is also larger but within tolerance. One treatment course simulation varies by 2.1% from the convolution volume at 7920 cGy. For both methods, all critical structures aside from the LNT structure remain below plan criteria for all simulations. The LNT volume in simulated treatment courses differs by less than 0.1% from convolution for both methods. While each simulated random treatment course yields slightly different doses, the variation is within typical clinical tolerances. In this study, 100% of simulations produce dose distributions that deliver >7524 cGy (95% of the prescription dose) for both PTP-based and margin-based plans. This exceeds the 90% of patients expected when using the margin formula of van Herk *et al.* and is due to the fact that only random setup uncertainties are considered.

Margin-based planning and PTP planning are successfully completed on all patient plans. A comparison of isodose profiles on a transverse slice through the isocenter for one patient with PTP-based and margin-based (with and without convolution) plans is shown in Fig. 2. As is typical in dose-volume based optimization, final plans result in a trade-off between the objective function criteria, with not all treatment objectives being fully met. All plans meet the specified criteria for left femur and right femur using both methods. One margin-based planning patient and a different PTP patient exceed the bladder maximum dose objective. All other bladder objectives are met for all patients. One PTP patient exceeds the 8470 cGy rectum maximum dose objective by 0.3 cGy. Two margin-based plans and two PTP-based plans exceed the rectum 7500 cGy objective (by 36 and 3 cGy for the margin-based plans and by 5 and 103 cGy for the PTP-based plans; the 3 and 103 cGy deviations are for the same patient). All other rectum objectives are met for all patients.

Physician review of the plans indicates that the PTP-based plan is preferred over the margin-based plan for 21 out of 28 total patients. For one patient, the clinician indicated that there is no preference between plans. For two of the patients,

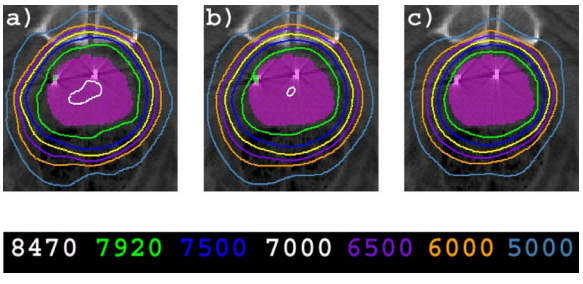

FIG. 2. Typical isodose profiles on a transverse slice passing through the isocenter for (a) the optimized margin-based plan, without inclusion of the effect of the random patient setup errors, (b) the optimized margin-based plan, with inclusion of the random patient setup errors, and (c) the PTP-based plan, which inherently incorporates the effect of random patient setup errors.

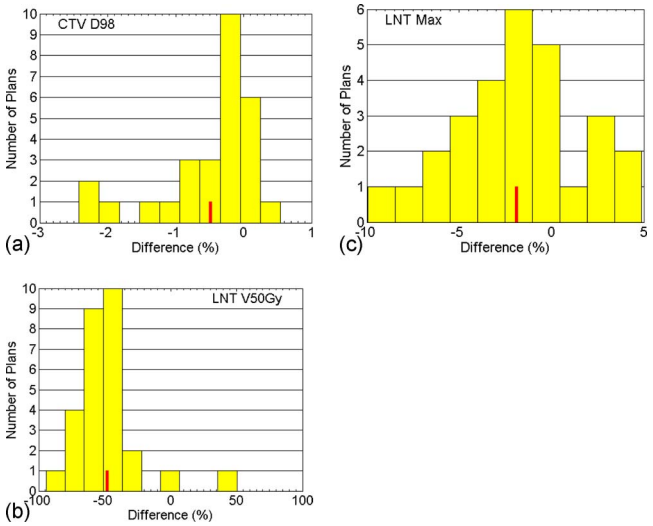

FIG. 3. (a) The percentage difference in the CTV doses to 98% of the volume between the margin-based and PTP-based plans for each patient. The average difference of −0.5% is indicated by the small bar. Negative values indicate a lower dose for the PTP-based plans. 0.5% corresponds to a 39.6 cGy difference. (b) The percentage difference in the LNT volumes receiving 5000 cGy. The average difference of −48% is indicated by the small bar. Negative values indicate a lower volume for the PTP-based plans. 48% corresponds to a 409 cc reduction in volume. (c) The percentage difference in the local normal tissue maximum doses between the margin-based and PTP-based plans for each patient. The average difference of −1.9% is indicated by the small bar. 1.9% corresponds to a 120.7 cGy difference.

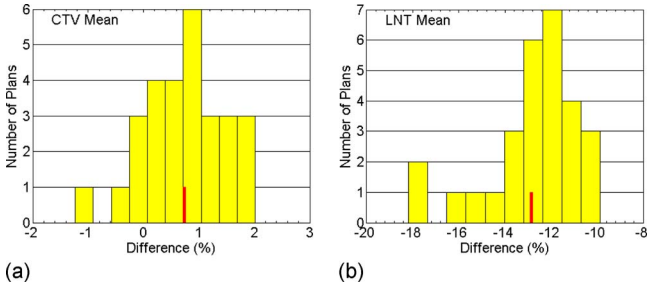

FIG. 4. (a) The percentage difference in CTV mean dose between the margin-based and PTP-based plans for each patient. The average difference of 0.7% is indicated by the small bar. Negative values indicate a lower dose for the PTP plans. 0.7% corresponds toh a 60.1 cGy difference. (b) The percentage difference in LNT mean dose between the margin-based and PTP-based plans for each patient. The average difference of 12.9% is indicated by the small bar. 12.9% corresponds to a 268 cGy difference.

the margin-based plan is preferred due to a slightly greater amount of the rectum exposed to high doses in the PTP plan. For four of the patients, the physician rejected both of the autogenerated plans due to the high dose to the critical structures. For two additional patients, the physician would reject only the margin-based plan. None of the PTP-based plans are rejected without the margin-based plan for the same patient being rejected. In a true clinical setting, optimization parameters for failing plans would have been modified to meet the planning criteria; however, for consistency, standard criteria are used for all plan evaluations in this study. Histograms of per-patient deviations in the dose-volume indices, $\Delta=100(1-D_{V_x}^{\mathrm{PTP}}/D_{V_x}^{\mathrm{MP}})$ or $\Delta=100(1-V_{D_y}^{\mathrm{PTP}}/V_{D_y}^{\mathrm{MP}})$, where D_{V_x} is the dose received by V_x percentage of the volume for the structure indicated and V_{D_y} is the volume receiving a dose of D_y for the structure indicated, are shown in Fig. 3. Summary results of DVH analysis are shown in Table IV. Averaged over all patients, the CTV D_{98} is 0.5% lower for PTP as compared to margin-based planning. The CTV volume receiving 7920 cGy does not differ significantly for this objective ($p=0.092$). All p values are obtained from a two-tailed paired t test. The maximum 8470 cGy dose objective shows no significant differences between PTP- and margin-based planning ($p=0.44$). PTP shows a 48% decrease in volume receiving the 5000 cGy maximum dose objective for LNT with $p<0.0001$. There is a 1.9% decrease in the maximum dose delivered to the target with $p=0.0095$.

Histograms of per-patient deviations in the mean dose, $\Delta=100(1-\bar{D}^{\mathrm{PTP}}/\bar{D}^{\mathrm{MP}})$, where $\bar{D}$ is the mean dose delivered to the structure indicated, are shown in Fig. 4. Summary results of mean dose analysis are shown in Table V. The CTV on average receives a slightly higher mean dose (+0.74%, $p<0.0001$). PTP results in a significantly ($p<0.0001$) lower mean dose to critical structures. Mean doses to all critical structures on all patient plans are reduced compared with margin-based plans as follows: Bladder, −14.2%; rectum, −8%; left femur, −11.3%; right femur, −11%; and LNT, −12.9%.

Histograms of absolute per-patient deviations in the $P+$, TCP, and NTCP, $\Delta=B^{\mathrm{PTP}}-B^{\mathrm{MP}}$, where B is the $P+$, TCP, or

TABLE IV. Mean, maximum, minimum, and p value for the difference in doses and difference in volumes between margin-based and PTP-based plans for the listed objectives. Plan objectives not listed were met by both methods for all plans. Δ is used to indicate "difference in."

Structure	Dose (cGy)	Volume (%)	Δdose (%)	Max. (%)	Min. (%)	p	Δvolume (%)	Max. (%)	Min. (%)	P
Target	>7920	98	−0.5	0.6	−2.4	0.0013	−0.4	4.7	−3.0	0.0916
	<8470	2	0.1	1.4	−0.7	0.1040	66.6	780.1	−86.6	0.4415
Rectum	<7500	15	[a]							
	<8470		[b]							
Bladder	<8470		[c]							
LNT	<5000		−1.9	4.9	−10.0	0.0095	−47.9	50.2	−94.4	<0.0001

[a]All plans met objectives except for two PTP-based plans and two margin-based plans.
[b]All plans met criteria except for one PTP-based plan.
[c]All plans met criteria except for one PTP-based plan and one margin-based plan.

TABLE V. Mean, maximum, and minimum differences in mean doses between margin-based and PTP-based plans, with associated p values for objective structures. Δ is used to indicate "difference in."

Structure	Δmean (%)	Max. (%)	Min. (%)	p
CTV	0.7	2.0	−1.2	<0.0001
Rectum	−8.0	−1.6	−15.5	<0.0001
Bladder	−14.2	−4.5	−26.4	<0.0001
Left Femur	−11.3	−5.0	−20.6	<0.0001
Right Femur	−11.1	−3.0	−18.5	<0.0001
LNT	−12.9	−9.9	−18.2	<0.0001

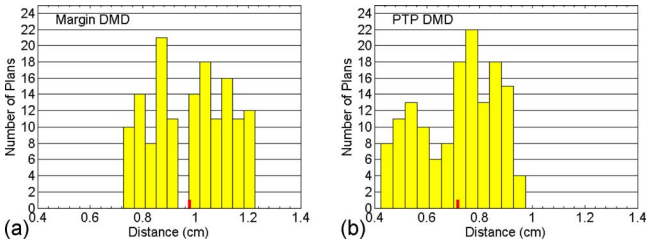

FIG. 6. Dosimetric margin distributions for sample (a) margin-based plan and (b) PTP-based plan. The average dosimetric margin for margin-based plans is 9.8 mm as indicated by the bar on (a). The average dosimetric margin for PTP plans is 7.2 mm as indicated by the bar on (b).

NTCP value for the structure indicated, are shown in Fig. 5. Summary results of $P+$, TCP, and NTCP analysis are shown in Table VI. The PTP-based plans on average show an absolute increase in $P+$ of +2.5% over margin-based plans. ($p=0.0002$). The TCP for both PTP-based and margin-based plans are equal at 99.9% for all but one plan. That plan shows an increase in TCP of 0.01% from 88.1% to 89.2% for the PTP-based plan. The rectum NTCP decreases for PTP-based plans by an average of 1.9% with $p=0.0014$. Rectal NTCP differences range from an increase of 2.8% to a decrease of 7% for PTP. Bladder NTCP values decrease on average by 0.7%, $p<0.0001$. LNT NTCP is decreased by 0.06%, $p=0.0028$. The left and right femurs for all patients for both PTP-based and margin-based plans have 0 NTCP.

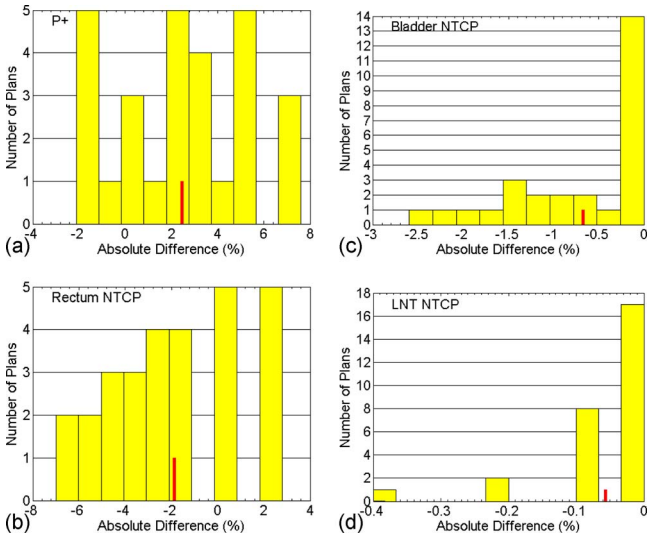

FIG. 5. (a) The absolute difference in $P+$ between the margin-based and PTP-based plans for each patient. The average difference of 2.45% is indicated by the small bar. Positive values indicate a better treatment outcome for the PTP-based plans. (b) The absolute difference in rectum NTCPs between the margin-based and PTP-based plans for each patient. The average difference of 1.9% is indicated by the small bar. Negative values indicate a lower complication rate for the PTP-based plans. (c) The absolute difference in bladder NTCPs between the margin-based and PTP-based plans for each patient. The average difference of 0.7% is indicated by the small bar. (d) The absolute difference in LNT NTCPs between the margin-based and PTP-based plans for each patient. The average difference of 0.06% is indicated by the small bar.

For all patients, PTP gives 0 NTCP for LNT. Five margin-based plans have an NTCP of 0.01 for LNT; all other plans have 0 NTCP for LNT.

A histogram of the 7100 cGy DMDs for the margin-based and PTP-based plans for a sample patient is shown in Fig. 6. Table VII shows the summary of the DMD values. For each patient, the average dosimetric margin for the PTP-based plans is less than that for the margin-based plans. The average dosimetric margin over all patients at 7100 cGy shows a significant ($p<0.0001$) difference between margin-based (0.90 cm) and PTP-based (0.65 mm) plans. For 25 out of 28 patients, the dosimetric margin at 7100 cGy for PTP-based plans is smaller than that of the margin-based plans in all of the 146 evaluated directions. The average dosimetric margin over all patients at 3960 cGy shows a significant ($p<0.0001$) difference between margin-based (1.90 cm) and PTP-based (1.60 cm) plans. For 27 of the patients, the dosimetric margin at 3960 cGy for PTP-based plans is smaller than that of margin-based plans in all of the 146 evaluated directions. PTP produces plans that are more conformal resulting in smaller dosimetric margins and a reduction in doses outside of the target. For PTP-based plans a slight increase (1.6%) in monitor units is observed compared to margin-based plans; this indicates little increase in the complexity of PTP-based plans.

The sensitivity of the structure dose coverage to the setup uncertainty estimate used in optimization is tested for both margin-based and PTP-based plans. Table VIII displays the difference in mean dose when the patient-specific random setup uncertainty σ_T is double and half the value that is used for the optimization. If the patient setup uncertainty is decreased with respect to the estimated uncertainty used during planning ($\sigma_T<\sigma$), mean dose for both PTP-based and margin-based plans increases for all structures except the LNT structure which reports a lower mean dose from both methods. With increased setup uncertainty during treatment, the converse holds true. These results are consistent with a decrease/increase in the dose blurring as the setup uncertainty is reduced/increased. Table IX compares the plans using the optimization DVH indices for unmet criteria. Again, consistent with dose blurring, as treatment uncertainty increases, the dose to the target decreases and deviation between target simulation dose increases. Dose to critical structures decreases as well as the deviation between OAR

TABLE VI. Mean, maximum, and minimum differences in *P*+, TCP, and NTCP between margin-based and PTP-based plans with associated *p* values for objective structures. Δ is used to indicate "difference in."

Structure	Type	Δmean (%)	Max. (%)	Min. (%)	*P*
All	*P*+	2.45	7.60	−2.10	0.0002
CTV	TCP	0.01	0.30	0.00	0.3262
Rectum	NTCP	−1.88	2.80	−7.00	0.0014
Bladder	NTCP	−0.67	0.00	−2.60	<0.0001
Left femur	NTCP	0.00	0.00	0.00	–
Right femur	NTCP	0.00	0.00	0.00	–
LNT	NTCP	−0.06	0.00	−0.40	0.0028

simulation dose as uncertainty increases. For $\sigma_T=6$ mm, all PTP- and margin-based plans failed to meet the CTV $D_{98}\geq 7920$ cGy dose criteria; however, eight PTP and six margin-based plans that initially failed to meet the CTV $D_{\max}<8470$ cGy then met the criteria, consistent with dose blurring. With $\sigma_T=6$ mm, no critical structure doses exceeded planning criteria. For $\sigma_T=1.5$ mm, 23 PTP plans and 10 margin-based plans that initially did not fully meet the CTV $D_{98}\geq 7920$ cGy criteria then met the criteria. However, two additional PTP and four additional margin-based plans failed to meet the $D_{\max}<8470$ cGy criteria. Furthermore, four additional OAR criteria were not met with $\sigma_T=1.5$ mm for both the PTP- and margin-based plans. Adequate coverage is achieved if the uncertainty during treatment is less than or equal to the uncertainty used during the planning process for either margin-based planning or PTP. When the uncertainty during treatment is greater than the uncertainty used during the planning process, both methods have reduced coverage. These results demonstrate that if uncertainty is underestimated, PTP methods will produce acceptable coverage. In the case of uncertainty being overestimated, neither PTP- nor margin-based planning will produce the required coverage. In both PTP- and margin-based planning, if there is low confidence in the uncertainty estimate, it is best to overestimate the uncertainty to ensure coverage.

IV. DISCUSSION

In this study, a simple method for incorporating random patient setup uncertainty into plan optimization is implemented. This method does not require changing the objective functions used in optimization. The results show that PTP-based plans produce similar target coverage to margin-based plans while reducing dose to critical structures and LNT and produce more conformal plans without increasing complexity. This simple method of incorporating random errors into treatment optimization is significant since it is a straightforward method to improve the therapeutic ratio that can be implemented into an arbitrary optimization system.

PTP allows for uncertainties to be handled directly by the optimizer. This allows an optimal solution to be generated that does not require the addition of margins. PTP optimized plans result in a tighter dosimetric margin around the target. Margin-based plans using a fixed expansion tend to generate effective dosimetric margins that are larger than the planning margin.[34] This larger margin results in more normal tissue receiving therapeutic doses.

Our findings that PTP reduces normal tissue doses and NTCP are similar to the findings of previous studies. For focal liver tumors, Balter *et al.* reported that convolving the dose with a population-based random Gaussian can reduce the effective treatment volume by 6%–8% as compared to a margin-based approach.[37] Yang *et al.* reported that incorporating uncertainty around targets and OARs by way of a score function composed of scores on multiple shifted planning scans weighted by their probability resulted in greater OAR sparing when compared to margin-based approaches, including methods that incorporate a PRV margin.[31]

As is demonstrated in Fig. 2, incorporating the effects of random setup errors into the dose evaluation results in a blurring of the patient dose distribution. This finding is in agreement with numerous previous authors.[6,38] Although it is trivial to incorporate such a blurring into the dose calculation and display process and require very little additional computational overhead, clinically, no treatment planning systems

TABLE VII. Mean, maximum, and minimum dosimetric margins for 7100 and 3960 cGy for both margin-based and PTP-based plans with *p* values of the difference between margin-based and PTP-based plans.

	7100 cGy			3960 cGy		
Dose	Mean (cm)	Max. (cm)	Min. (cm)	Mean. (cm)	Max. (cm)	Min. (cm)
Margin	0.90	1.63	0.37	1.90	4.11	0.92
PTP	0.65	1.47	0.17	1.60	3.67	0.62
P	<0.0001			<0.0001		

TABLE VIII. Differences in the structure mean dose values when the patient plan is subject to half (σ_T=1.5 mm) and double (σ_T=6 mm) the estimated (σ=3 mm) random uncertainty used during the optimization for margin-based and PTP-based plans.

		Half (%)	Double (%)
Margin	Bladder	0.3	−1.0
	CTV	0.2	−1.6
	LNT	−0.4	1.8
	Left femur	0.3	−1.1
	Right femur	0.4	−1.3
	Rectum	0.3	−1.0
PTP	Bladder	0.1	−0.2
	CTV	0.4	−2.6
	LNT	−0.3	1.6
	Left femur	0.3	−1.2
	Right femur	0.4	−1.3
	Rectum	0.3	−1.0

do this. Currently, plans are presented to the physician showing isodose profiles and DVHs as if the patient is in an identical treatment position with respect to the beams during each treatment delivery. By viewing a static dose distribution, the gradients in the dose distributions evaluated by the clinicians are sharper than what is actually achieved during multifractional treatment delivery. A method more representative of the actual patient dose is to include the best estimate of the random component of the random patient setup uncertainty into the dose calculation, either using the fluence convolution[39] or dose convolution[38] approaches prior to displaying isodose and DVHs. For margin-based planning, such analysis would require evaluating DVHs for structures with margins added that only account for systematic setup errors or evaluation of the coverage probability. It is possible, though not quantifiable at this point, that displaying a more clinically realistic dose distribution to the clinician could alter treatment planning decisions.

For the purposes of this study, other than the sensitivity study, exact knowledge of the random uncertainty distribution was assumed. Exact knowledge of the random uncertainty distribution can only be had after an entire treatment course has been completed. Random uncertainty estimates are commonly obtained from a large population of similar patients. Additionally from a large population of patients, the uncertainty in the random setup uncertainty estimate can be obtained. With knowledge of the uncertainty in the random uncertainty estimate, a planning setup uncertainty can be chosen based upon a percentage of the uncertainty distribution. It may be the case that the best value used in planning is the *N*th percentile of the distribution of uncertainty estimates, where *N* is the percentage of patients. For this case, 90% would correspond with the margin formulations of van Herk *et al.*[4–6]

In this study, we assume that systematic setup uncertainties are negligible. While clinically unrealistic, use of adaptive therapy setup protocols,[13,14] where the patient position is imaged for the first several (approximately five) fractions, then repositioned based on the systematic error derived from those measurements, has been shown to significantly reduce systematic setup errors. Even if systematic errors persist, the methods used in this study are still relevant. When systematic errors remain, a margin can be added around the structures to account for systematic uncertainty alone while allowing PTP to account for random uncertainty.

While this study only accounted for random rigid patient setup variations, other random uncertainties such as intrafraction motion that can be modeled using a PDF could be incorporated using similar methods. Evaluation of these uncertainties is left to future studies.

V. CONCLUSIONS

A PTP method that directly incorporates random uncertainty into the standard IMRT optimization of a commercial TPS has been implemented and tested. PTP results generated using this implementation are compared with margin-based plans. PTP-based plans show similar coverage to the margin-based plans. A small reduction in the dose to the target planning objectives is observed but dose to the local normal tissue structure is significantly reduced. OARs and LNT show

TABLE IX. Mean dose and standard deviation over 28 patients for the listed criteria for plans optimized with σ=3 mm but recomputed with σ_T=1.5, 3, and 6 mm. As uncertainty increases, the dose at target objectives decreases and vice-versa. As uncertainty increases, the dose at OAR objectives decreases and vice-versa. Objectives not listed were met by all plans.

		1.5 mm		3 mm		6 mm	
	Dose	PTP	Margin	PTP	Margin	PTP	Margin
CTV	98% (cGy)	8005	7974	7878	7930	7198	7494
	Standard deviation (cGy)	48	30	69	38	153	133
Rectum	25% (cGy)	5441	5797	5382	5743	5193	5554
	Standard deviation (cGy)	864	796	852	783	805	743
Rectum	15% (cGy)	6507	6811	6434	6734	6189	6486
	Standard deviation (cGy)	744	672	727	650	669	600

decreased mean dose using PTP methods as compared to margin-based methods while target mean dose slightly increases. Biological indices indicate that PTP has a similar TCP with reduced NTCP resulting in a higher $P+$. Effective dosimetric margins are smaller in PTP-based plans as compared to margin-based plans indicating more conformal plans. PTP produces plans that maintain similar target coverage while reducing dose to all other structures.

The use of fluence convolution to simulate the dose blurring effect of the 30-fraction treatment courses is valid. Compared with average from delivery simulations, fluence convolution-based target doses and volumes differed by $<0.1\%$. Use of convolution instead of simulation during optimization is within clinical tolerance.

The sensitivity of PTP-based plans to deviations in the patient-specific uncertainty with respect to that used in planning is comparable to the sensitivity of margin-based plans. For both margin-based and PTP methods, if the setup uncertainty is less than what was used for planning, dose increases to the target and to nearby critical structures due to sharpening of the dose distribution. If the setup uncertainty is larger than what is used for planning, dose decreases to the target and to nearby critical structures due to blurring of the dose distribution

ACKNOWLEDGMENTS

The authors would like to thank Karl Bzdusek and Michael Kaus of Philips Medical Systems for providing the hooks required to develop the Pinnacle plugins necessary for this work, and Dr. Elizabeth Weiss and Nahla Sayah at VCU for generating contours and initial plans for these patients. Thanks also go to James Ververs for his assistance in proofing this article. This work is supported by NIH Grant Nos. P01CA116602 and T32CA113277.

[a]Electronic mail: jamoore@vcu.edu

[1]International Commission on Radiation Units and Measurements, *Prescribing, Recording, and Reporting Photon Beam Therapy* (International Commission on Radiation Units and Measurements, Bethesda, MD, 1993).
[2]International Commission on Radiation Units and Measurements, *Prescribing, Recording, and Reporting Photon Beam Therapy* (International Commission on Radiation Units and Measurements, Bethesda, MD, 1999).
[3]J. C. Stroom, H. C. de Boer, H. Huizenga, and A. G. Visser, "Inclusion of geometrical uncertainties in radiotherapy treatment planning by means of coverage probability," Int. J. Radiat. Oncol. Biol. Phys. **43**(4), 905–919 (1999).
[4]M. van Herk, P. Remeijer, C. Rasch, and J. V. Lebesque, "The probability of correct target dosage: Dose-population histograms for deriving treatment margins in radiotherapy," Int. J. Radiat. Oncol., Biol., Phys. **47**(4), 1121–1135 (2000).
[5]M. van Herk, "Errors and margins in radiotherapy," Semin. Radiat. Oncol. **14**(1), 52–64 (2004).
[6]M. van Herk, P. Remeijer, and J. V. Lebesque, "Inclusion of geometric uncertainties in treatment plan evaluation," Int. J. Radiat. Oncol., Biol., Phys. **52**(5), 1407–1422 (2002).
[7]A. Bel, P. H. Vos, P. T. Rodrigus, C. L. Creutzberg, A. G. Visser, J. C. Stroom, and J. V. Lebesque, "High-precision prostate cancer irradiation by clinical application of an offline patient setup verification procedure, using portal imaging," Int. J. Radiat. Oncol., Biol., Phys. **35**(2), 321–332 (1996).
[8]H. C. de Boer and B. J. Heijmen, "A protocol for the reduction of systematic patient setup errors with minimal portal imaging workload," Int. J. Radiat. Oncol., Biol., Phys. **50**(5), 1350–1365 (2001).
[9]D. A. Jaffray, J. H. Siewerdsen, J. W. Wong, and A. A. Martinez, "Flat-panel cone-beam computed tomography for image-guided radiation therapy," Int. J. Radiat. Oncol., Biol., Phys. **53**(5), 1337–1349 (2002).
[10]J. Lattanzi, S. McNeeley, W. Pinover, E. Horwitz, I. Das, T. E. Schultheiss, and G. E. Hanks, "A comparison of daily CT localization to a daily ultrasound-based system in prostate cancer," Int. J. Radiat. Oncol., Biol., Phys. **43**(4), 719–725 (1999).
[11]D. Litzenberg, L. A. Dawson, H. Sandler, M. G. Sanda, D. L. McShan, R. K. Ten Haken, K. L. Lam, K. K. Brock, and J. M. Balter, "Daily prostate targeting using implanted radiopaque markers," Int. J. Radiat. Oncol., Biol., Phys. **52**(3), 699–703 (2002).
[12]T. T. Nuver, M. S. Hoogeman, P. Remeijer, M. van Herk, and J. V. Lebesque, "An adaptive off-line procedure for radiotherapy of prostate cancer," Int. J. Radiat. Oncol., Biol., Phys. **67**(5), 1559–1567 (2007).
[13]M. S. Hoogeman, M. van Herk, J. de Bois, and J. V. Lebesque, "Strategies to reduce the systematic error due to tumor and rectum motion in radiotherapy of prostate cancer," Radiother. Oncol. **74**(2), 177–185 (2005).
[14]D. Yan, E. Ziaja, D. Jaffray, J. Wong, D. Brabbins, F. Vicini, and A. Martinez, "The use of adaptive radiation therapy to reduce setup error: A prospective clinical study," Int. J. Radiat. Oncol., Biol., Phys. **41**(3), 715–720 (1998).
[15]C. Baum, M. Alber, M. Birkner, and F. Nusslin, "Treatment simulation approaches for the estimation of the distributions of treatment quality parameters generated by geometrical uncertainties," Phys. Med. Biol. **49**(24), 5475–5488 (2004).
[16]C. Baum, M. Alber, M. Birkner, and F. Nusslin, "Robust treatment planning for intensity modulated radiotherapy of prostate cancer based on coverage probabilities," Radiother. Oncol. **78**(1), 27–35 (2006).
[17]M. Birkner, D. Yan, M. Alber, J. Liang, and F. Nusslin, "Adapting inverse planning to patient and organ geometrical variation: Algorithm and implementation," Med. Phys. **30**(10), 2822–2831 (2003).
[18]T. C. Chan, T. Bortfeld, and J. N. Tsitsiklis, "A robust approach to IMRT optimization," Phys. Med. Biol. **51**(10), 2567–2583 (2006).
[19]M. Chu, Y. Zinchenko, S. G. Henderson, and M. B. Sharpe, "Robust optimization for intensity modulated radiation therapy treatment planning under uncertainty," Phys. Med. Biol. **50**(23), 5463–5477 (2005).
[20]J. G. Li and L. Xing, "Inverse planning incorporating organ motion," Med. Phys. **27**(7), 1573–1578 (2000).
[21]J. Lof, B. K. Lind, and A. Brahme, "Optimal radiation beam profiles considering the stochastic process of patient positioning in fractionated radiation therapy," Inverse Probl. **11**(6), 1189–1209 (1995).
[22]J. Lof, B. K. Lind, and A. Brahme, "An adaptive control algorithm for optimization of intensity modulated radiotherapy considering uncertainties in beam profiles, patient set-up and internal organ motion," Phys. Med. Biol. **43**(6), 1605–1628 (1998).
[23]D. Maleike, J. Unkelbach, and U. Oelfke, "Simulation and visualization of dose uncertainties due to interfractional organ motion," Phys. Med. Biol. **51**(9), 2237–2252 (2006).
[24]D. L. McShan, M. L. Kessler, K. Vineberg, and B. A. Fraass, "Inverse plan optimization accounting for random geometric uncertainties with a multiple instance geometry approximation (MIGA)," Med. Phys. **33**(5), 1510–1521 (2006).
[25]H. Rehbinder, C. Forsgren, and J. Lof, "Adaptive radiation therapy for compensation of errors in patient setup and treatment delivery," Med. Phys. **31**(12), 3363–3371 (2004).
[26]A. Trofimov, E. Rietzel, H. M. Lu, B. Martin, S. Jiang, G. T. Chen, and T. Bortfeld, "Temporo-spatial IMRT optimization: Concepts, implementation and initial results," Phys. Med. Biol. **50**(12), 2779–2798 (2005).
[27]J. Unkelbach and U. Oelfke, "Inclusion of organ movements in IMRT treatment planning via inverse planning based on probability distributions," Phys. Med. Biol. **49**(17), 4005–4029 (2004).
[28]J. Unkelbach and U. Oelfke, "Incorporating organ movements in IMRT treatment planning for prostate cancer: minimizing uncertainties in the inverse planning process," Med. Phys. **32**(8), 2471–2483 (2005).
[29]J. Unkelbach and U. Oelfke, "Incorporating organ movements in inverse planning: assessing dose uncertainties by Bayesian inference," Phys. Med. Biol. **50**(1), 121–139 (2005).
[30]M. G. Witte, J. van der Geer, C. Schneider, J. V. Lebesque, M. Alber, and M. van Herk, "IMRT optimization including random and systematic geometric errors based on the expectation of TCP and NTCP," Med. Phys. **34**(9), 3544–3555 (2007).

[31]J. Yang, G. S. Mageras, S. V. Spirou, A. Jackson, E. Yorke, C. C. Ling, and C. S. Chui, "A new method of incorporating systematic uncertainties in intensity-modulated radiotherapy optimization," Med. Phys. **32**(8), 2567–2579 (2005).
[32]T. Craig, E. Wong, G. Bauman, J. Battista, and J. Van Dyk, "Impact of geometric uncertainties on evaluation of treatment techniques for prostate cancer," Int. J. Radiat. Oncol., Biol., Phys. **62**(2), 426–436 (2005).
[33]T. Craig, J. Battista, and J. Van Dyk, "Limitations of a convolution method for modeling geometric uncertainties in radiation therapy. II. The effect of a finite number of fractions," Med. Phys. **30**(8), 2012–2020 (2003).
[34]J. J. Gordon and J. V. Siebers, "Evaluation of dosimetric margins in prostate IMRT treatment plans," Med. Phys. **35**(2), 569–575 (2008).
[35]G. A. Ezzell, J. M. Galvin, D. Low, J. R. Palta, I. Rosen, M. B. Sharpe, P. Xia, Y. Xiao, L. Xing, and C. X. Yu, "Guidance document on delivery, treatment planning, and clinical implementation of IMRT: Report of the IMRT Subcommittee of the AAPM Radiation Therapy Committee," Med. Phys. **30**(8), 2089–2115 (2003).
[36]B. Fraass, K. Doppke, M. Hunt, G. Kutcher, G. Starkschall, R. Stern, and J. Van Dyke, "American Association of Physicists in Medicine Radiation Therapy Committee Task Group 53: Quality assurance for clinical radiotherapy treatment planning," Med. Phys. **25**(10), 1773–1829 (1998).
[37]J. M. Balter, K. K. Brock, K. L. Lam, D. Tatro, L. A. Dawson, D. L. McShan, and R. K. Ten Haken, "Evaluating the influence of setup uncertainties on treatment planning for focal liver tumors," Int. J. Radiat. Oncol., Biol., Phys. **63**(2), 610–614 (2005).
[38]J. Leong, "Implementation of random positioning error in computerised radiation treatment planning systems as a result of fractionation," Phys. Med. Biol. **32**(3), 327–334 (1987).
[39]W. A. Beckham, P. J. Keall, and J. V. Siebers, "A fluence-convolution method to calculate radiation therapy dose distributions that incorporate random set-up error," Phys. Med. Biol. **47**(19), 3465–3473 (2002).
[40]A. K. Agren Cronqvist, P. Källman, I. Turesson, and A. Brahme, "Volume and heterogeneity dependence of the dose-response relationship for head and neck tumours," Acta Oncol. (Madr.) **34**(6), 851–860 (1995).
[41]E. W. Korevaar, H. Huizenga, J. Lof, J. C. Stroom, J. W. Leer, and A. Brahme, "Investigation of the added value of high-energy electrons in intensity-modulated radiotherapy: Four clinical cases," Int. J. Radiat. Oncol., Biol., Phys. **52**(1), 236–253 (2002).
[42]A. A. Perez, M. V. Pilepich, and F. Zivnuska, "Tumor control in definitive irradiation of localized carcinoma of the prostate," Int. J. Radiat. Oncol., Biol., Phys. **12**(4), 523–531 (1986).

Appendix II

Comparisons of Treatment Optimization Directly Incorporating Systematic Patient Setup Uncertainty with a Margin-based Approach

Joseph A. Moore

J. J. Gordon

Mitchell Anscher

Joaquin Silva

Jeffrey V Siebers

Submitted to Medical Physics

Comparisons of Treatment Optimization Directly Incorporating Systematic Patient Setup Uncertainty with a Margin-based Approach

Joseph A. Moore[1], J. James. Gordon[1], Mitchell Anscher[1], Joaquin Silva[2], Jeffrey V Siebers[1]

[1]Department of Radiation Oncology

Virginia Commonwealth University

Richmond, Virginia 23298

[2]Department of Therapeutic Radiology-Radiation Oncology

University of Minnesota

Minneapolis, MN 55455

Submitted to: Medical Physics

Keywords: IMRT, prostate, probabilistic planning, setup errors, margins

Abstract

Purpose: To develop a probabilistic treatment planning (PTP) method which is robust to systematic patient setup errors and to compare PTP plans with plans generated using a Planning Target Volume (PTV) margin optimized to give the same target coverage probability as the PTP plan.

Methods: Plans adhering to the RT0G-0126 protocol are developed for 28 prostate patients using PTP and margin-based planning. For PTP, an objective function that simultaneously considers multiple possible patient positions is developed. PTP plans are optimized using Clinical Target Volume (CTV) structures and Organ at Risk (OAR) structures. The desired CTV coverage probability is 95%. Plans that cannot achieve a 95% CTV coverage probability are re-optimized with a desired CTV coverage probability reduced by 5% until the desired CTV coverage probability is achieved. Margin-based plans are created which achieve the same CTV coverage probability as the PTP plans by iterative adjustment of the CTV-to-PTV margin. Post optimization, probabilistic dose volume coverage metrics are used to compare the plans.

Results: For equivalent target coverage probability, PTP plans significantly reduce coverage probability for rectum objectives (-17% for D_{35}<65Gy, p=0.0010; -23% for D_{25}<70Gy, p<0.0001; and -27% for D_{15}<75Gy, p<0.0001). Physician assessment indicates PTP plans are entirely preferred 71% of the time while margin-based plans are entirely preferred 7% of the time.

Conclusions: For plans having the same target coverage probability, PTP has potential to reduce rectal doses while maintaining CTV coverage probability. In blind comparisons, physicians prefer PTP plans over optimized margin plans. (Work supported by NIH P01CA116602 and T32CA113277)

Introduction

In planning fractionated external beam radiation therapy, treatment plans developed should be robust to random and systematic inter-fractional patient setup errors to ensure the target volume receives a tumoricidal dose and that organ at risk doses are kept below complication thresholds. The common approach to accommodate setup errors is use a planning target volume (PTV) as a surrogate for the clinical target volume (CTV) during the planning process.[1, 2] The intent of the PTV is to ensure that the CTV receives the prescription dose for an expected percentage of the setup errors. Geometrically, this is accomplished by expanding the CTV by a margin to create the PTV. Margin recipes have been developed which suggest the margin size as functions of the standard deviations (SDs) of random and systematic errors. [3-6] In principle, site and institution-specific SDs can be obtained by direct measurements of a suitable population of patients and margins directly computed. In practice, margins are based on clinical experience and are applied as uniform expansions of the CTV in 3-dimensions, with possible adjustment depending on the site, and adjacent critical structures. In either case, due to the fact that the dose distribution imperfectly conforms to the PTV volume, the percentage of setup errors in which the CTV receives the prescribed dose level can differ from what is expected for a given PTV margin. [7, 8] The CTV coverage is dictated by the treated volume, which is only indirectly a function of the PTV.

An alternative to margins is to use probabilistic treatment planning (PTP) or robust optimization methods, which ensure CTV coverage by optimizing the treatment plan dose distribution while incorporating the effects of the patient setup uncertainty.[9-22] PTP methods do not require specification of PTVs or planning risk volumes (PRVs). Instead, given the

probability distributions of setup errors, the plan optimization constructs a treated volume to meet the planning criteria without constricting the dose to predefined PTVs/PRVs. When the locational probability distributions of a CTV and organs at risk (OAR) volumes overlap, PTP optimization can directly optimize the trade-offs. PTP permits creation of non-uniform static dose distributions to meet the planning goals when the cumulative effect of patient setup errors are folded into the dose evaluation.

Potential benefits of PTP have been documented for methods designed to accommodate just the random component of the positioning uncertainty[16, 17, 20], and the combined effects of random and systematic positioning uncertainties[9, 13-15, 18, 21, 22]. Considering only the random component, using a dose convolution approach, Balter *et al.*[17] found that PTP reduces the treated volume by 6-8% as compared to a margin based approach for focal liver tumors. Using multiple offset replicas of a the patient's geometry to accommodate random errors, McShan et al.[20] confirmed that PTP reduced normal tissue doses and created plans which were more robust to positioning errors than margin-based plans. For prostate, Moore *et al.*[16] used a fluence convolution to mimic the random patient positioning variability in the accelerator coordinate system and found that PTP reduced the dose to local normal tissue by 48% and increased the probability of uncomplicated tumor control (P+) by 2.5% compared to margin-based methods.

Considering both random and systematic errors, using a stochastic optimization of P+ including the effects of setup uncertainties, Lof et al.[9] demonstrated the potential for PTP to increase P+ compared to margin-based methods. For various treatment sites and using different Effective Uniform Dose (EUD)-based PTP optimization approaches, Baum et al.[22] ,

Birkner et al. [18], Yang et al. [21], and Witte et al.[13] each found increased OAR sparing compared to a margin-based methods. Yang confirmed improved OAR sparing even over methods that incorporate an ICRU 62 PRV.[21] Gordon et al.[14 15] used probabilistic DVH-based coverage criteria, evaluated via sampling setup error probability distribution functions, as an optimization goal, and found that, compared with standard margins, a ~20% average reduction in volume receiving the treatment dose could be achieved while maintaining desired target coverage probabilities, or an increased target coverage probability could be achieved for same OAR dose.[14] While the potential benefits of PTP using EUD or specialized coverage-based objective functions seem clear, except for Gordon et al[14, 15] who used 27/28 prostate patients and Witte et al. who used 19 prostate patients, these prior PTP studies are mainly demonstration studies, limited to at most 3 patients per treatment site. Furthermore, none of these studies is backed up with physician evaluation of the resultant treatment plans.

The purpose of this work is to explicitly incorporate dosimetric effects of random and systematic setup uncertainties into treatment plan optimization by performing a joint optimization over multiple probable patient setup positions. Due to its ability to consider relative locations of targets and risk structures during the optimization, it is hypothesized that this optimization method will produce plans with similar target coverage while reducing the dose received by treatment risk structures compared with margin-based plans. This is evaluated by comparing the PTP plans with margin-based plans. The primary differences from previous work include study of a large patient population, use of dose-volume objectives for optimization, and analysis with coverage probability, probabilistic dose-volume histograms, and physician assessment.

Methods and Materials

This study compares margin-based and PTP-based treatment plans for a series of 28 prostate patients. For each patient, the process is split into three steps: (1) a PTP plan is created and the coverage probability is evaluated; (2) a margin-based plan is created with the same coverage probability (within tolerance) as the PTP plan; (3) metrics are compiled for each plan and used for plan comparison. This process is repeated until the entire patient population has been analyzed. Figure 1 shows the overall flow of the comparison process. The patient contouring and planning steps are described in detail in the sub-sections below.

Planning parameters

Imaging and contour data from 28 prostate patients treated under an approved institutional review board protocol are used in this study. The plan used for the patient treatment is discarded and new plans are generated for this virtual plan comparison study. Patient plans are generated with a research version of Pinnacle^3 8.1y (Philips Medical Systems, Fitchburg, WI) using a 7-beam setup with beam angles of 30^o, 80^o, 130^o, 180^o, 230^o, 280^o and 330^o, with the 180^o beam corresponding with a posterior beam. The dose matrix resolution of 4×4×4 mm^3 is used during the intensity modulation optimization. The CTV is defined as the prostate plus seminal vesicles. PTP directly uses the CTV during the optimization. For margin-based planning, the PTV is a uniform expansion of the CTV. The size of the CTV-to-PTV margin is adjusted to match the CTV coverage achieved during the PTP planning (described below). The optimization objectives are based on the RTOG-0126 protocol (shown in Table 1). The PTP plans use custom objective functions (described below) while the margin-based plans use the

standard objective functions available in Pinnacle. The patient setup errors are assumed to be normally distributed with a standard deviation in systematic uncertainty of 3 mm in each direction and the standard deviation in the random setup error of 3 mm. The use of normally distributed setup errors equal in each direction for this planning comparison study is justified in the discussion.

Probabilistic treatment planning

The main PTP optimization (Figure 2) consists of two stages; creating an initial PTP plan followed by adjusting objective function weights to achieve acceptable coverage. To improve efficiency, the PTP optimization (Figure 4) is wrapped in a loop (Figure 3) which progressively increases the number of systematic errors sampled during the optimization. At the core of the PTP optimization is computation of the objective function and gradients used for updating the beam intensity profiles during the optimization. At initiation, objectives and weights are defined as shown in Table 1. An additional zero-weight target objective is added using a contour created by expanding the CTV contour by 1 cm. This objective ensures that active intensity values exist in locations where the target can be shifted to during the optimization. Since this objective has zero weight, it has no effect on the solution other than setting the initial intensities.

The general flow of creating an initial PTP plan is shown in Figure 3. At initiation, the optimizer defines an initial uniform beam intensity which fully covers structures identified as target objectives for each beam. Systematic setup errors are simulated by shifting the dose distribution with respect to the patient anatomy and evaluating the objective function multiple

times during the optimization. Initially, the number of systematic offsets $nSys = 8$. Optimization proceeds till convergence, then $nSys$ is doubled and the inner optimization process restarts using the last intensity matrix as the initial intensity matrix. When $nSys = 128$ the initial PTP optimization is complete.

The inner loop of the PTP process is shown in Figure 4. Note that initiating the process with the intensity matrix optimized in prior iterations, the process is jump-started permitting convergence with fewer iterations. Random setup uncertainties are incorporated into the optimization process in the dose computation step by convolving each beam's incident fluence with a σ=3 mm Gaussian in the dose calculation process. See (Moore et al. 2009) for details. Following dose computation, the planning objective function is evaluated for a sequence of $nSys$ randomly sampled patient systematic errors. Assuming the dose distribution in the accelerator coordinate system is invariant to small patient shifts[23], a systematic setup error corresponds with an offset of the dose distribution with respect to the patient's anatomy. Offsets s are sampled from a Gaussian distribution with Σ=3 mm. Each sampled systematic setup error s and associated objective function F_s (described below) evaluation therefore corresponds with a probable treatment course. Every s generates an objective function gradient matrix, $G_{i,s}$, where the 3D matrix contains elements for each voxel i of the dose matrix. The cumulative objective function gradient for each voxel G_i is used to update the beam intensity matrix during the optimization, and the total objective function F is used to evaluate optimization convergence. The optimization terminates when the objective function F changes by less than 1×10^{-6} from the value in a preceding iteration or when 500 iterations have been completed.

Objective function

Dose-volume based objective functions are used in the simultaneous optimization over multiple sampled systematic errors. A standard maximum dose-volume objective function can be expressed as

$$f^{MaxDVH} = \frac{1}{N_{roi}}\left(p \sum_{i}^{N_{roi}} H\left(D_{V_{Rx}} - D_i\right) \cdot H(D_i - D_{Rx}) \cdot (D_i - D_{Rx})^2 \right)$$

where N_{roi} is the number of voxels in the region of interest (ROI) in which the dose-volume objective is being applied, p is the relative weight of the objective and is used when multiple objective functions are summed, D_{Rx} is the desired prescription dose, $D_{V_{Rx}}$is the dose at the prescription volume such that $V\left(D_{V_{Rx}}\right) = V_{Rx}$, D_i is the dose in voxel i and H is the Heaviside function. A minimum dose-volume objective, f^{MinDVH}, can be similarly defined. Details of dose-volume-based objective functions are described by Wu and Mohan[24].

In PTP optimization the dose-volume objective function is evaluated for multiple potential treatment courses. Each treatment course is represented by a systematic shift s of the patient anatomy. For a given shift, s, the objective function is calculated by replacing D_i with the value from the shifted anatomy D_{i+s} and calculating $D_{V_{Rx}}$ for the shifted dose distribution $D_{V_{Rx},s}$ giving

$$f_s^{MaxDVH} = \frac{1}{N_{roi}}\left(p \sum_{i}^{N_{roi}} H\left(D_{V_{Rx},s} - D_{i+s}\right) \cdot H(D_{i+s} - D_{Rx}) \cdot (D_{i+s} - D_{Rx})^2 \right)$$

The total objective function for a single ROI is obtained by summing over each systematic error sampled:

$$f = \sum_{s}^{nSys} f_s^{MaxDVH}$$

This results in each shifted anatomy contributing a component of the total objective function effectively creating a simultaneous optimization over all sampled shifts.

Note that in the equations above, a Heaviside function dependent on $D_{V_{Rx,o},s}$ is used such as $H\left(D_{V_{Rx,o},s} - D_{i+s}\right)$. $D_{V_{Rx,o},s}$ is dependent on the dose distribution underlying a specific shift and must be recomputed for each shift. Generally, $D_{V_{Rx,o},s}$ will vary from shift to shift and thus changes the range of voxels the objective function operates on.

Weight-adjusted PTP plan

Post initial optimization, the PTP plan is adjusted to ensure that the CTV D_{98} dose volume metric achieves a desired coverage probability[14, 15] Q_D, where the Q_D gives the probability of a treatment course meeting the specified dose volume metric. To obtain a plan with the desired Q_D, the planning objective weights are adjusted using an iterative binary search. Only rectum and bladder weights are changed, and adjusted bladder weights are equal to adjusted rectum weights. Initially, the desired coverage probability (Q_D) is set to 95%. The iterative binary search investigates the weight range between 0 and 100, and halves the search range at each step until the desired weight is located. If the desired Q_D cannot be achieved, Q_D is reduced by 5% and the search process re-initiated until an achievable value is reached. The iterative weight search process is stopped when the achieved coverage is within 0.5% of the desired coverage or the change in weight would be less than 1. The end result of this process is the final optimized PTP plan with a known Q_D.

Coverage optimized margin plan

To provide a fair comparison between margin-based planning and PTP, a margin-based plan is created which as the same Q_D as the final PTP plan. The method used to create a margin-based plan with a specific Q_D is similar to the iterative procedure described by Gordon et al.[15] The objective function weights for the margin-based plan are given in Table 1. A uniform CTV-to-PTV margin M_T is used. To enforce OAR avoidance, each OAR structure is expanded by 1 cm to produce a PRV. Note, this 1 cm margin roughly corresponds with the value which would be recommended using the van Herk and Stroom margin formulas.[4-6] The PRVs are not changed during the margin optimization process, but the CTV margin M_T is permitted to vary in the range of 0 cm to 1.0 cm. Similar to the process used to determine appropriate weights for the PTP plan, a binary search algorithm is used to cut the range of margin values in half at each step until the desired coverage probability is reached. The iterative process is stopped when the achieved coverage is within 0.5% of the desired coverage, or the change in margin would be less than 0.05 cm.

Comparison Metrics

For both the final optimized PTP plan and the coverage optimized margin plan, coverage probabilities for all planning structures are computed along with Probabilistic Dose Volume Histograms (PDVHs) and Dose Volume Coverage Maps (DVCMs)[15] using the methods developed by Gordon et al[7, 14]. A DVCM is a probability map which gives the probability of dose-volume values for a simulated set of setup errors. A DVCM is constructed by generating DVHs for many systematic shifts and computing the probability that the DVH curve lies above each dose-

volume point. For this study, DVCMs are created assuming normally distributed 3 mm systematic and 3 mm random setup errors. Coverage values are read off at DVCM dose-volume pairs. To compare PTP and margin-based plans, coverage values are output for each optimization criteria dose volume pair. A PDVH is a pseudo DVH created by interconnecting points at a given probability level on a DVCM. To assist in plan comparison, DVCMs are imported into Matlab for display. Planning criteria for each structure are overlaid on the DVCMs to ease data interpretation. For a given patient, coverage values for two different planning scenarios can be compared by looking at the difference in the DVCMs. Dose-Volume Coverage Difference Maps are computed by subtracting one DVCM from another, e.g. the DVCM from the margin-based plan is subtracted from the DVCM from the PTP plan. DVCDM map values range from -1 to 1. Negative values indicate that the PTP plan has lower coverage for the dose-volume pair and positive values indicate that the PTP-base plan has a higher coverage for the dose volume pair. To avoid dose interpolation errors, dose is recomputed on a $2\times2\times2$ mm^3 grid prior to coverage probability evaluations.

For comparing CTV PDVHs, 95 percentile values are used, which means that DVH values for 95% of the errors simulated will lie above the PDVH curve. For OARs, 5 percentile values are used so that 5% of the with-error simulated DVH values lie below the PDVH curve.

For each patient, DVHs and PDVHs for PTP and margin-based plans are also evaluated by two physicians to determine plan acceptability and preference. DVH and PDVH curves are generated and displayed for the target, bladder, rectum, left femur and right femur structures. PDVHs are computed as above. For targets, DVHs were presented for nominal PTVs obtained by expanding the CTVs uniformly by 0.7cm, except posteriorly where the expansion is 0.3cm.

These nominal PTVs were used in preference to the actual PTVs used in optimizing margin-based plans, since they corresponded to current clinical practice at our institution, and therefore produced target DVHs that the physician could compare to familiar clinical examples. All curves for a given analysis type are presented on a single plot for each patient. Markers are placed on the graph to indicate the planning objectives used during optimization. To avoid bias, PTP and margin-based plans for each patient are randomized and labeled as A or B. Plots are presented to the physician to determine if a plan would be acceptable to treat and if both plans are acceptable, which plan would be the preferred plan to treat the patient.

Results

An example of a static DVH and a PDVH is shown in Figure 5. Table 2 lists the physician preference for each plan. Using static DVH plots for comparison, both physicians prefer the PTP plan for 23 patients while the margin plan is preferred for 2 patients. For 3 patients, one physician prefers the PTP plan, while the other prefers the margin plan. Using PDVH plots for comparison, both physicians prefer the PTP plan for 21 patients while the margin plan is preferred for 4 patients. For 3 patients, one physician prefers the PTP plan while the other prefers the margin plan. For 20 of the 28 patients, all physicians prefer the PTP plans using all assessment methods. The margin plan is preferred using all methods for only 2 patients.

For all patients, the margin required to meet the coverage in the PTP plan was recorded. The average margin required to match the PTP plan was 0.60 cm (min 0.46 cm, max 0.97 cm, SD 0.11 cm). The van Herk margin formula (VHMF) suggests a margin of 0.96 cm. This value only matched one sample using the optimized margin method, all others were lower. The specific

plan which matched the VHMF produced 99.8% coverage probability to the CTV for the margin plan and 99.6% coverage for the PTP plan. The margin suggested by the VHMF being larger than the margin required using iterative margin expansion is consistent with the results shown by Gordon et al.[7] In that work, it was shown that the volume receiving the prescription dose, termed the treated volume in ICRU nomenclature, is larger than the CTV-to-PTV margin, therefore yields greater coverage.

DVCMs and DVCDMs for the CTV, bladder, rectum and femur for Patient 1 are shown in Figure 6. The trends in the data found for Patient 1 are typical of those for other patients. For the CTV, the DVCMs are similar, but not identical. Similarity is expected since the margin-based plan optimization is adjusted to provide the same coverage as the PTP plan. The CTV D_{98} dose-volume objective has on average 90% coverage probability. Above D_{98}, dose coverage rapidly drops falling off towards the D_2 objective, with 45% at D_2. The rapid dose fall-off results from the upper and lower optimization DVH objectives which are set to achieve a uniform CTV dose. The DVCDM, which compares the PTP and margin-based DVCMs, shows a difference band with a width of ~1 Gy. These minor differences are expected since, although the margin-based coverage was optimized to be equivalent, even if the margin and PTP-based coverage values are equivalent at D_{98}, coverage diverges at other dose values since the PTP and margin-based dose distributions differ. Although the primary convergence criterion requires coverage probability agreement within 0.5%, for some patients, target coverage differs by up to 8%. In the margin-based plans, target coverage can be very sensitive to slight changes in margin, thus it was not feasible to achieve exactly the same coverage as in the PTP plans. However, slight

differences in target coverage were evaluated by physicians in their assessment of plans, and were judged not to be clinically significant.

Larger differences in DVCMs are observed for the OARs as shown in Figure 6. To understand the clinical meaning of the differences observed, it is it is useful to sub-divide OAR DVCMs into 3 regions as shown in Figure 7: Region A is completely below the plan optimization objectives. Differences in region A can be considered to be unimportant as they are below the plan objectives. If doses in region A are deemed to be important for planning, an objective should be added to control dose in these areas, resulting in the point being moved to either region B or C. Region B is completely above the plan optimization objectives and is a clinically important region since this is where the optimizer failed to reduce the dose below the plan objectives. Region C is the intermediate region near the plan objectives, and is also clinically important since it demonstrates the objective function tradeoffs as the plan optimizer finds a solution.

The general trends seen for Patient 1 are evident for all patients: when an OAR dose is near the plan objectives, PTP reduces dose coverage in that region. This shows as blue in the DVCDM. However, PTP increases dose coverage at dose-volume regions well below the objective values. This shows as red in the DVCDM. From the methods used in this study, it cannot be determined if the increased OAR volumes receiving low doses is inherent to PTP or if adding dose-volume objectives for the lower volumes would push the dose to unspecified tissues. PTP shows higher coverage – the probability of the DVH curve exceeding the dose for a given volume – for all OARs in region A well below the planning objectives. For the bladder, neither method shows coverage in region B, while both methods show coverage in region C.

PTP plans showed higher bladder coverage in region C for 9 out of 28 patients, while 5 patients showed higher coverage in the margin-based plans. For the rectum, none of the PTP plans showed coverage in region B while 7 out of 28 patients showed coverage in the margin-based plans. Margin-based plans showed higher rectal coverage in region C for 20 out of 28 patients while PTP plans show rectal coverage in region C for only one patient. For the femur, neither method shows coverage in region B. Femoral coverage is very low in both methods in region C. For the left femur a small dose tail extends out to the 5000cGy max dose objective in 21 out of 28 PTP plans, and 12 out of 28 for margin-based plans. For the right femur the tail reached the objective in 22 out of 28 PTP plans, and 12 out of 28 margin-based plans.

The average coverage probability for each structure is shown in Table 3. Target coverage probability is generally the same for each patient due to the design of the study. The average difference in coverage probability between PTP and margin plans is 0.7% +/- 2.7%. The difference is not significant ($p=0.17$) with a paired t-test.

For organs at risk, the average coverage probability over all patients for PTP plans decreased 17% for the rectum $D_{35}<65$Gy objective ($p=0.010$) as compared to margin-based plans, decreased 23% for the rectum $D_{25}<70$Gy objective ($p<0.0001$) and decreased 27% for the rectum $D_{15}<75$Gy objective ($p<0.0001$). The bladder coverage changes are smaller, with PTP resulting in $D_{50}<65$Gy increased by 2% ($p=0.0005$), $D_{35}<70$Gy increased by 3% ($p=0.156$), $D_{15}<80$Gy decreased by 6% ($p=0.0146$), left femur 50Gy max increased by 4% ($p=0.0078$) and right femur increased by 6% ($p=0.0024$) when compared to margin-based plans. Coverage for other objectives did not change significantly.

Discussion

This study assumes random and systematic setup errors with standard deviations equal to 3 mm in each direction to simulate setup uncertainties. These numbers are typical of setup error values reported in the literature for (implanted marker-based) image alignment.[4, 5, 13, 18, 25, 26] For the comparison purposes of this study, matching the setup-error to the clinical setup error is not required. While the general PTP method described in this paper allows non-normally distributed errors, unequal errors in each direction, and for tissue deformation, margin-based methods typically are not based on these assumptions. Standard margin formulas[3-6] assume normally distributed setup errors, and clinically, margins are typically chosen to be uniform in all directions around a structure, with occasional trimming to avoid nearby organs at risk. Use of normally distributed errors with the same standard deviation in each direction for PTP, while simplistic, realistically mimics the assumptions made in margin based planning, but disregards the flexibility of PTP to address non-normal motion or tissue deformations. Thus, bias introduced by assuming uniform and normally distributed errors will be in favor of the margin based approach. Nonetheless, the results demonstrate the advantages of PTP even when the assumptions of margin-based planning are followed.

In the plan assessment stage, both static DVHs and PDVHs are used in this work. A comparison of static DVH and PDVH curves are displayed in Figure 5. A static DVH represents a single patient setup. To ensure setup uncertainties are considered in planning, PTV DVHs are used to represent the DVH of the CTV.[1] For OARs, ideally PRVs are used to represent likely dose distributions to underlying structures. However, often PRVs are not used in planning, resulting in overly optimistic dose representation. A PDVH curve represents the DVH for a specified

coverage probability. For the curves demonstrated in this work, the probability of CTV doses exceeding the PDVH is 95% and the probability of the dose to the critical structures being lower than the PDVH is 95%. Therefore, it is expected that in 95% of cases, the plan will perform better than the displayed curves.

Comparison of DVHs and PDVHs (e.g. Figure 5 and Figure 8) show that although margin-based plans seemingly meet or nearly meet the OAR optimization criteria when evaluated based on static DVHs, PDVH evaluation reveals a strong likelihood that the optimization criteria will be exceeded. Independent of the planning method, it would be prudent to provide physicians with the PDVH information for plan evaluation to allow incorporation of this information in the plan approval decision making process. Plans which have a significant probability of overdosing OARs should be rejected.

To directly compare margin-based planning to PTP, patient specific coverage optimized margins were used in this study. In routine clinical practice, it is more common to use the same margin for each patient. An accepted method would be to use the van Herk margin formulation to determine the margin, which, for the setup errors assumed in this study would have yielded a margin of approximately 1 cm. Plans produced with a 1 cm margin would have resulted in both higher target coverage probability and an increase in dose to nearby local structures (an increased coverage probability for critical structures) compared to the optimized margins used in this study.

Due to conflicting planning goals produced by PTV and PRV overlap structures and other considerations, PRV margins are often not used in conjunction with PTV-based planning. The 1 cm OAR-to-PRV margins used in this study therefore result in a level of OAR protection often

not afforded by PTV-based planning. If the margin-based portion of this study would be repeated with zero OAR-to-PRV margins, OAR-to-PRV margins equal to the CTV-to-PTV margins, or any value less than 1 cm, the resultant optimized dose distributions would increase OAR doses, further exemplifying the advantages of PTP.

The work in this study required a great amount of computational resources. An average optimization including weight adjustment took nearly two days on a single 2.83 GHz processor. This is unrealistic in a clinical scenario. Fortunately, the methods proposed here can be easily parallelized. Computation of gradients and objective functions for different shifts are independent of each other. With a multiple processor machine or cluster, computation of shifts could be spread to multiple CPUs. Further enhancements and optimization of the code may also reduce the time required.

Conclusions

For the same CTV coverage probability, PTP results in a reduced rectal dose. DVCDMs show that dose is decreased in the neighborhood of the optimization constraints, while dose is increased in unconstrained areas. Physician assessment indicates that PTP plans are preferred by all physicians and assessment methods 71% of the time, while optimized margin-based plans are preferred by all physicians and assessment methods 7% of the time. Significant reductions in coverage of the rectal objectives were achieved (16-27%) though small increases in coverage of the bladder and femurs were observed (2-6%)

Acknowledgements

The author would like to thank Karl Bzdusek and Michael Kaus from Philips Medical Systems for providing assistance in developing code within Pinnacle Treatment Planning System used in this work. This work is supported by NIH grants P01CA116602 and T32CA113277, and a research contract from Philips Medical Systems.

References

1. International Commission on Radiation Units and Measurements., *Prescribing, recording, and reporting photon beam therapy*. (International Commission on Radiation Units and Measurements, Bethesda, Md., 1999).
2. International Commission on Radiation Units and Measurements., *Prescribing, recording, and reporting photon beam therapy*. (International Commission on Radiation Units and Measurements, Bethesda, MD, 1993).
3. M. van Herk, "Errors and margins in radiotherapy," Semin Radiat Oncol **14**, 52-64 (2004).
4. M. van Herk, P. Remeijer and J. V. Lebesque, "Inclusion of geometric uncertainties in treatment plan evaluation," Int J Radiat Oncol Biol Phys **52**, 1407-1422 (2002).
5. M. van Herk, P. Remeijer, C. Rasch and J. V. Lebesque, "The probability of correct target dosage: dose-population histograms for deriving treatment margins in radiotherapy," Int J Radiat Oncol Biol Phys **47**, 1121-1135 (2000).
6. J. C. Stroom, H. C. de Boer, H. Huizenga and A. G. Visser, "Inclusion of geometrical uncertainties in radiotherapy treatment planning by means of coverage probability," Int J Radiat Oncol Biol Phys **43**, 905-919 (1999).
7. J. J. Gordon and J. V. Siebers, "Evaluation of dosimetric margins in prostate IMRT treatment plans," Med Phys **35**, 569-575 (2008).
8. J. J. Gordon, A. J. Crimaldi, M. Hagan, J. Moore and J. V. Siebers, "Evaluation of clinical margins via simulation of patient setup errors in prostate IMRT treatment plans," Med Phys **34**, 202-214 (2007).
9. J. Lof, B. K. Lind and A. Brahme, "An adaptive control algorithm for optimization of intensity modulated radiotherapy considering uncertainties in beam profiles, patient set-up and internal organ motion," Phys Med Biol **43**, 1605-1628 (1998).
10. J. Unkelbach and U. Oelfke, "Incorporating organ movements in inverse planning: assessing dose uncertainties by Bayesian inference," Phys Med Biol **50**, 121-139 (2005).
11. J. Unkelbach and U. Oelfke, "Inclusion of organ movements in IMRT treatment planning via inverse planning based on probability distributions," Phys Med Biol **49**, 4005-4029 (2004).
12. J. Unkelbach and U. Oelfke, "Incorporating organ movements in IMRT treatment planning for prostate cancer: minimizing uncertainties in the inverse planning process," Med Phys **32**, 2471-2483 (2005).
13. M. G. Witte, J. van der Geer, C. Schneider, J. V. Lebesque, M. Alber and M. van Herk, "IMRT optimization including random and systematic geometric errors based on the expectation of TCP and NTCP," Med Phys **34**, 3544-3555 (2007).
14. J. J. Gordon, N. Sayah, E. Weiss and J. V. Siebers, "Coverage optimized planning: probabilistic treatment planning based on dose coverage histogram criteria," Med Phys **37**, 550-563 (2010).
15. J. J. Gordon and J. V. Siebers, "Coverage-based treatment planning: optimizing the IMRT PTV to meet a CTV coverage criterion," Med Phys **36**, 961-973 (2009).

16. J. A. Moore, J. J. Gordon, M. S. Anscher and J. V. Siebers, "Comparisons of treatment optimization directly incorporating random patient setup uncertainty with a margin-based approach," Med Phys **36**, 3880-3890 (2009).
17. J. M. Balter, K. K. Brock, K. L. Lam, D. Tatro, L. A. Dawson, D. L. McShan and R. K. Ten Haken, "Evaluating the influence of setup uncertainties on treatment planning for focal liver tumors," Int J Radiat Oncol Biol Phys **63**, 610-614 (2005).
18. M. Birkner, D. Yan, M. Alber, J. Liang and F. Nusslin, "Adapting inverse planning to patient and organ geometrical variation: algorithm and implementation," Med Phys **30**, 2822-2831 (2003).
19. W. A. Beckham, P. J. Keall and J. V. Siebers, "A fluence-convolution method to calculate radiation therapy dose distributions that incorporate random set-up error," Phys Med Biol **47**, 3465-3473 (2002).
20. D. L. McShan, M. L. Kessler, K. Vineberg and B. A. Fraass, "Inverse plan optimization accounting for random geometric uncertainties with a multiple instance geometry approximation (MIGA)," Med Phys **33**, 1510-1521 (2006).
21. J. Yang, G. S. Mageras, S. V. Spirou, A. Jackson, E. Yorke, C. C. Ling and C. S. Chui, "A new method of incorporating systematic uncertainties in intensity-modulated radiotherapy optimization," Med Phys **32**, 2567-2579 (2005).
22. C. Baum, M. Alber, M. Birkner and F. Nusslin, "Robust treatment planning for intensity modulated radiotherapy of prostate cancer based on coverage probabilities," Radiother Oncol **78**, 27-35 (2006).
23. T. Craig, J. Battista and J. Van Dyk, "Limitations of a convolution method for modeling geometric uncertainties in radiation therapy. II. The effect of a finite number of fractions," Med Phys **30**, 2012-2020 (2003).
24. Q. Wu and R. Mohan, "Algorithms and functionality of an intensity modulated radiotherapy optimization system," Med Phys **27**, 701-711 (2000).
25. C. Baum, M. Alber, M. Birkner and F. Nusslin, "Treatment simulation approaches for the estimation of the distributions of treatment quality parameters generated by geometrical uncertainties," Phys Med Biol **49**, 5475-5488 (2004).
26. T. Craig, E. Wong, G. Bauman, J. Battista and J. Van Dyk, "Impact of geometric uncertainties on evaluation of treatment techniques for prostate cancer," Int J Radiat Oncol Biol Phys **62**, 426-436 (2005).

Figures

Table 1: Planning objectives according to RTOG-0126 with initial weights used in optimization

Structure	Type	Dose (cGy)	Volume (%)	Weight
Target	Min DVH	7920	98	100
Target	Max DVH	8470	2	90
Rectum	Max DVH	6000	50	80
Rectum	Max DVH	6500	35	80
Rectum	Max DVH	7000	25	80
Rectum	Max DVH	7500	15	80
Rectum	Max Dose	8470		80
Bladder	Max DVH	6500	50	80
Bladder	Max DVH	7000	35	80
Bladder	Max DVH	7500	25	80
Bladder	Max DVH	8000	15	80
Bladder	Max Dose	8470		80
Left Femur	Max DVH	3500	50	20
Left Femur	Max Dose	5000		20
Right Femur	Max DVH	3500	50	20
Right Femur	Max Dose	5000		20

480 **Table 2: Physician assessment of PTP and margin-based plans. Preferred plan is indicated for each physician using Probability Dose Volume Histograms or static Dose-Volume Histograms.**

	PDVH		Static DVH	
Patient	Physician 1	Physician 2	Physician 1	Physician 2
1	PTP	PTP	PTP	PTP
2	PTP	PTP	PTP	PTP
3	PTP	PTP	PTP	PTP
4	PTP	PTP	PTP	PTP
5	PTP	PTP	PTP	PTP
6	PTP	PTP	PTP	PTP
7	PTP	PTP	PTP	PTP
8	PTP	PTP	PTP	PTP
9	PTP	PTP	PTP	PTP
10	Margin	Margin	Margin	Margin
11	PTP	PTP	PTP	PTP
12	Margin	Margin	Margin	PTP
13	PTP	PTP	PTP	PTP
14	PTP	PTP	PTP	PTP
15	PTP	PTP	PTP	PTP
16	Margin	PTP	PTP	PTP
17	PTP	PTP	PTP	PTP
18	PTP	PTP	PTP	PTP
19	PTP	PTP	PTP	PTP
20	Margin	PTP	PTP	PTP
21	PTP	PTP	PTP	Margin
22	PTP	PTP	PTP	PTP
23	PTP	PTP	PTP	PTP
24	PTP	PTP	PTP	PTP
25	PTP	PTP	PTP	PTP
26	Margin	Margin	Margin	Margin
28	Margin	PTP	PTP	Margin
30	Margin	Margin	PTP	PTP

Table 3: Coverage for PTP and Margin plans at planning objectives. Change represents coverage of PTP plan less coverage of margin plan. Significance is a result of a 2-sided paired t-test.

Structure	Volume (%)	Dose (cGy)	PTP	Margin	Change	p
BLADDER	50	6500	3	1	2	0.0005
BLADDER	35	7000	10	6	3	0.0156
BLADDER	25	7500	10	11	-1	0.7609
BLADDER	15	8000	5	11	-6	0.0146
BLADDER	0	8470	37	22	14	0.1084
CTV	98	7920	90	91	-1	0.2292
CTV	2	8470	45	32	12	0.2328
FEMUR_LT	50	3500	0	0	0	n/a
FEMUR_LT	0	5000	5	1	4	0.0078
FEMUR_RT	50	3500	0	0	0	n/a
FEMUR_RT	0	5000	6	0	6	0.0024
RECTUM	50	6000	1	6	-5	0.0962
RECTUM	35	6500	9	26	-17	0.0010
RECTUM	25	7000	18	41	-23	0.0000
RECTUM	15	7500	28	55	-27	0.0000
RECTUM	0	8470	19	10	9	0.1794

485

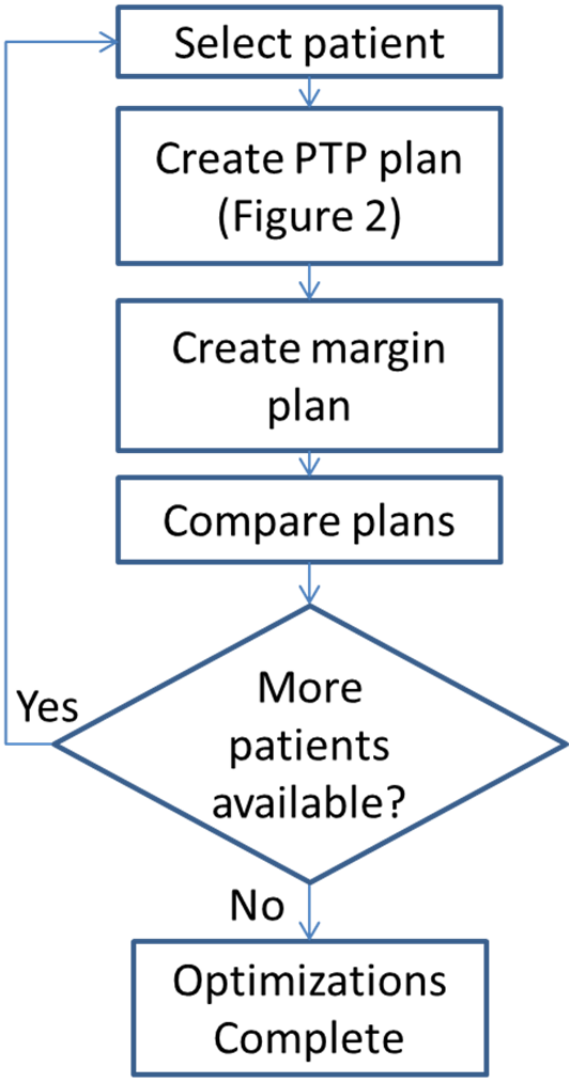

Figure 1: Flow chart describing overall comparison process

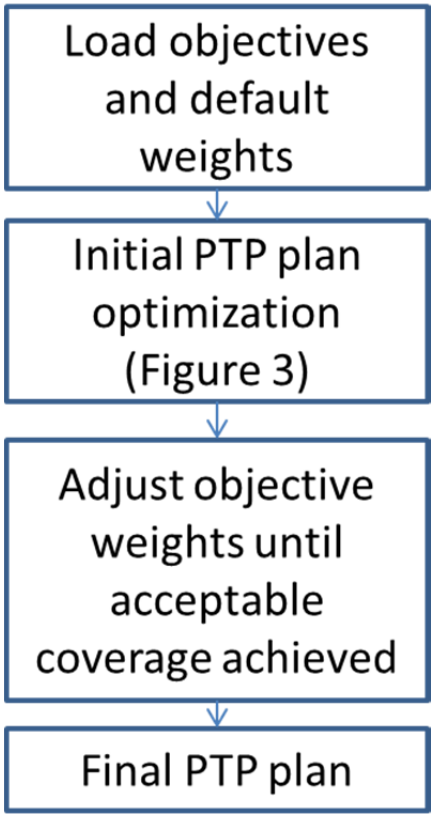

Figure 2: Process for generating the final optimized PTP plan

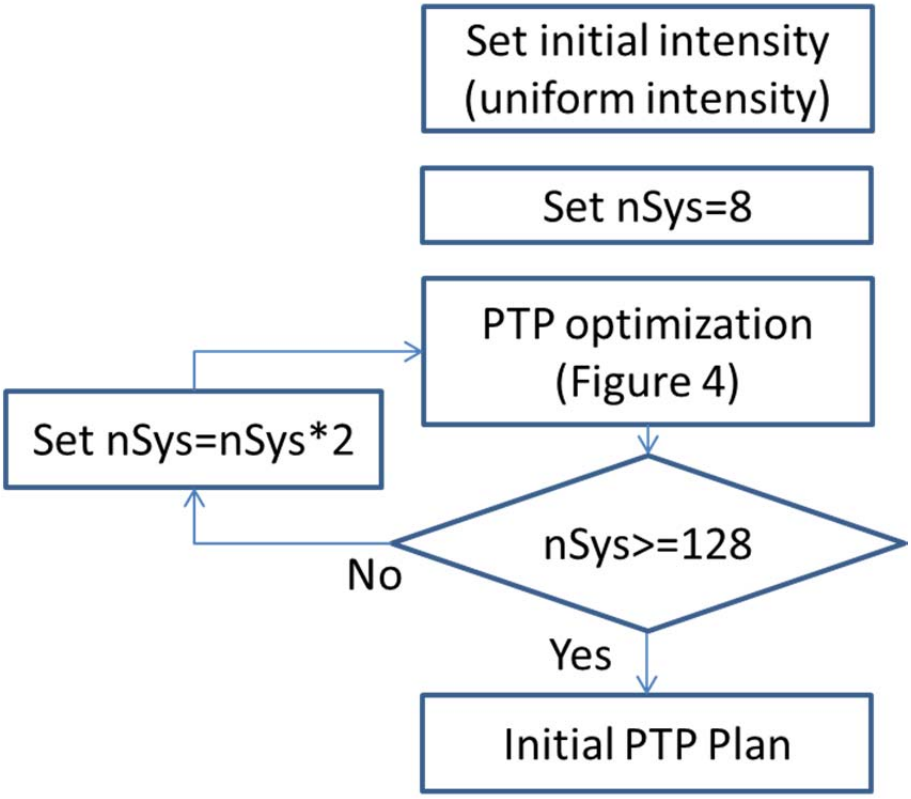

490

Figure 3: Process for generating the initial PTP plan. nSys is the number of systematic shifts used during the PTP optimization process.

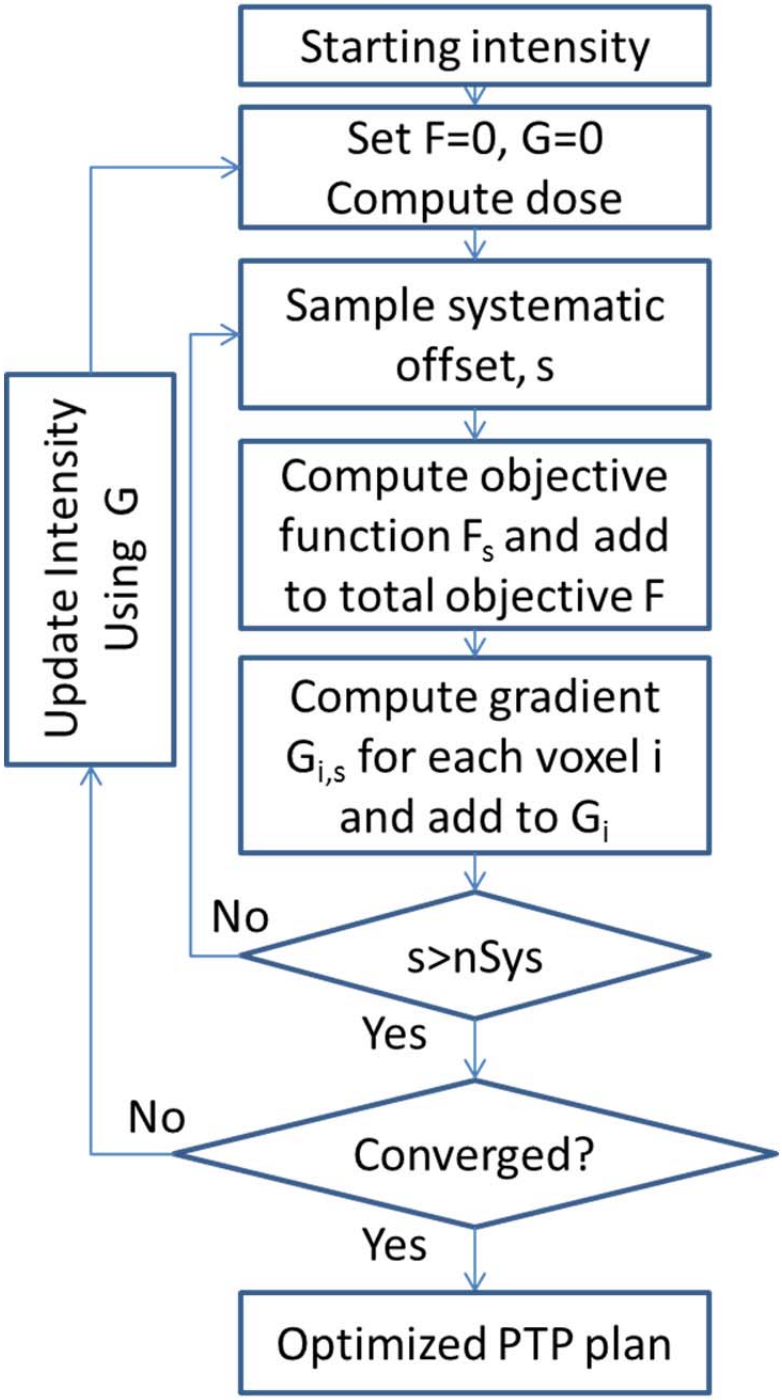

Figure 4: PTP Process to generate an optimized plan accounting for systematic uncertainty. F is the total objective score, G is the total gradient matrix containing the first derivative of the objective function G_i for each voxel i. F_s is the objective function score for shift s

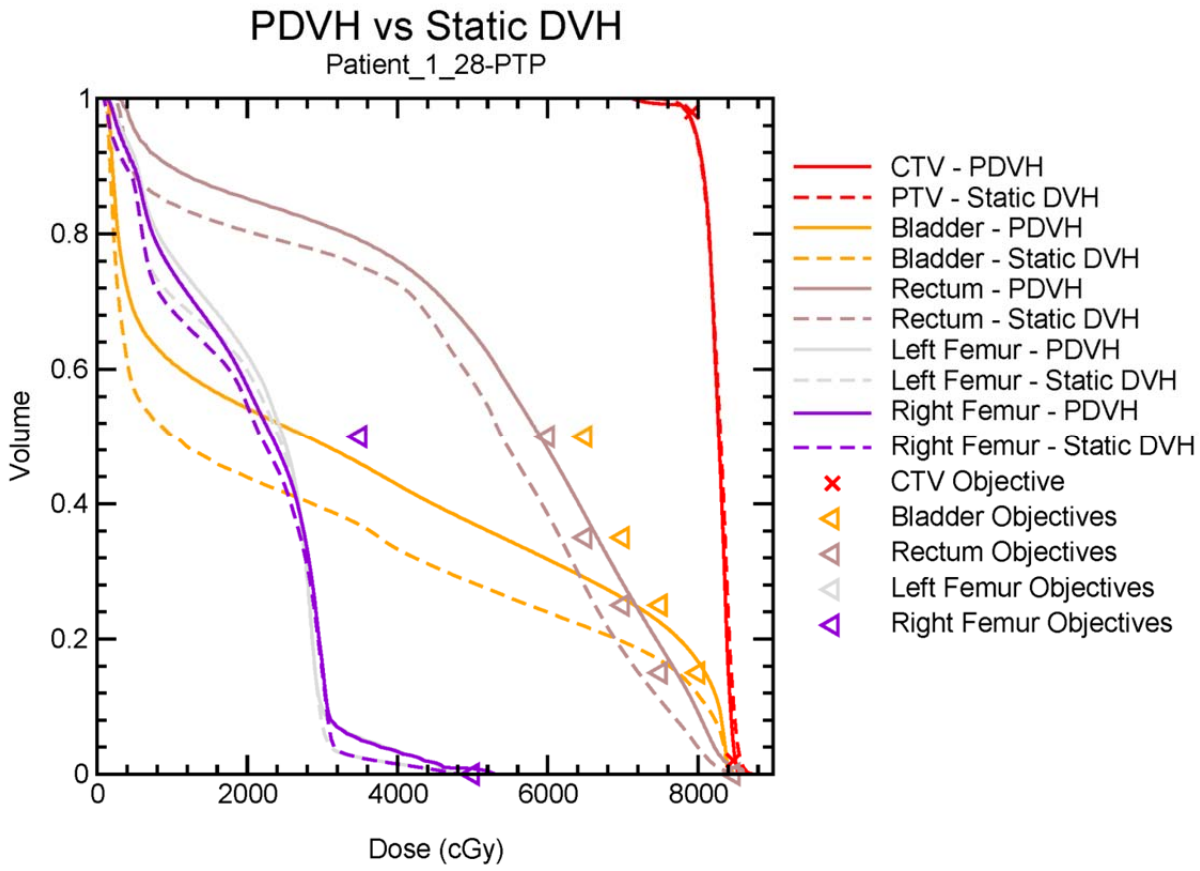

Figure 5: Static DVH and PDVH curves for the CTV, bladder, rectum, left femur and right femur for the PTP generated for Patient 1. Solid lines represent PDVH curves and dashed lines represent static DVH. Objectives used during optimization are given as triangles.

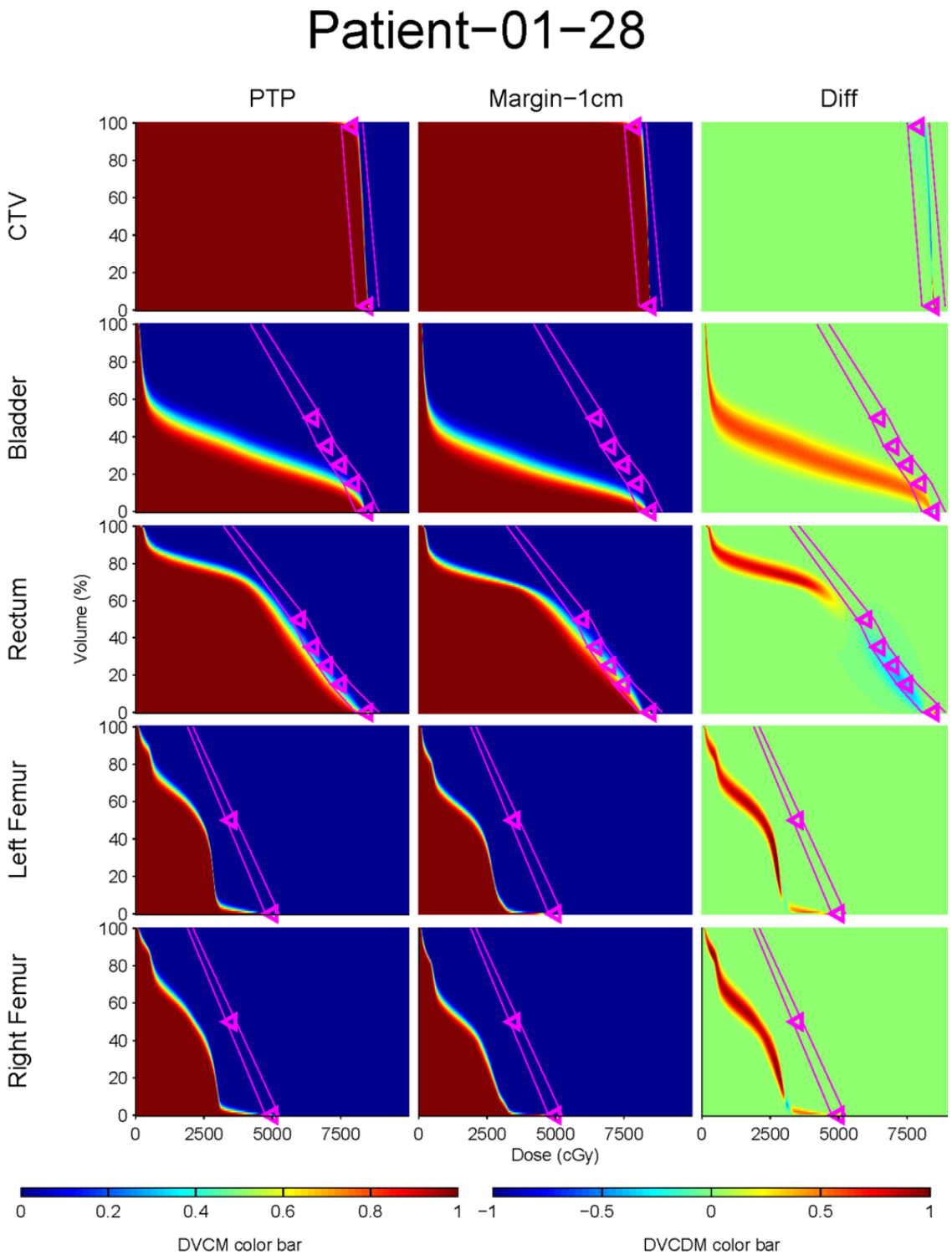

Figure 6: Dose-volume coverage maps (DVCM) and dose-volume coverage difference maps (DVCDM) for the CTV, bladder, rectum and femur for Patient 1. The DVCM indicates the probability that the dose-volume level is achieved in a given treatment course. Triangles on the DVCM indicate the dose-volume planning objectives used during plan optimization. The DVCDM compares the PTP and the margin-based plans. Values less than zero (blue regions) indicate lower doses by the PTP plan compared with the margin plan. Values greater than zero (red regions) indicate higher doses by the PTP plan.

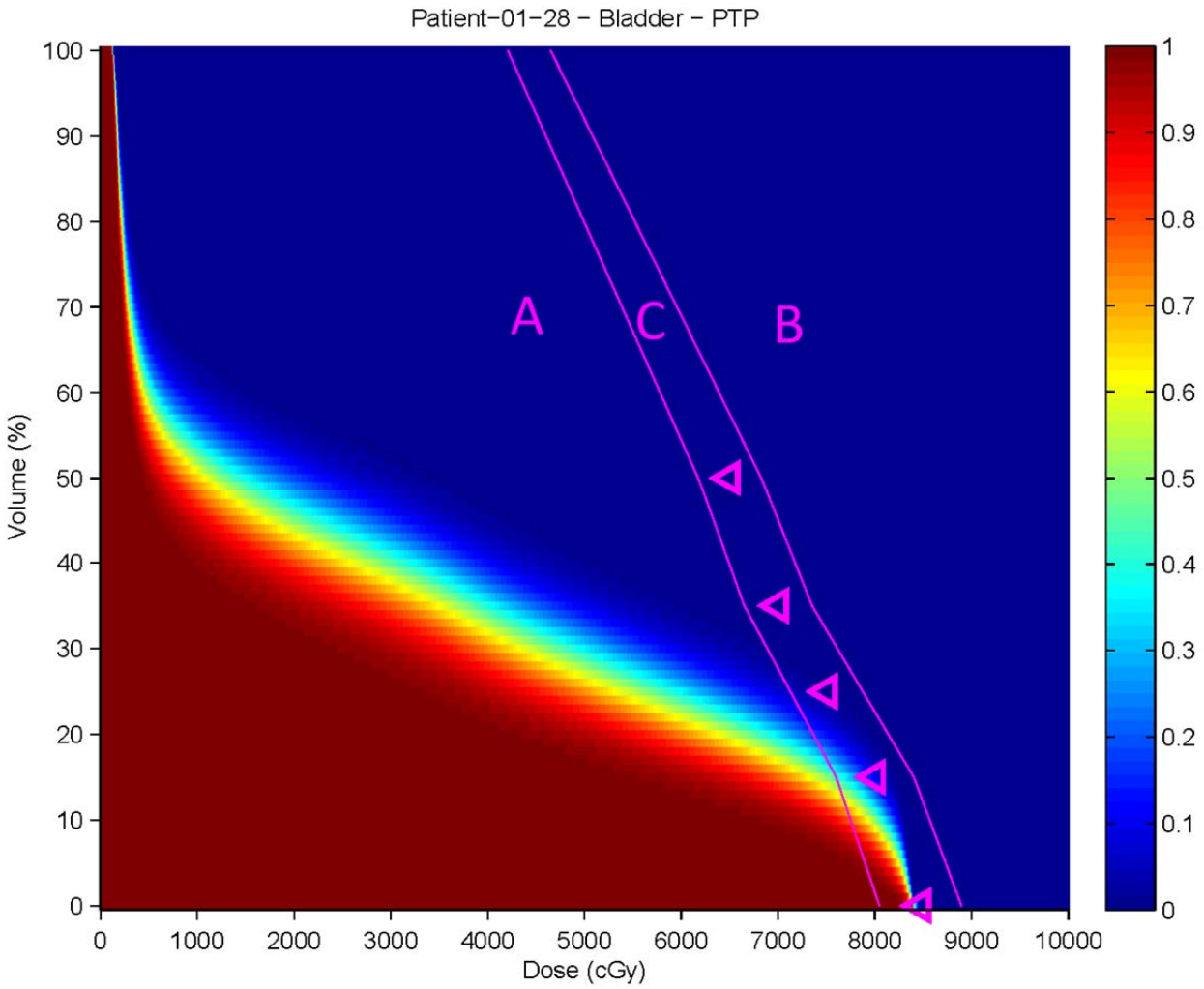

510 **Figure 7: Regions of a DVCM. Region A is below the plan objectives, Region B is above the plan objectives and Region C is the intermediate area near the plan objectives.**

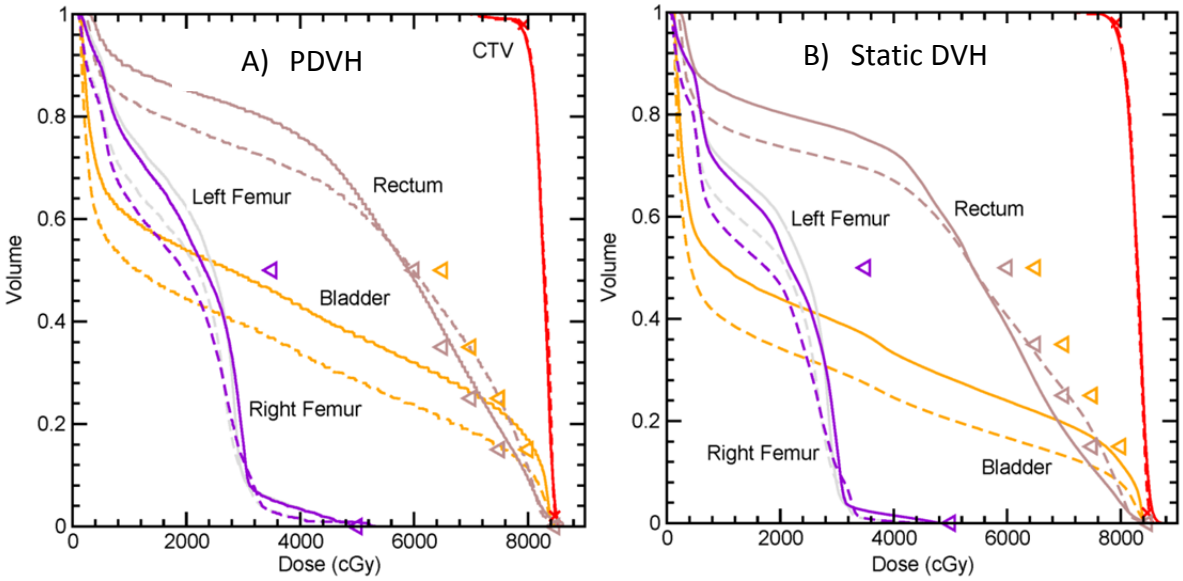

Figure 8: (A) Probability Dose-Volume Histogram for the 95% percentile DVH for the CTV and 5% DVH for the Bladder, Rectum and Femurs for PTP and margin-based plans. (B) Static Dose-Volume Histograms for the CTV, bladder, rectum, left femur and right femur for PTP and margin-based plans. Solid lines represent PDVH curves for the PTP plan and dashed lines represent the margin-based plan. Objectives used during optimization are given as triangles.

Appendix III

Dose-Volume Coverage Maps for all patients used in study. For each patient, DVCMs for PTP plans and margin-based plans are displayed with the Dose-Volume Coverage Difference Map. Maps for the CTV, bladder, rectum, left femur and right femur are presented. For DVCMs, values of 1 indicate 100% coverage probability of the dose-volume point for a given structure for all simulated offsets. Values of 0 indicate zero coverage probability of the dose-volume point for a given structure for any simulated offset. For DVCDMs, positive values indicate greater coverage probability by the PTP plan, while negative values indicate greater coverage probability by the margin-based plan.

Patient−01

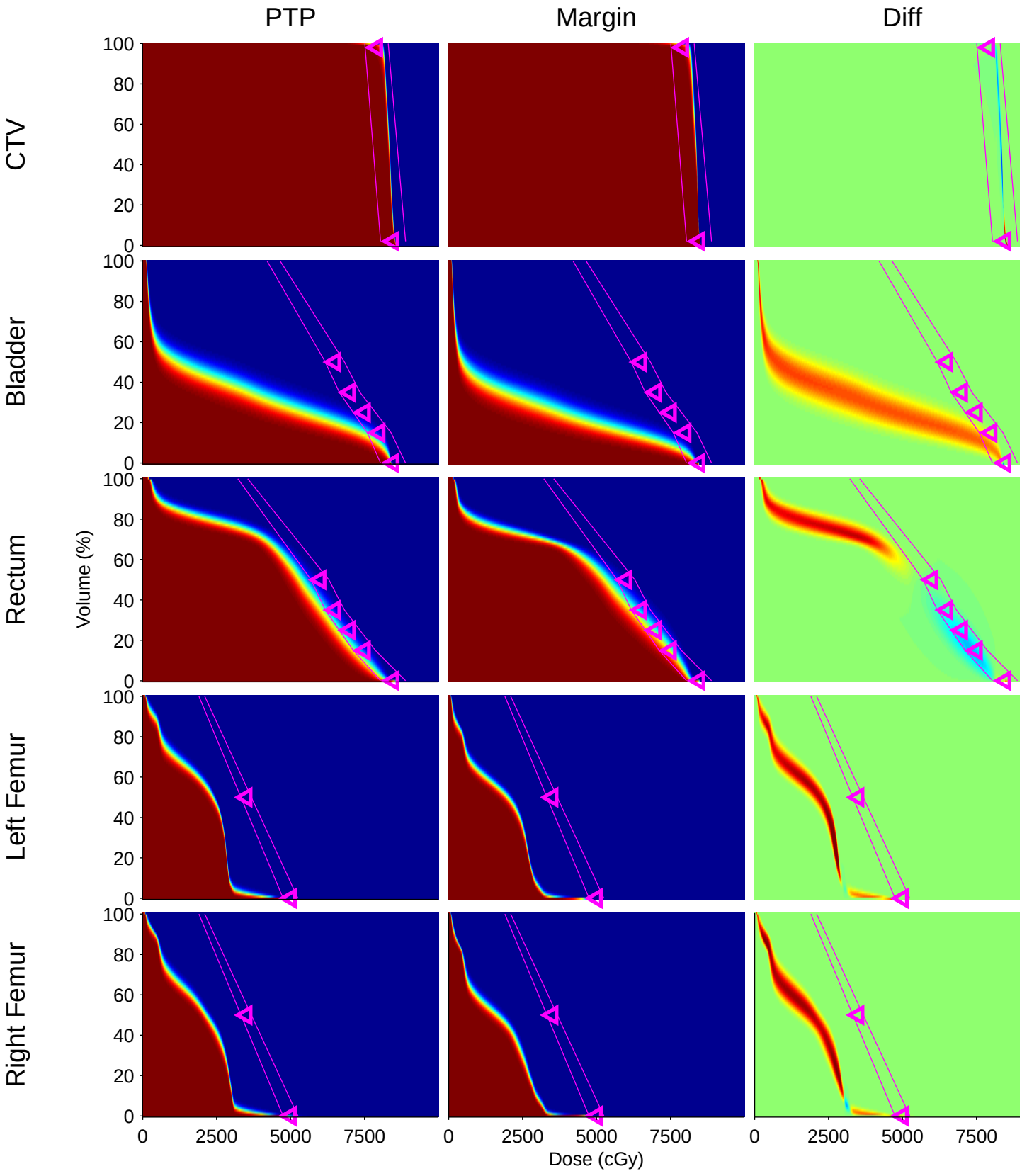
PTP
Margin
Diff
CTV
Bladder
Rectum
Left Femur
Right Femur
Volume (%)
0
20
40
60
80
100
0
2500
5000
7500
Dose (cGy)
0
0.2
0.4
0.6
0.8
1
DVCM color bar
−1
−0.5
0
0.5
1
DVCDM color bar

Patient−02

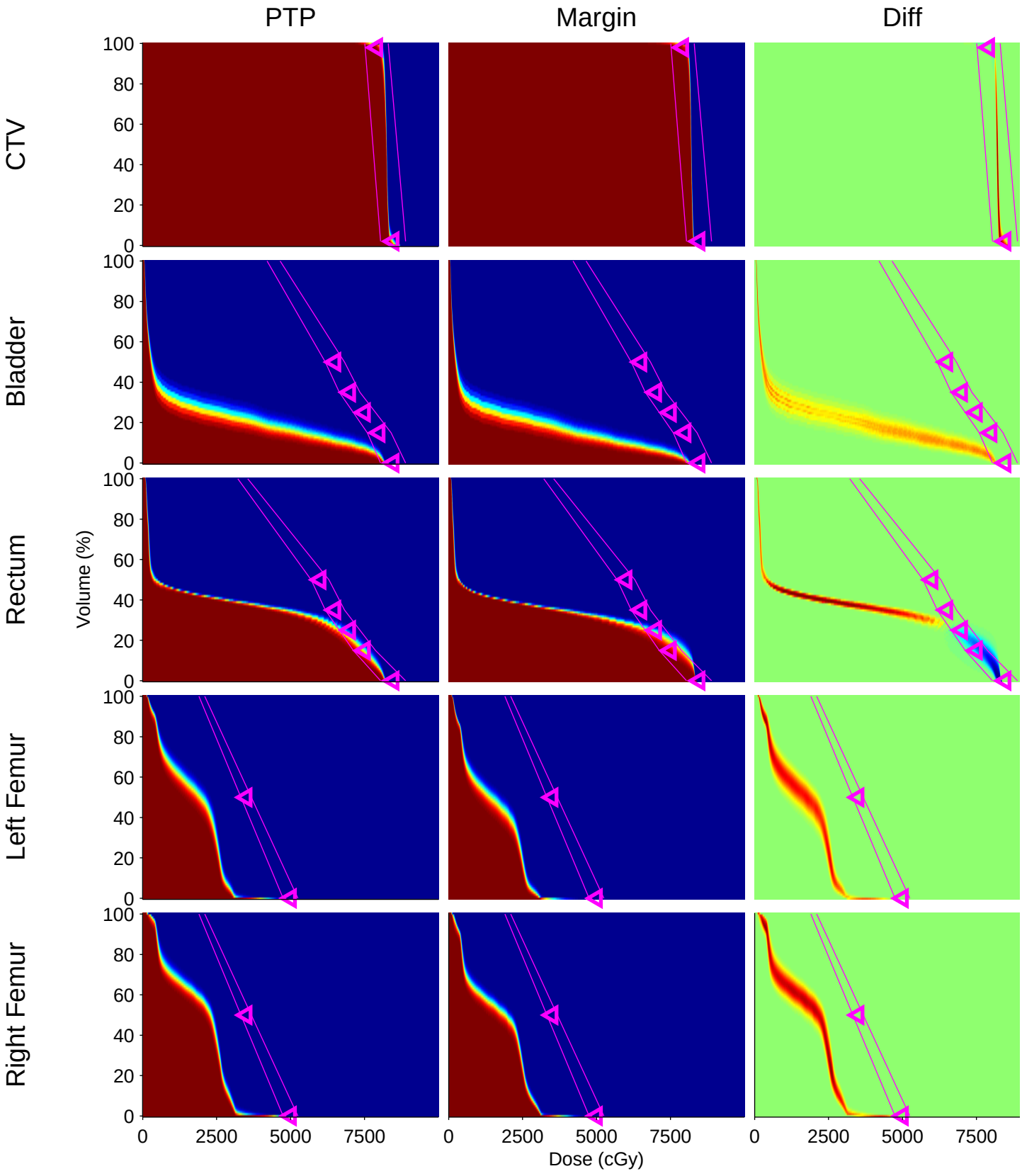
PTP
Margin
Diff
CTV
Bladder
Rectum
Left Femur
Right Femur
Volume (%)
0
20
40
60
80
100
0
2500
5000
7500
Dose (cGy)
0
0.2
0.4
0.6
0.8
1
DVCM color bar
−1
−0.5
0
0.5
1
DVCDM color bar

Patient−03

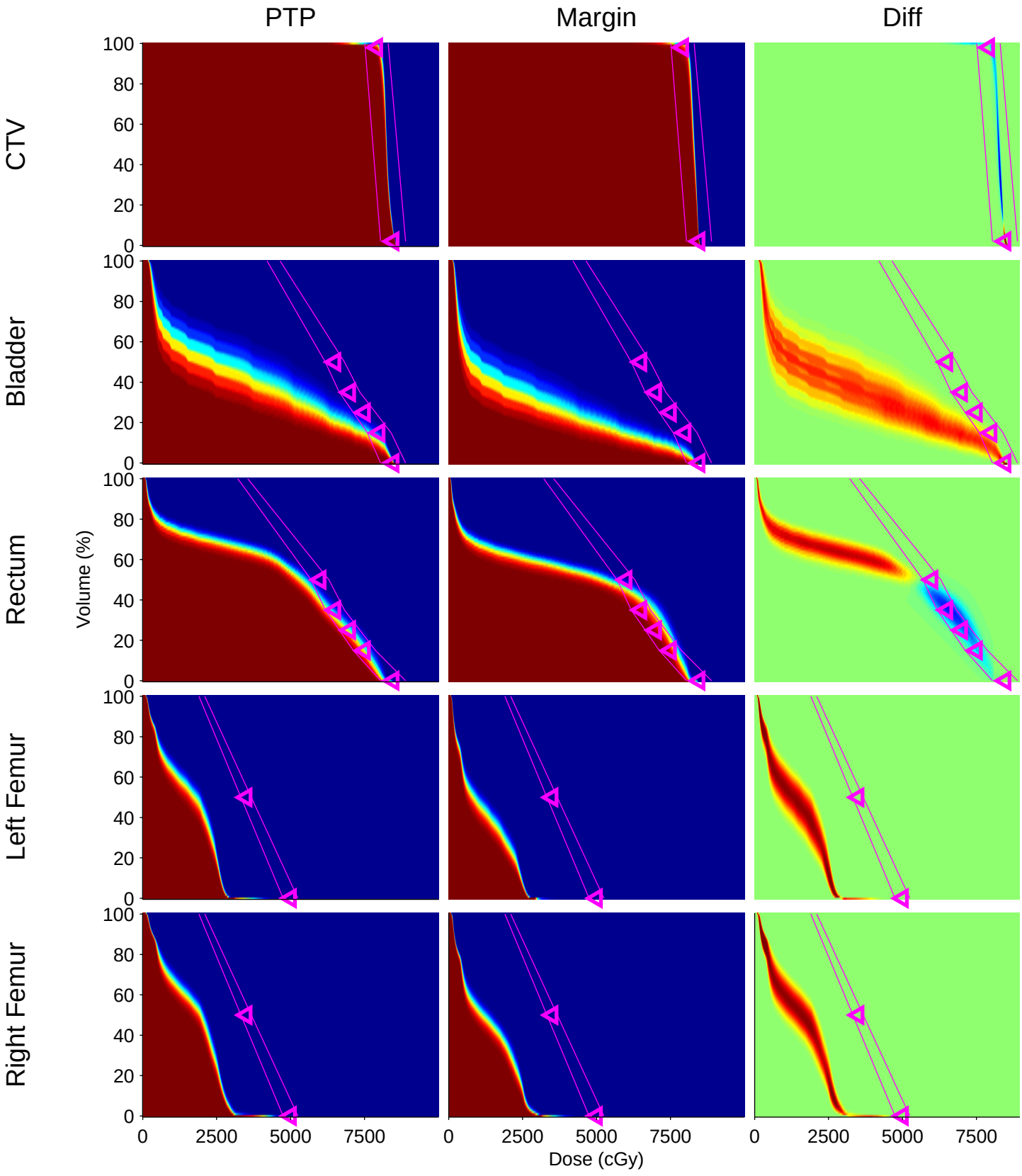
PTP
Margin
Diff
CTV
Bladder
Rectum
Left Femur
Right Femur
Volume (%)
0
20
40
60
80
100
0
2500
5000
7500
Dose (cGy)
0
0.2
0.4
0.6
0.8
1
DVCM color bar
−1
−0.5
0
0.5
1
DVCDM color bar

Patient−04

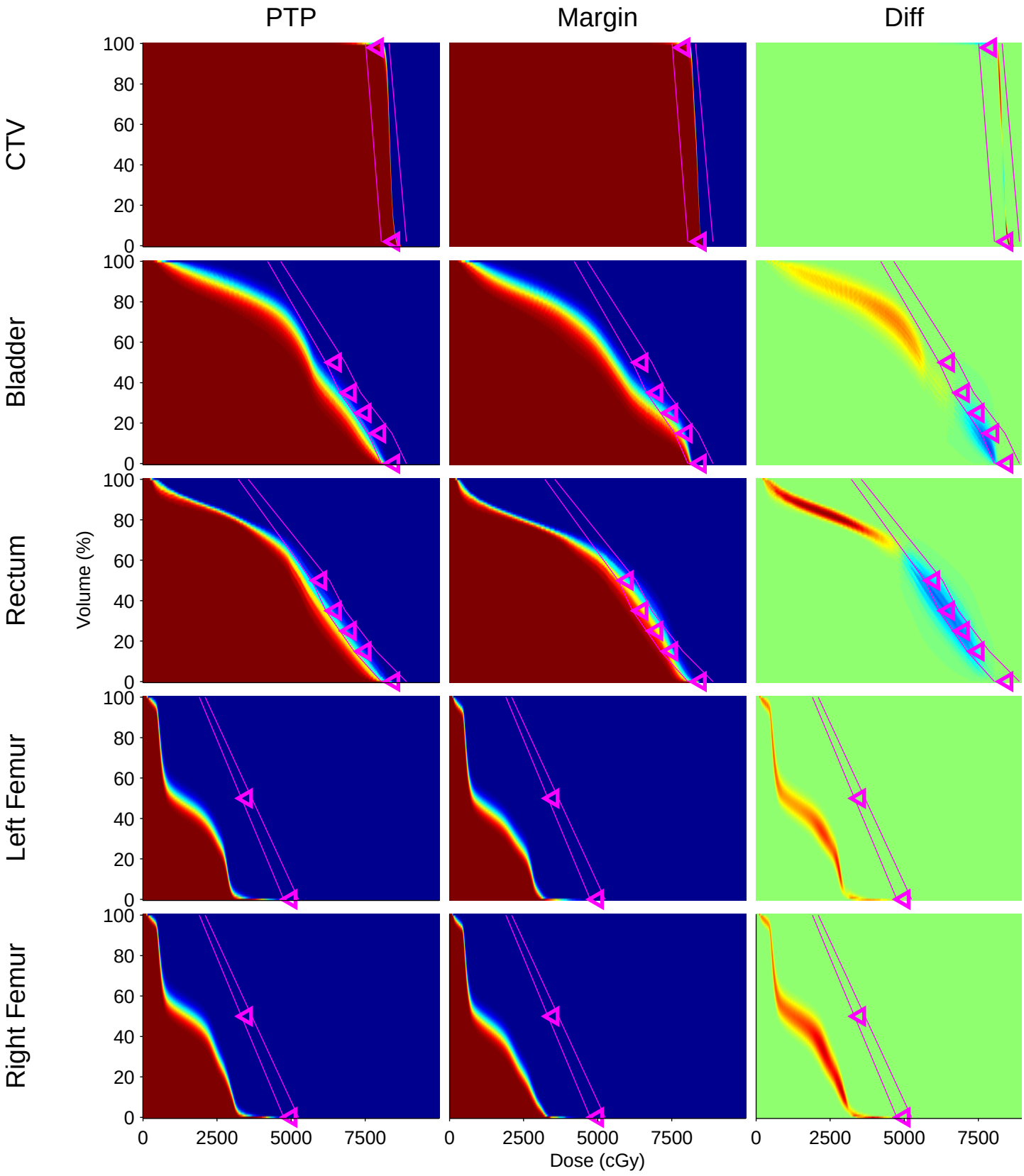
PTP
Margin
Diff
CTV
Bladder
Rectum
Left Femur
Right Femur
Volume (%)
0
20
40
60
80
100
0
2500
5000
7500
Dose (cGy)
0
0.2
0.4
0.6
0.8
1
DVCM color bar
−1
−0.5
0
0.5
1
DVCDM color bar

Patient−05

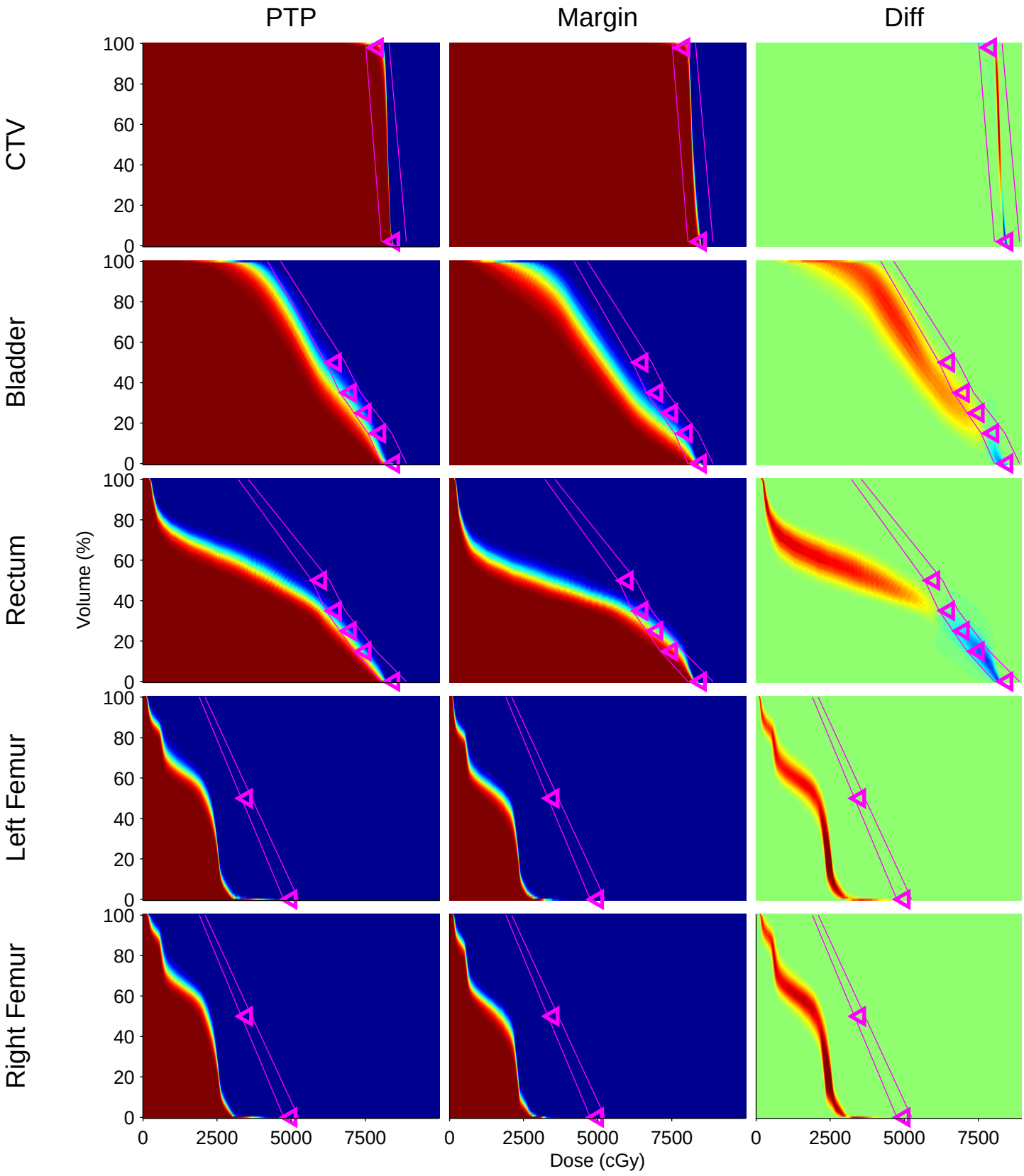
PTP
Margin
Diff
CTV
Bladder
Rectum
Left Femur
Right Femur
Volume (%)
0
20
40
60
80
100
0
2500
5000
7500
Dose (cGy)
0
0.2
0.4
0.6
0.8
1
DVCM color bar
−1
−0.5
0
0.5
1
DVCDM color bar

Patient−06

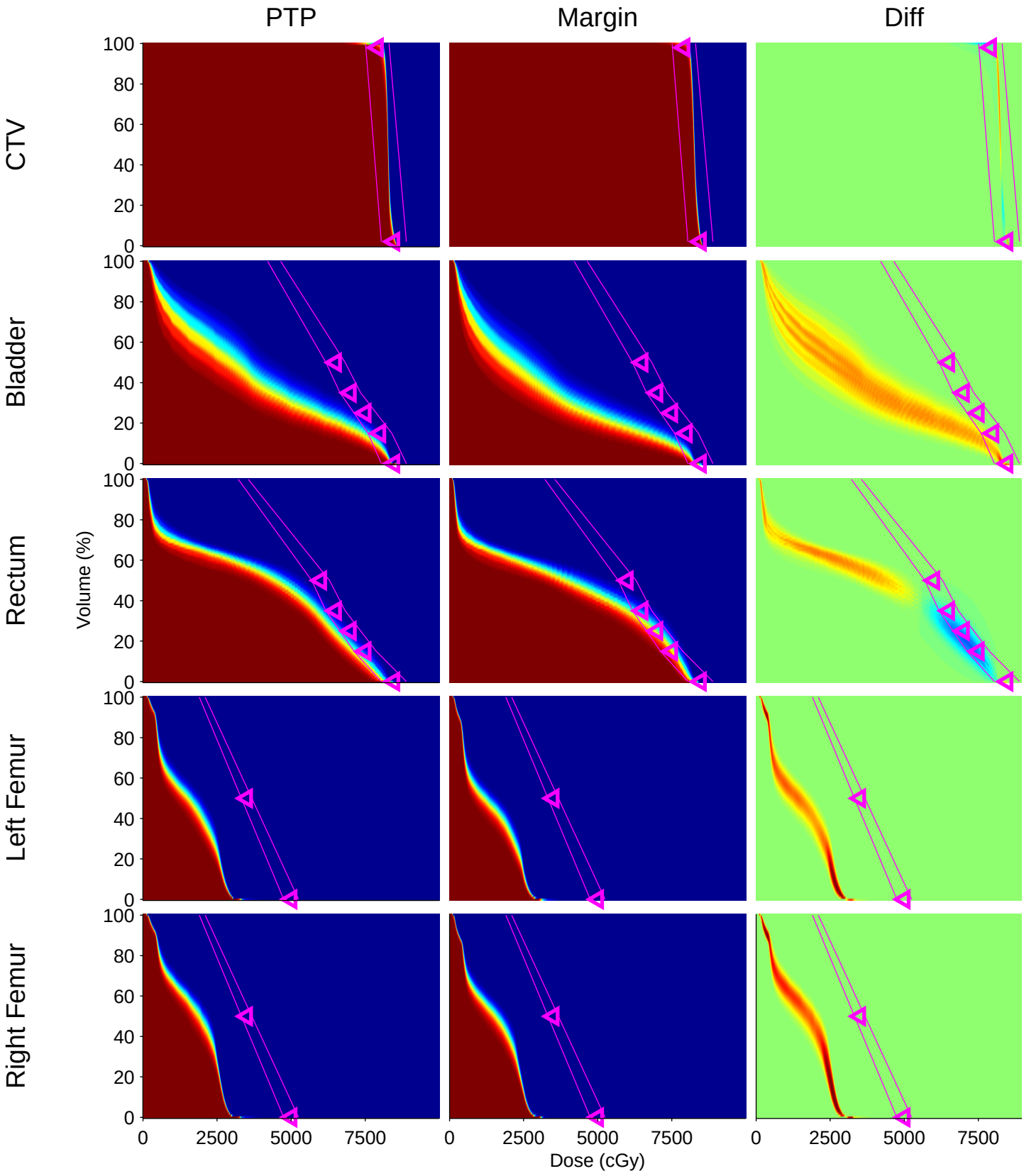
PTP
Margin
Diff
CTV
Bladder
Rectum
Left Femur
Right Femur
Volume (%)
0
20
40
60
80
100
0
2500
5000
7500
Dose (cGy)
0
0.2
0.4
0.6
0.8
1
DVCM color bar
−1
−0.5
0
0.5
1
DVCDM color bar

Patient−07

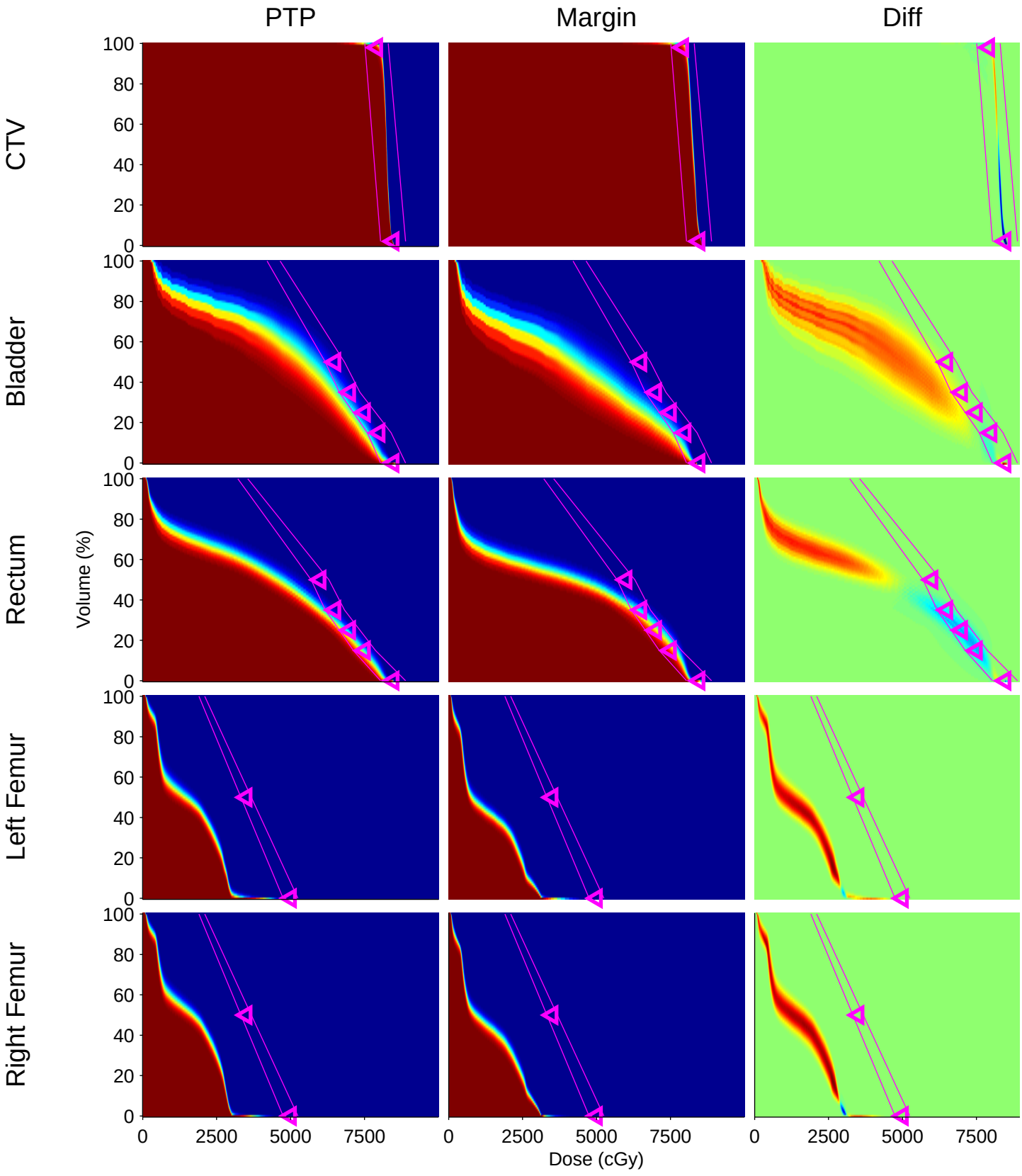
PTP
Margin
Diff
CTV
Bladder
Rectum
Left Femur
Right Femur
Volume (%)
0
20
40
60
80
100
0
2500
5000
7500
Dose (cGy)
0
0.2
0.4
0.6
0.8
1
DVCM color bar
−1
−0.5
0
0.5
1
DVCDM color bar

Patient−08

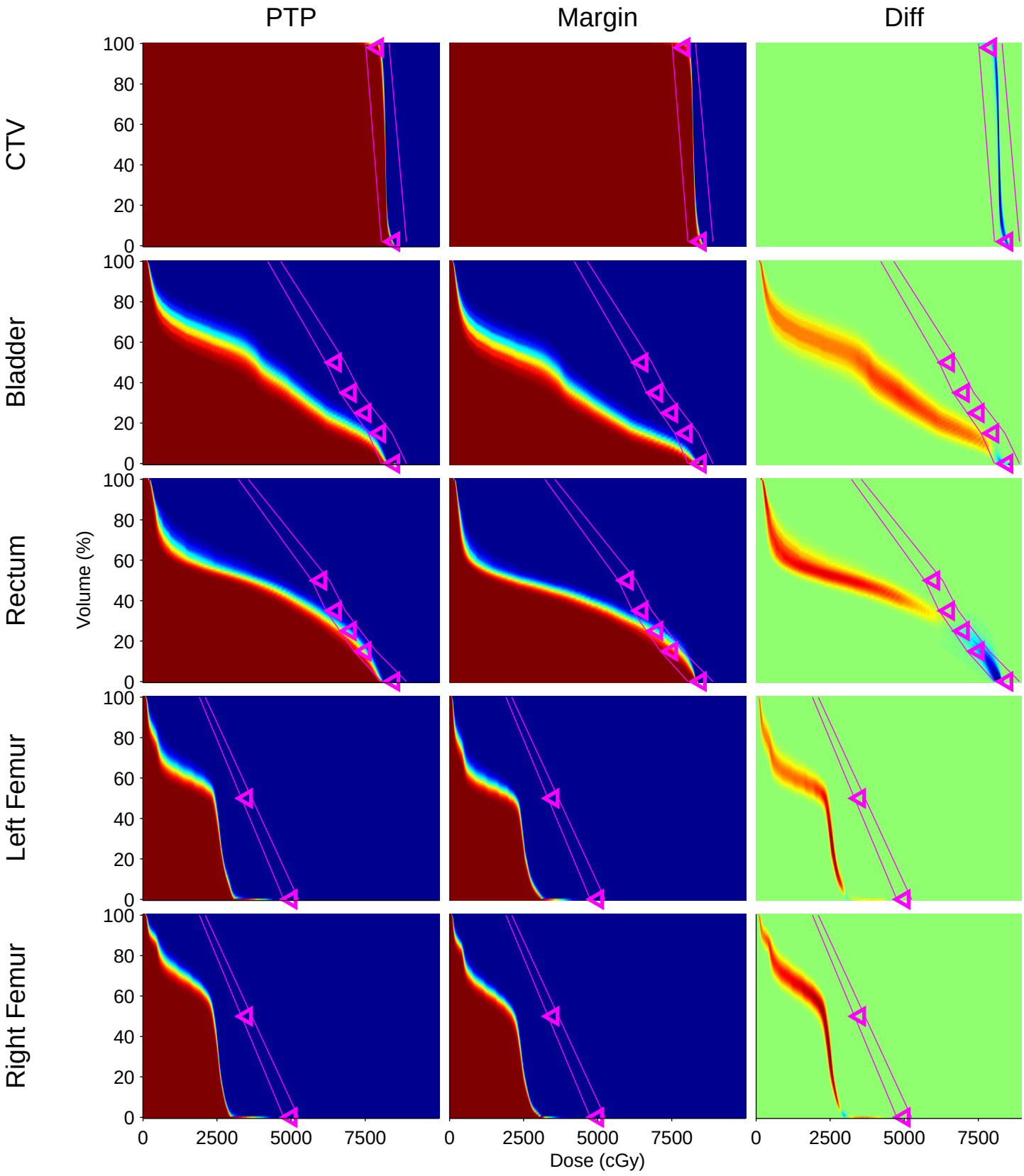
PTP
Margin
Diff
CTV
Bladder
Rectum
Left Femur
Right Femur
Volume (%)
0
20
40
60
80
100
0
2500
5000
7500
Dose (cGy)
0
0.2
0.4
0.6
0.8
1
DVCM color bar
−1
−0.5
0
0.5
1
DVCDM color bar

Patient−09

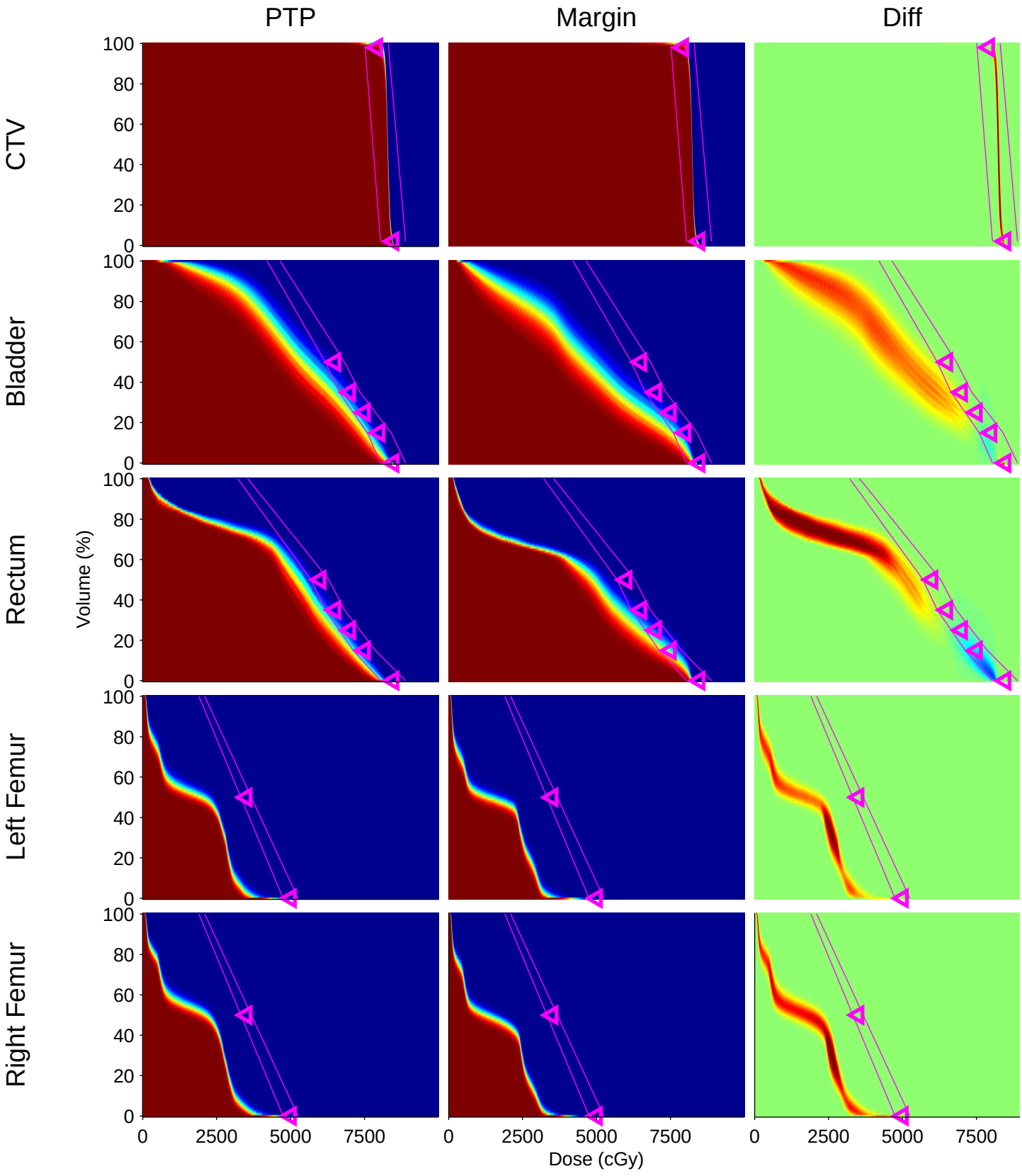
PTP
Margin
Diff
CTV
Bladder
Rectum
Left Femur
Right Femur
Volume (%)
0
20
40
60
80
100
0
2500
5000
7500
Dose (cGy)
0
0.2
0.4
0.6
0.8
1
DVCM color bar
−1
−0.5
0
0.5
1
DVCDM color bar

Patient−10

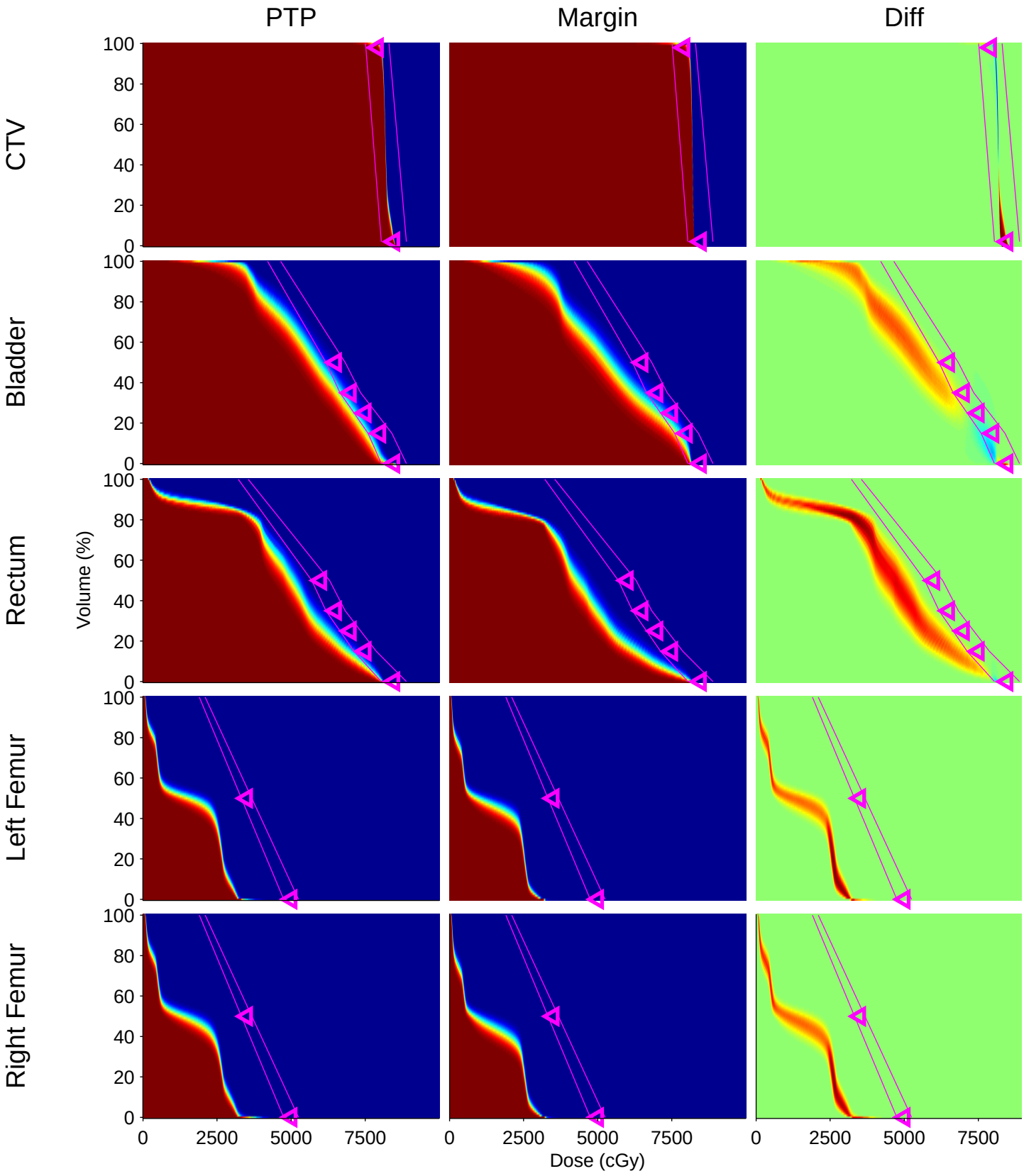
PTP
Margin
Diff
CTV
Bladder
Rectum
Left Femur
Right Femur
Volume (%)
0
20
40
60
80
100
0
2500
5000
7500
Dose (cGy)
0
0.2
0.4
0.6
0.8
1
DVCM color bar
−1
−0.5
0
0.5
1
DVCDM color bar

Patient−11

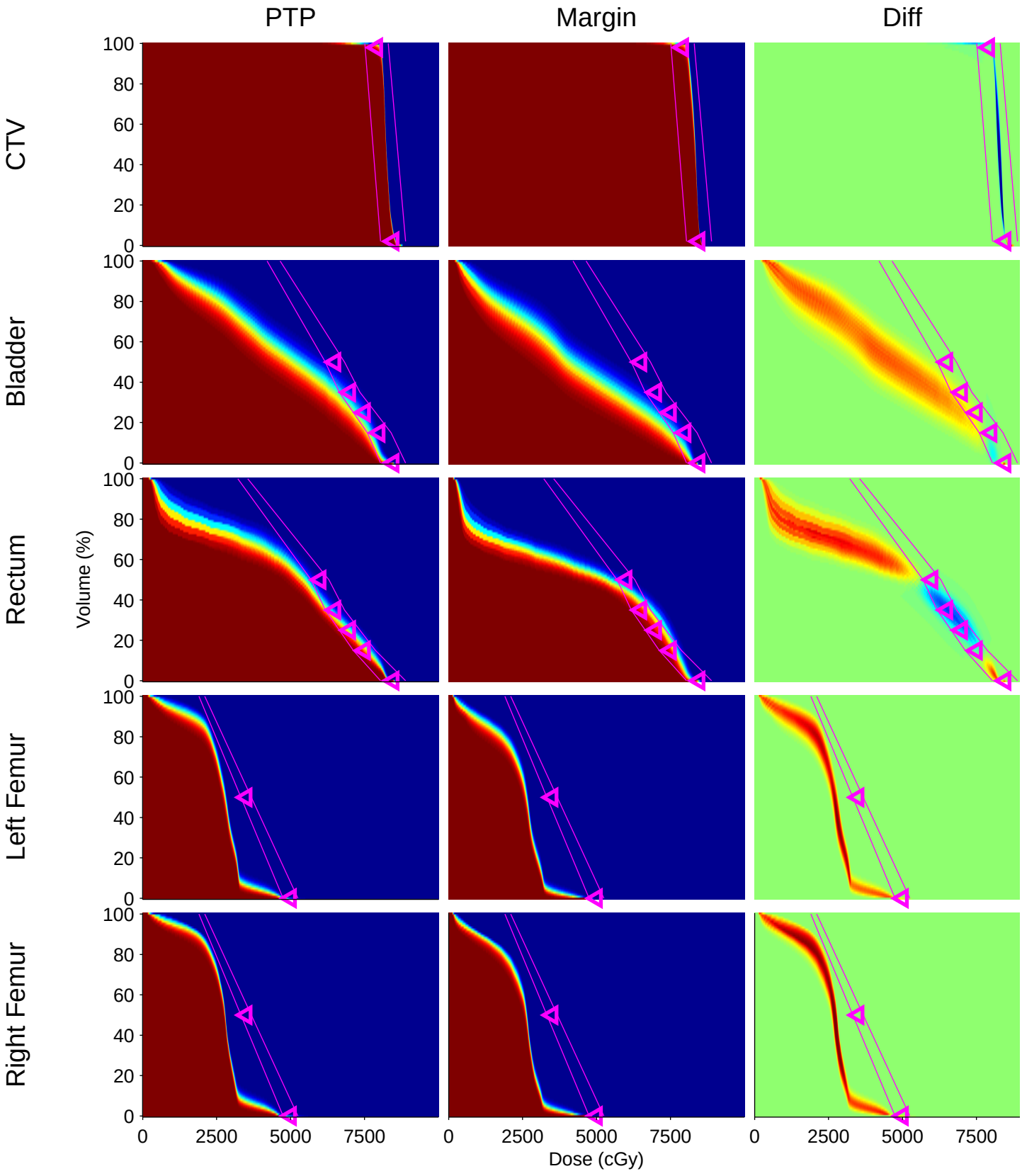
PTP
Margin
Diff
CTV
Bladder
Rectum
Left Femur
Right Femur
Volume (%)
0
20
40
60
80
100
0
2500
5000
7500
Dose (cGy)
0
0.2
0.4
0.6
0.8
1
DVCM color bar
−1
−0.5
0
0.5
1
DVCDM color bar

Patient−12

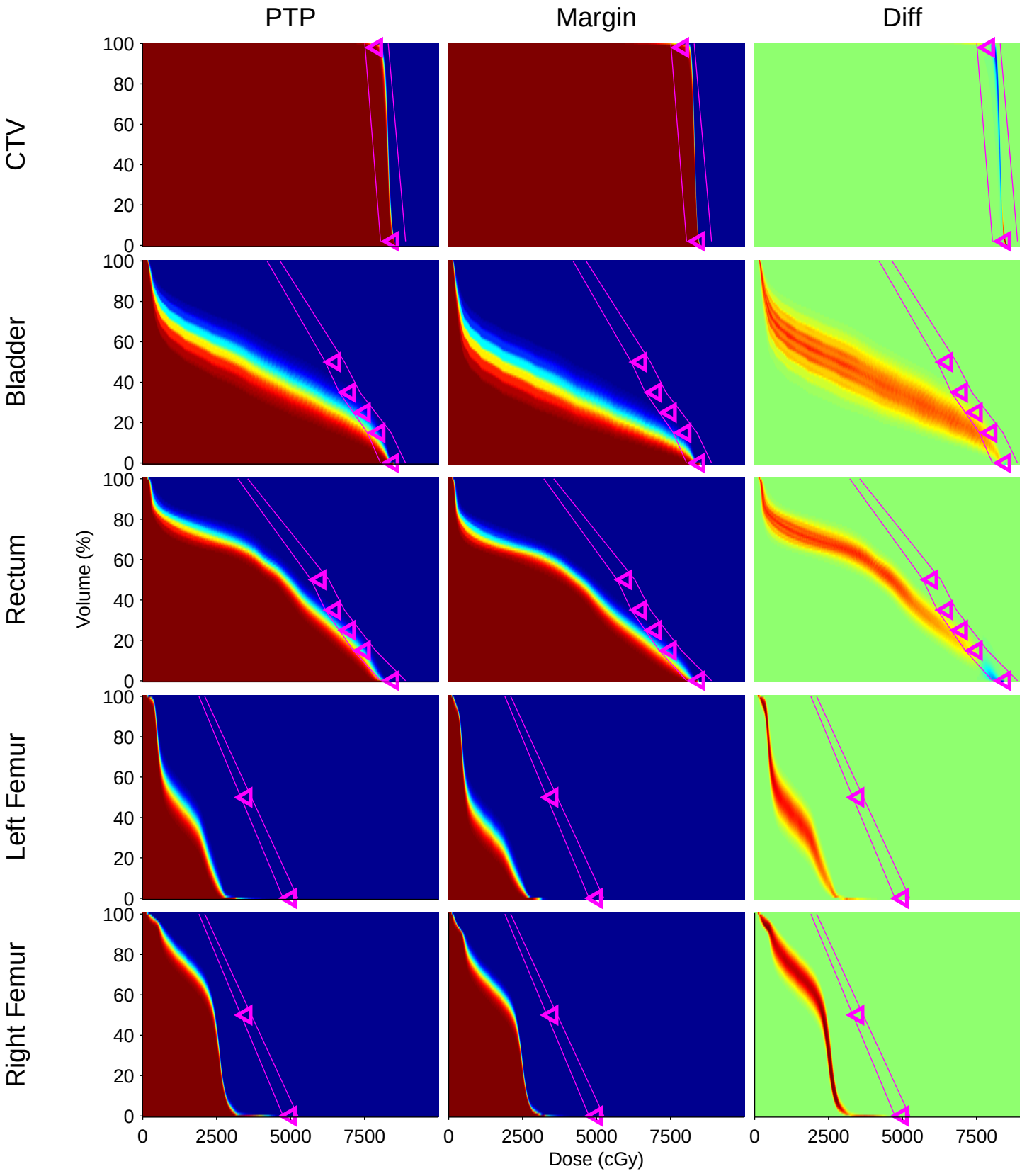
PTP
Margin
Diff
CTV
Bladder
Rectum
Left Femur
Right Femur
Volume (%)
0
20
40
60
80
100
0
2500
5000
7500
Dose (cGy)
0
0.2
0.4
0.6
0.8
1
DVCM color bar
−1
−0.5
0
0.5
1
DVCDM color bar

Patient−13

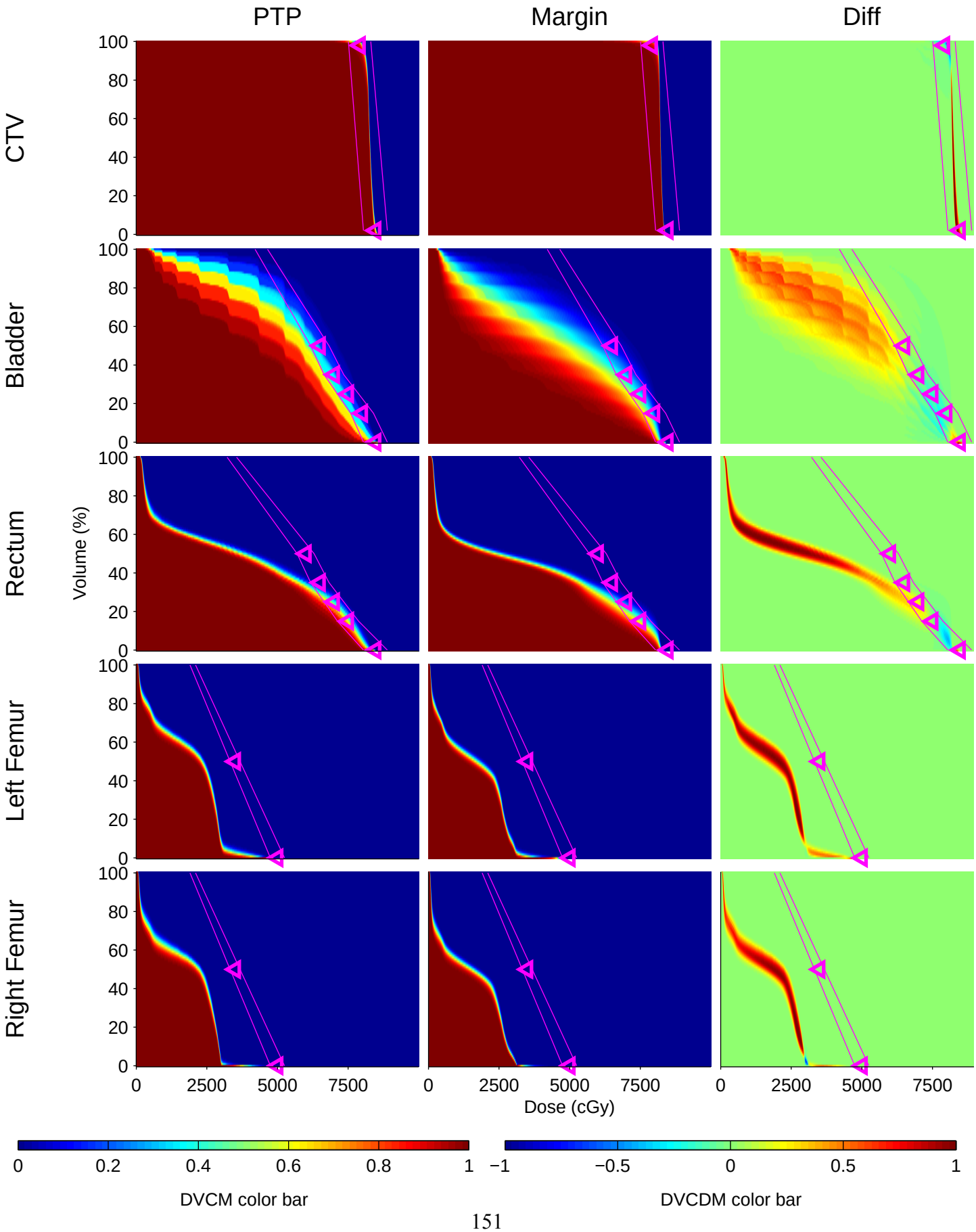
PTP
Margin
Diff
CTV
Bladder
Rectum
Left Femur
Right Femur
Volume (%)
0
20
40
60
80
100
0
2500
5000
7500
Dose (cGy)
0
0.2
0.4
0.6
0.8
1
DVCM color bar
−1
−0.5
0
0.5
1
DVCDM color bar

Patient−14

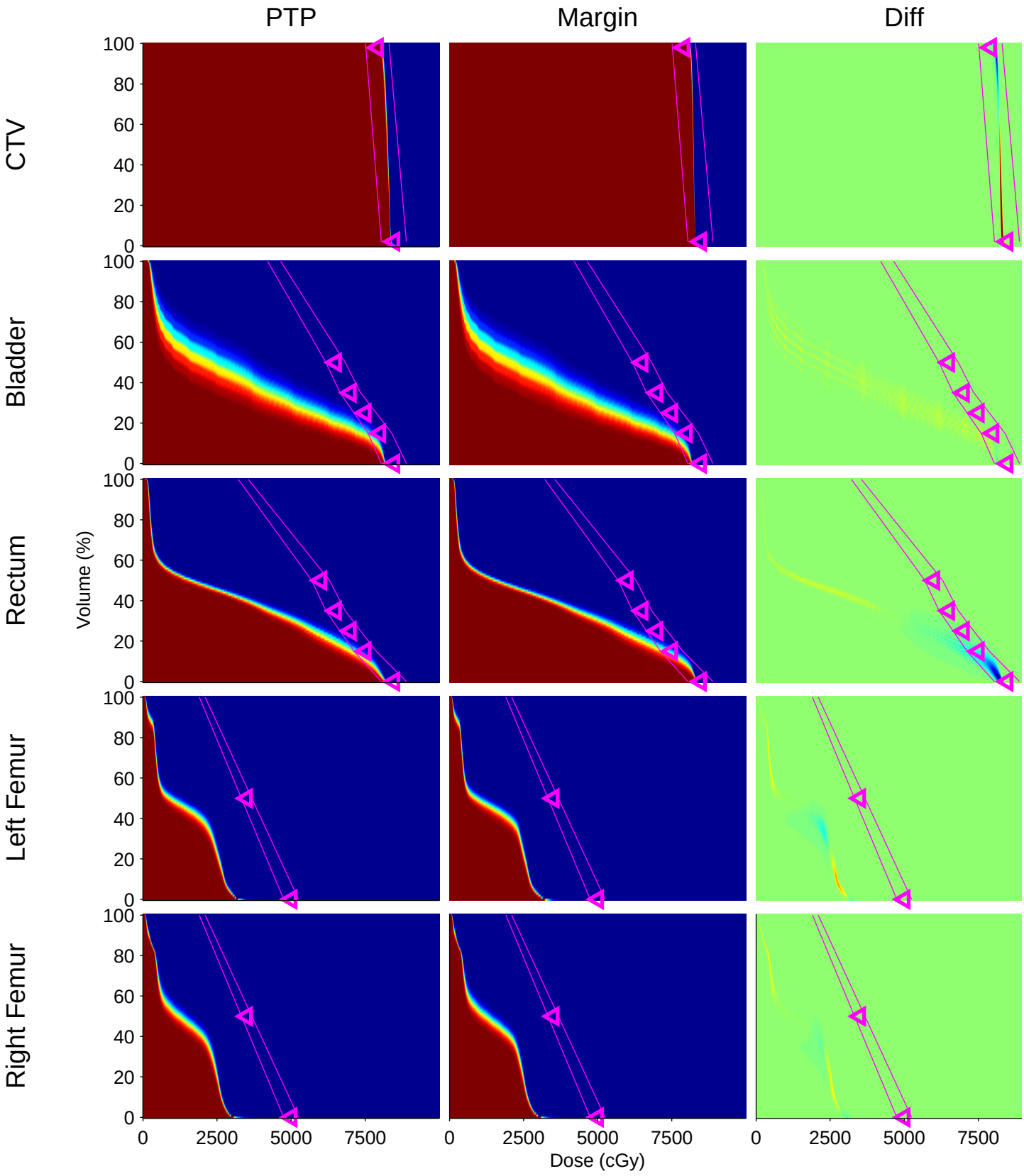
PTP
Margin
Diff
CTV
Bladder
Rectum
Left Femur
Right Femur
Volume (%)
0
20
40
60
80
100
0
2500
5000
7500
Dose (cGy)
0
0.2
0.4
0.6
0.8
1
DVCM color bar
−1
−0.5
0
0.5
1
DVCDM color bar

Patient−15

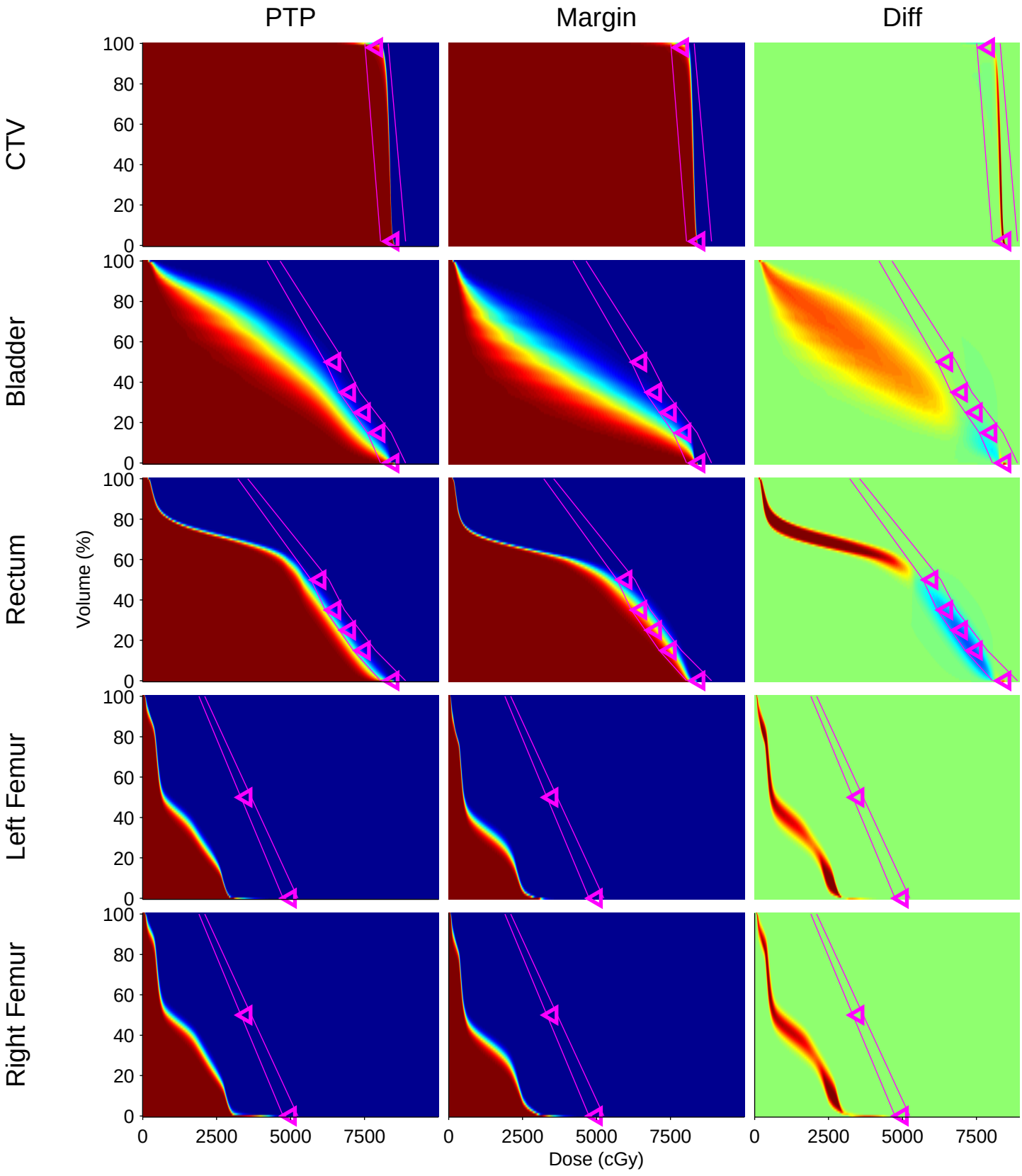
PTP
Margin
Diff
CTV
Bladder
Rectum
Left Femur
Right Femur
Volume (%)
0
20
40
60
80
100
0
2500
5000
7500
Dose (cGy)
0
0.2
0.4
0.6
0.8
1
DVCM color bar
−1
−0.5
0
0.5
1
DVCDM color bar

Patient−16

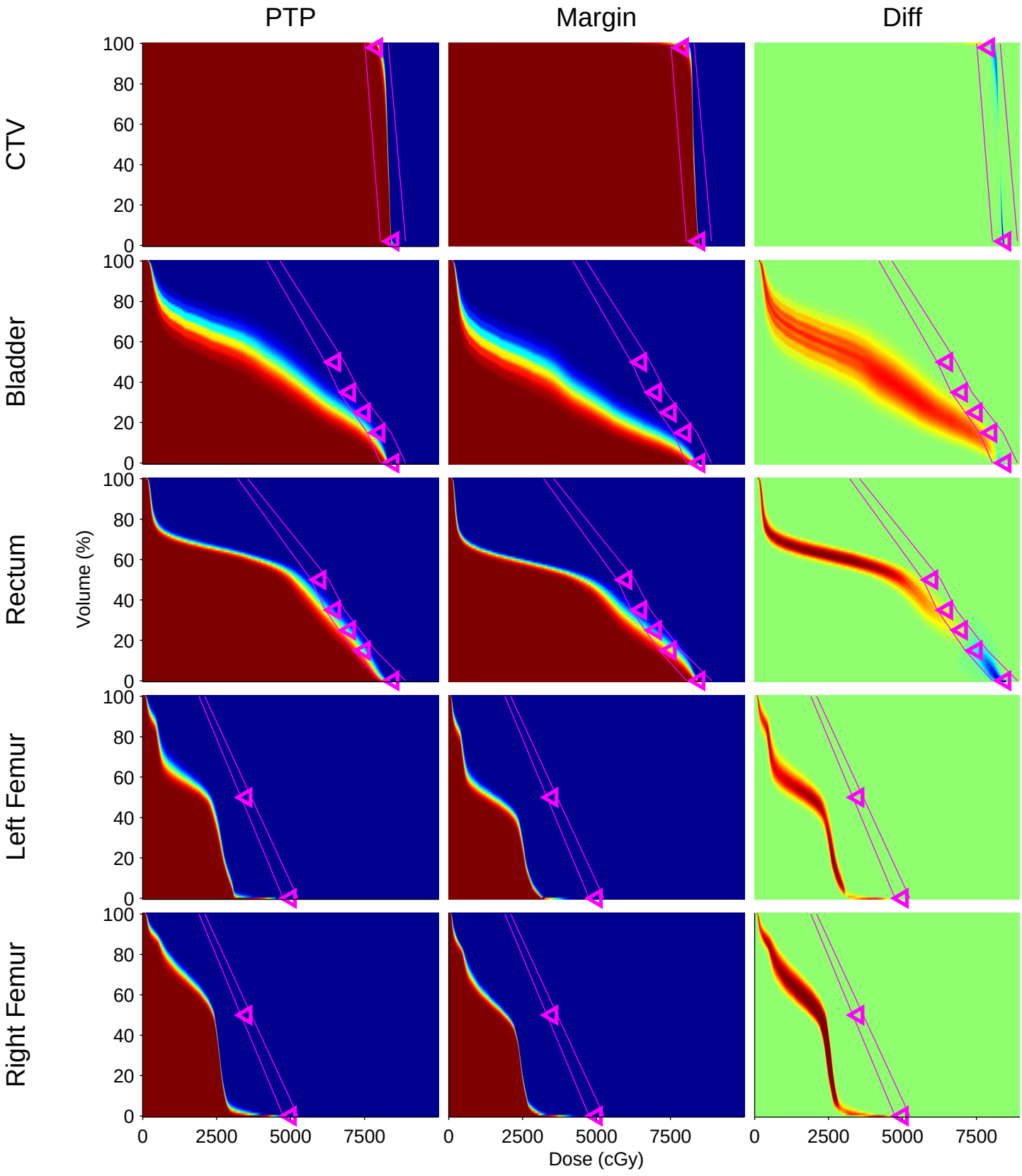
PTP
Margin
Diff
CTV
Bladder
Rectum
Left Femur
Right Femur
Volume (%)
0
20
40
60
80
100
0
2500
5000
7500
Dose (cGy)
0
0.2
0.4
0.6
0.8
1
DVCM color bar
−1
−0.5
0
0.5
1
DVCDM color bar

Patient−17

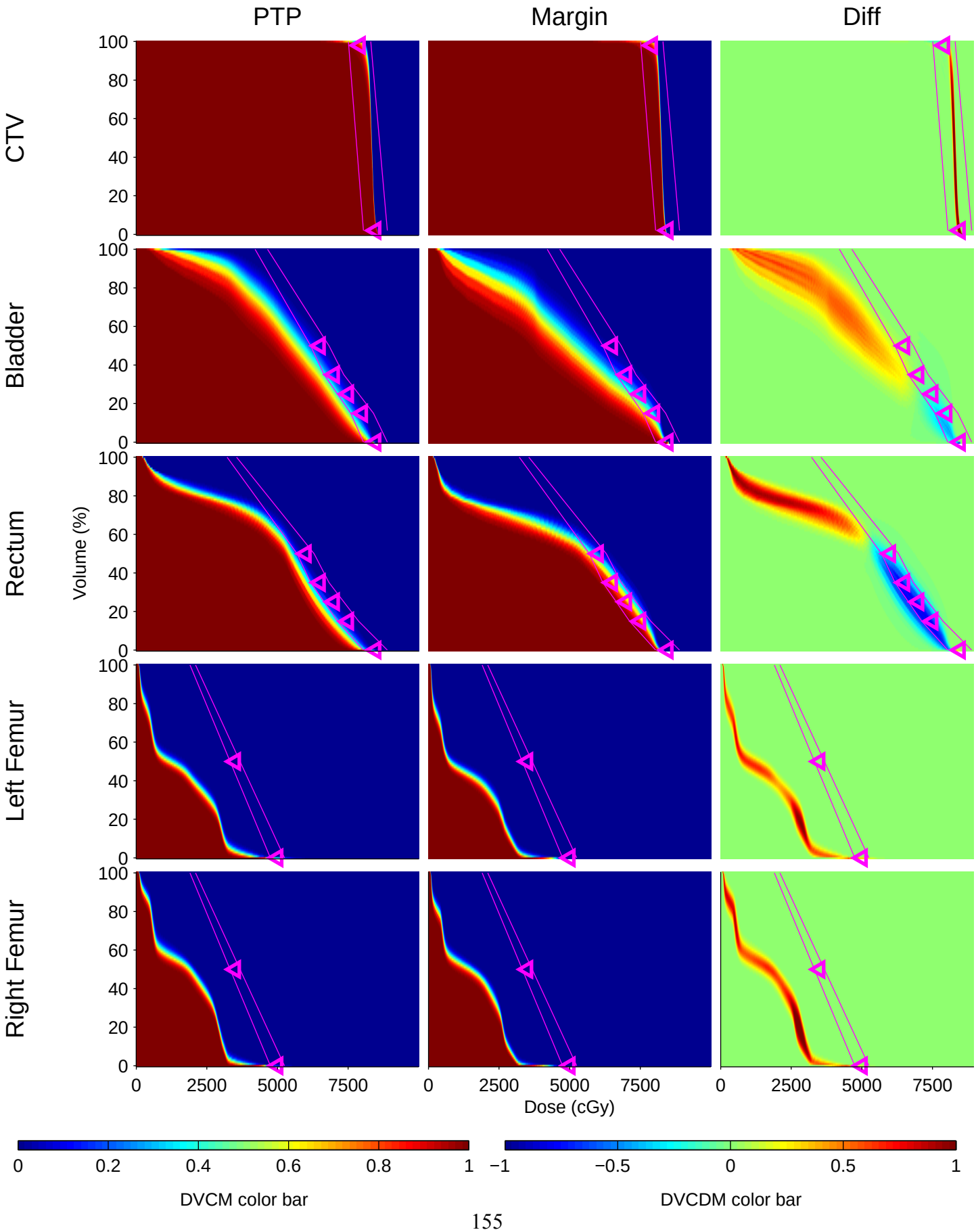
PTP
Margin
Diff
CTV
Bladder
Rectum
Left Femur
Right Femur
Volume (%)
0
20
40
60
80
100
0
2500
5000
7500
Dose (cGy)
0
0.2
0.4
0.6
0.8
1
DVCM color bar
−1
−0.5
0
0.5
1
DVCDM color bar

Patient−18

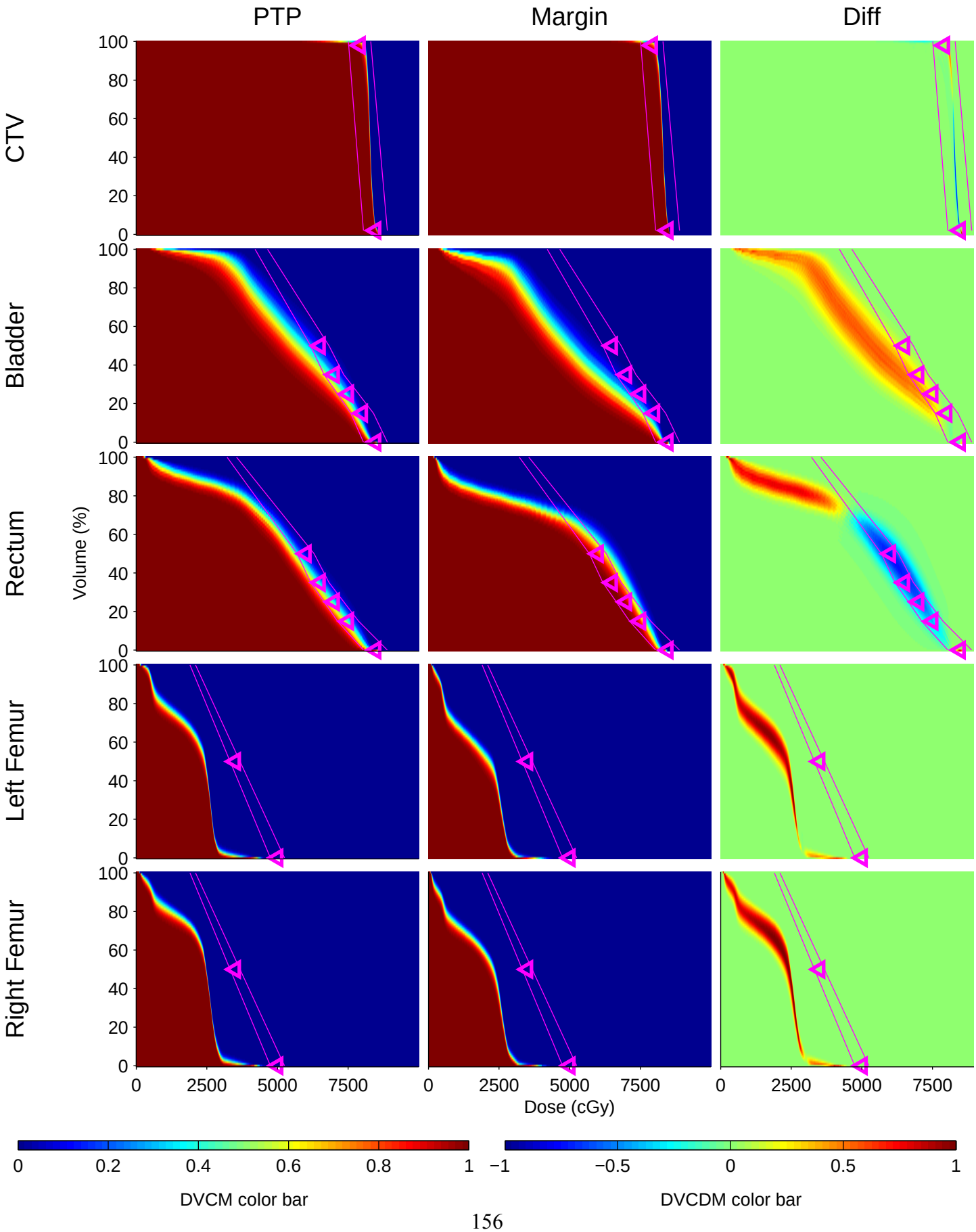
PTP
Margin
Diff
CTV
Bladder
Rectum
Left Femur
Right Femur
Volume (%)
0
20
40
60
80
100
0
2500
5000
7500
Dose (cGy)
0
0.2
0.4
0.6
0.8
1
DVCM color bar
−1
−0.5
0
0.5
1
DVCDM color bar

Patient−19

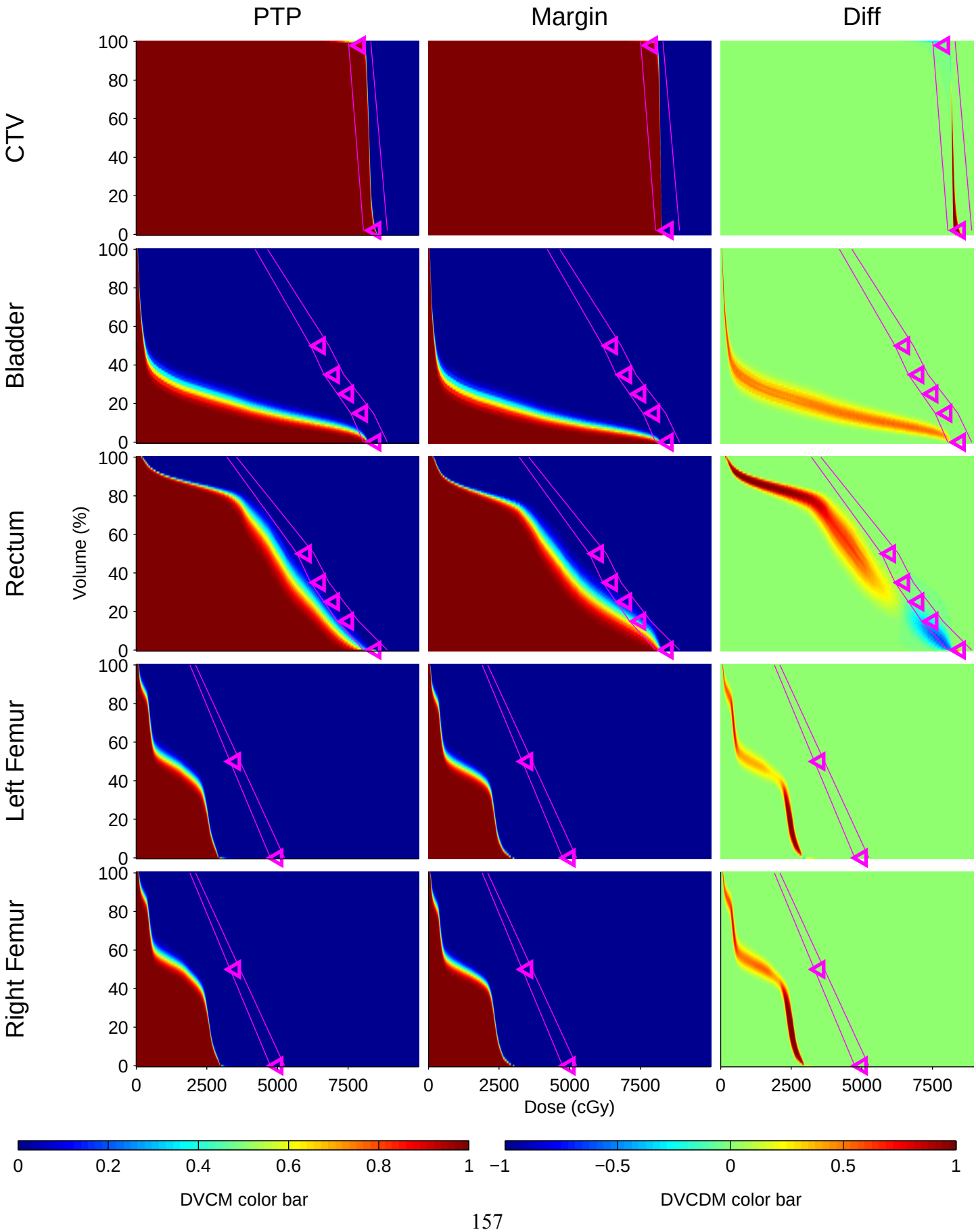
PTP
Margin
Diff
CTV
Bladder
Rectum
Left Femur
Right Femur
Volume (%)
0
20
40
60
80
100
0
2500
5000
7500
Dose (cGy)
0
0.2
0.4
0.6
0.8
1
DVCM color bar
−1
−0.5
0
0.5
1
DVCDM color bar

Patient−20

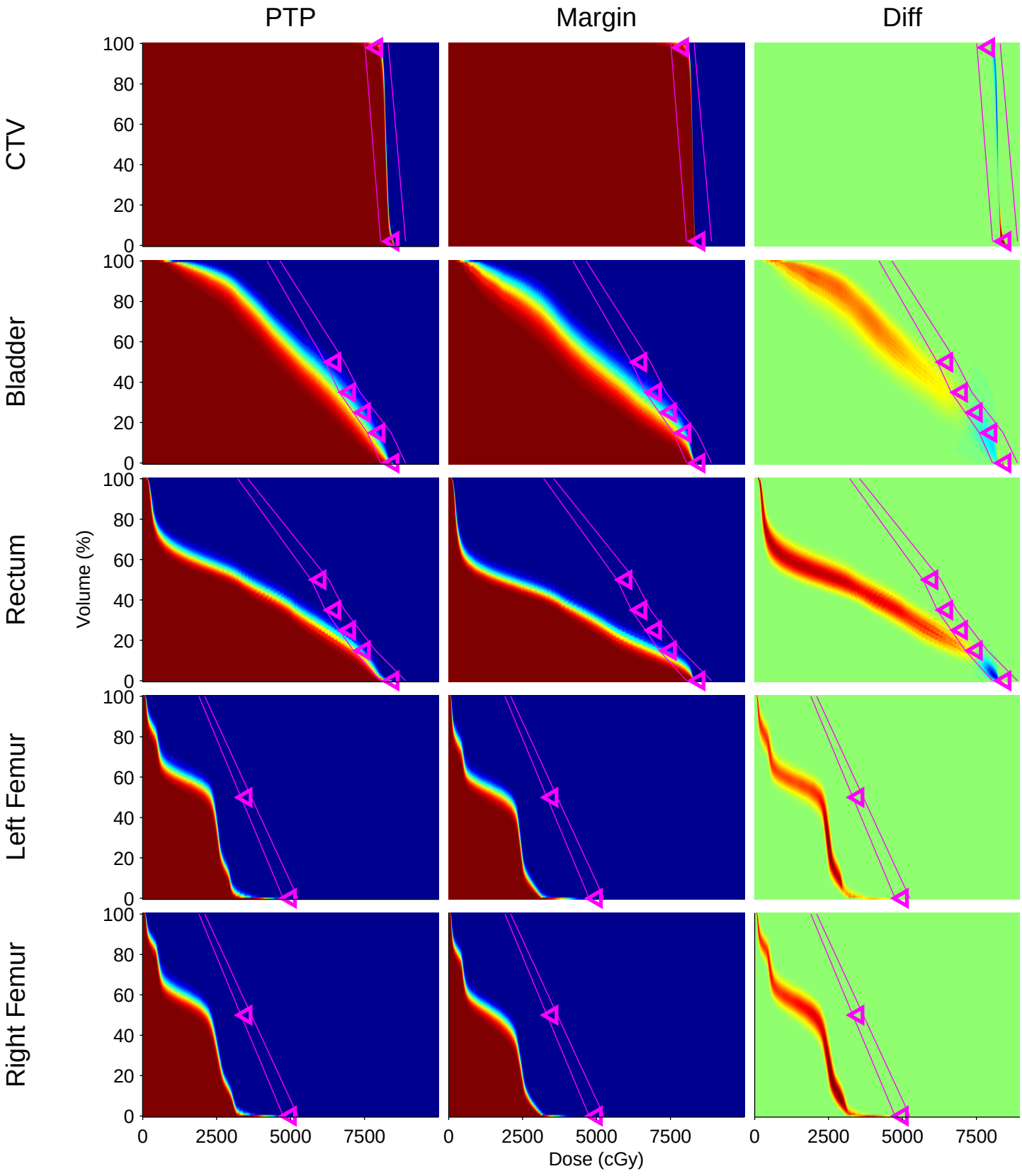
PTP
Margin
Diff
CTV
Bladder
Rectum
Left Femur
Right Femur
Volume (%)
0
20
40
60
80
100
0
2500
5000
7500
Dose (cGy)
0
0.2
0.4
0.6
0.8
1
DVCM color bar
−1
−0.5
0
0.5
1
DVCDM color bar

Patient−21

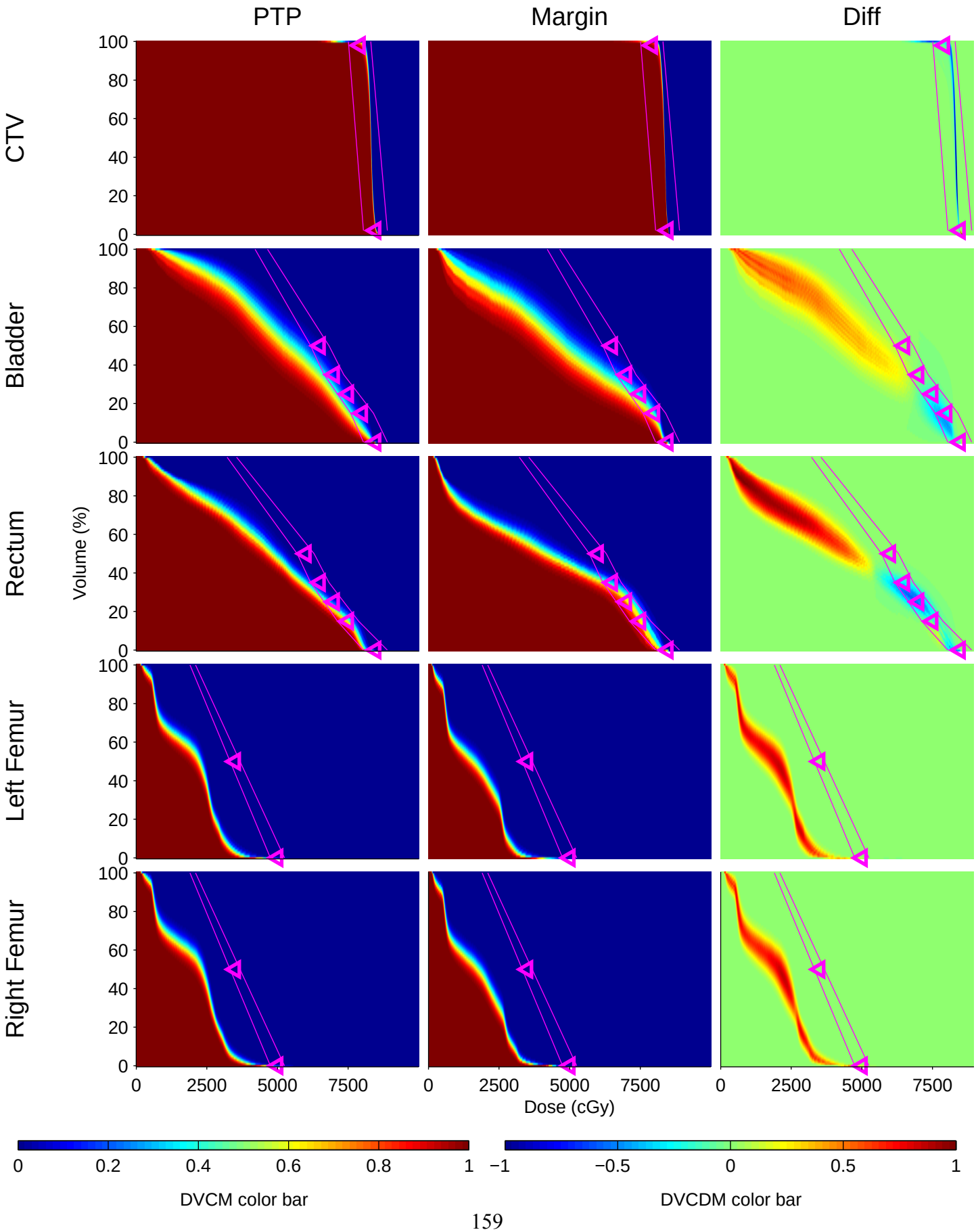
PTP
Margin
Diff
CTV
Bladder
Rectum
Left Femur
Right Femur
Volume (%)
0
20
40
60
80
100
0
2500
5000
7500
Dose (cGy)
0
0.2
0.4
0.6
0.8
1
DVCM color bar
−1
−0.5
0
0.5
1
DVCDM color bar

Patient−22

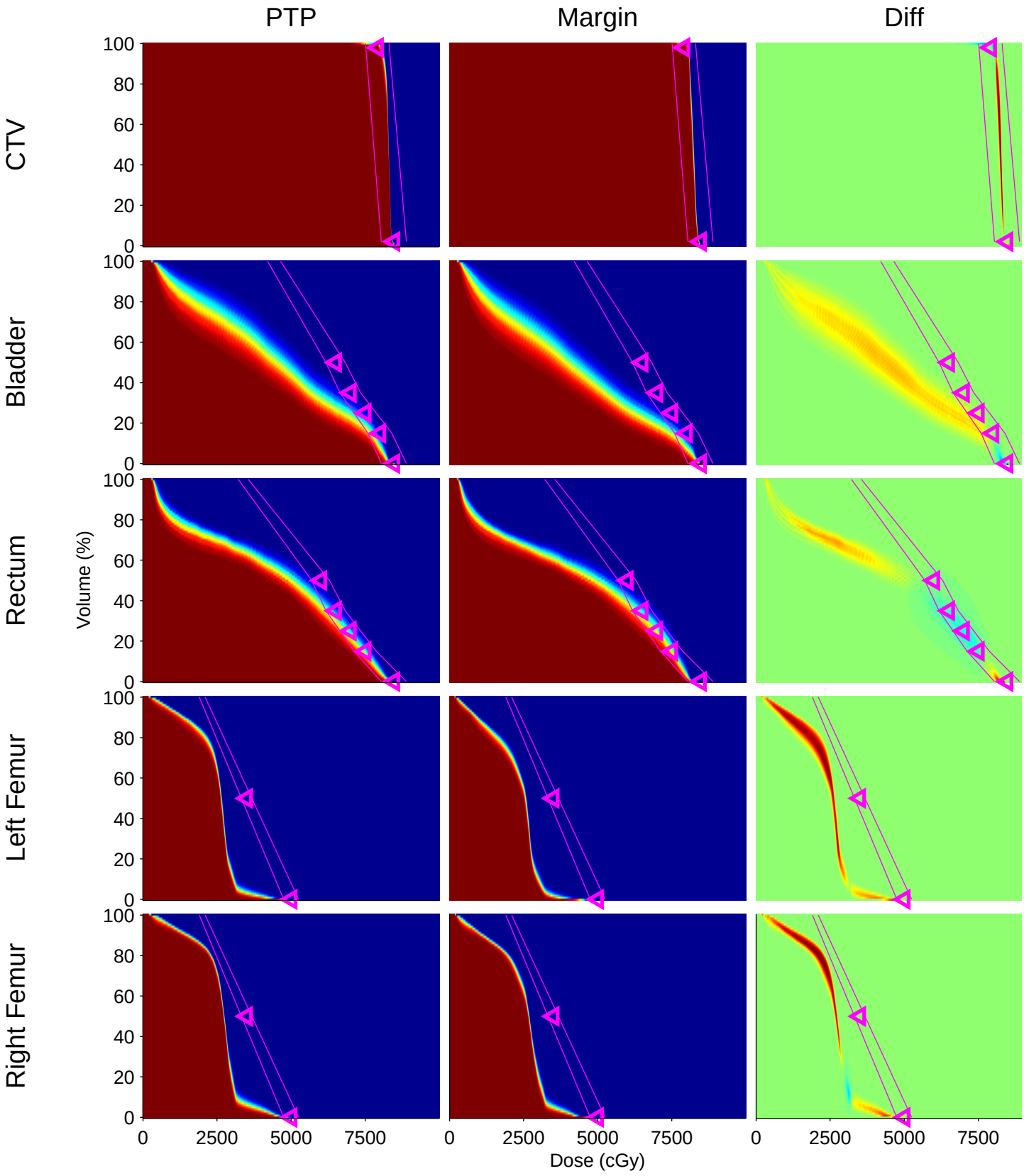
PTP
Margin
Diff
CTV
Bladder
Rectum
Left Femur
Right Femur
Volume (%)
0
20
40
60
80
100
0
2500
5000
7500
Dose (cGy)
0
0.2
0.4
0.6
0.8
1
DVCM color bar
−1
−0.5
0
0.5
1
DVCDM color bar

Patient−23

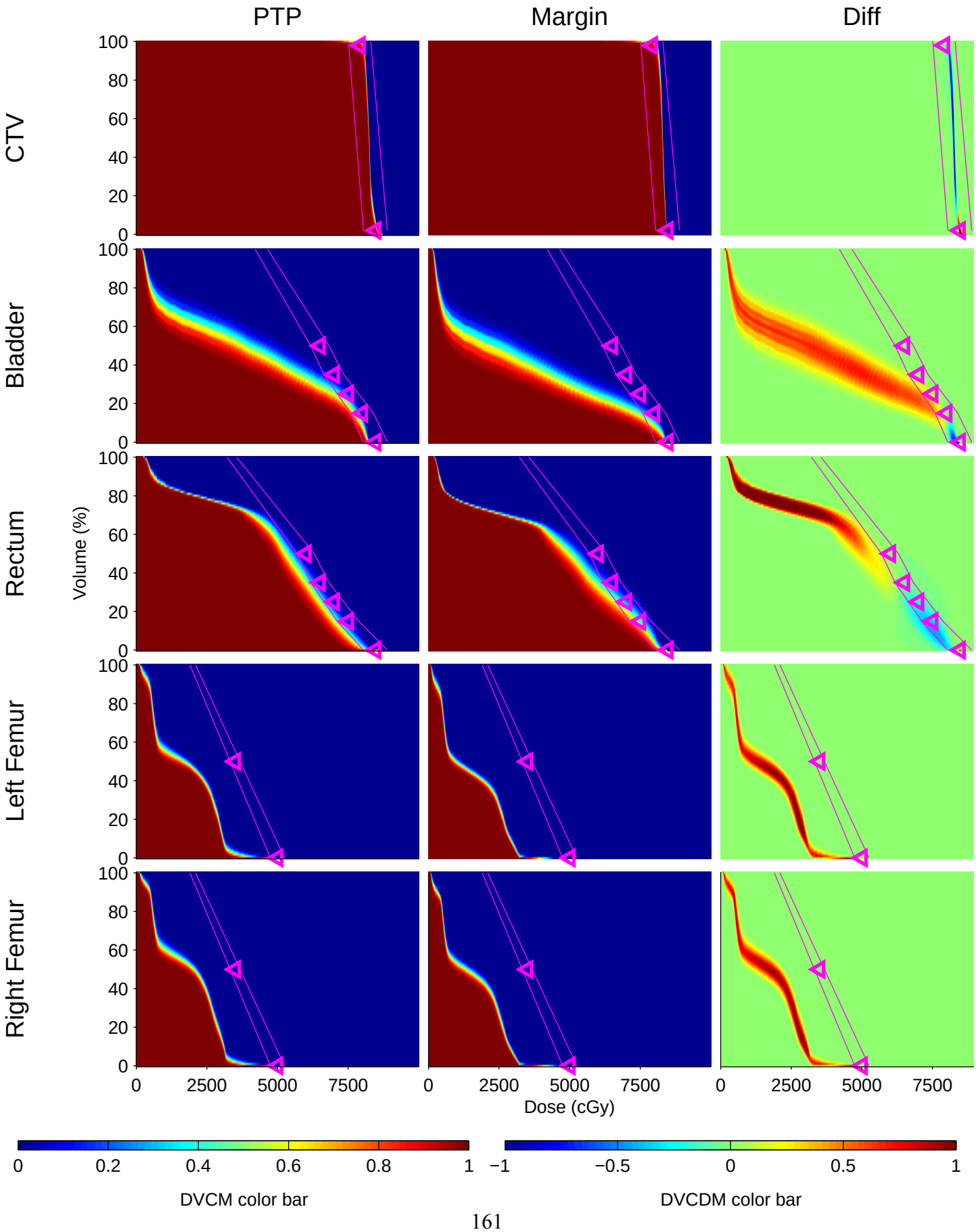
PTP
Margin
Diff
CTV
Bladder
Rectum
Left Femur
Right Femur
Volume (%)
0
20
40
60
80
100
0
2500
5000
7500
Dose (cGy)
0
0.2
0.4
0.6
0.8
1
DVCM color bar
−1
−0.5
0
0.5
1
DVCDM color bar

Patient−24

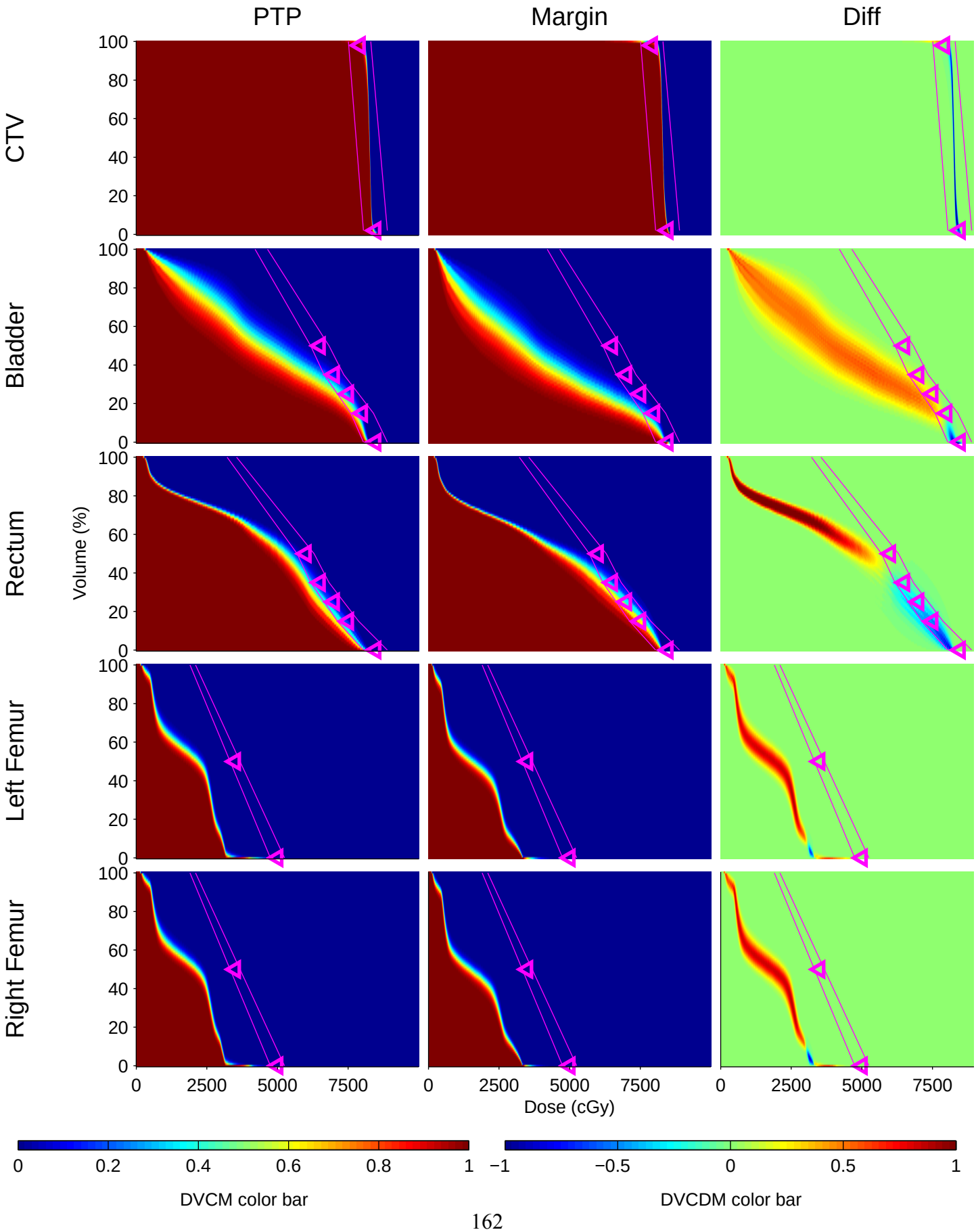
PTP
Margin
Diff
CTV
Bladder
Rectum
Left Femur
Right Femur
Volume (%)
0
20
40
60
80
100
0
2500
5000
7500
Dose (cGy)
0
0.2
0.4
0.6
0.8
1
DVCM color bar
−1
−0.5
0
0.5
1
DVCDM color bar

Patient−25

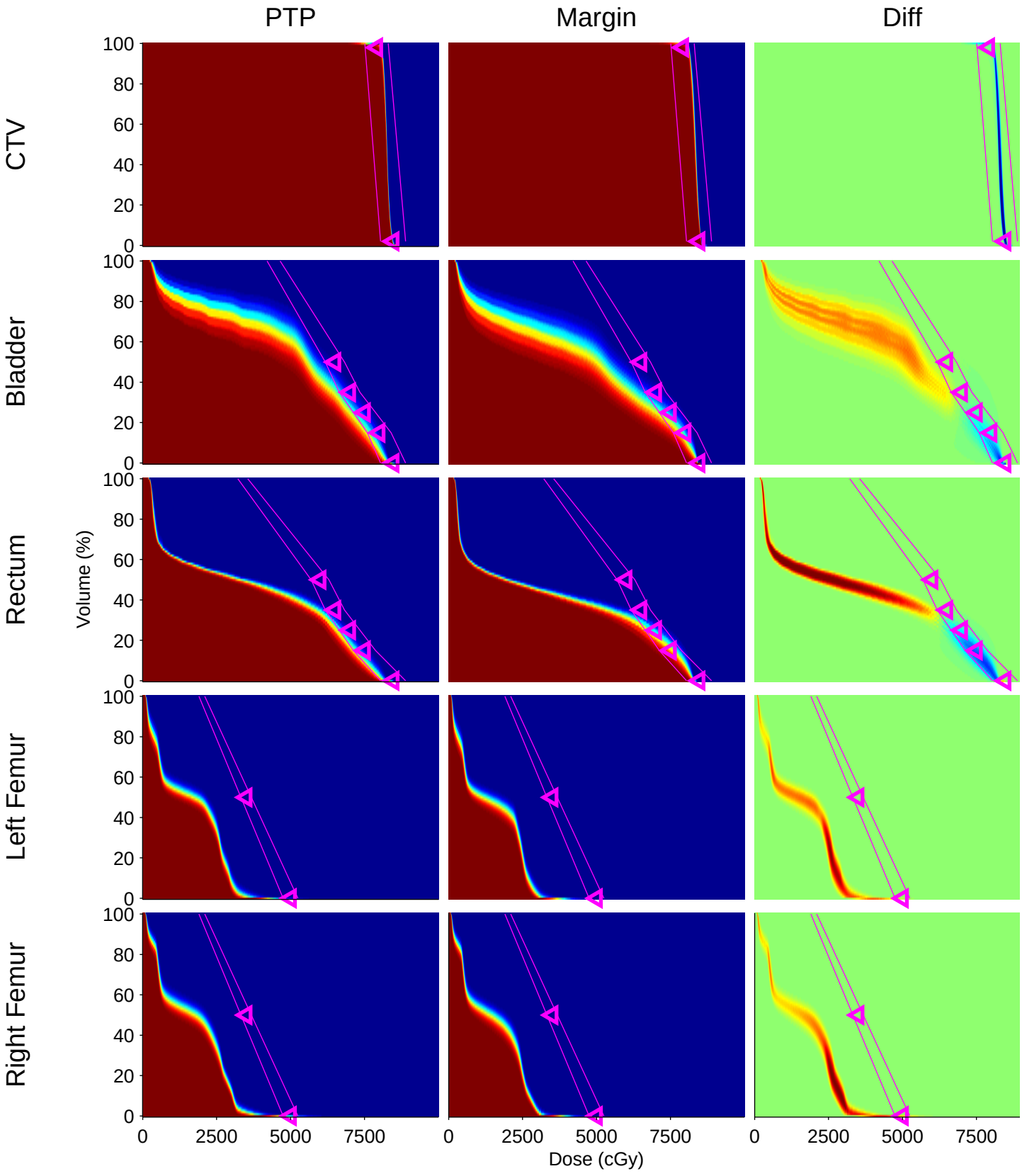
PTP
Margin
Diff
CTV
Bladder
Rectum
Left Femur
Right Femur
Volume (%)
0
20
40
60
80
100
0
2500
5000
7500
Dose (cGy)
0
0.2
0.4
0.6
0.8
1
DVCM color bar
−1
−0.5
0
0.5
1
DVCDM color bar

Patient−26

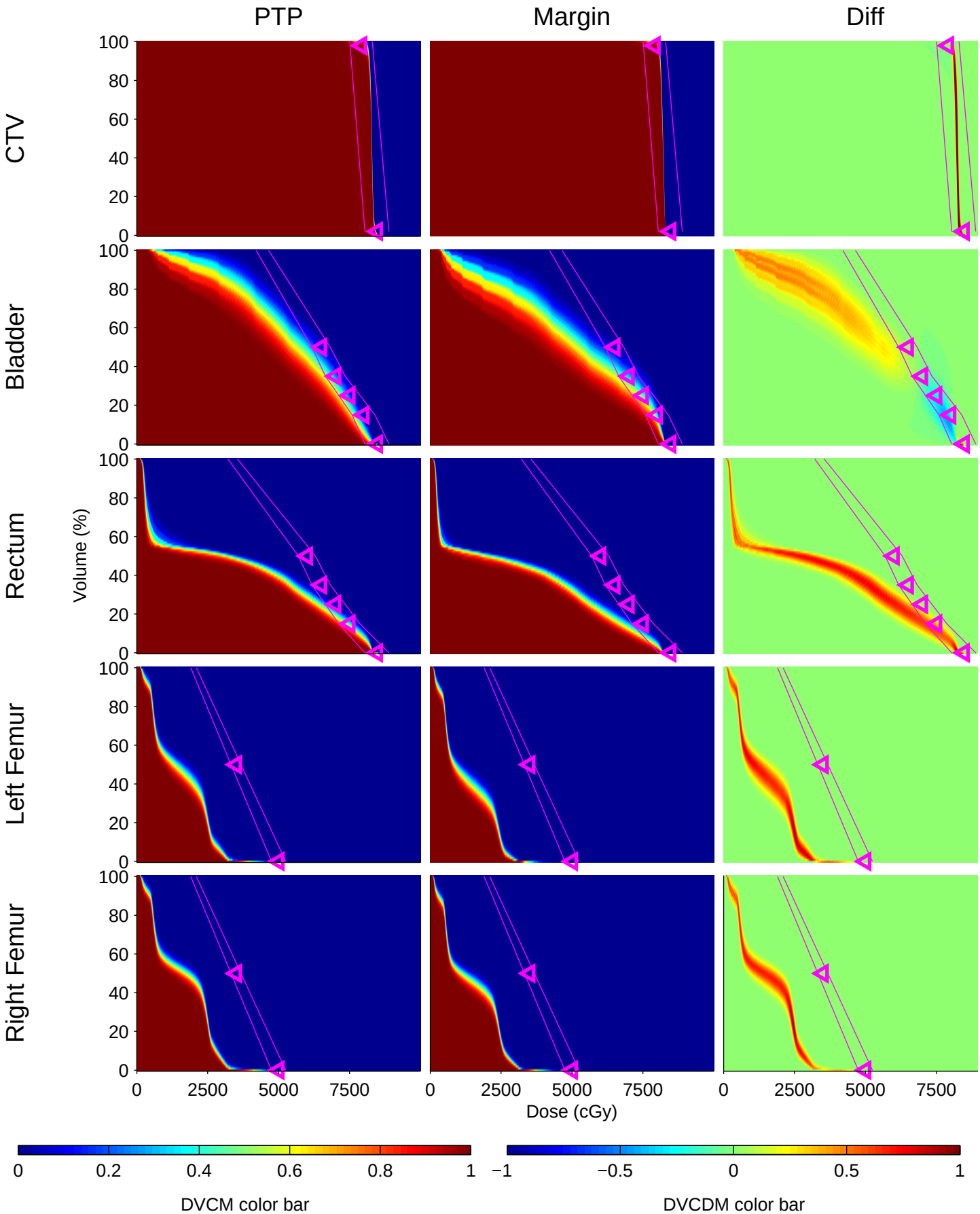
PTP
Margin
Diff
CTV
Bladder
Rectum
Left Femur
Right Femur
Volume (%)
0
20
40
60
80
100
0
2500
5000
7500
Dose (cGy)
0
0.2
0.4
0.6
0.8
1
DVCM color bar
−1
−0.5
0
0.5
1
DVCDM color bar

Patient−28

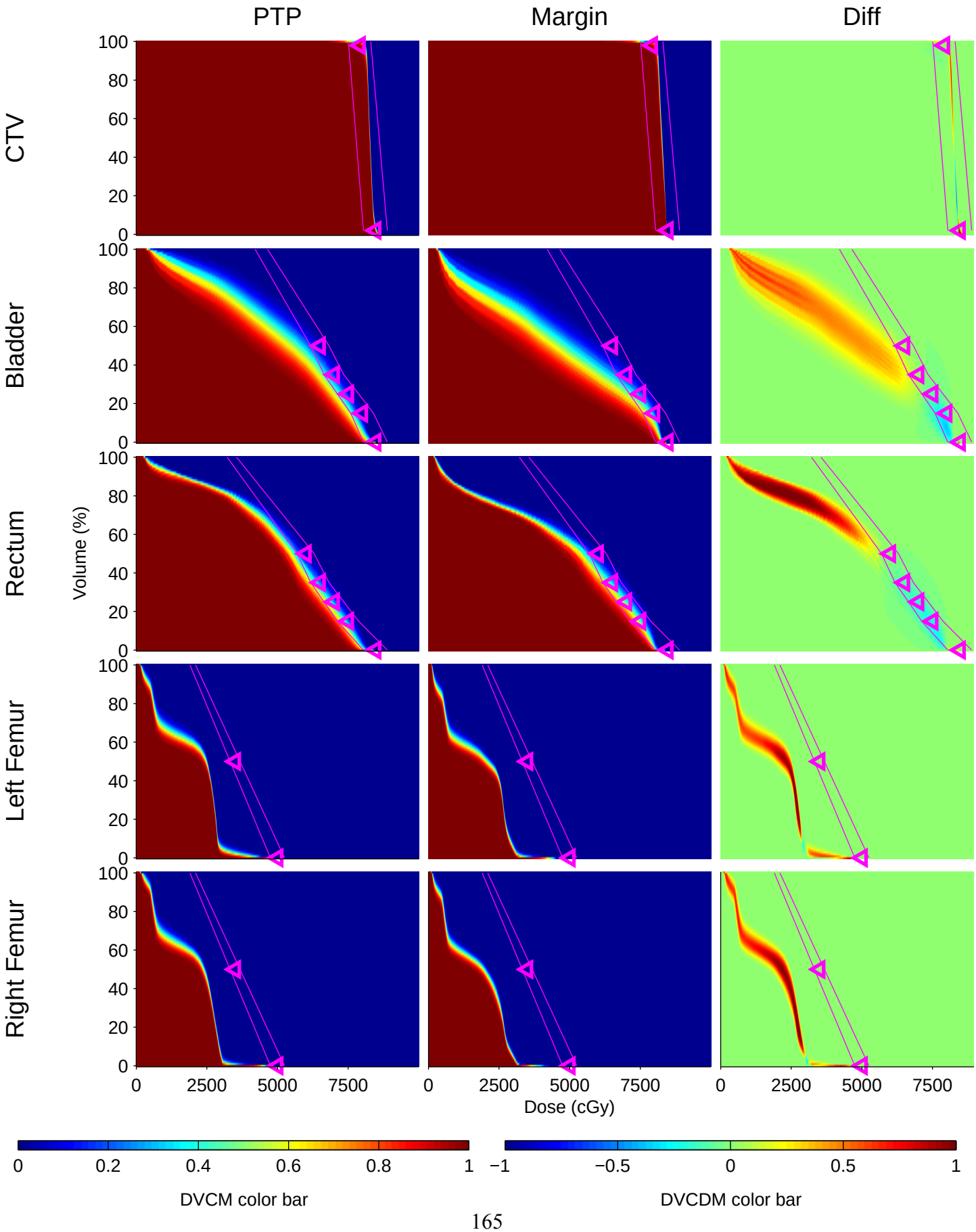
PTP
Margin
Diff
CTV
Bladder
Rectum
Left Femur
Right Femur
Volume (%)
0
20
40
60
80
100
0
2500
5000
7500
Dose (cGy)
0
0.2
0.4
0.6
0.8
1
DVCM color bar
−1
−0.5
0
0.5
1
DVCDM color bar

Patient−30

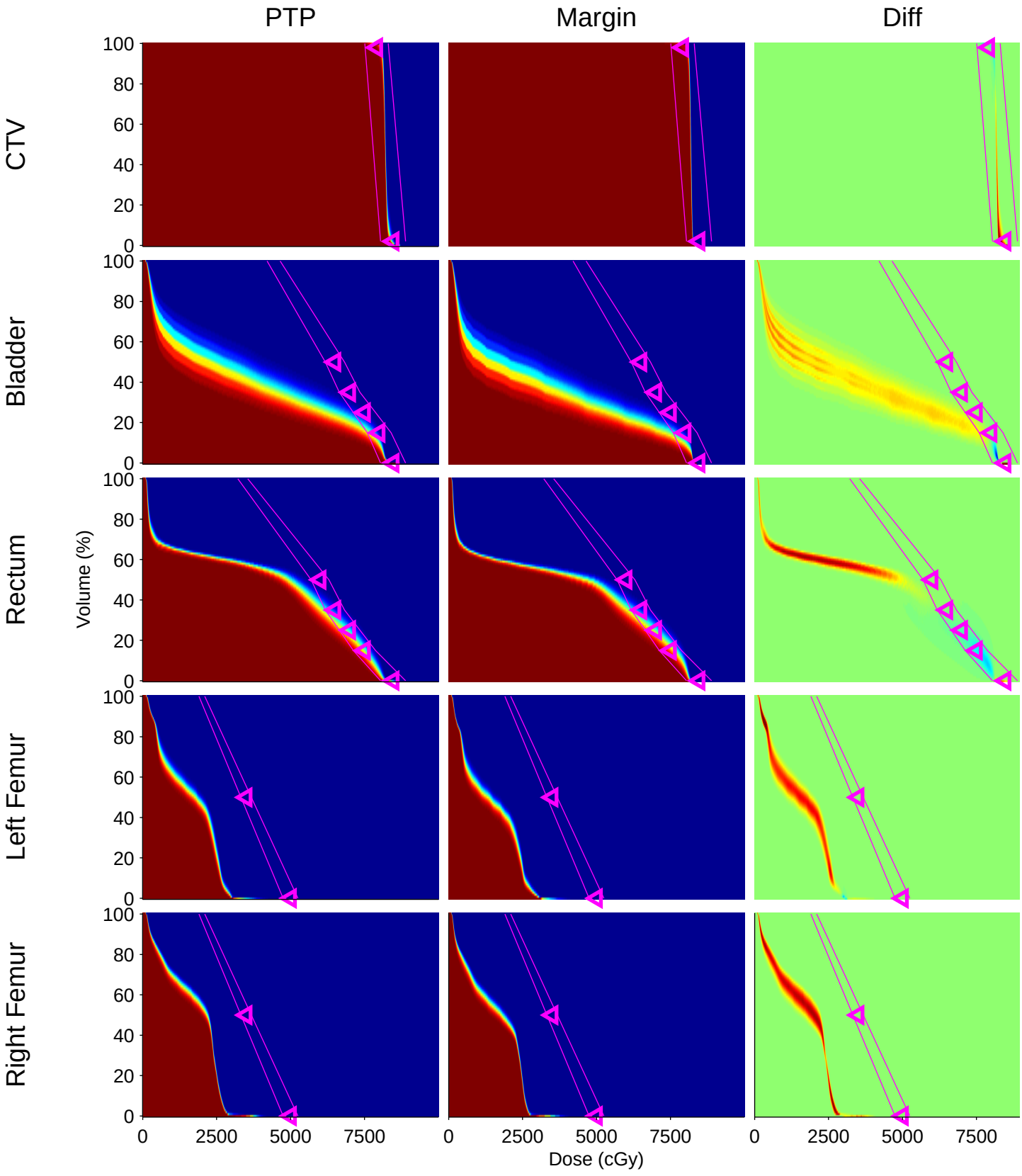
PTP
Margin
Diff
CTV
Bladder
Rectum
Left Femur
Right Femur
Volume (%)
0
20
40
60
80
100
0
2500
5000
7500
Dose (cGy)
0
0.2
0.4
0.6
0.8
1
DVCM color bar
−1
−0.5
0
0.5
1
DVCDM color bar

Appendix IV: Static Dose-Volume Histograms

Static Dose-Volume Histogram plots for all patients used in this study. For each patient, a DVH curve is plotted for CTV, rectum, bladder, left and right femur. Solid lines indicate PTP plans and dashed lines indicate margin-based plans.

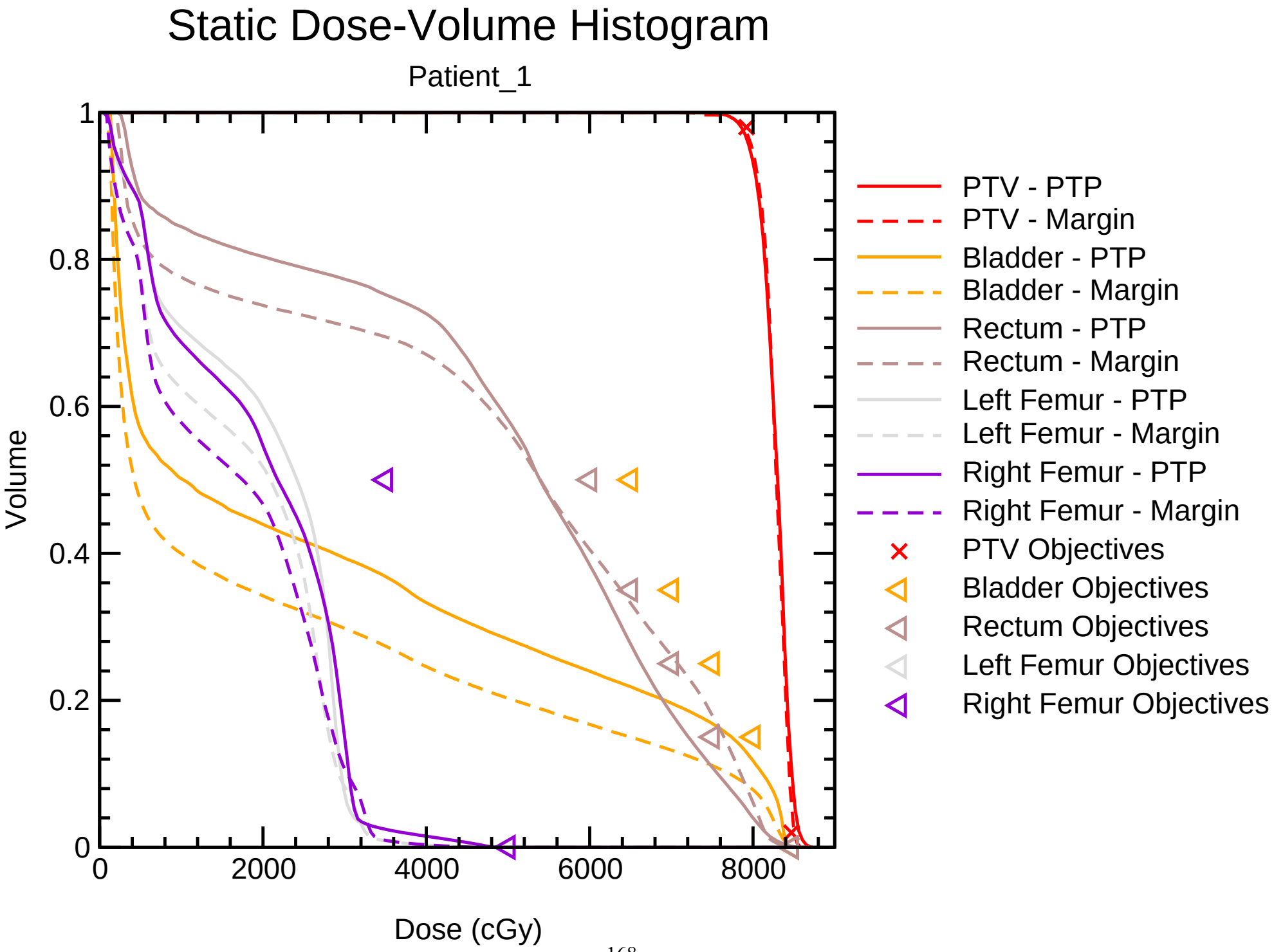
Static Dose-Volume Histogram
Patient_1
Volume
Dose (cGy)
0
0.2
0.4
0.6
0.8
1
0
2000
4000
6000
8000
PTV - PTP
PTV - Margin
Bladder - PTP
Bladder - Margin
Rectum - PTP
Rectum - Margin
Left Femur - PTP
Left Femur - Margin
Right Femur - PTP
Right Femur - Margin
PTV Objectives
Bladder Objectives
Rectum Objectives
Left Femur Objectives
Right Femur Objectives

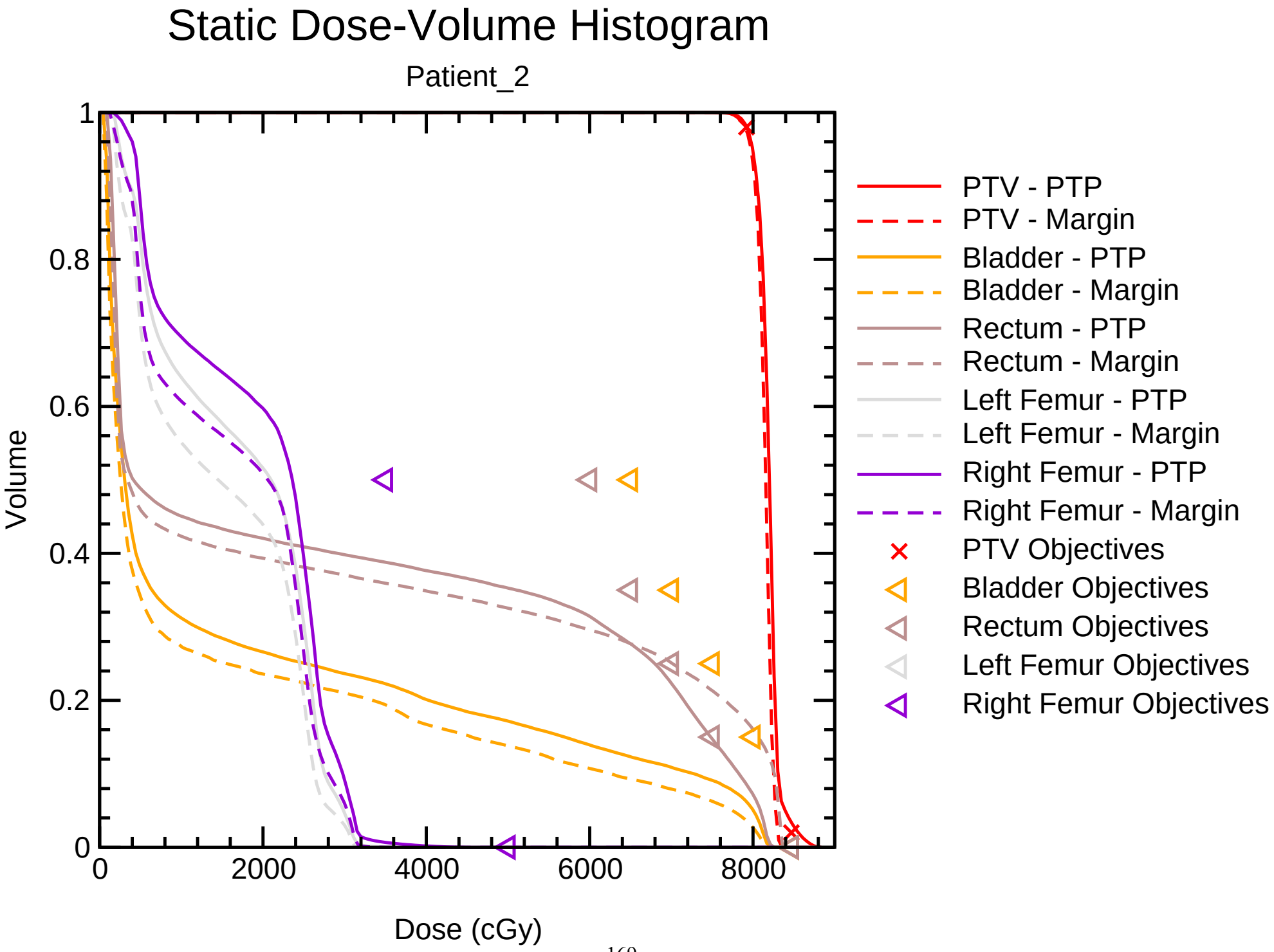
Static Dose-Volume Histogram
Patient_2
Volume
Dose (cGy)
0
0.2
0.4
0.6
0.8
1
0
2000
4000
6000
8000
PTV - PTP
PTV - Margin
Bladder - PTP
Bladder - Margin
Rectum - PTP
Rectum - Margin
Left Femur - PTP
Left Femur - Margin
Right Femur - PTP
Right Femur - Margin
PTV Objectives
Bladder Objectives
Rectum Objectives
Left Femur Objectives
Right Femur Objectives

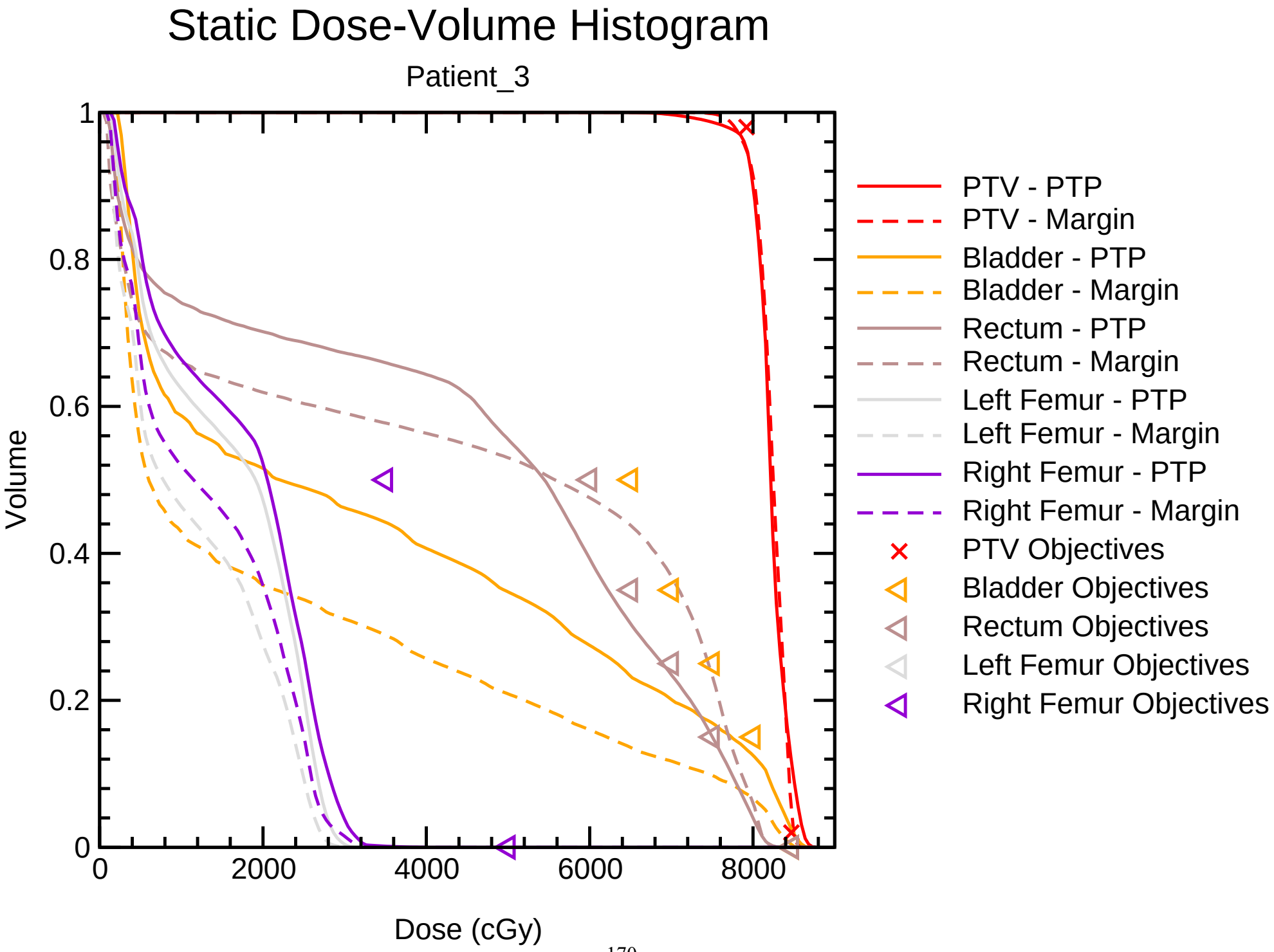
Static Dose-Volume Histogram
Patient_3
Volume
Dose (cGy)
0
0.2
0.4
0.6
0.8
1
0
2000
4000
6000
8000
PTV - PTP
PTV - Margin
Bladder - PTP
Bladder - Margin
Rectum - PTP
Rectum - Margin
Left Femur - PTP
Left Femur - Margin
Right Femur - PTP
Right Femur - Margin
PTV Objectives
Bladder Objectives
Rectum Objectives
Left Femur Objectives
Right Femur Objectives

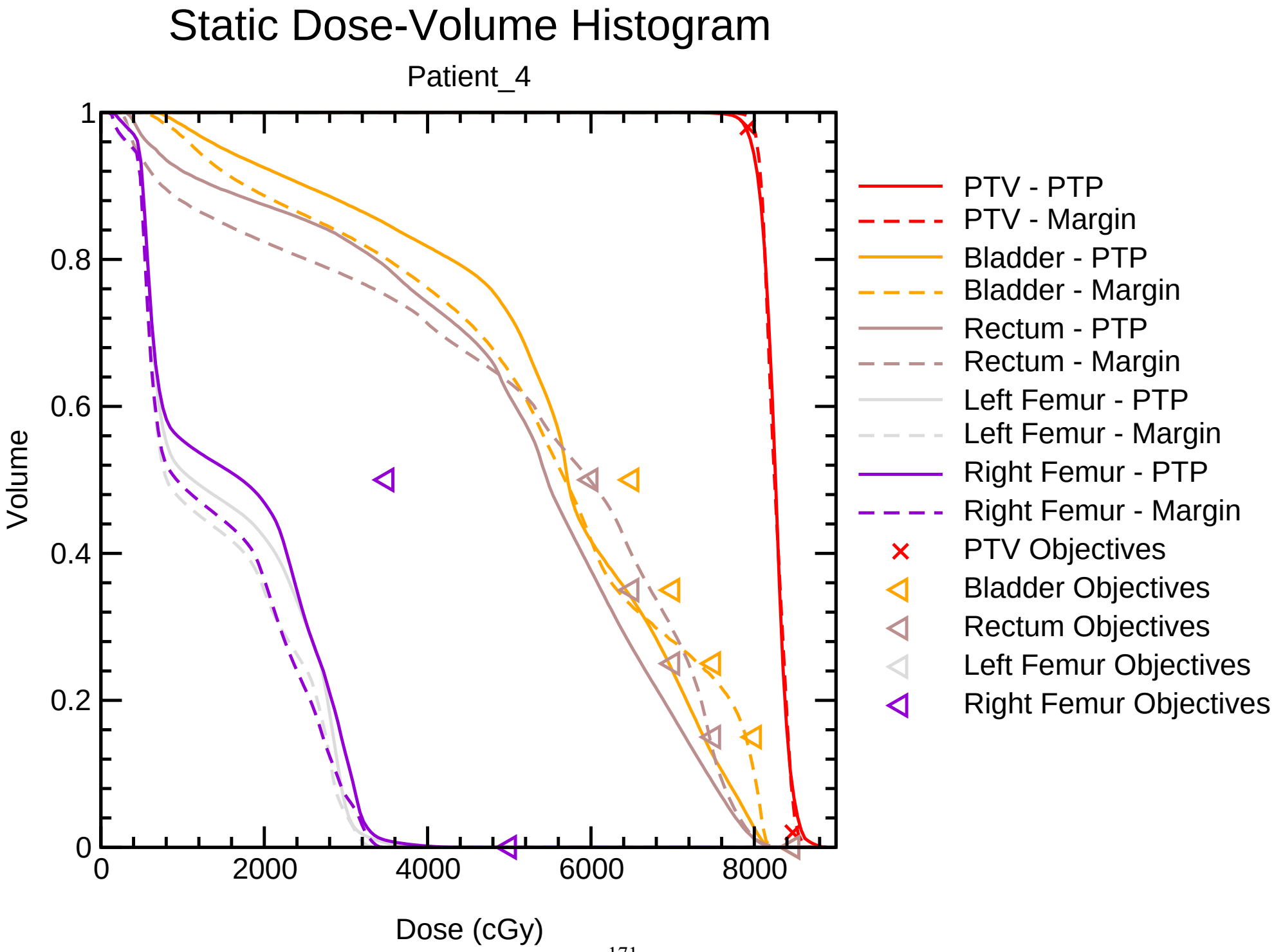
Static Dose-Volume Histogram
Patient_4
Volume
Dose (cGy)
0
0.2
0.4
0.6
0.8
1
0
2000
4000
6000
8000
PTV - PTP
PTV - Margin
Bladder - PTP
Bladder - Margin
Rectum - PTP
Rectum - Margin
Left Femur - PTP
Left Femur - Margin
Right Femur - PTP
Right Femur - Margin
PTV Objectives
Bladder Objectives
Rectum Objectives
Left Femur Objectives
Right Femur Objectives

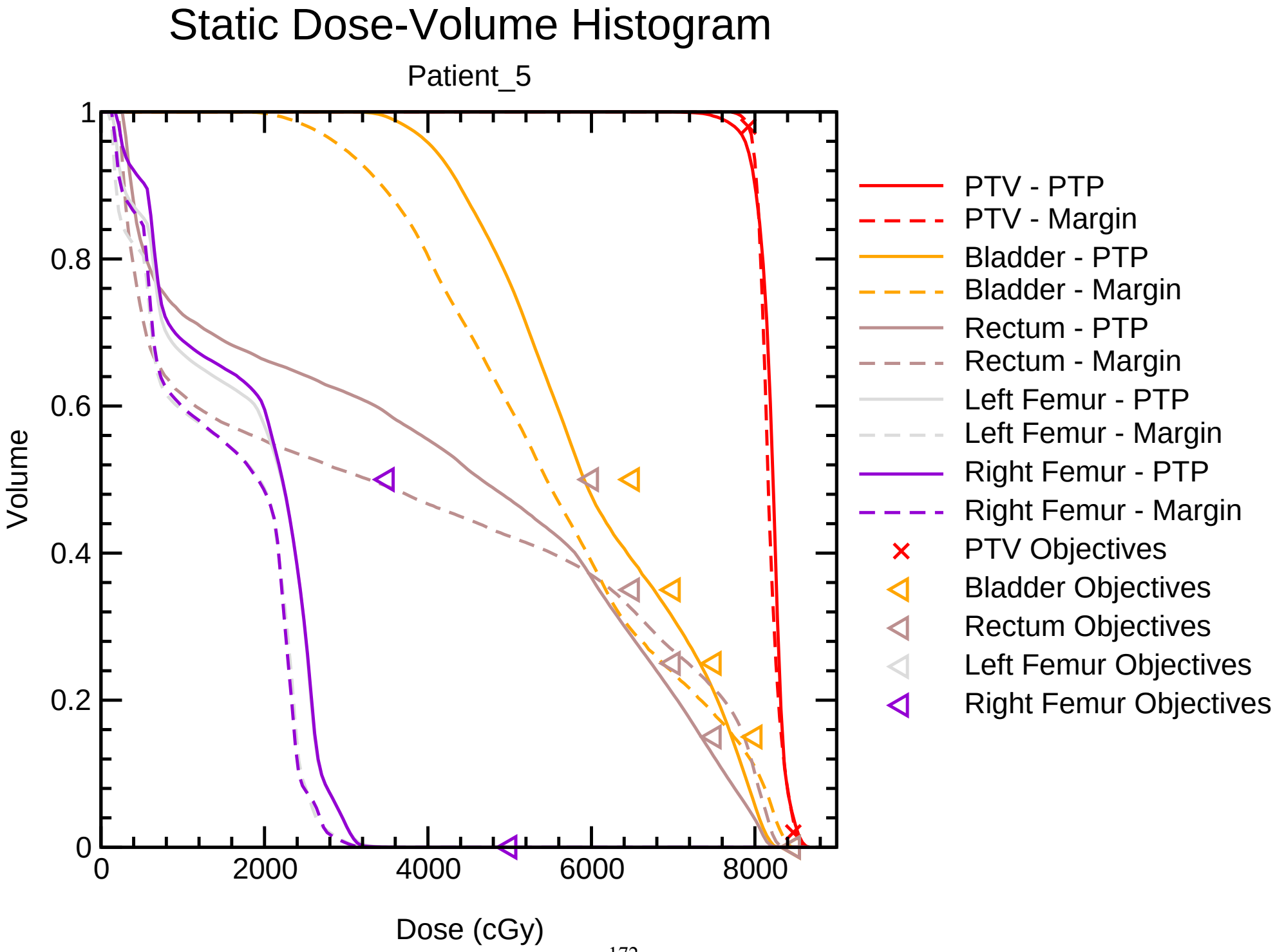
Static Dose-Volume Histogram
Patient_5
Volume
Dose (cGy)
0
0.2
0.4
0.6
0.8
1
0
2000
4000
6000
8000
PTV - PTP
PTV - Margin
Bladder - PTP
Bladder - Margin
Rectum - PTP
Rectum - Margin
Left Femur - PTP
Left Femur - Margin
Right Femur - PTP
Right Femur - Margin
PTV Objectives
Bladder Objectives
Rectum Objectives
Left Femur Objectives
Right Femur Objectives

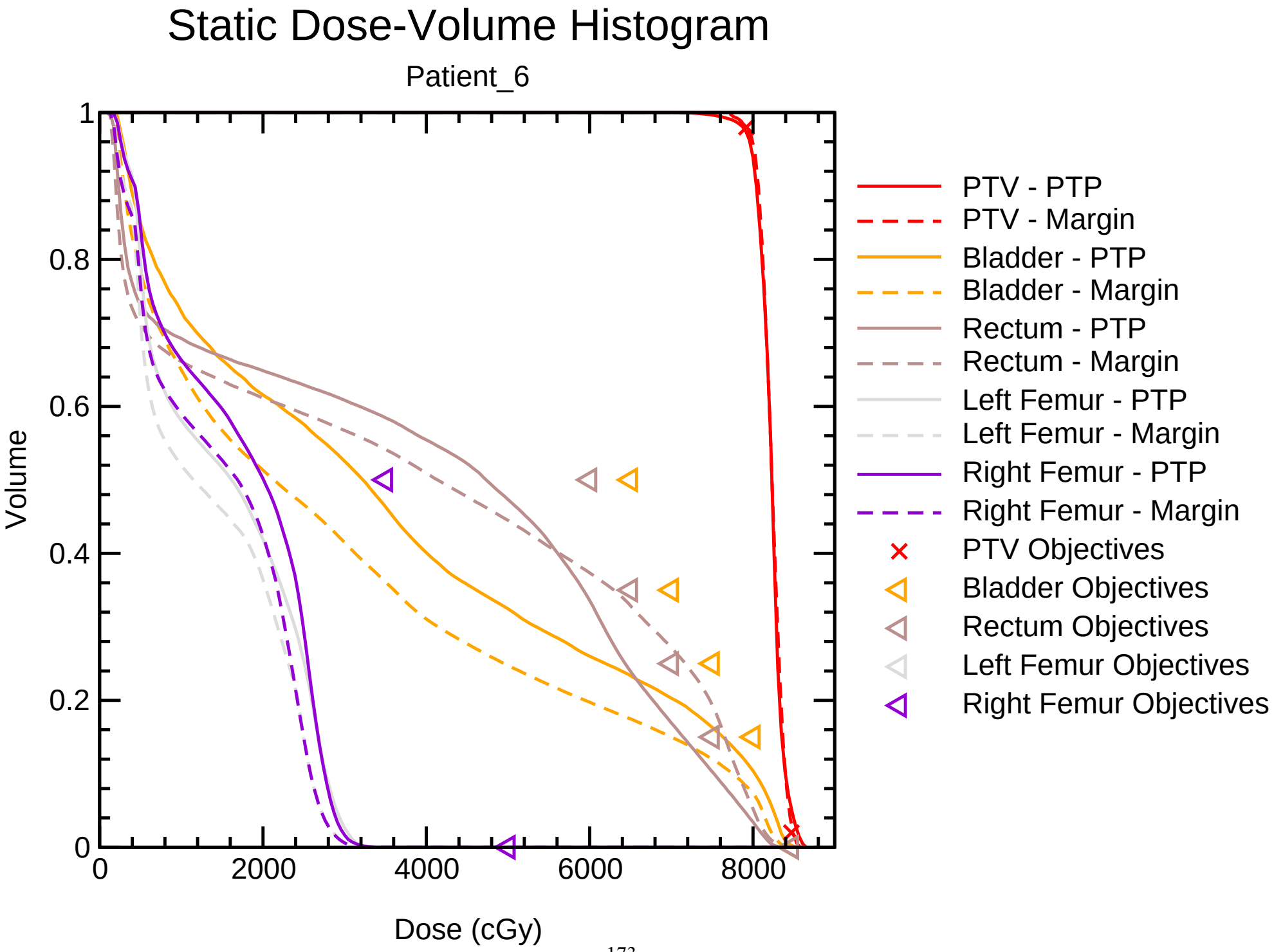
Static Dose-Volume Histogram
Patient_6
Volume
Dose (cGy)
0
0.2
0.4
0.6
0.8
1
0
2000
4000
6000
8000
PTV - PTP
PTV - Margin
Bladder - PTP
Bladder - Margin
Rectum - PTP
Rectum - Margin
Left Femur - PTP
Left Femur - Margin
Right Femur - PTP
Right Femur - Margin
PTV Objectives
Bladder Objectives
Rectum Objectives
Left Femur Objectives
Right Femur Objectives

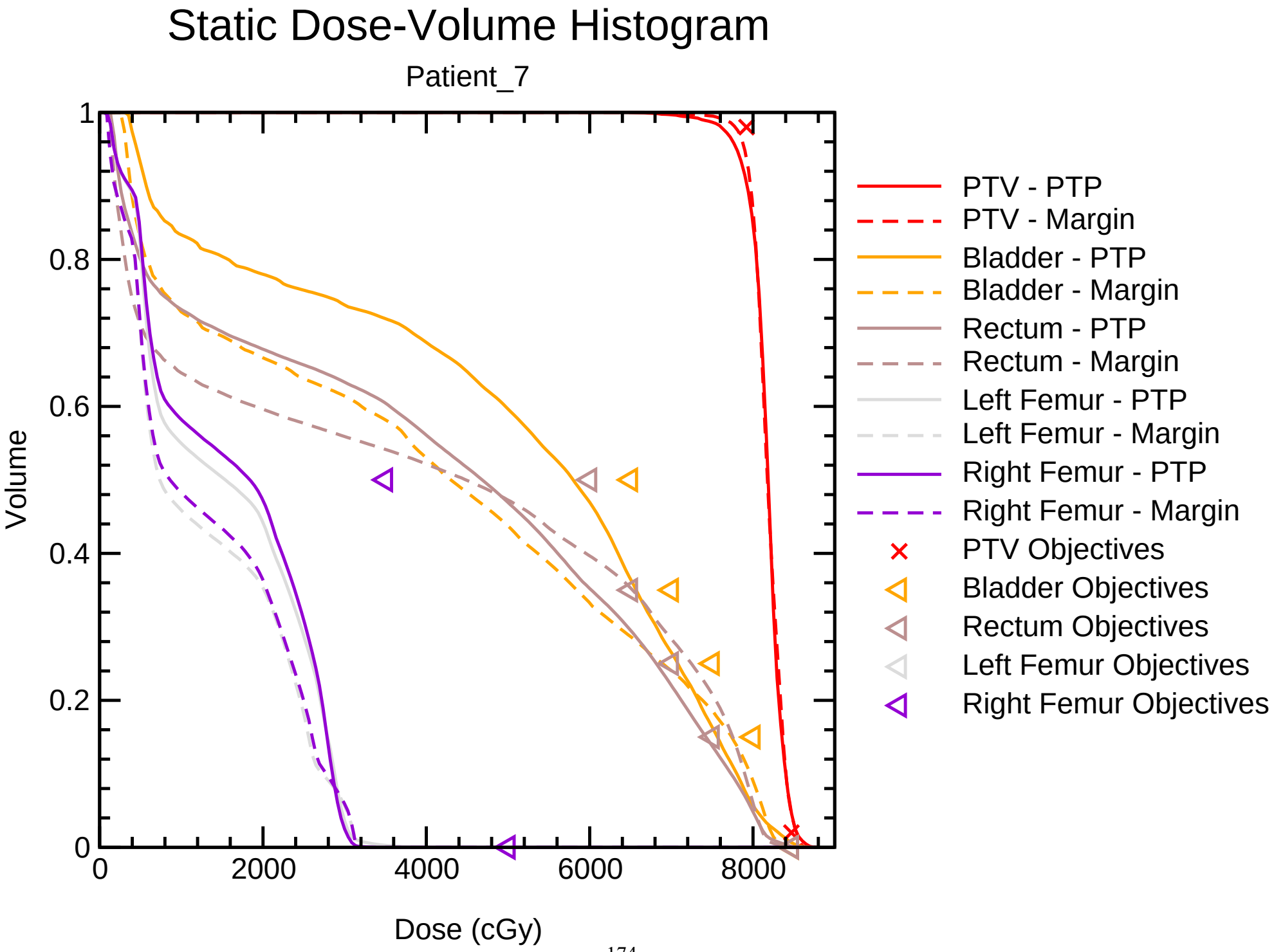
Static Dose-Volume Histogram
Patient_7
Volume
Dose (cGy)
0
0.2
0.4
0.6
0.8
1
0
2000
4000
6000
8000
PTV - PTP
PTV - Margin
Bladder - PTP
Bladder - Margin
Rectum - PTP
Rectum - Margin
Left Femur - PTP
Left Femur - Margin
Right Femur - PTP
Right Femur - Margin
PTV Objectives
Bladder Objectives
Rectum Objectives
Left Femur Objectives
Right Femur Objectives

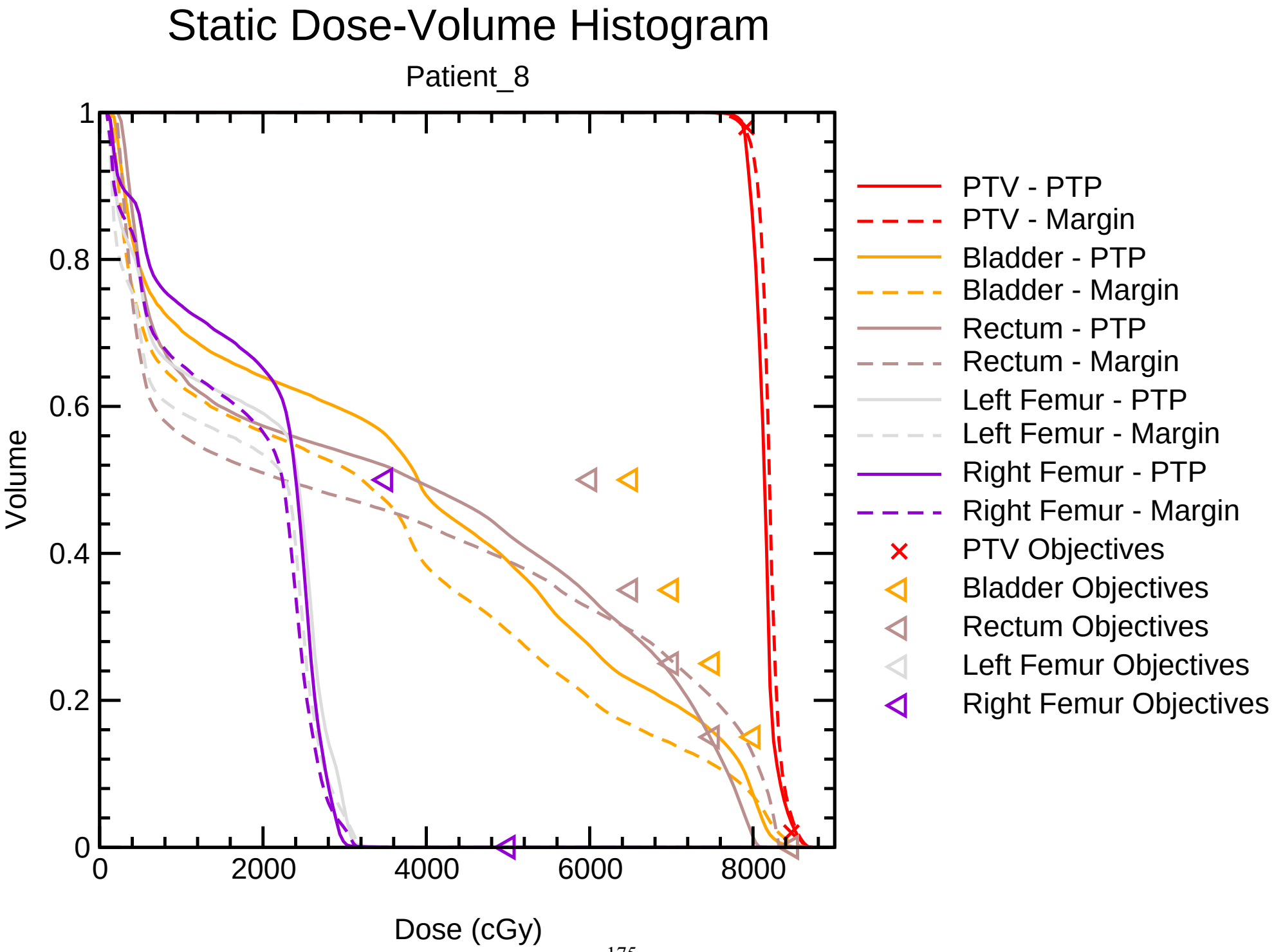
Static Dose-Volume Histogram
Patient_8
Volume
Dose (cGy)
0
0.2
0.4
0.6
0.8
1
0
2000
4000
6000
8000
PTV - PTP
PTV - Margin
Bladder - PTP
Bladder - Margin
Rectum - PTP
Rectum - Margin
Left Femur - PTP
Left Femur - Margin
Right Femur - PTP
Right Femur - Margin
PTV Objectives
Bladder Objectives
Rectum Objectives
Left Femur Objectives
Right Femur Objectives

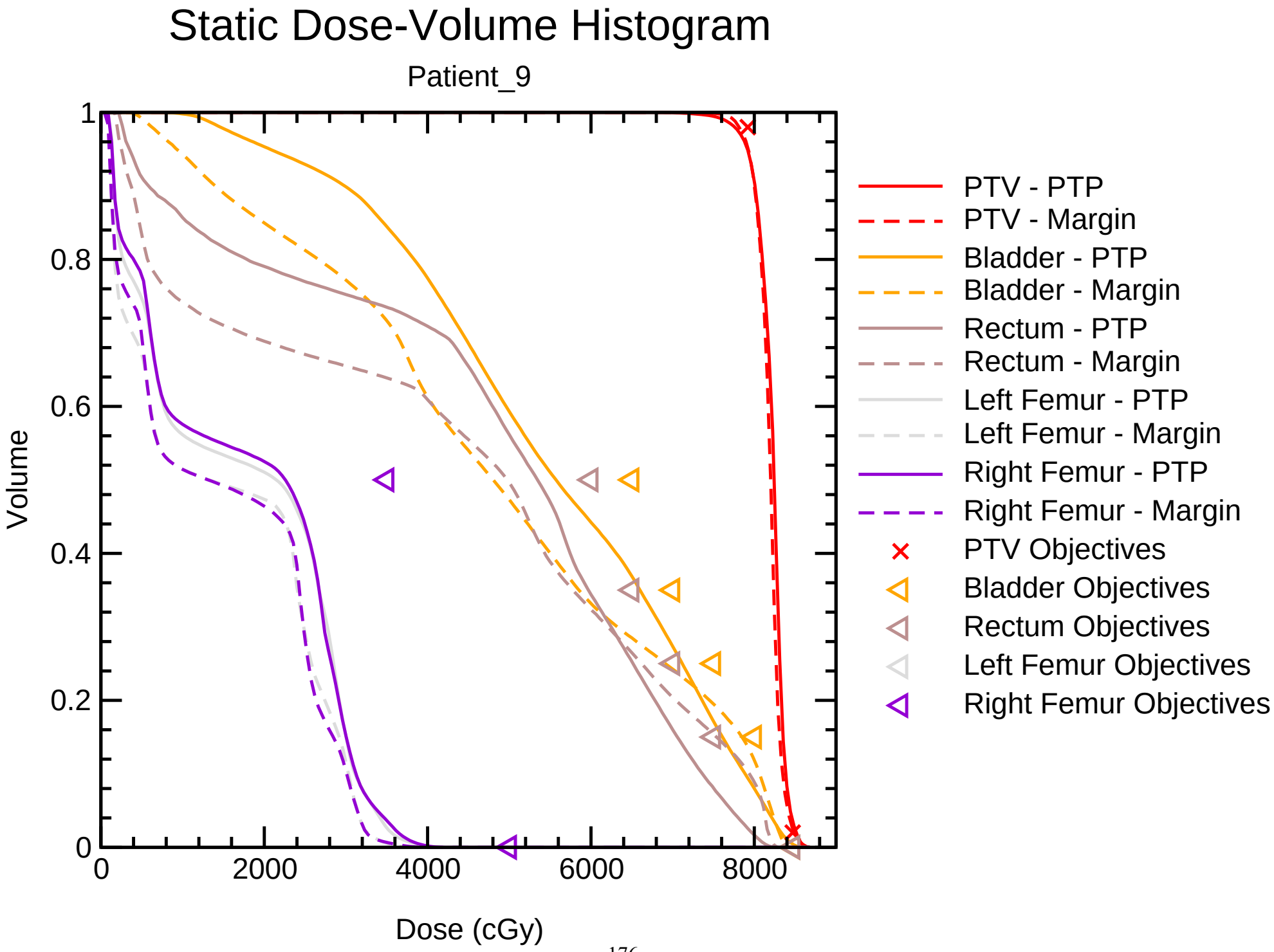
Static Dose-Volume Histogram
Patient_9
Volume
Dose (cGy)
0
0.2
0.4
0.6
0.8
1
0
2000
4000
6000
8000
PTV - PTP
PTV - Margin
Bladder - PTP
Bladder - Margin
Rectum - PTP
Rectum - Margin
Left Femur - PTP
Left Femur - Margin
Right Femur - PTP
Right Femur - Margin
PTV Objectives
Bladder Objectives
Rectum Objectives
Left Femur Objectives
Right Femur Objectives

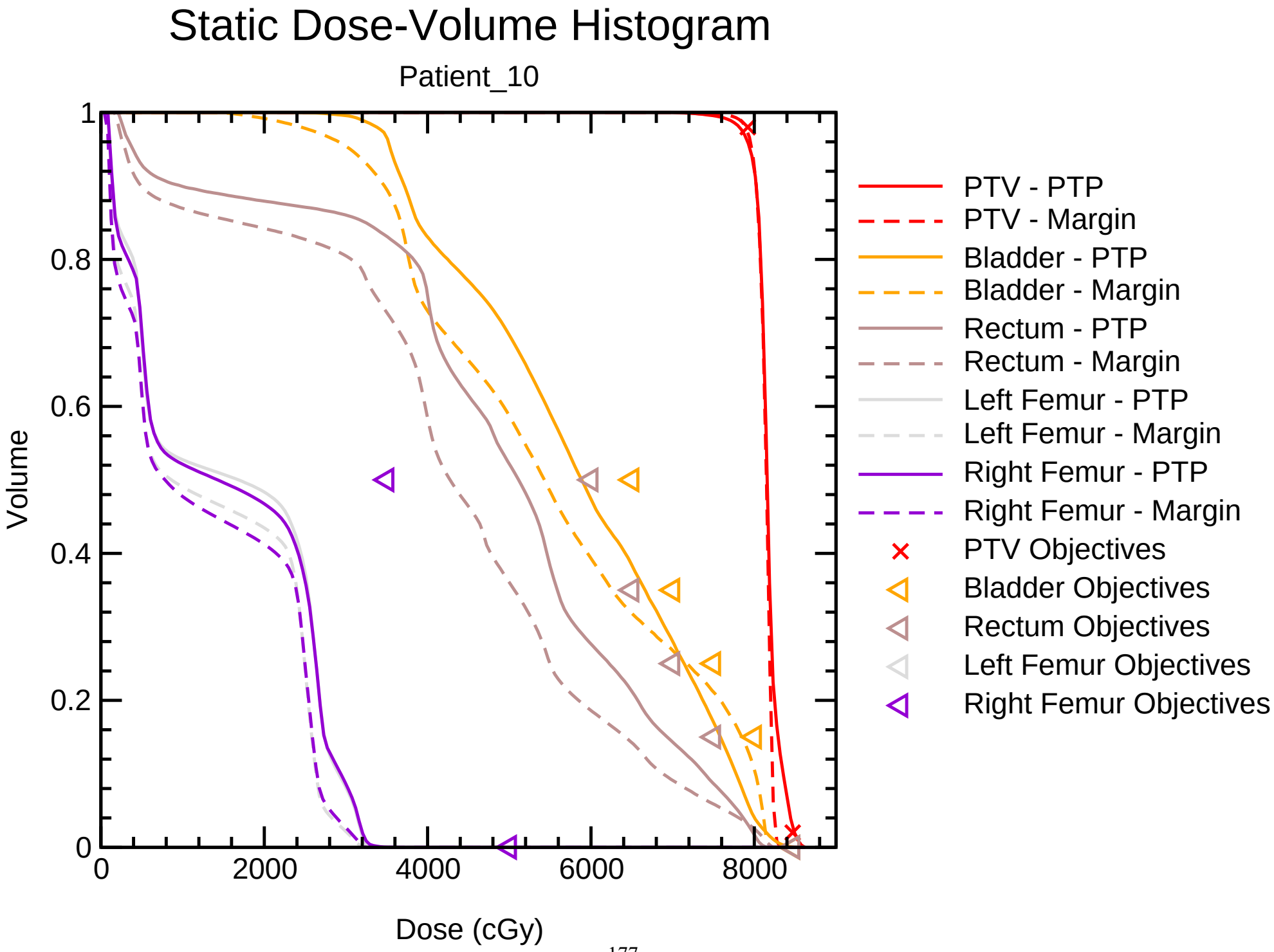
Static Dose-Volume Histogram
Patient_10
Volume
Dose (cGy)
0
0.2
0.4
0.6
0.8
1
0
2000
4000
6000
8000
PTV - PTP
PTV - Margin
Bladder - PTP
Bladder - Margin
Rectum - PTP
Rectum - Margin
Left Femur - PTP
Left Femur - Margin
Right Femur - PTP
Right Femur - Margin
PTV Objectives
Bladder Objectives
Rectum Objectives
Left Femur Objectives
Right Femur Objectives

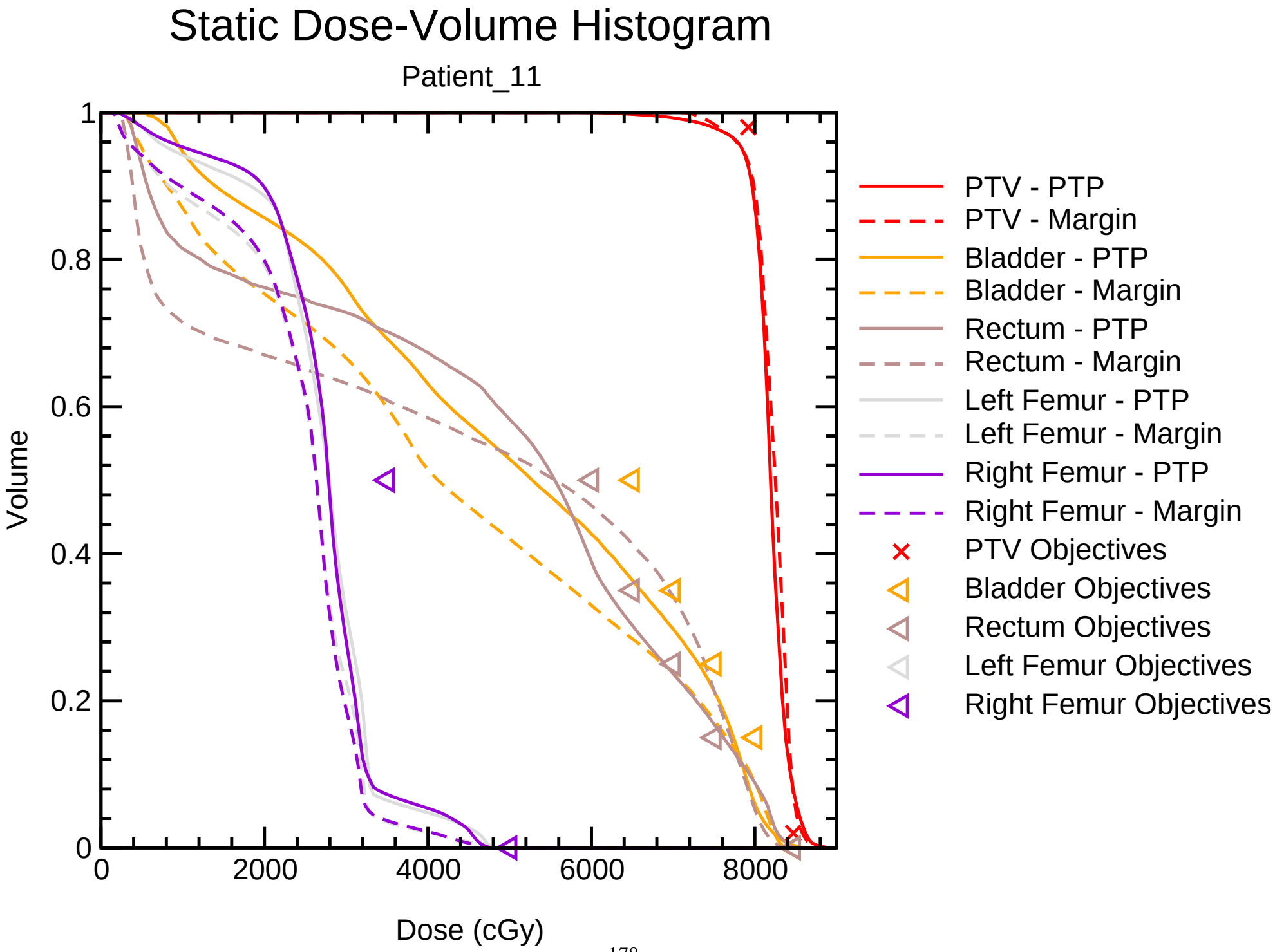
Static Dose-Volume Histogram
Patient_11
Volume
Dose (cGy)
0
0.2
0.4
0.6
0.8
1
0
2000
4000
6000
8000
PTV - PTP
PTV - Margin
Bladder - PTP
Bladder - Margin
Rectum - PTP
Rectum - Margin
Left Femur - PTP
Left Femur - Margin
Right Femur - PTP
Right Femur - Margin
PTV Objectives
Bladder Objectives
Rectum Objectives
Left Femur Objectives
Right Femur Objectives

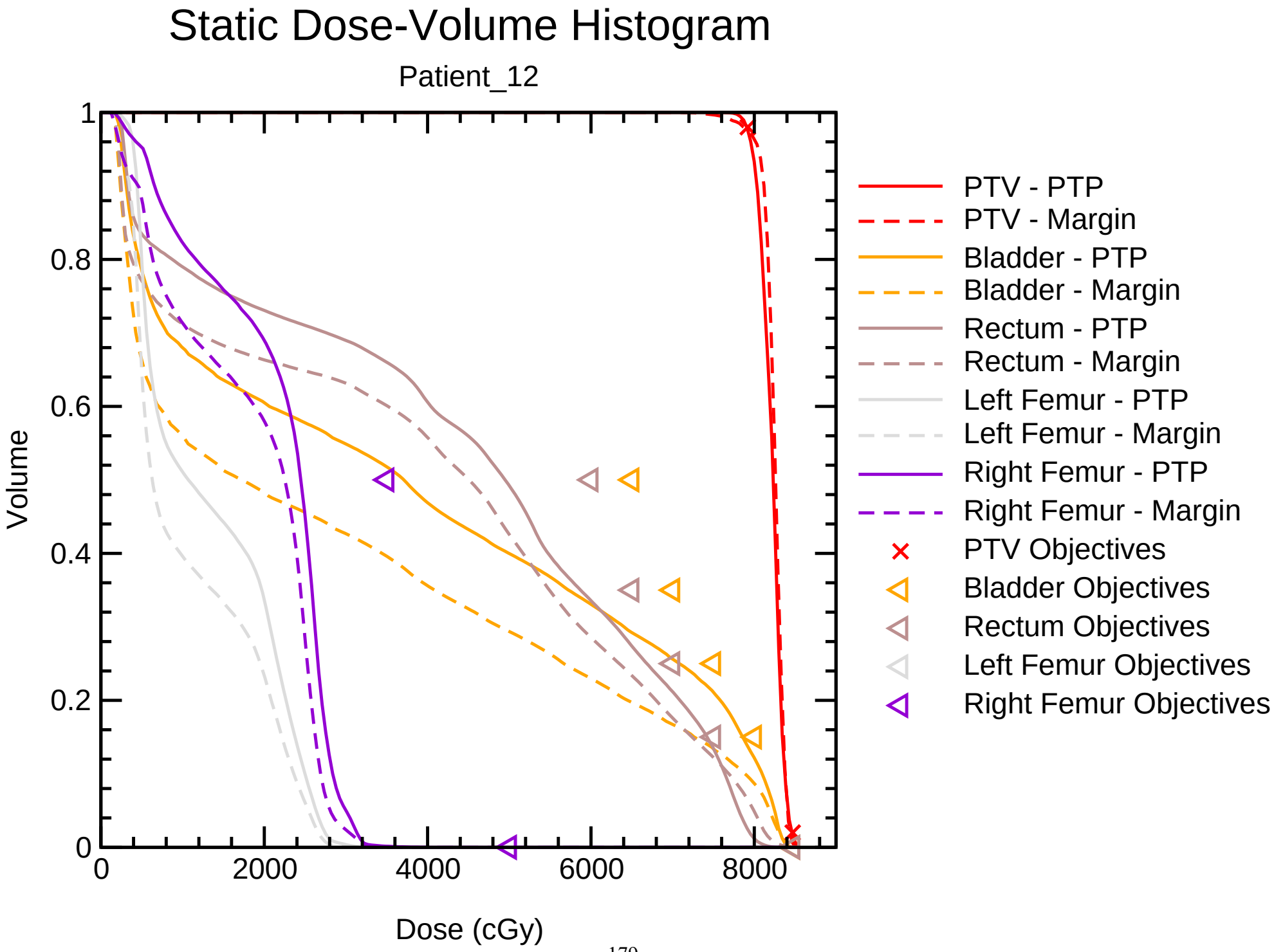
Static Dose-Volume Histogram
Patient_12
Volume
Dose (cGy)
0
0.2
0.4
0.6
0.8
1
0
2000
4000
6000
8000
PTV - PTP
PTV - Margin
Bladder - PTP
Bladder - Margin
Rectum - PTP
Rectum - Margin
Left Femur - PTP
Left Femur - Margin
Right Femur - PTP
Right Femur - Margin
PTV Objectives
Bladder Objectives
Rectum Objectives
Left Femur Objectives
Right Femur Objectives

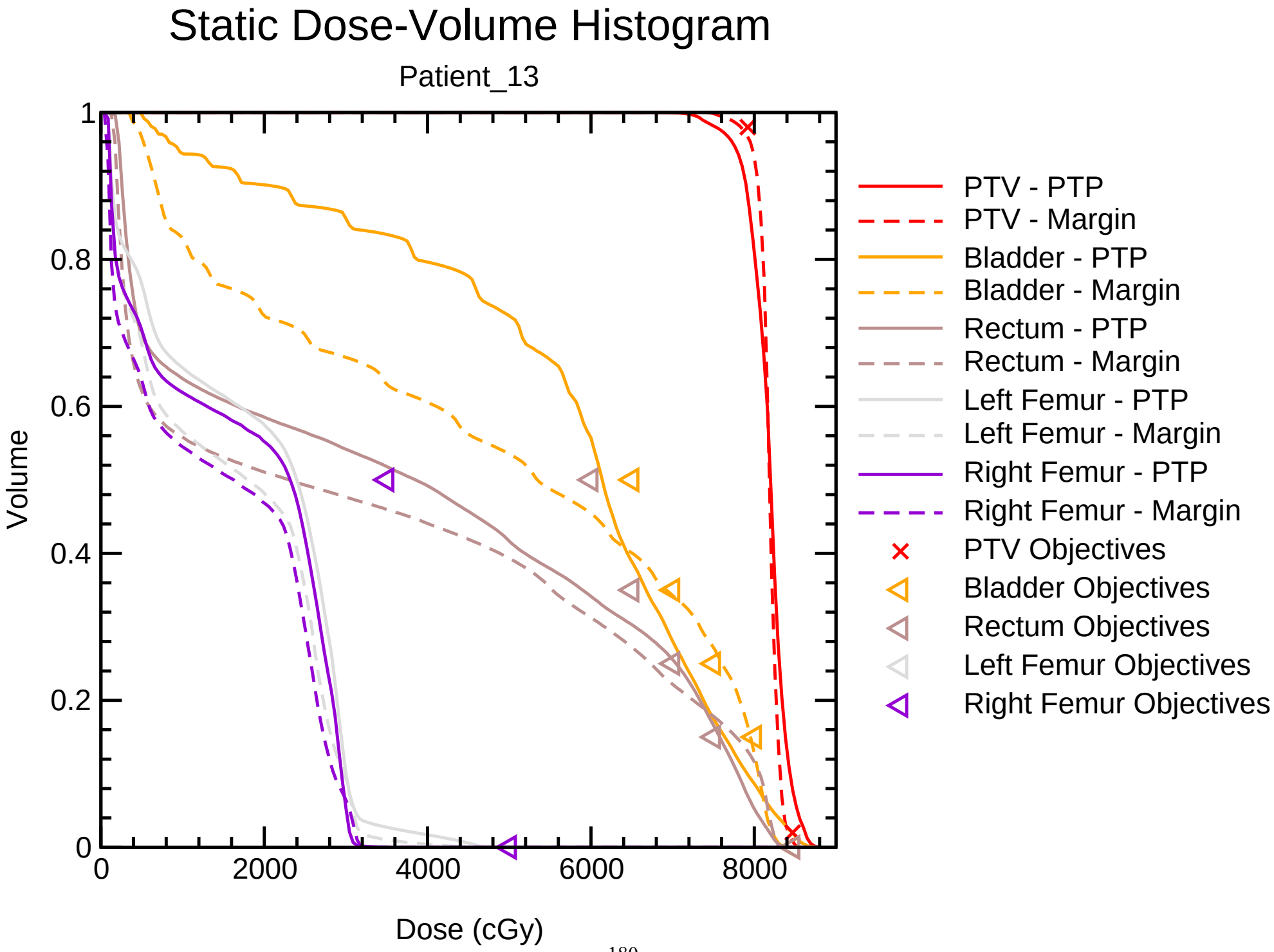
Static Dose-Volume Histogram
Patient_13
Volume
Dose (cGy)
0
0.2
0.4
0.6
0.8
1
0
2000
4000
6000
8000
PTV - PTP
PTV - Margin
Bladder - PTP
Bladder - Margin
Rectum - PTP
Rectum - Margin
Left Femur - PTP
Left Femur - Margin
Right Femur - PTP
Right Femur - Margin
PTV Objectives
Bladder Objectives
Rectum Objectives
Left Femur Objectives
Right Femur Objectives

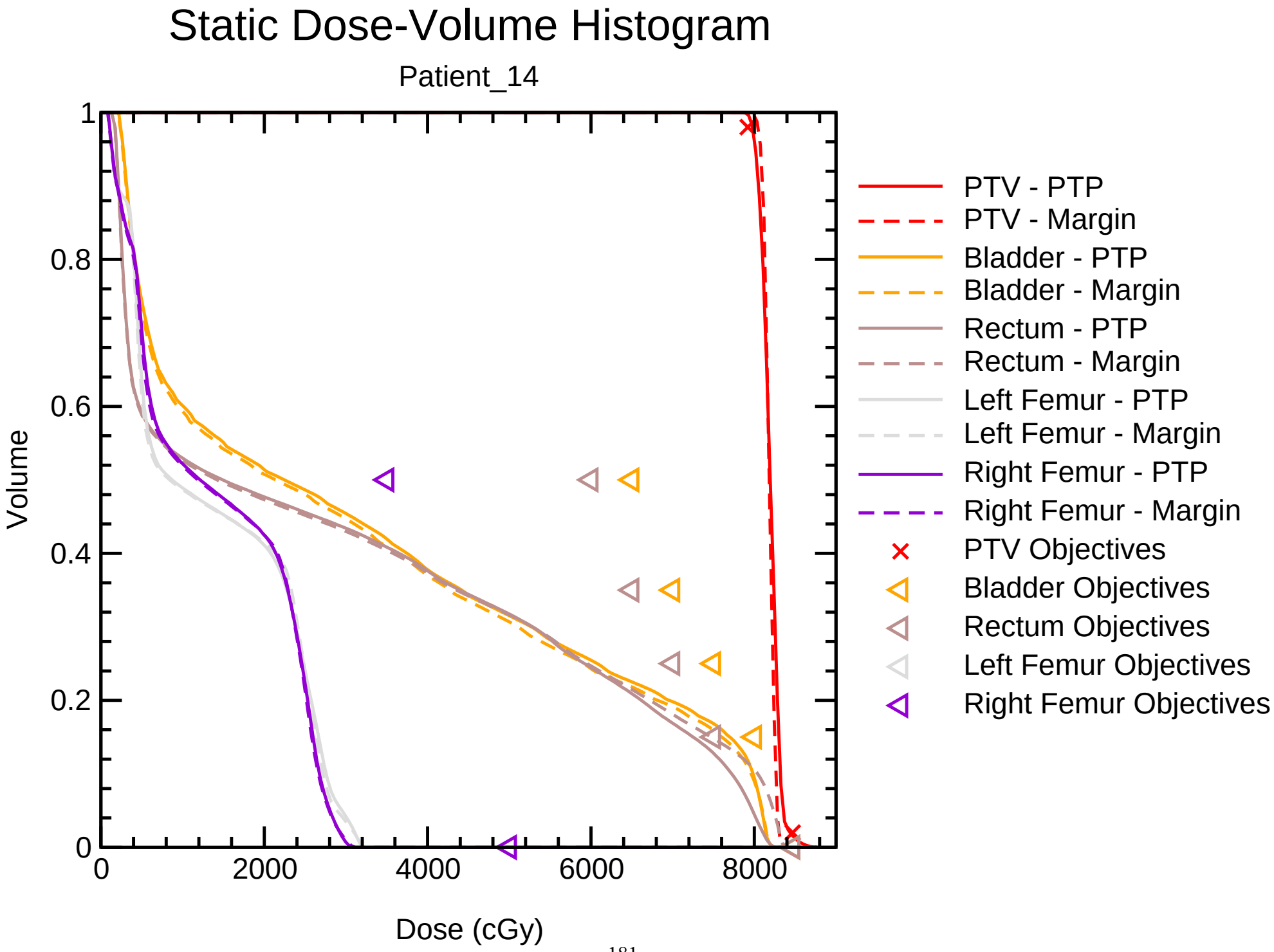
Static Dose-Volume Histogram
Patient_14
Volume
Dose (cGy)
0
0.2
0.4
0.6
0.8
1
0
2000
4000
6000
8000
PTV - PTP
PTV - Margin
Bladder - PTP
Bladder - Margin
Rectum - PTP
Rectum - Margin
Left Femur - PTP
Left Femur - Margin
Right Femur - PTP
Right Femur - Margin
PTV Objectives
Bladder Objectives
Rectum Objectives
Left Femur Objectives
Right Femur Objectives

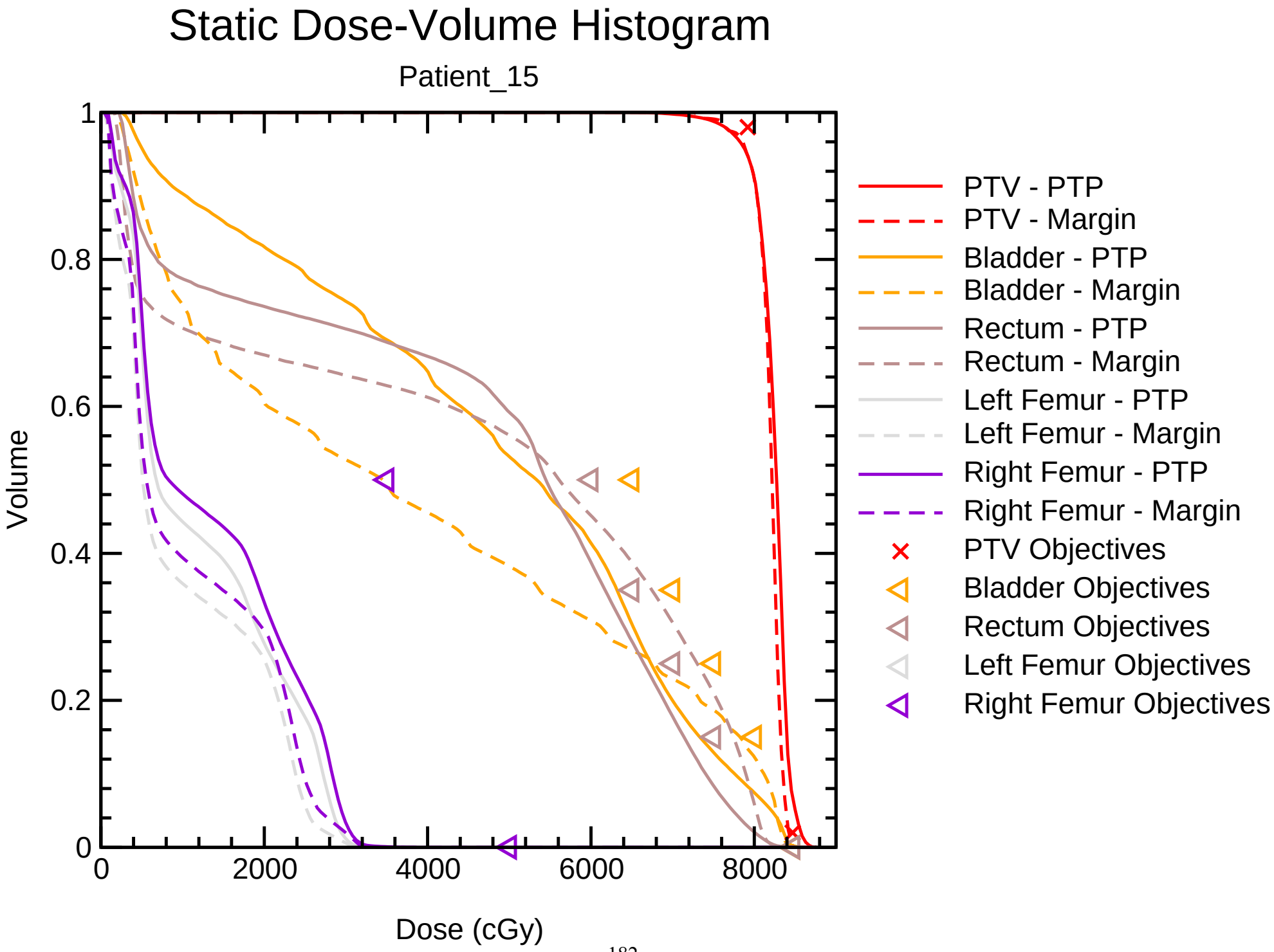
Static Dose-Volume Histogram
Patient_15
Volume
Dose (cGy)
0
0.2
0.4
0.6
0.8
1
0
2000
4000
6000
8000
PTV - PTP
PTV - Margin
Bladder - PTP
Bladder - Margin
Rectum - PTP
Rectum - Margin
Left Femur - PTP
Left Femur - Margin
Right Femur - PTP
Right Femur - Margin
PTV Objectives
Bladder Objectives
Rectum Objectives
Left Femur Objectives
Right Femur Objectives

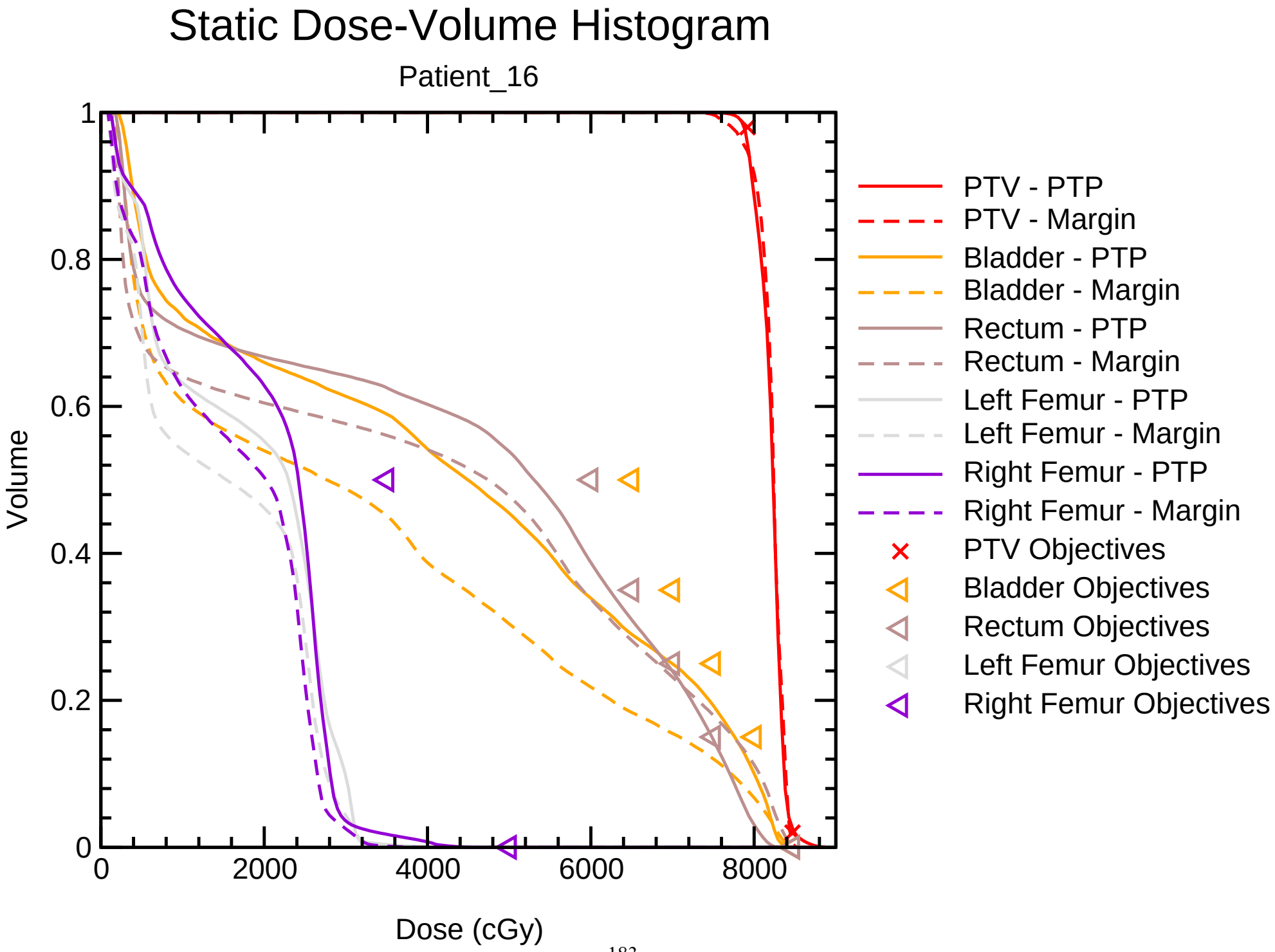
Static Dose-Volume Histogram
Patient_16
Volume
Dose (cGy)
0
0.2
0.4
0.6
0.8
1
0
2000
4000
6000
8000
PTV - PTP
PTV - Margin
Bladder - PTP
Bladder - Margin
Rectum - PTP
Rectum - Margin
Left Femur - PTP
Left Femur - Margin
Right Femur - PTP
Right Femur - Margin
PTV Objectives
Bladder Objectives
Rectum Objectives
Left Femur Objectives
Right Femur Objectives

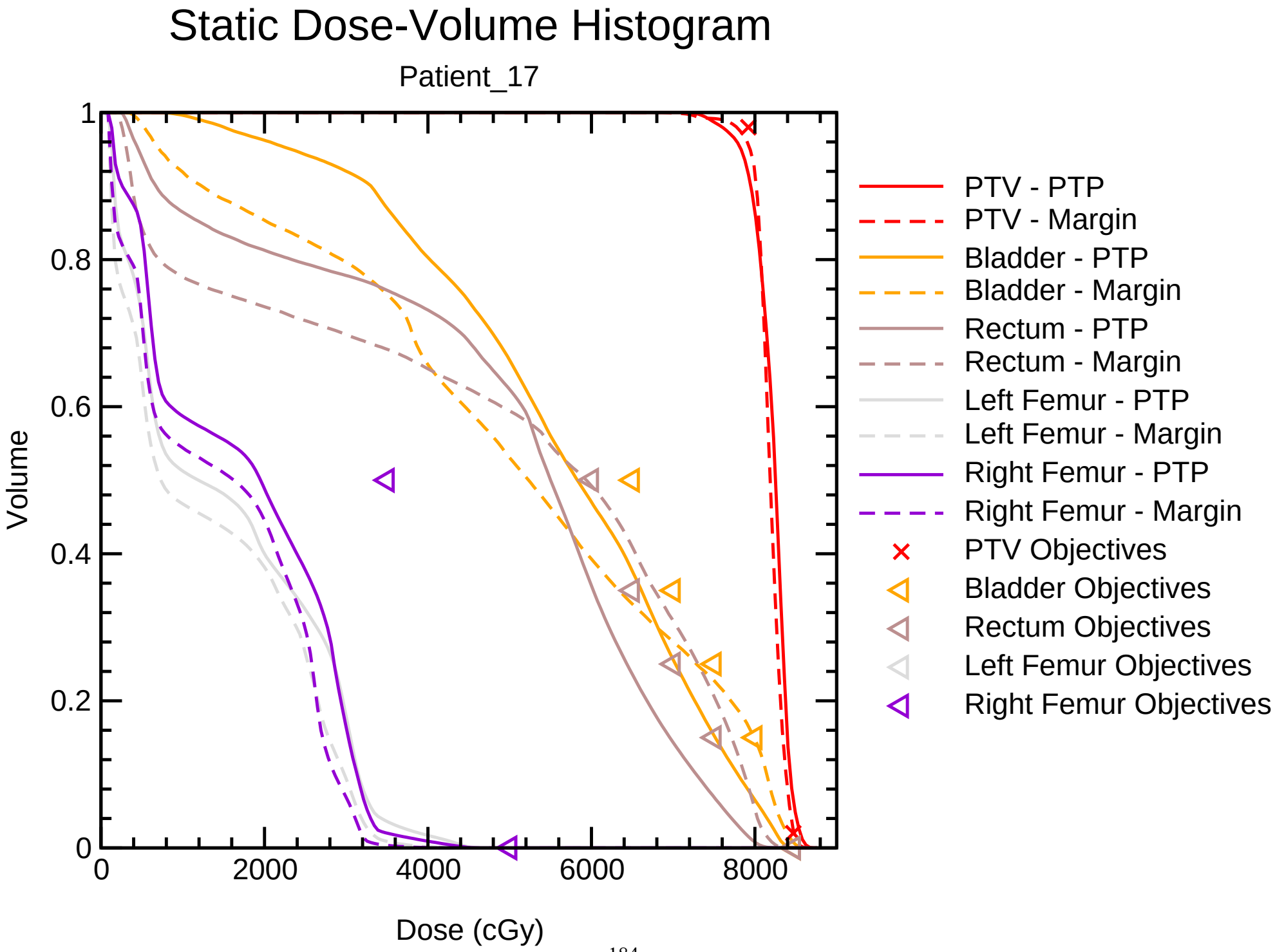
Static Dose-Volume Histogram
Patient_17
Volume
Dose (cGy)
0
0.2
0.4
0.6
0.8
1
0
2000
4000
6000
8000
PTV - PTP
PTV - Margin
Bladder - PTP
Bladder - Margin
Rectum - PTP
Rectum - Margin
Left Femur - PTP
Left Femur - Margin
Right Femur - PTP
Right Femur - Margin
PTV Objectives
Bladder Objectives
Rectum Objectives
Left Femur Objectives
Right Femur Objectives

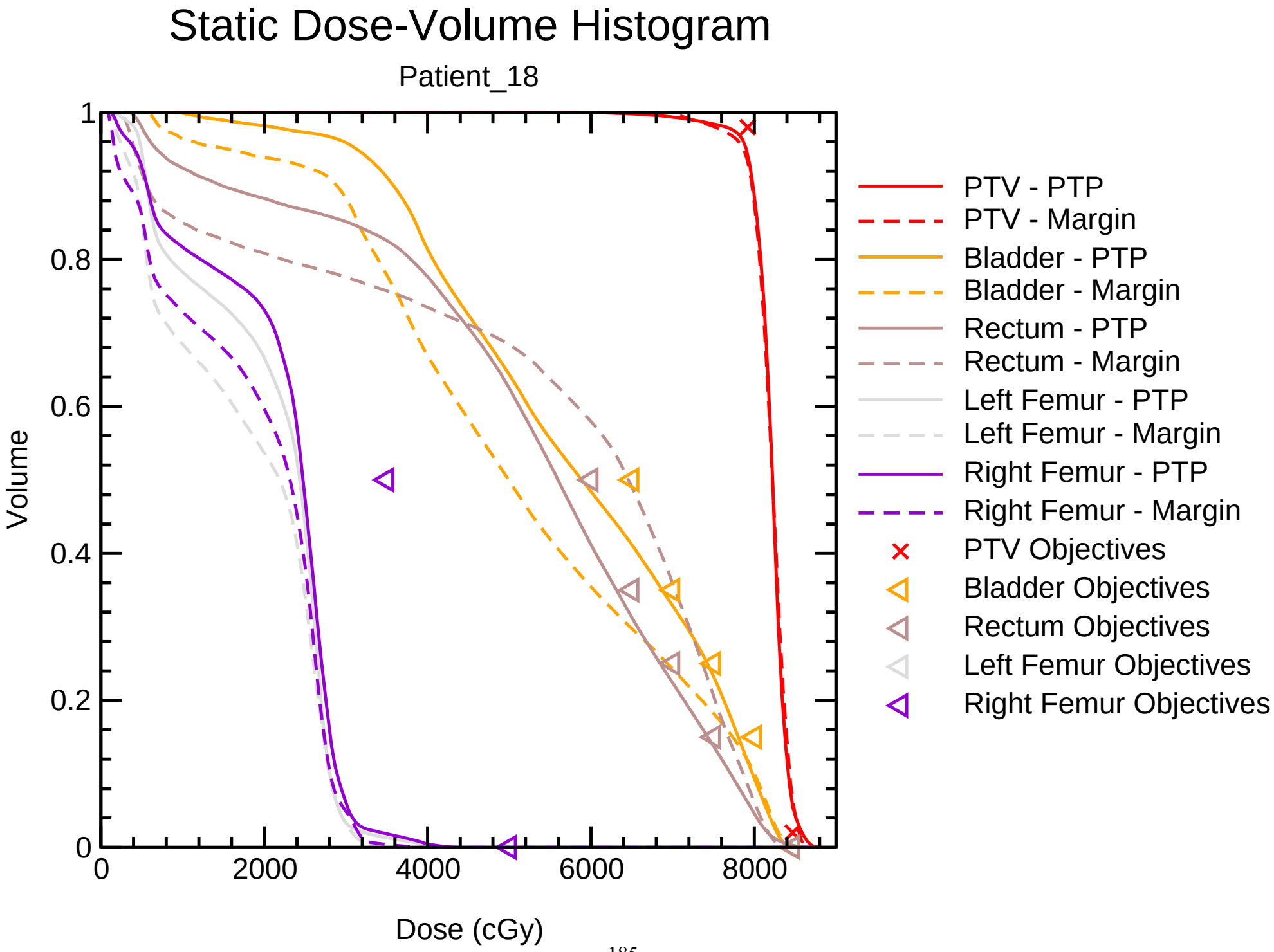
Static Dose-Volume Histogram
Patient_18
Volume
Dose (cGy)
0
0.2
0.4
0.6
0.8
1
0
2000
4000
6000
8000
PTV - PTP
PTV - Margin
Bladder - PTP
Bladder - Margin
Rectum - PTP
Rectum - Margin
Left Femur - PTP
Left Femur - Margin
Right Femur - PTP
Right Femur - Margin
PTV Objectives
Bladder Objectives
Rectum Objectives
Left Femur Objectives
Right Femur Objectives

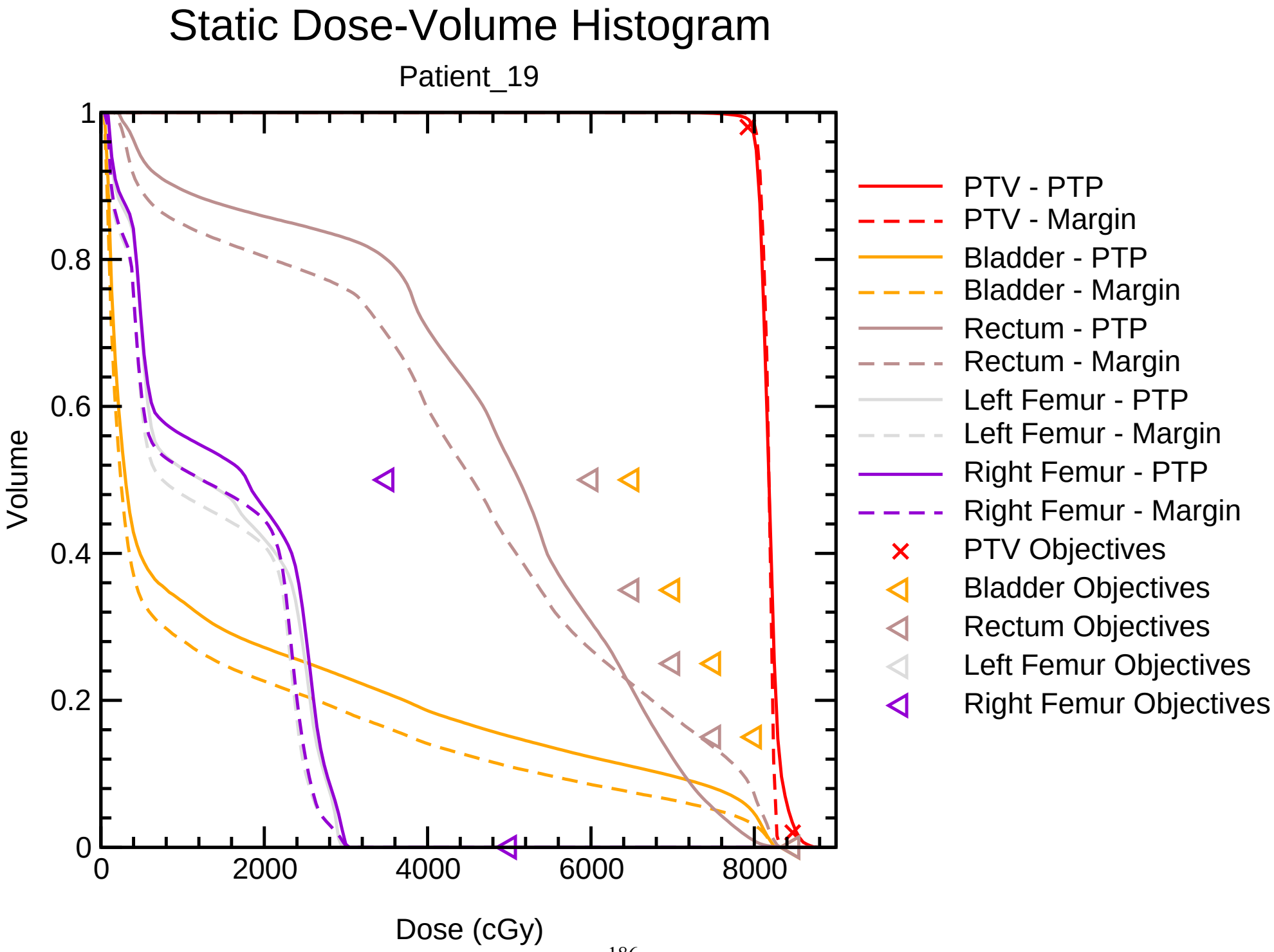
Static Dose-Volume Histogram
Patient_19
Volume
Dose (cGy)
0
0.2
0.4
0.6
0.8
1
0
2000
4000
6000
8000
PTV - PTP
PTV - Margin
Bladder - PTP
Bladder - Margin
Rectum - PTP
Rectum - Margin
Left Femur - PTP
Left Femur - Margin
Right Femur - PTP
Right Femur - Margin
PTV Objectives
Bladder Objectives
Rectum Objectives
Left Femur Objectives
Right Femur Objectives

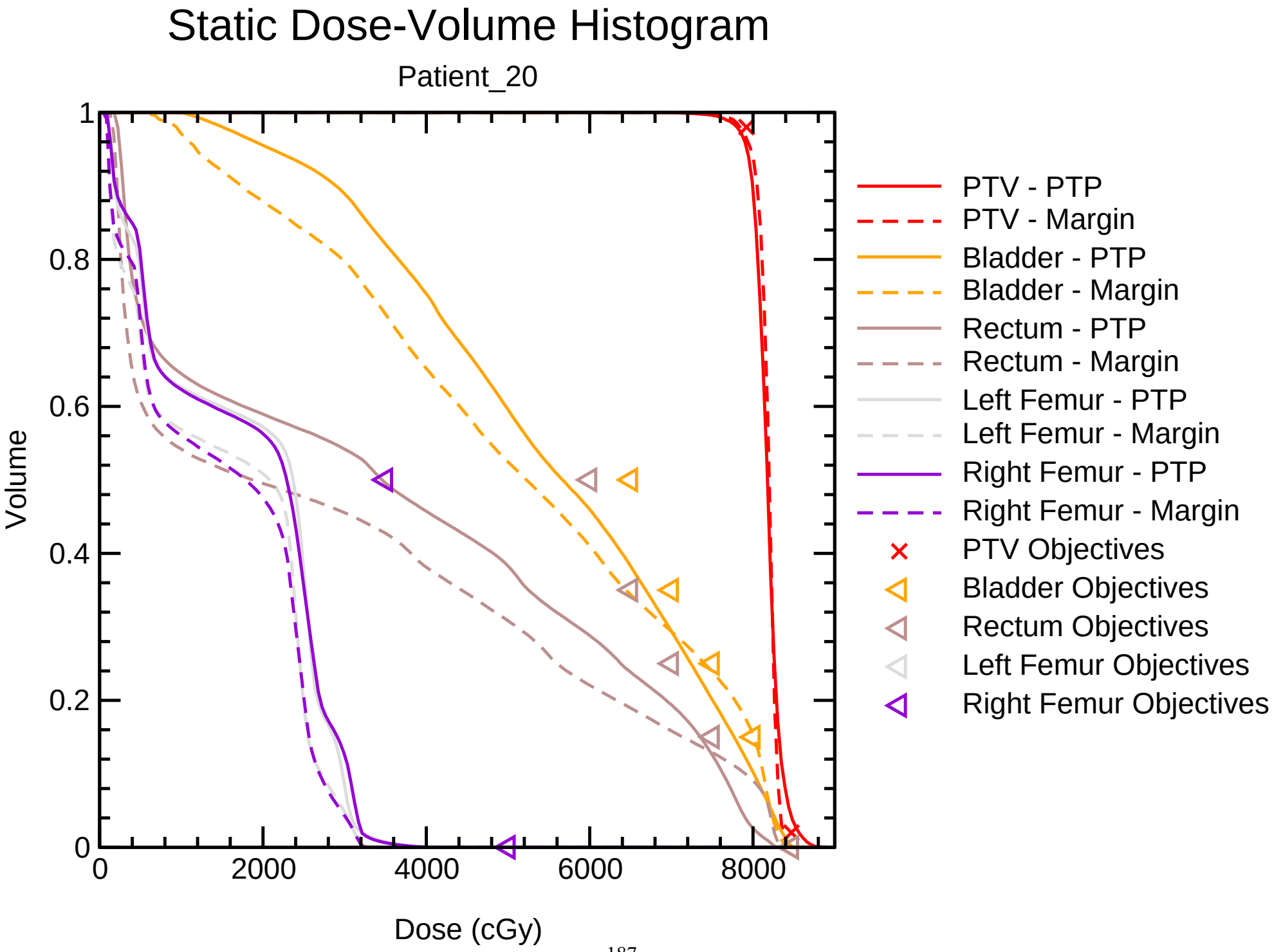
Static Dose-Volume Histogram
Patient_20
Volume
Dose (cGy)
0
0.2
0.4
0.6
0.8
1
0
2000
4000
6000
8000
PTV - PTP
PTV - Margin
Bladder - PTP
Bladder - Margin
Rectum - PTP
Rectum - Margin
Left Femur - PTP
Left Femur - Margin
Right Femur - PTP
Right Femur - Margin
PTV Objectives
Bladder Objectives
Rectum Objectives
Left Femur Objectives
Right Femur Objectives

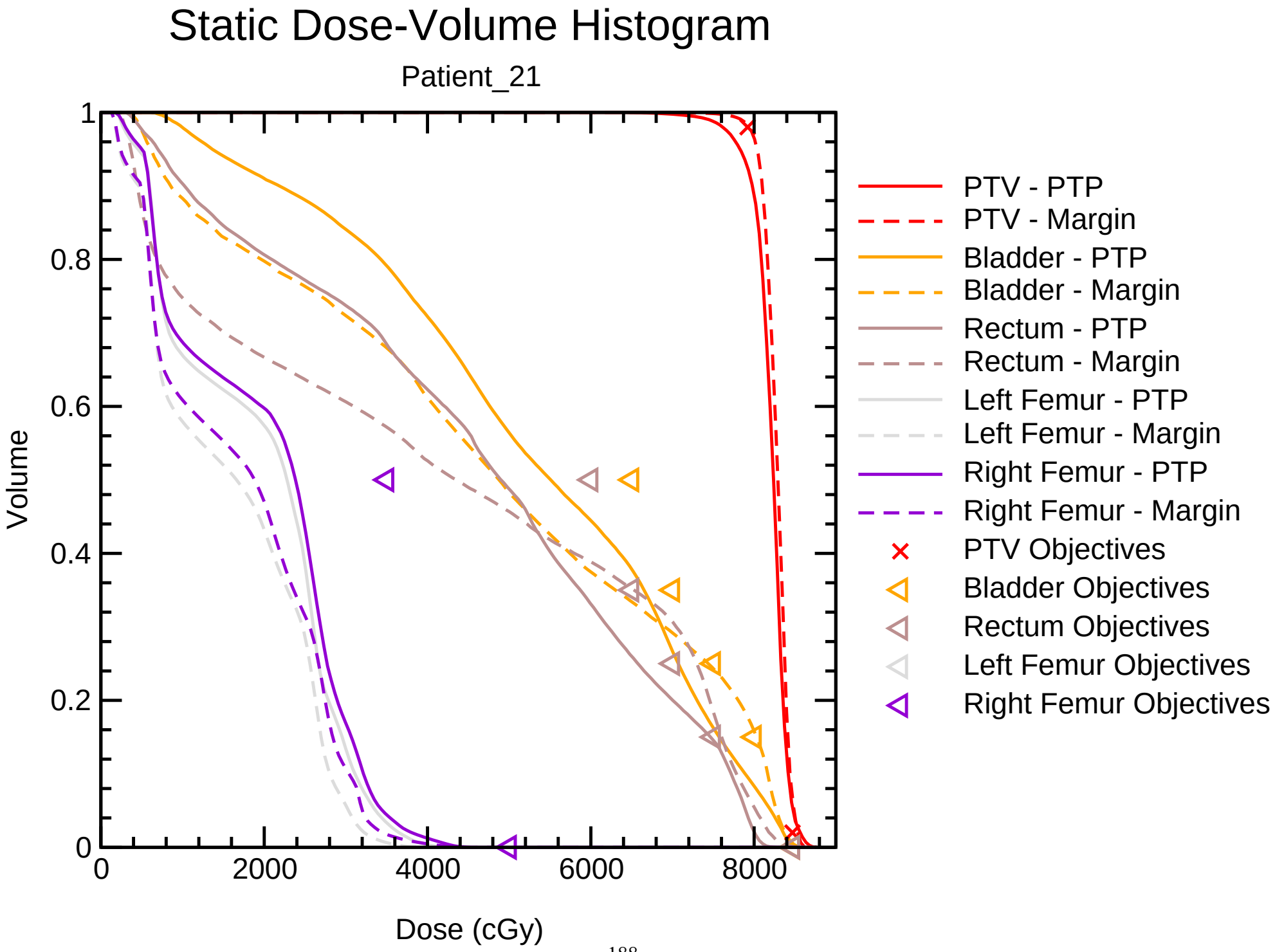
Static Dose-Volume Histogram
Patient_21
Volume
Dose (cGy)
0
0.2
0.4
0.6
0.8
1
0
2000
4000
6000
8000
PTV - PTP
PTV - Margin
Bladder - PTP
Bladder - Margin
Rectum - PTP
Rectum - Margin
Left Femur - PTP
Left Femur - Margin
Right Femur - PTP
Right Femur - Margin
PTV Objectives
Bladder Objectives
Rectum Objectives
Left Femur Objectives
Right Femur Objectives

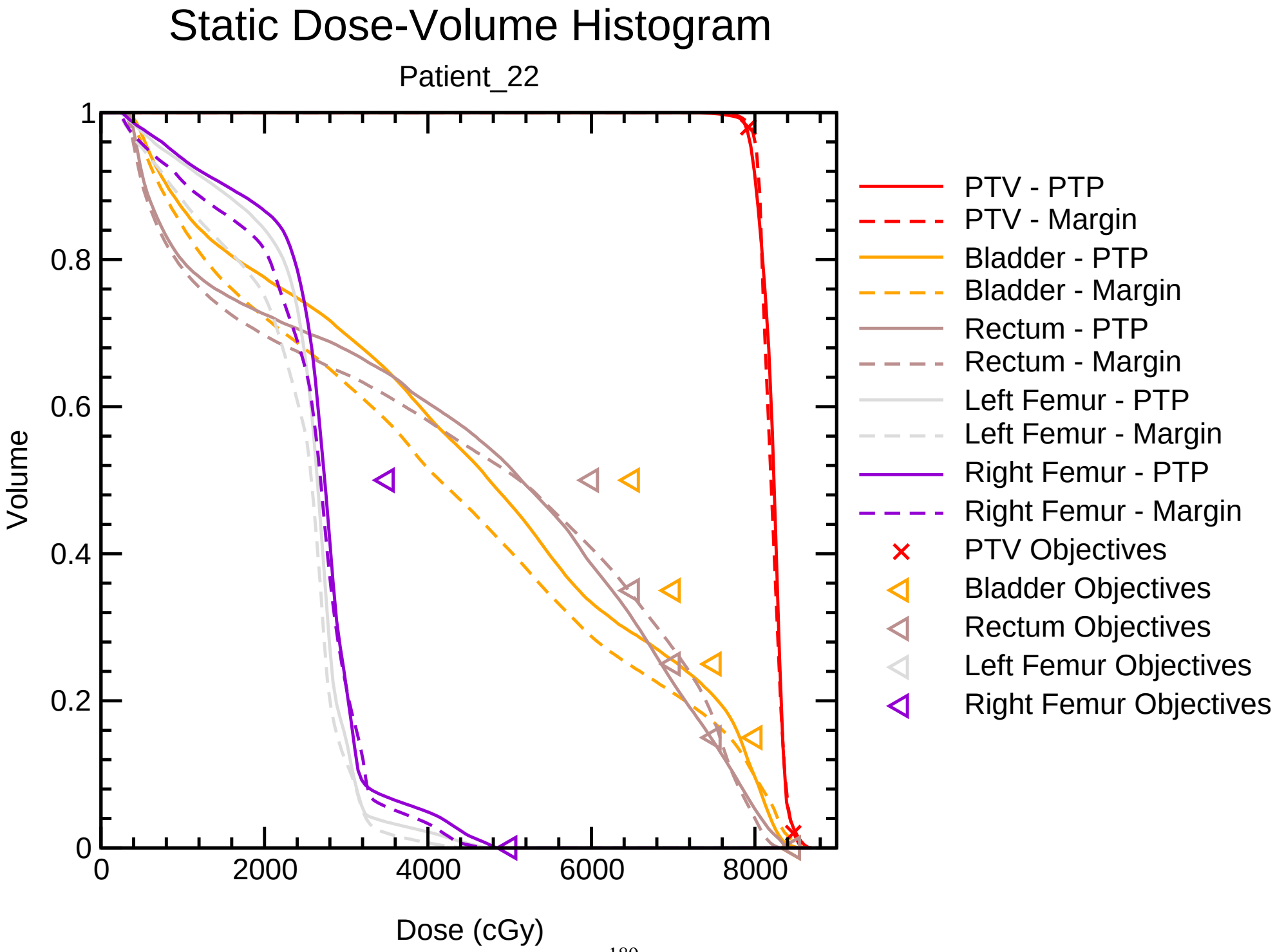
Static Dose-Volume Histogram
Patient_22
Volume
Dose (cGy)
0
0.2
0.4
0.6
0.8
1
0
2000
4000
6000
8000
PTV - PTP
PTV - Margin
Bladder - PTP
Bladder - Margin
Rectum - PTP
Rectum - Margin
Left Femur - PTP
Left Femur - Margin
Right Femur - PTP
Right Femur - Margin
PTV Objectives
Bladder Objectives
Rectum Objectives
Left Femur Objectives
Right Femur Objectives

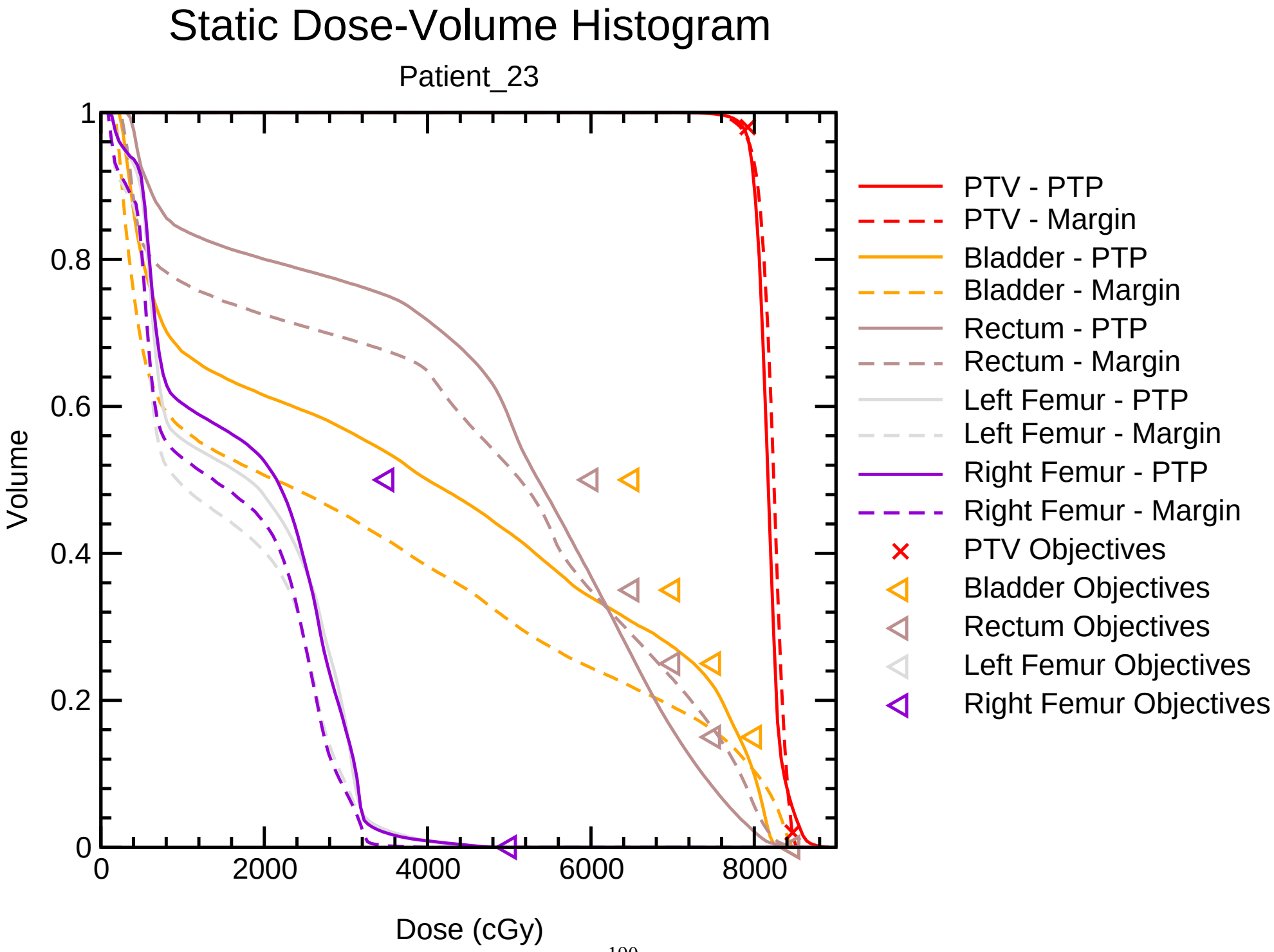
Static Dose-Volume Histogram
Patient_23
Volume
Dose (cGy)
0
0.2
0.4
0.6
0.8
1
0
2000
4000
6000
8000
PTV - PTP
PTV - Margin
Bladder - PTP
Bladder - Margin
Rectum - PTP
Rectum - Margin
Left Femur - PTP
Left Femur - Margin
Right Femur - PTP
Right Femur - Margin
PTV Objectives
Bladder Objectives
Rectum Objectives
Left Femur Objectives
Right Femur Objectives

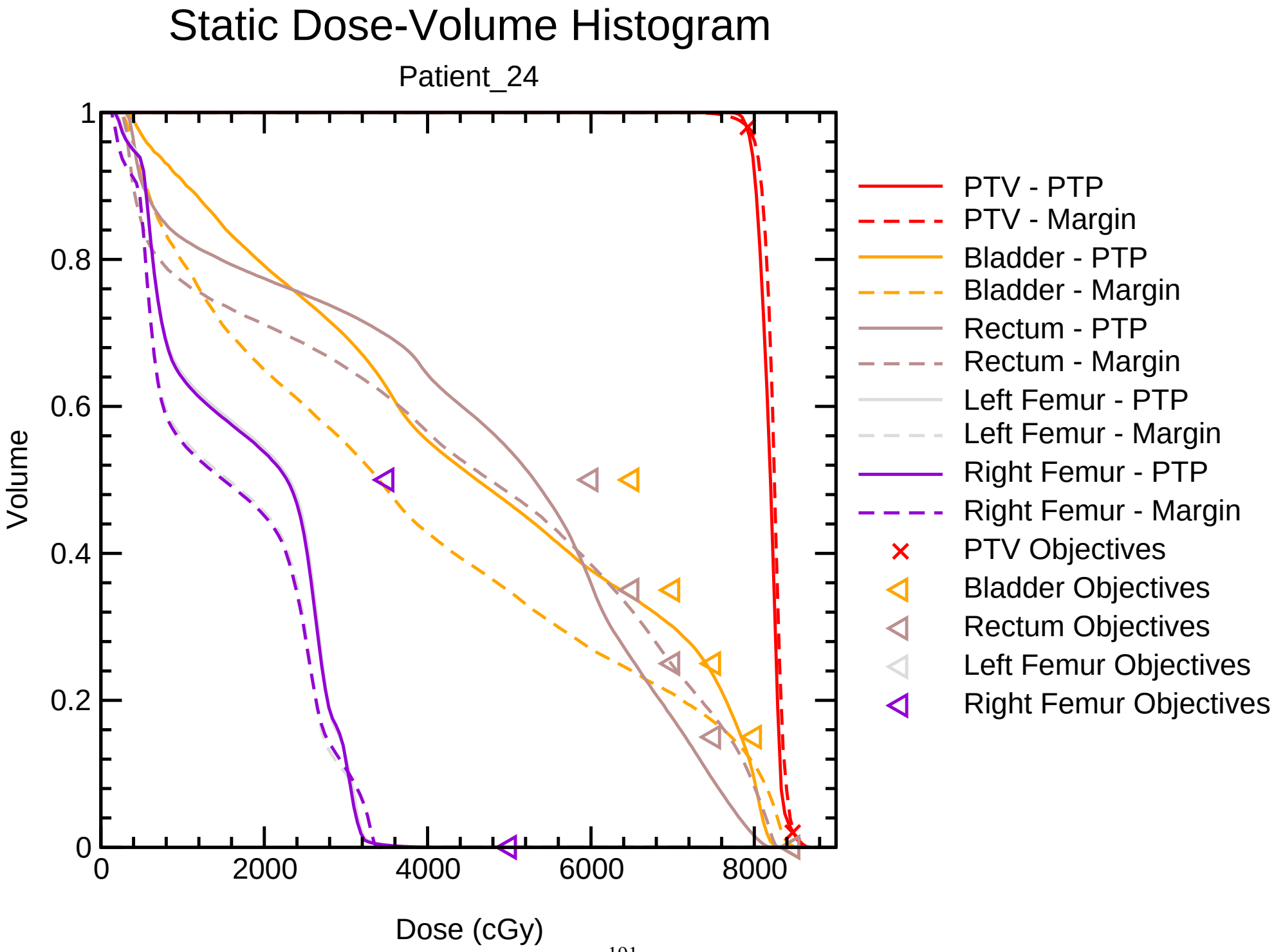
Static Dose-Volume Histogram
Patient_24
Volume
Dose (cGy)
0
0.2
0.4
0.6
0.8
1
0
2000
4000
6000
8000
PTV - PTP
PTV - Margin
Bladder - PTP
Bladder - Margin
Rectum - PTP
Rectum - Margin
Left Femur - PTP
Left Femur - Margin
Right Femur - PTP
Right Femur - Margin
PTV Objectives
Bladder Objectives
Rectum Objectives
Left Femur Objectives
Right Femur Objectives

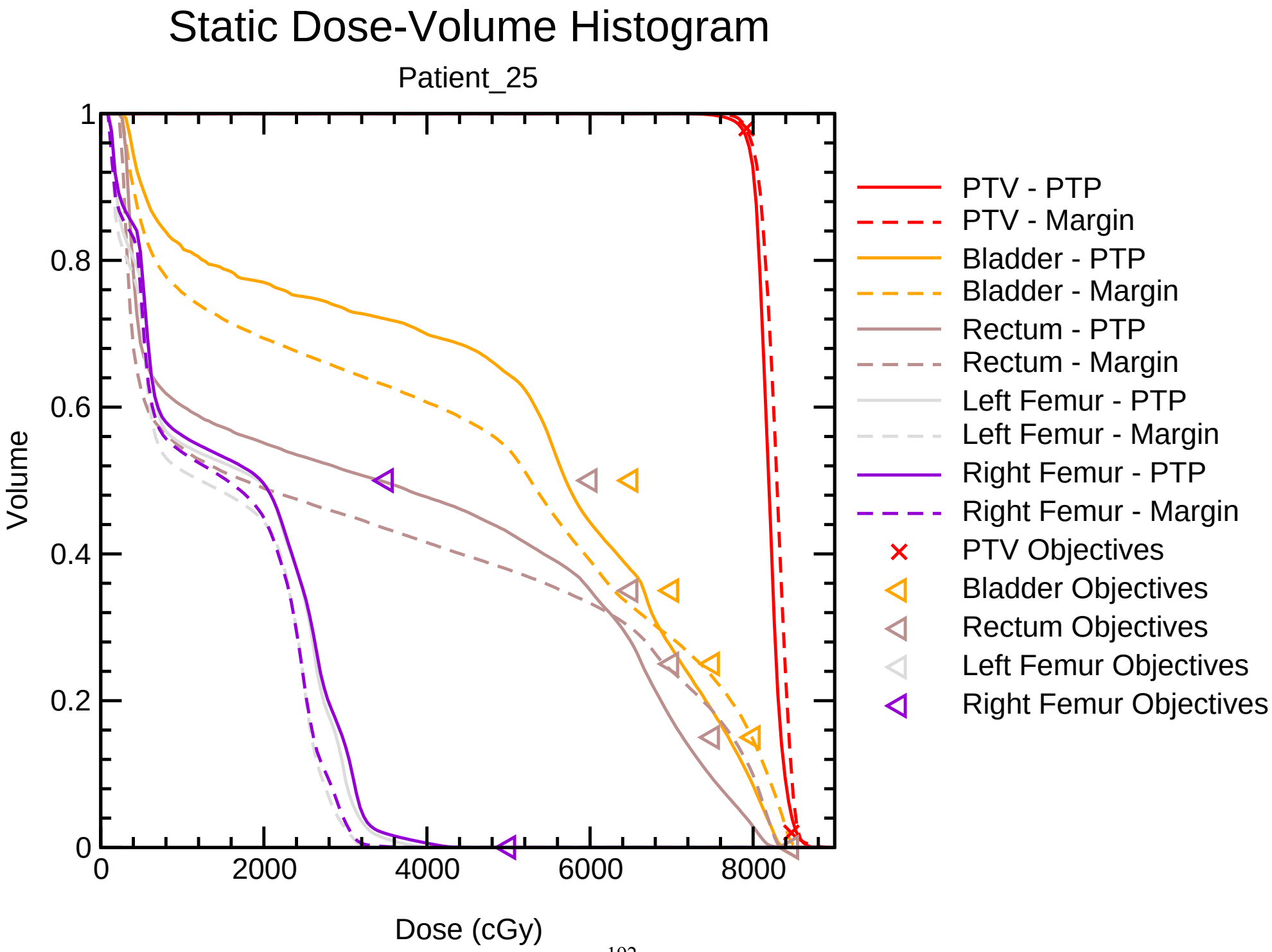
Static Dose-Volume Histogram
Patient_25
Volume
Dose (cGy)
0
0.2
0.4
0.6
0.8
1
0
2000
4000
6000
8000
PTV - PTP
PTV - Margin
Bladder - PTP
Bladder - Margin
Rectum - PTP
Rectum - Margin
Left Femur - PTP
Left Femur - Margin
Right Femur - PTP
Right Femur - Margin
PTV Objectives
Bladder Objectives
Rectum Objectives
Left Femur Objectives
Right Femur Objectives

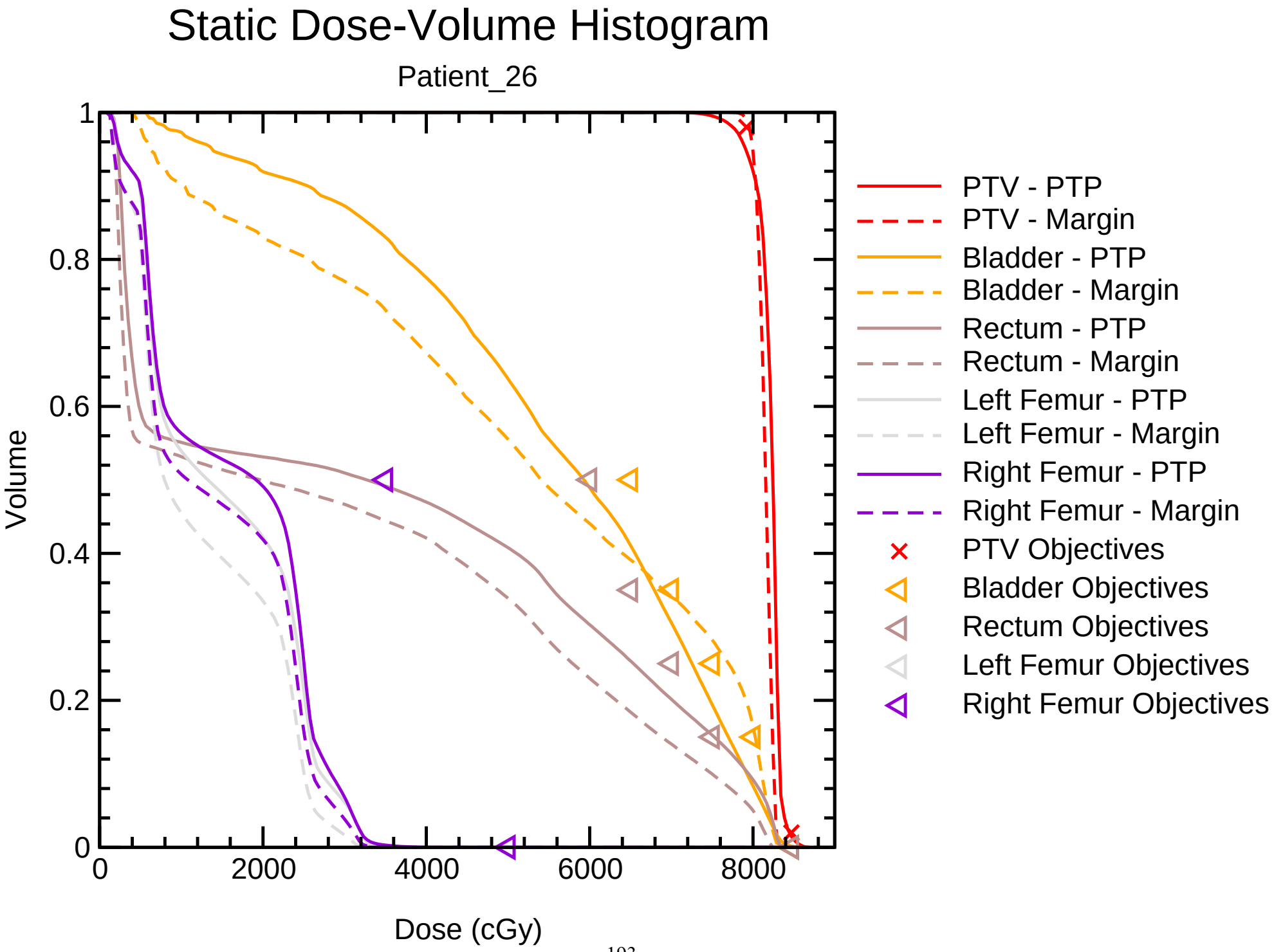
Static Dose-Volume Histogram
Patient_26
Volume
Dose (cGy)
0
0.2
0.4
0.6
0.8
1
0
2000
4000
6000
8000
PTV - PTP
PTV - Margin
Bladder - PTP
Bladder - Margin
Rectum - PTP
Rectum - Margin
Left Femur - PTP
Left Femur - Margin
Right Femur - PTP
Right Femur - Margin
PTV Objectives
Bladder Objectives
Rectum Objectives
Left Femur Objectives
Right Femur Objectives

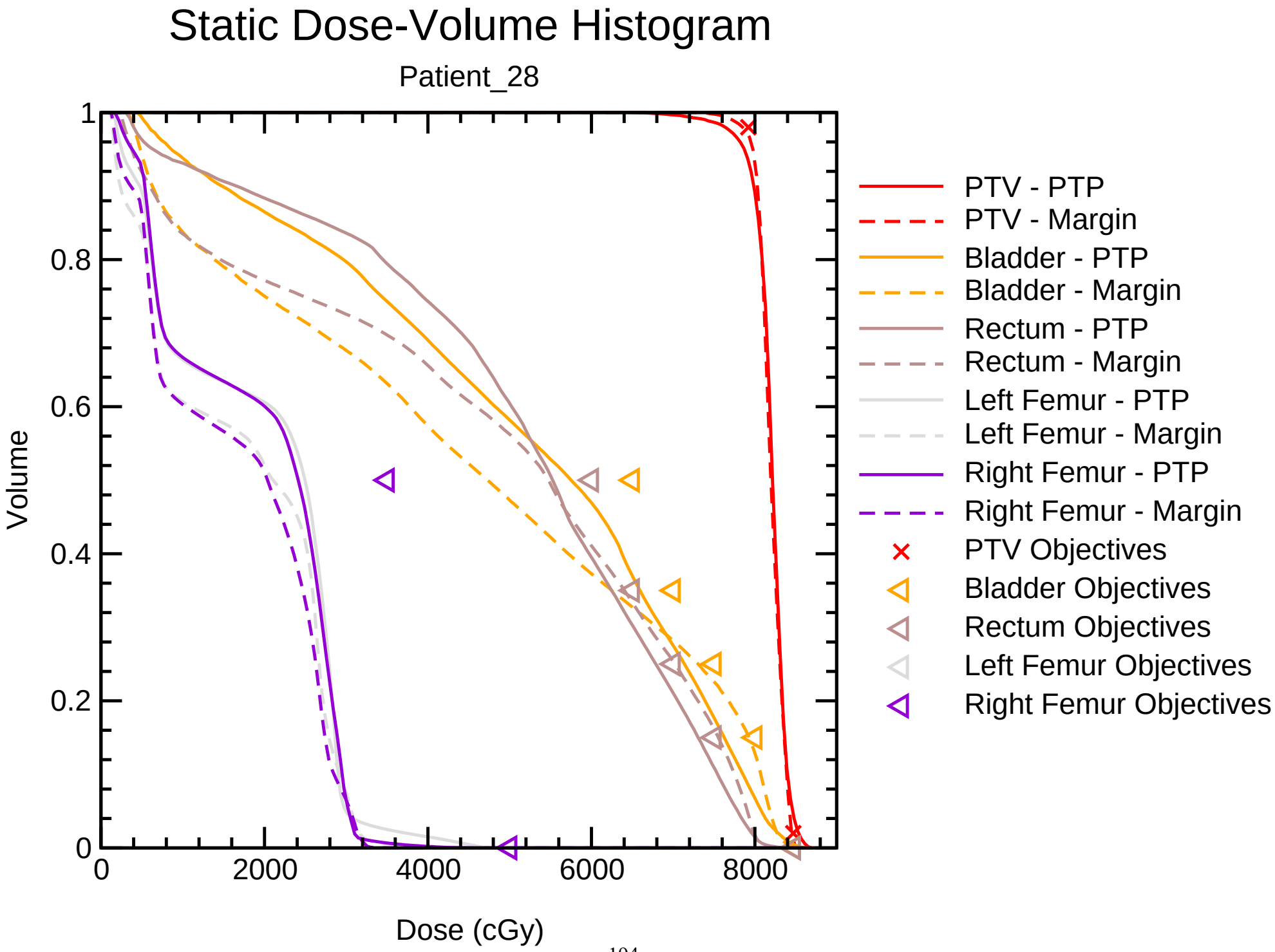
Static Dose-Volume Histogram
Patient_28
Volume
Dose (cGy)
0
0.2
0.4
0.6
0.8
1
0
2000
4000
6000
8000
PTV - PTP
PTV - Margin
Bladder - PTP
Bladder - Margin
Rectum - PTP
Rectum - Margin
Left Femur - PTP
Left Femur - Margin
Right Femur - PTP
Right Femur - Margin
PTV Objectives
Bladder Objectives
Rectum Objectives
Left Femur Objectives
Right Femur Objectives

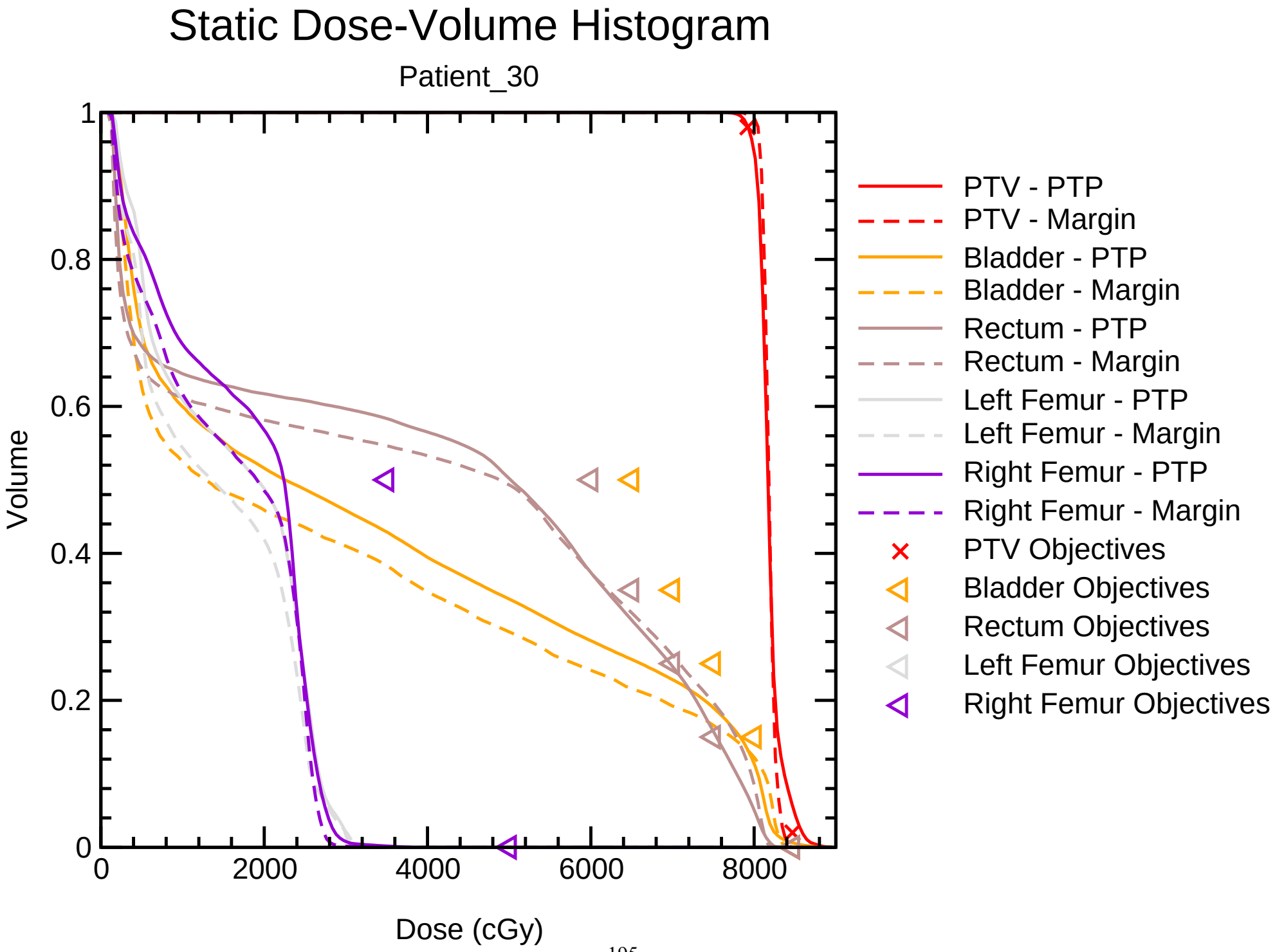
Static Dose-Volume Histogram
Patient_30
Volume
Dose (cGy)
0
0.2
0.4
0.6
0.8
1
0
2000
4000
6000
8000
PTV - PTP
PTV - Margin
Bladder - PTP
Bladder - Margin
Rectum - PTP
Rectum - Margin
Left Femur - PTP
Left Femur - Margin
Right Femur - PTP
Right Femur - Margin
PTV Objectives
Bladder Objectives
Rectum Objectives
Left Femur Objectives
Right Femur Objectives

Appendix V: Probability Dose-Volume Histograms

Probabilistic Dose-Volume Histogram plots for all patients used in this study. For each patient, a PDVH curve is plotted for CTV, rectum, bladder, left and right femur. Solid lines indicate PTP plans and dashed lines indicate margin-based plans. For target structures, the realized DVH curve will be above the PDVH curve 95% of the time. For OAR structures, the realized DVH curve will be below the PDVH curve 95% of the time.

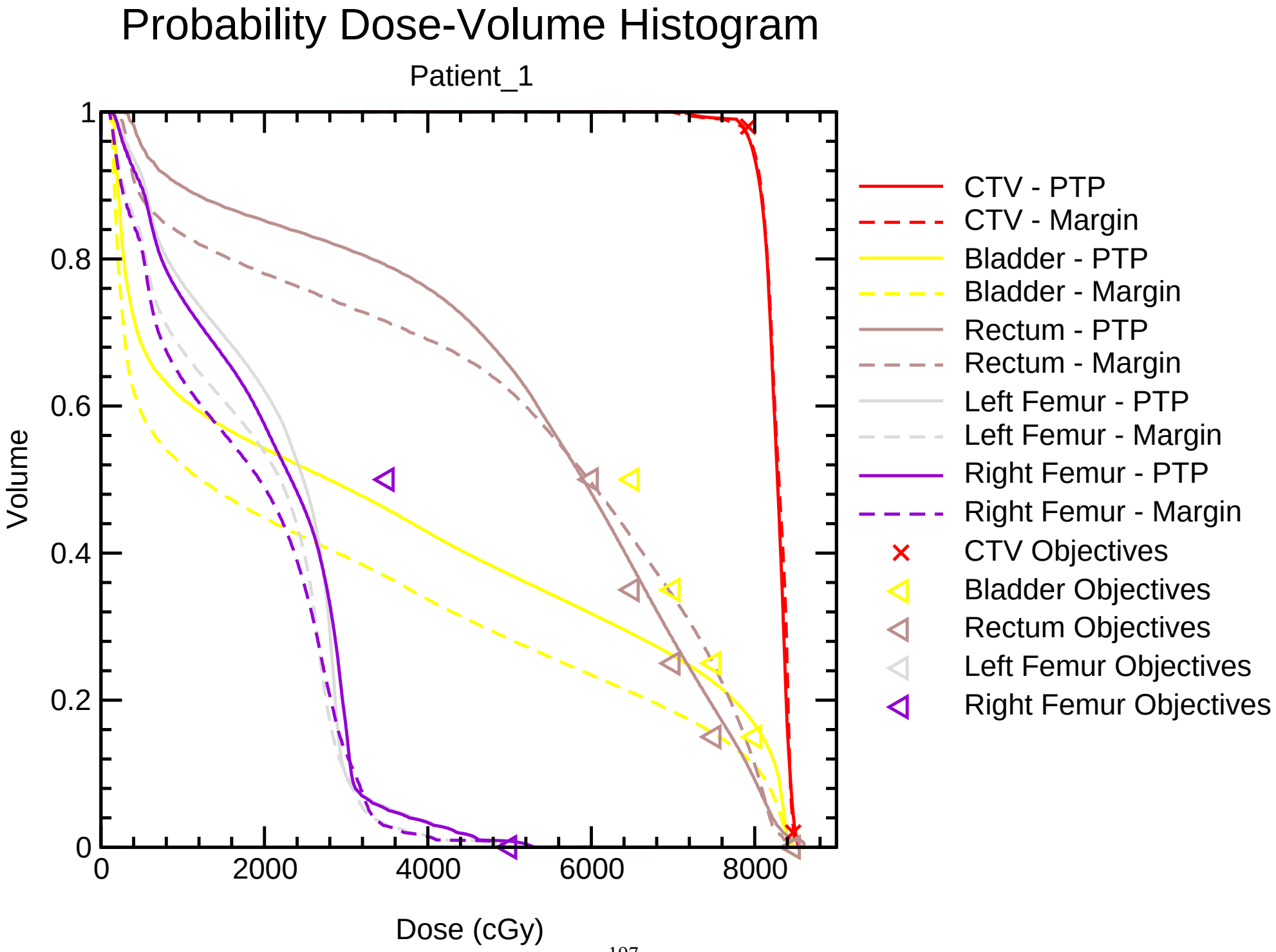
Probability Dose-Volume Histogram
Patient_1
Volume
Dose (cGy)
0
0.2
0.4
0.6
0.8
1
0
2000
4000
6000
8000
CTV - PTP
CTV - Margin
Bladder - PTP
Bladder - Margin
Rectum - PTP
Rectum - Margin
Left Femur - PTP
Left Femur - Margin
Right Femur - PTP
Right Femur - Margin
CTV Objectives
Bladder Objectives
Rectum Objectives
Left Femur Objectives
Right Femur Objectives

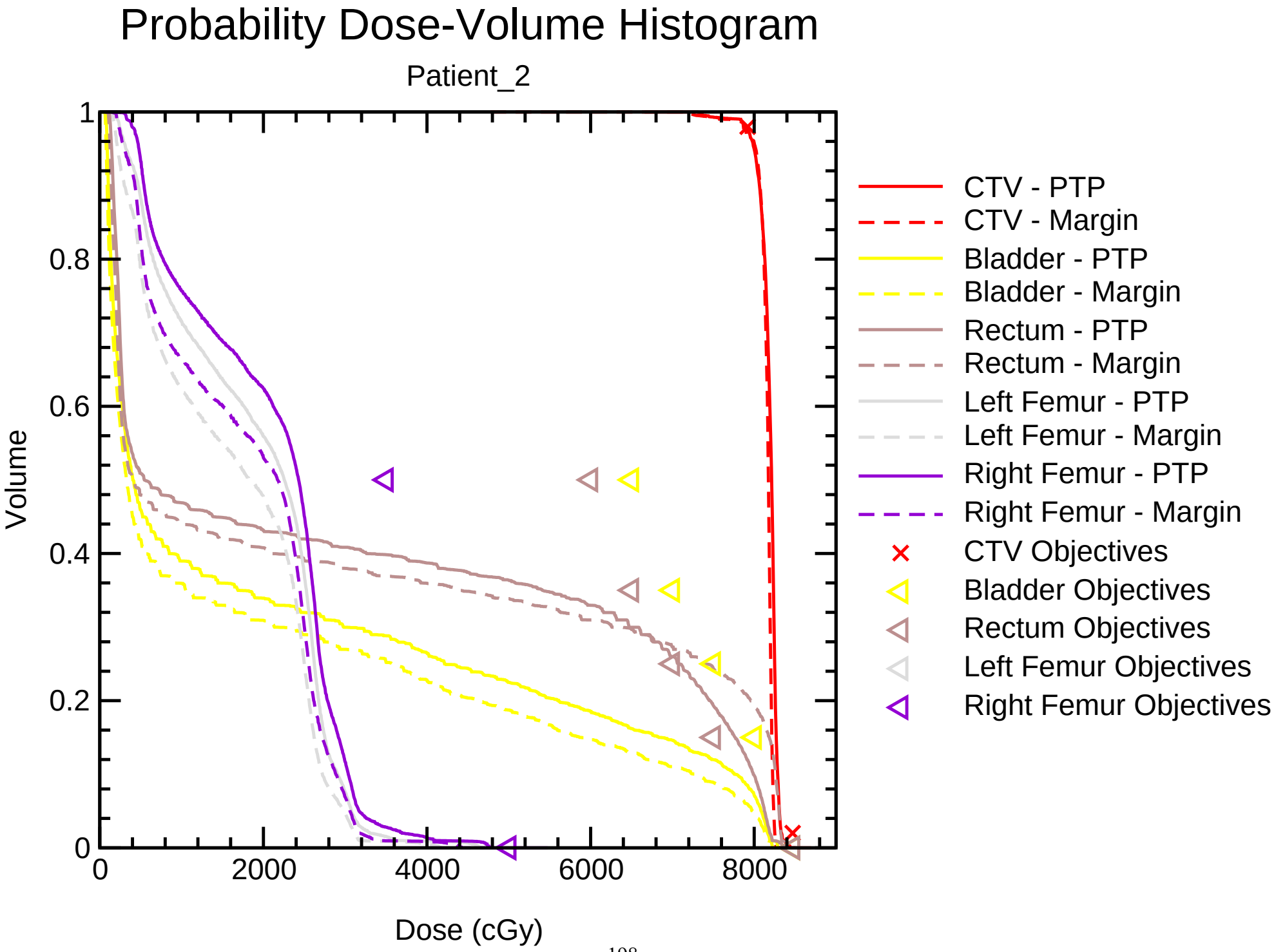
Probability Dose-Volume Histogram
Patient_2
Volume
Dose (cGy)
0
0.2
0.4
0.6
0.8
1
0
2000
4000
6000
8000
CTV - PTP
CTV - Margin
Bladder - PTP
Bladder - Margin
Rectum - PTP
Rectum - Margin
Left Femur - PTP
Left Femur - Margin
Right Femur - PTP
Right Femur - Margin
CTV Objectives
Bladder Objectives
Rectum Objectives
Left Femur Objectives
Right Femur Objectives

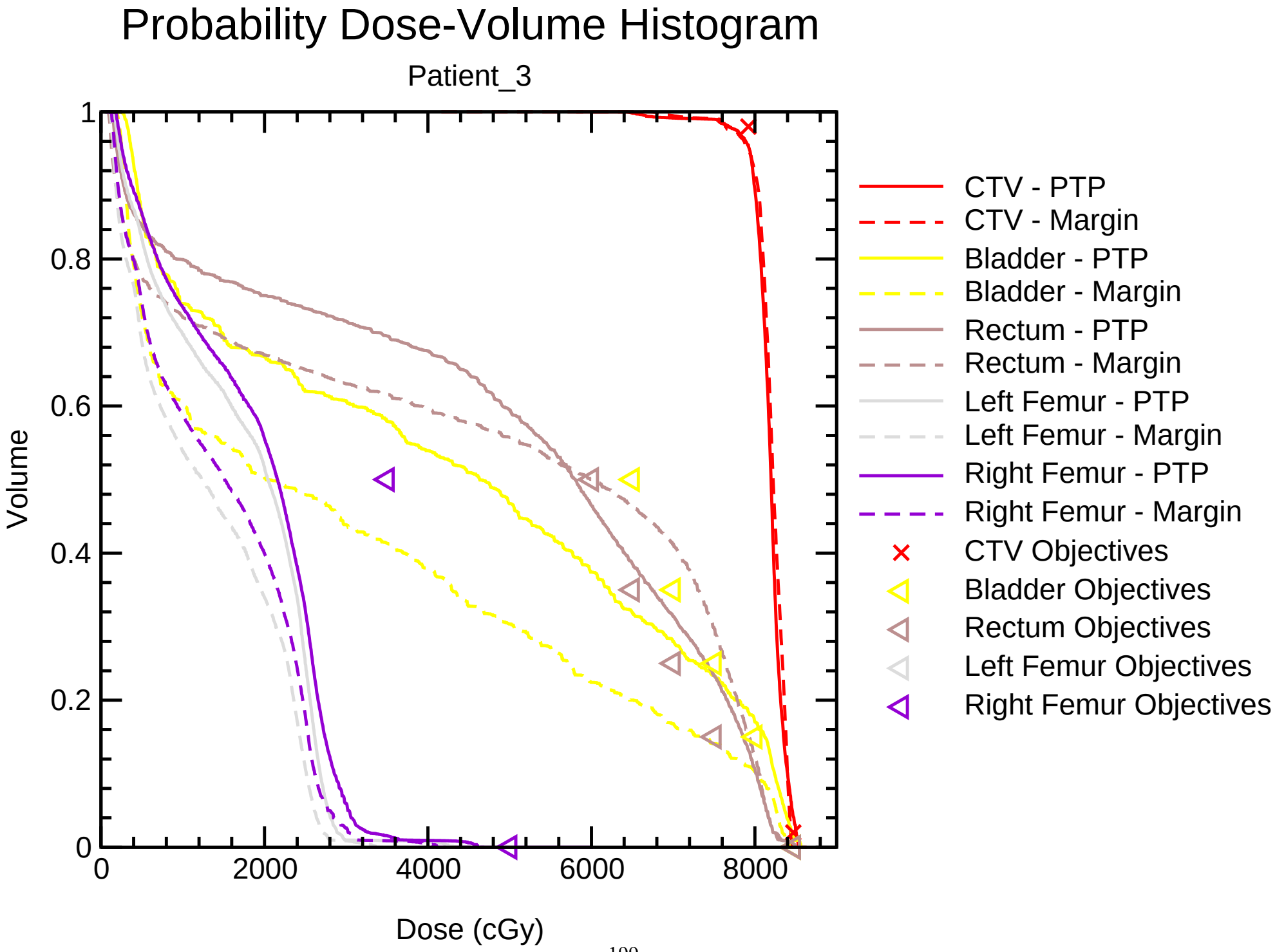
Probability Dose-Volume Histogram
Patient_3
Volume
Dose (cGy)
0
0.2
0.4
0.6
0.8
1
0
2000
4000
6000
8000
CTV - PTP
CTV - Margin
Bladder - PTP
Bladder - Margin
Rectum - PTP
Rectum - Margin
Left Femur - PTP
Left Femur - Margin
Right Femur - PTP
Right Femur - Margin
CTV Objectives
Bladder Objectives
Rectum Objectives
Left Femur Objectives
Right Femur Objectives

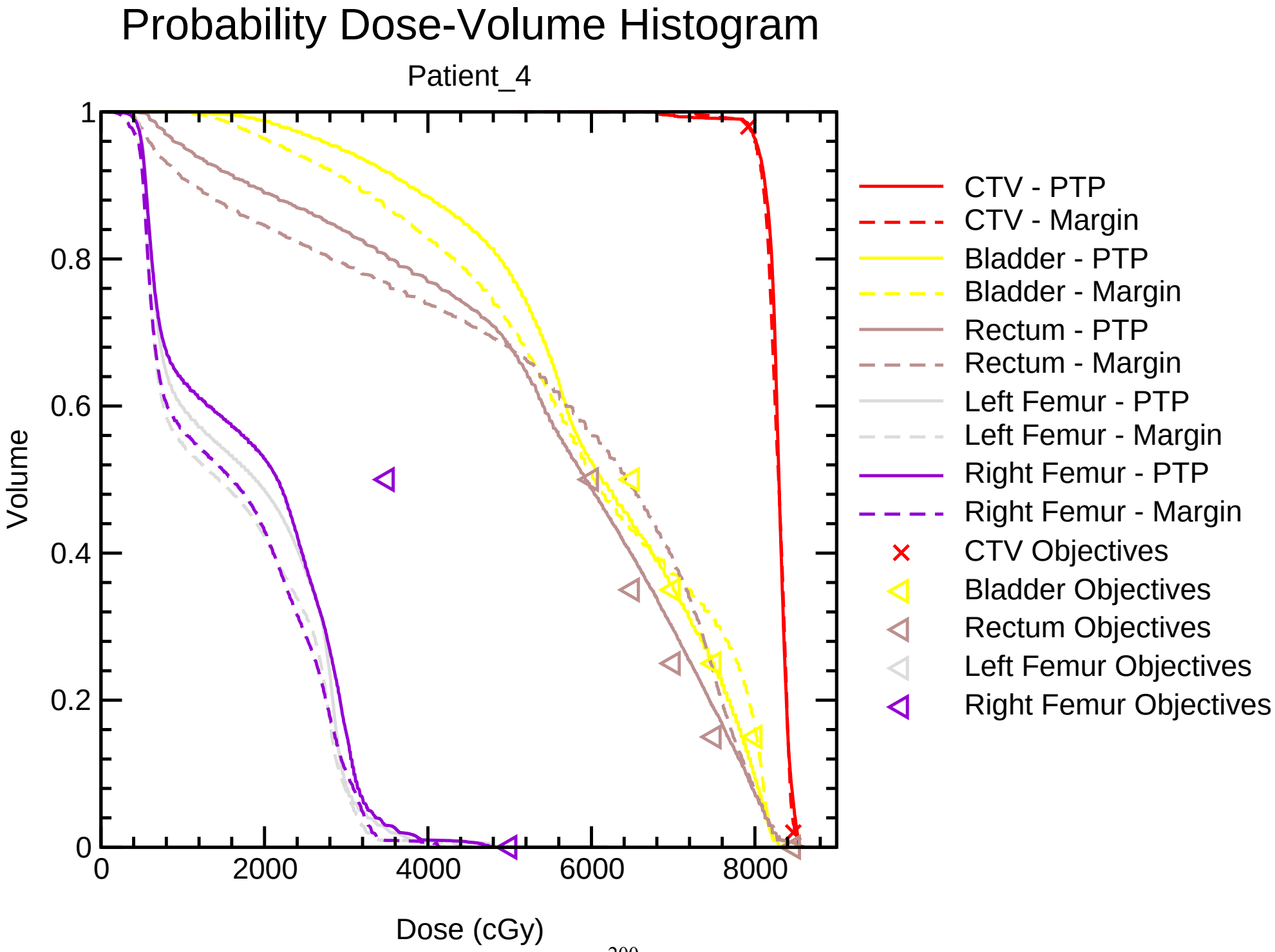
Probability Dose-Volume Histogram
Patient_4
Volume
Dose (cGy)
0
0.2
0.4
0.6
0.8
1
0
2000
4000
6000
8000
CTV - PTP
CTV - Margin
Bladder - PTP
Bladder - Margin
Rectum - PTP
Rectum - Margin
Left Femur - PTP
Left Femur - Margin
Right Femur - PTP
Right Femur - Margin
CTV Objectives
Bladder Objectives
Rectum Objectives
Left Femur Objectives
Right Femur Objectives

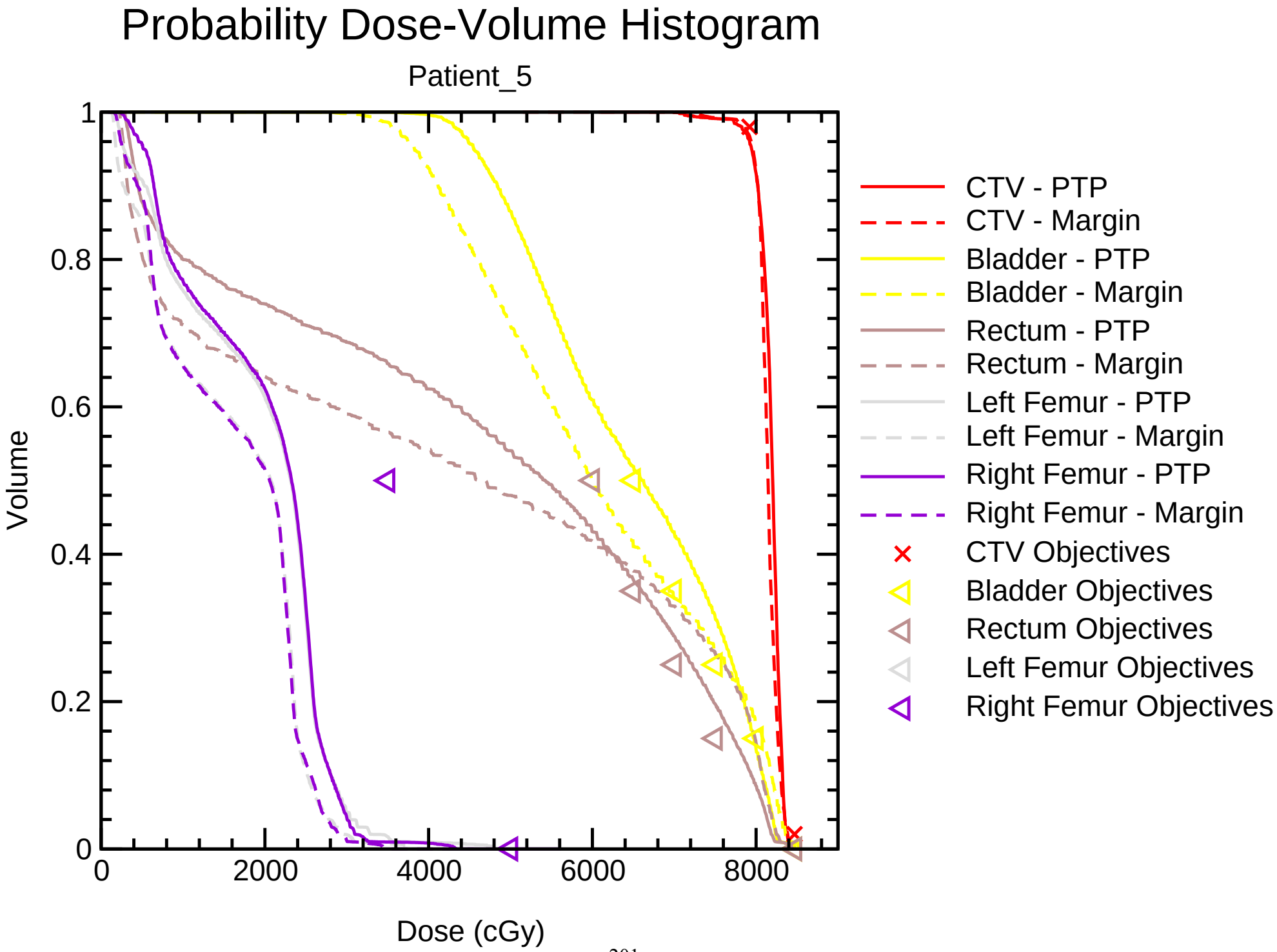
Probability Dose-Volume Histogram
Patient_5
Volume
Dose (cGy)
0
0.2
0.4
0.6
0.8
1
0
2000
4000
6000
8000
CTV - PTP
CTV - Margin
Bladder - PTP
Bladder - Margin
Rectum - PTP
Rectum - Margin
Left Femur - PTP
Left Femur - Margin
Right Femur - PTP
Right Femur - Margin
CTV Objectives
Bladder Objectives
Rectum Objectives
Left Femur Objectives
Right Femur Objectives

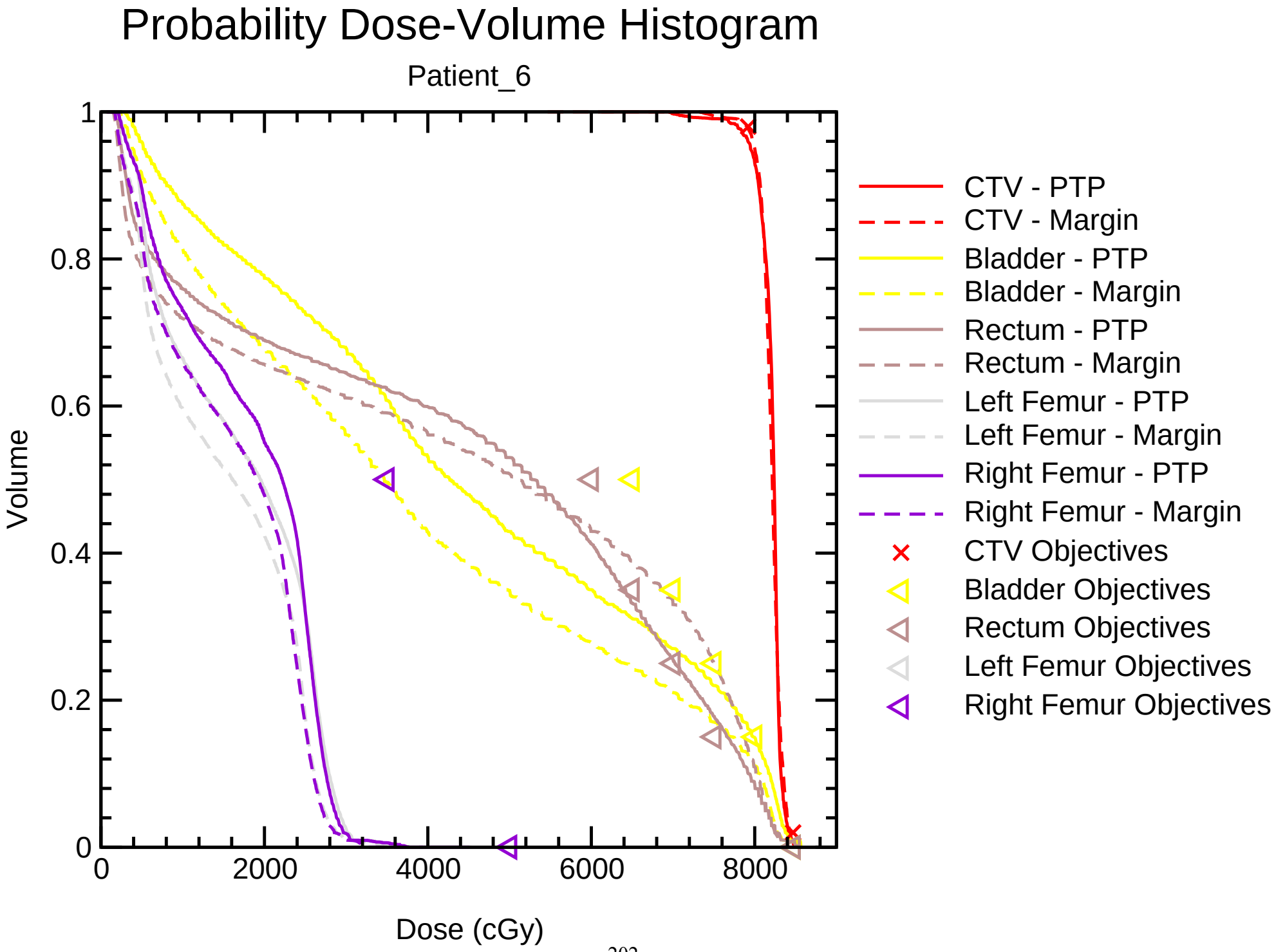
Probability Dose-Volume Histogram
Patient_6
Volume
Dose (cGy)
0
0.2
0.4
0.6
0.8
1
0
2000
4000
6000
8000
CTV - PTP
CTV - Margin
Bladder - PTP
Bladder - Margin
Rectum - PTP
Rectum - Margin
Left Femur - PTP
Left Femur - Margin
Right Femur - PTP
Right Femur - Margin
CTV Objectives
Bladder Objectives
Rectum Objectives
Left Femur Objectives
Right Femur Objectives

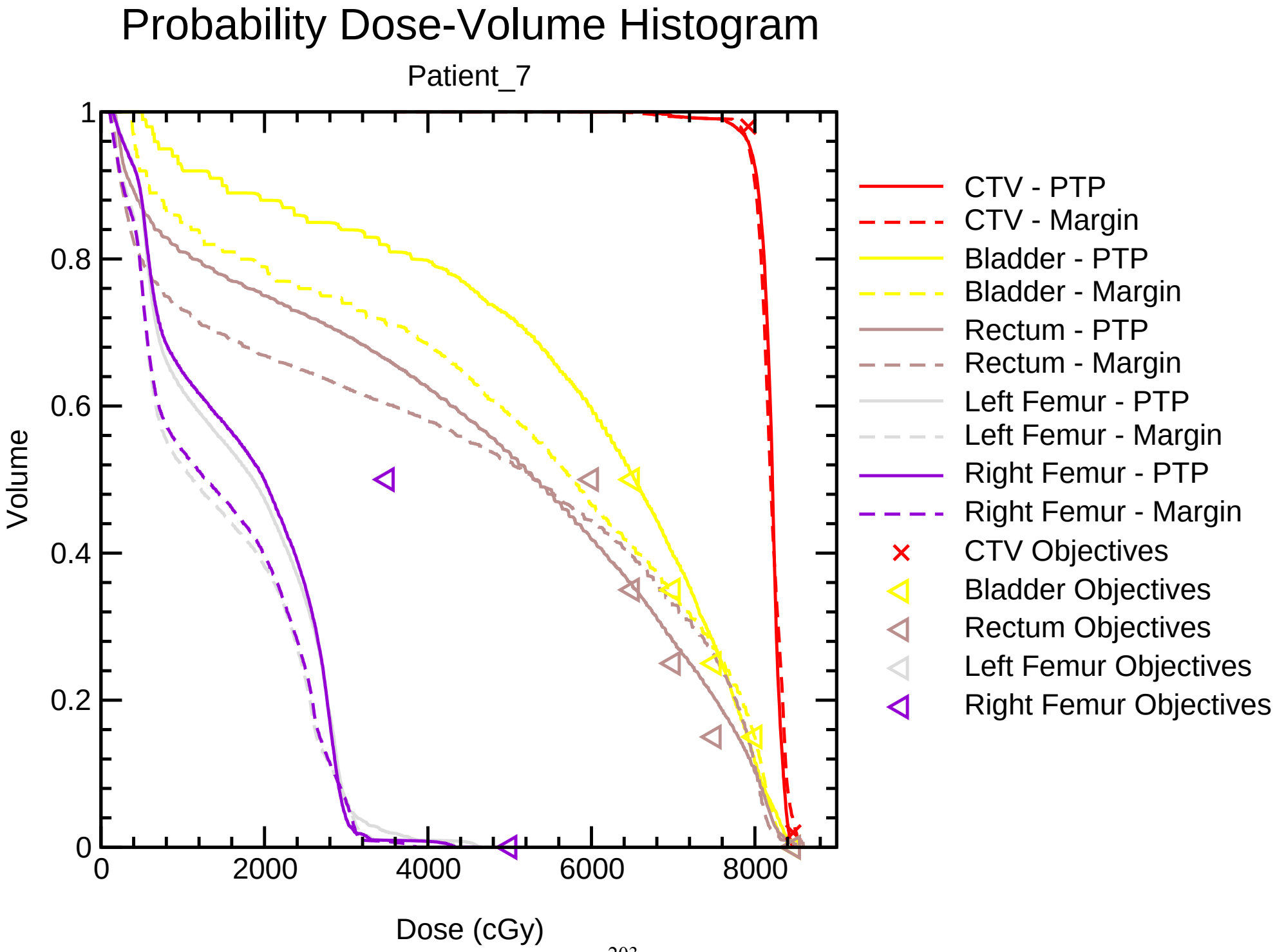
Probability Dose-Volume Histogram
Patient_7
Volume
Dose (cGy)
0
0.2
0.4
0.6
0.8
1
0
2000
4000
6000
8000
CTV - PTP
CTV - Margin
Bladder - PTP
Bladder - Margin
Rectum - PTP
Rectum - Margin
Left Femur - PTP
Left Femur - Margin
Right Femur - PTP
Right Femur - Margin
CTV Objectives
Bladder Objectives
Rectum Objectives
Left Femur Objectives
Right Femur Objectives

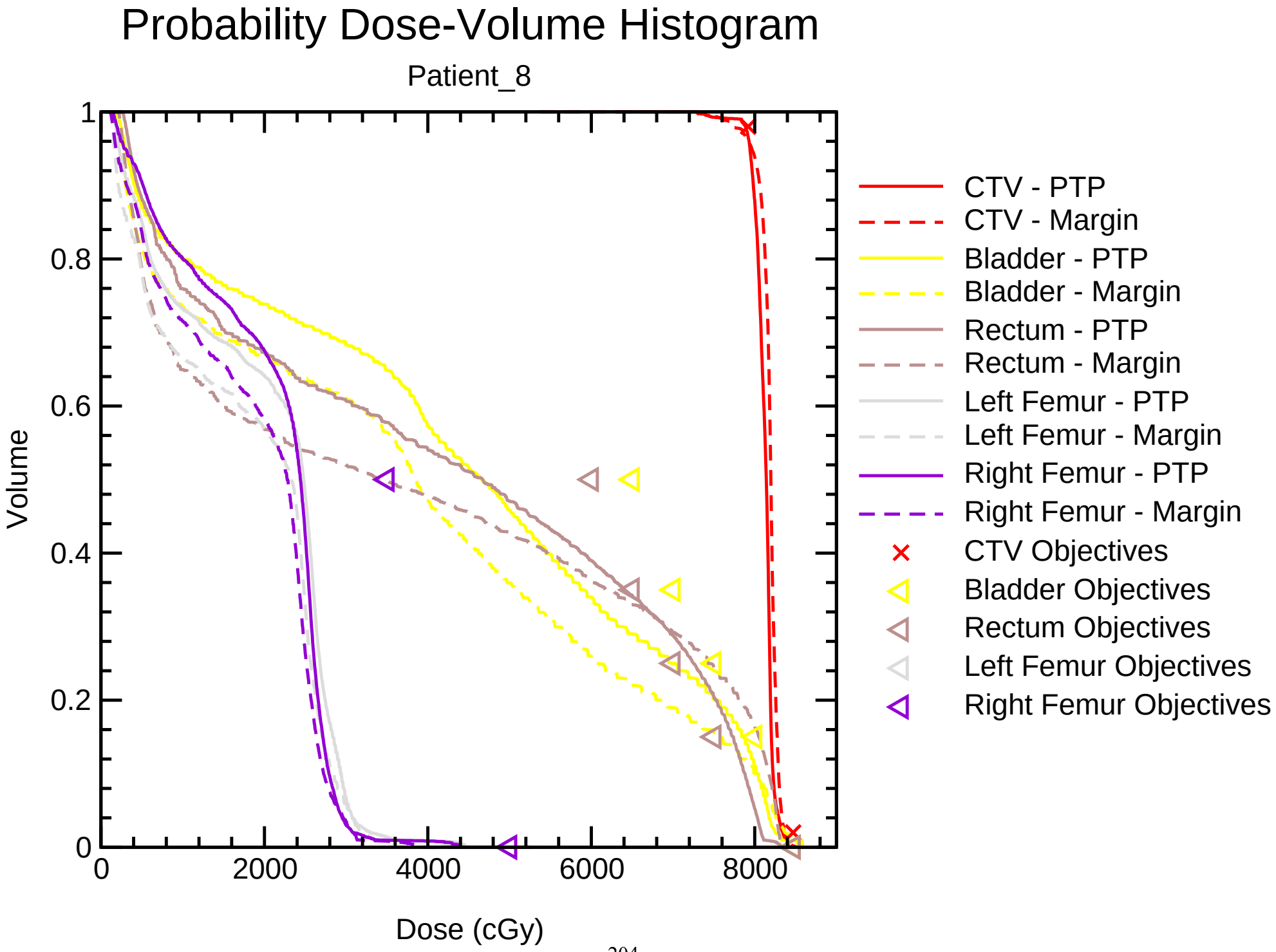
Probability Dose-Volume Histogram
Patient_8
Volume
Dose (cGy)
0
0.2
0.4
0.6
0.8
1
0
2000
4000
6000
8000
CTV - PTP
CTV - Margin
Bladder - PTP
Bladder - Margin
Rectum - PTP
Rectum - Margin
Left Femur - PTP
Left Femur - Margin
Right Femur - PTP
Right Femur - Margin
CTV Objectives
Bladder Objectives
Rectum Objectives
Left Femur Objectives
Right Femur Objectives

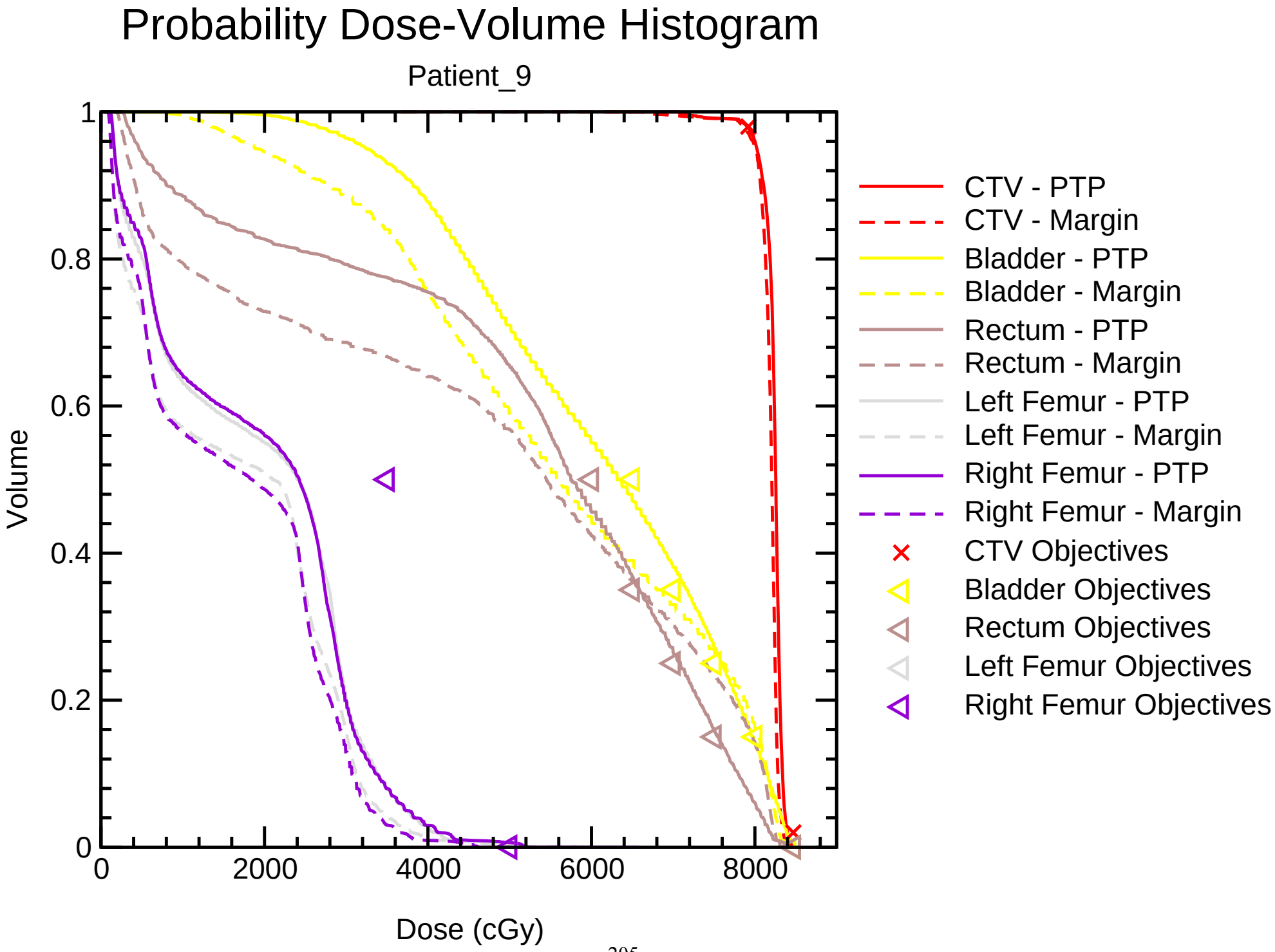
Probability Dose-Volume Histogram
Patient_9
Volume
Dose (cGy)
0
0.2
0.4
0.6
0.8
1
0
2000
4000
6000
8000
CTV - PTP
CTV - Margin
Bladder - PTP
Bladder - Margin
Rectum - PTP
Rectum - Margin
Left Femur - PTP
Left Femur - Margin
Right Femur - PTP
Right Femur - Margin
CTV Objectives
Bladder Objectives
Rectum Objectives
Left Femur Objectives
Right Femur Objectives

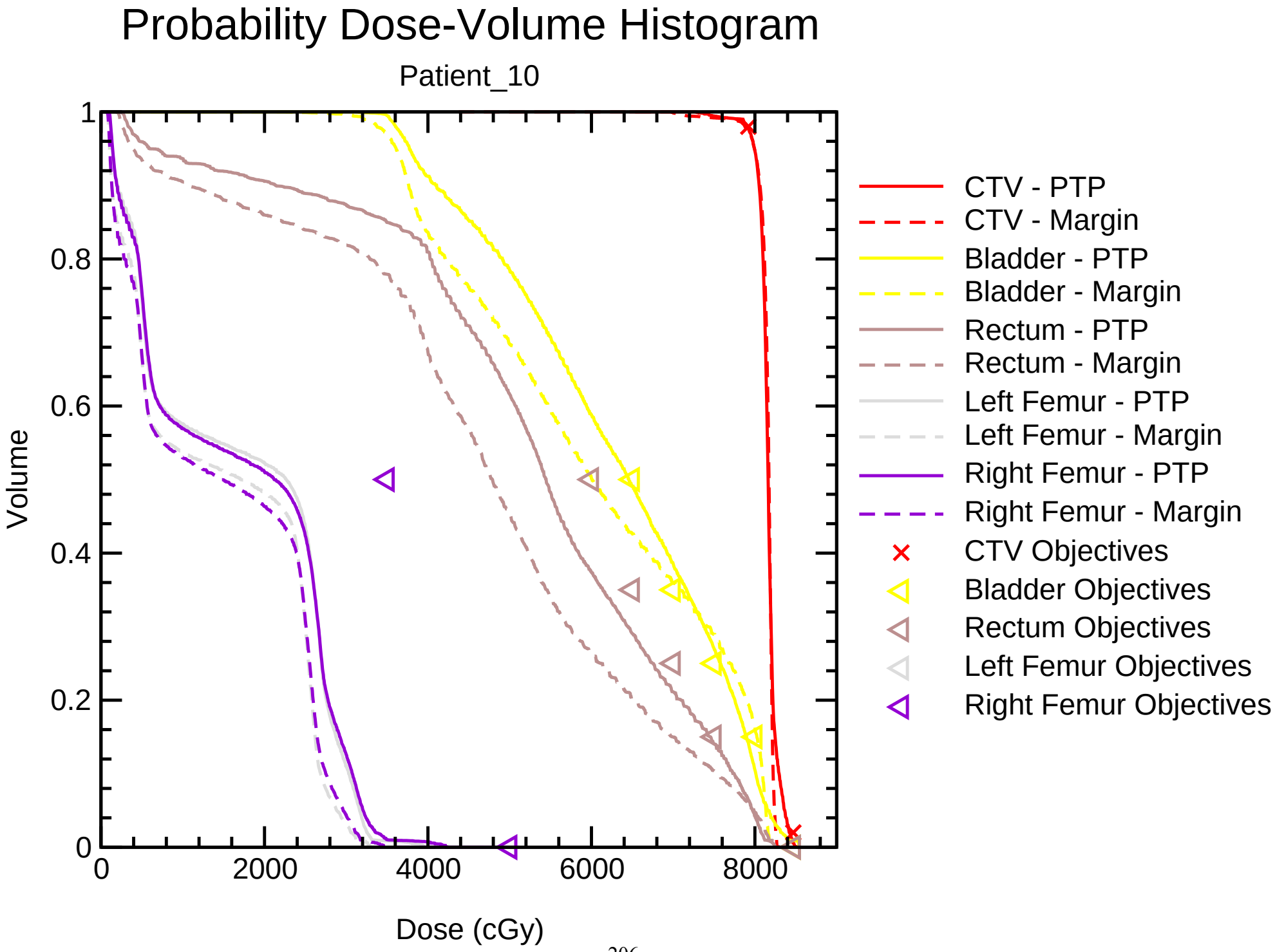
Probability Dose-Volume Histogram
Patient_10
Volume
Dose (cGy)
0
0.2
0.4
0.6
0.8
1
0
2000
4000
6000
8000
CTV - PTP
CTV - Margin
Bladder - PTP
Bladder - Margin
Rectum - PTP
Rectum - Margin
Left Femur - PTP
Left Femur - Margin
Right Femur - PTP
Right Femur - Margin
CTV Objectives
Bladder Objectives
Rectum Objectives
Left Femur Objectives
Right Femur Objectives

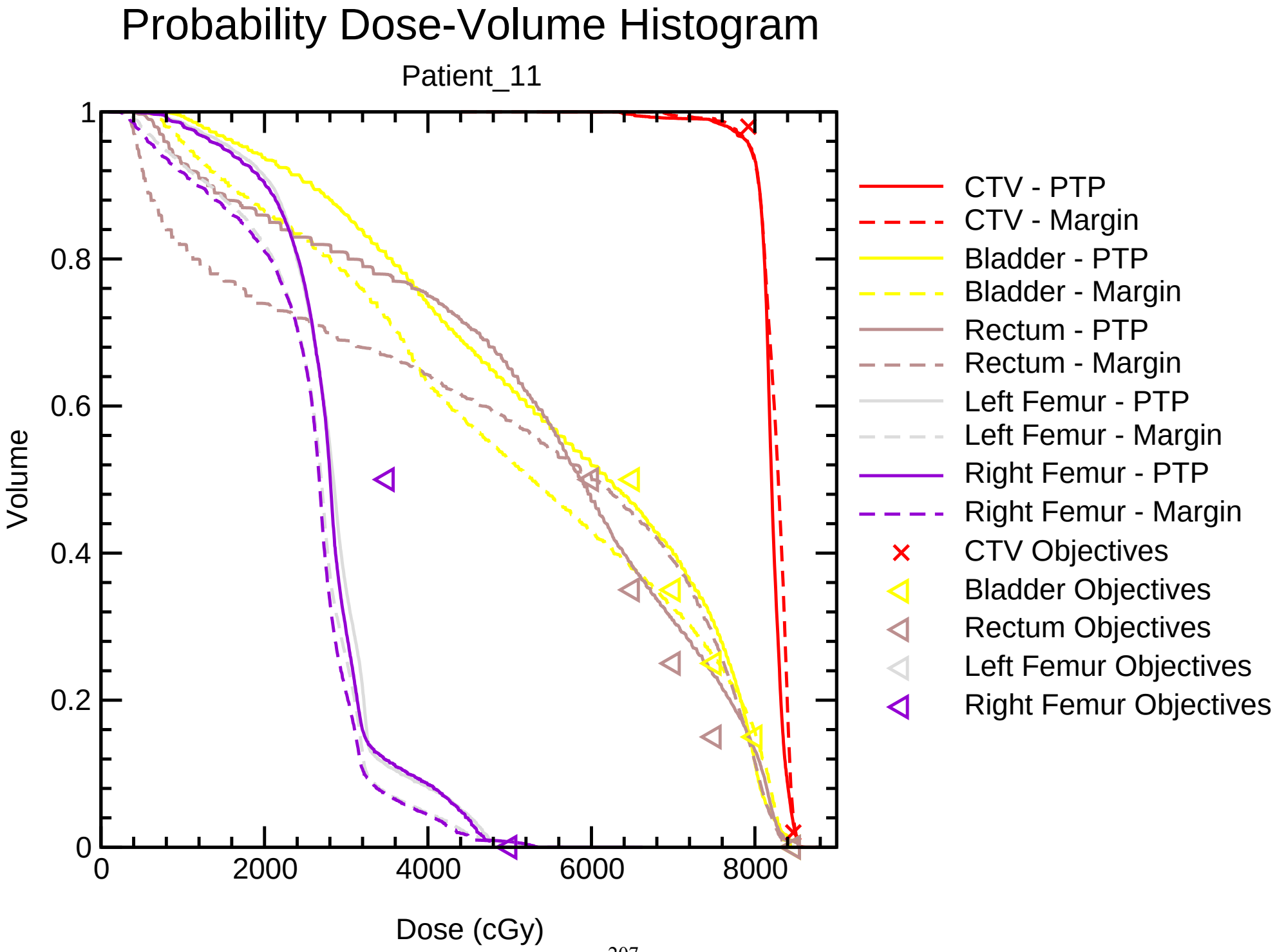
Probability Dose-Volume Histogram
Patient_11
Volume
Dose (cGy)
0
0.2
0.4
0.6
0.8
1
0
2000
4000
6000
8000
CTV - PTP
CTV - Margin
Bladder - PTP
Bladder - Margin
Rectum - PTP
Rectum - Margin
Left Femur - PTP
Left Femur - Margin
Right Femur - PTP
Right Femur - Margin
CTV Objectives
Bladder Objectives
Rectum Objectives
Left Femur Objectives
Right Femur Objectives

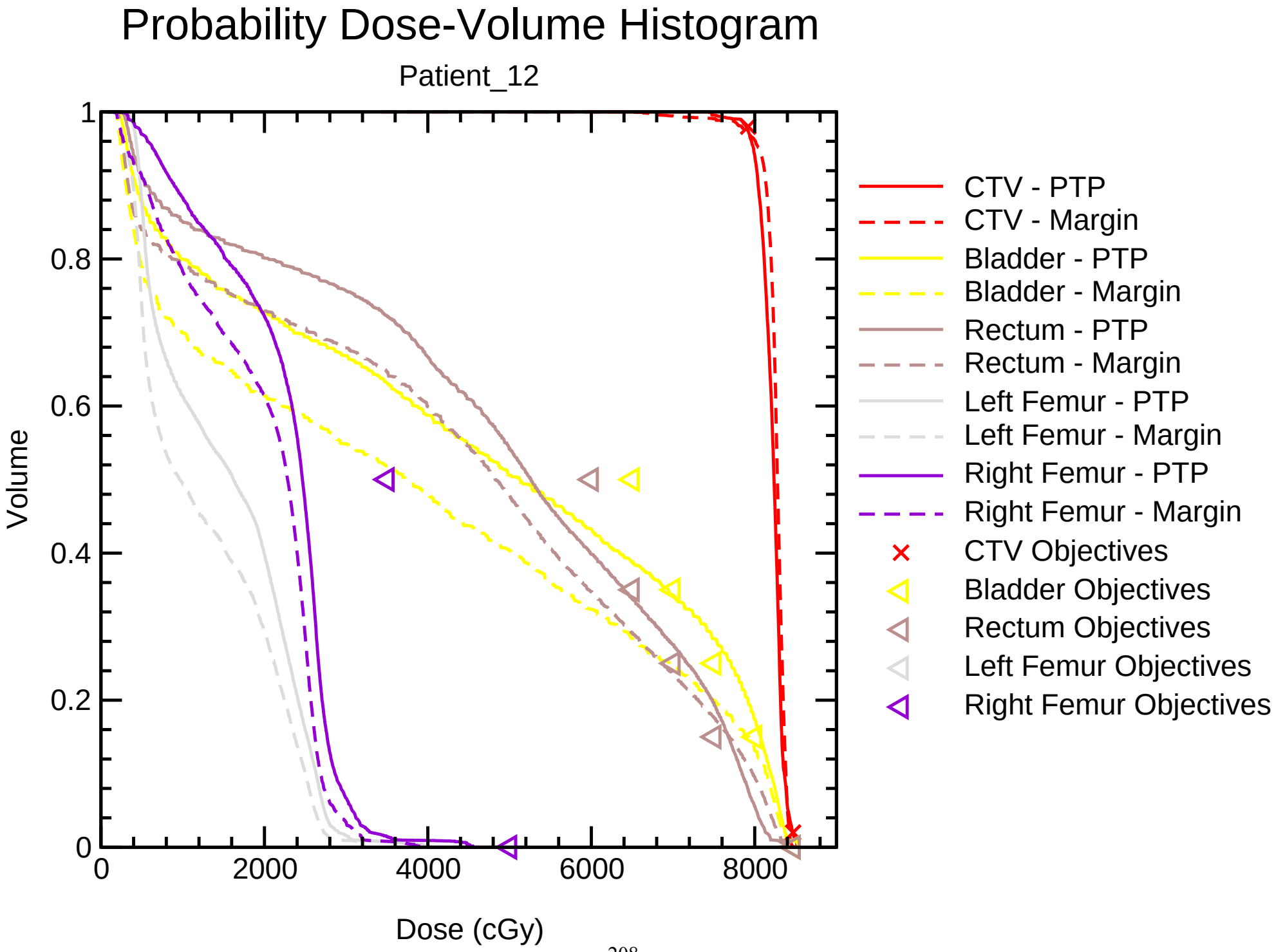
Probability Dose-Volume Histogram
Patient_12
Volume
Dose (cGy)
0
0.2
0.4
0.6
0.8
1
0
2000
4000
6000
8000
CTV - PTP
CTV - Margin
Bladder - PTP
Bladder - Margin
Rectum - PTP
Rectum - Margin
Left Femur - PTP
Left Femur - Margin
Right Femur - PTP
Right Femur - Margin
CTV Objectives
Bladder Objectives
Rectum Objectives
Left Femur Objectives
Right Femur Objectives

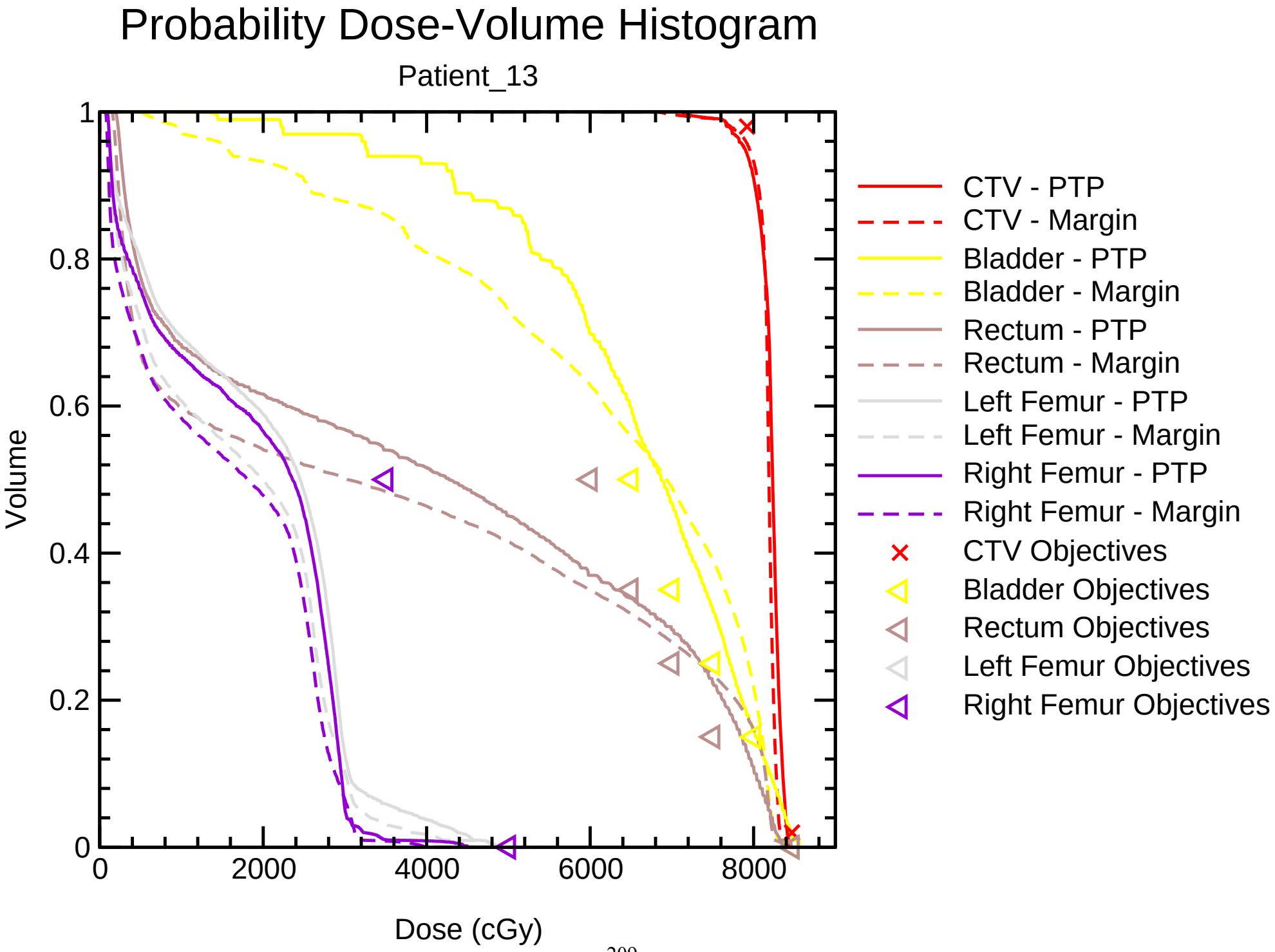
Probability Dose-Volume Histogram
Patient_13
Volume
Dose (cGy)
0
0.2
0.4
0.6
0.8
1
0
2000
4000
6000
8000
CTV - PTP
CTV - Margin
Bladder - PTP
Bladder - Margin
Rectum - PTP
Rectum - Margin
Left Femur - PTP
Left Femur - Margin
Right Femur - PTP
Right Femur - Margin
CTV Objectives
Bladder Objectives
Rectum Objectives
Left Femur Objectives
Right Femur Objectives

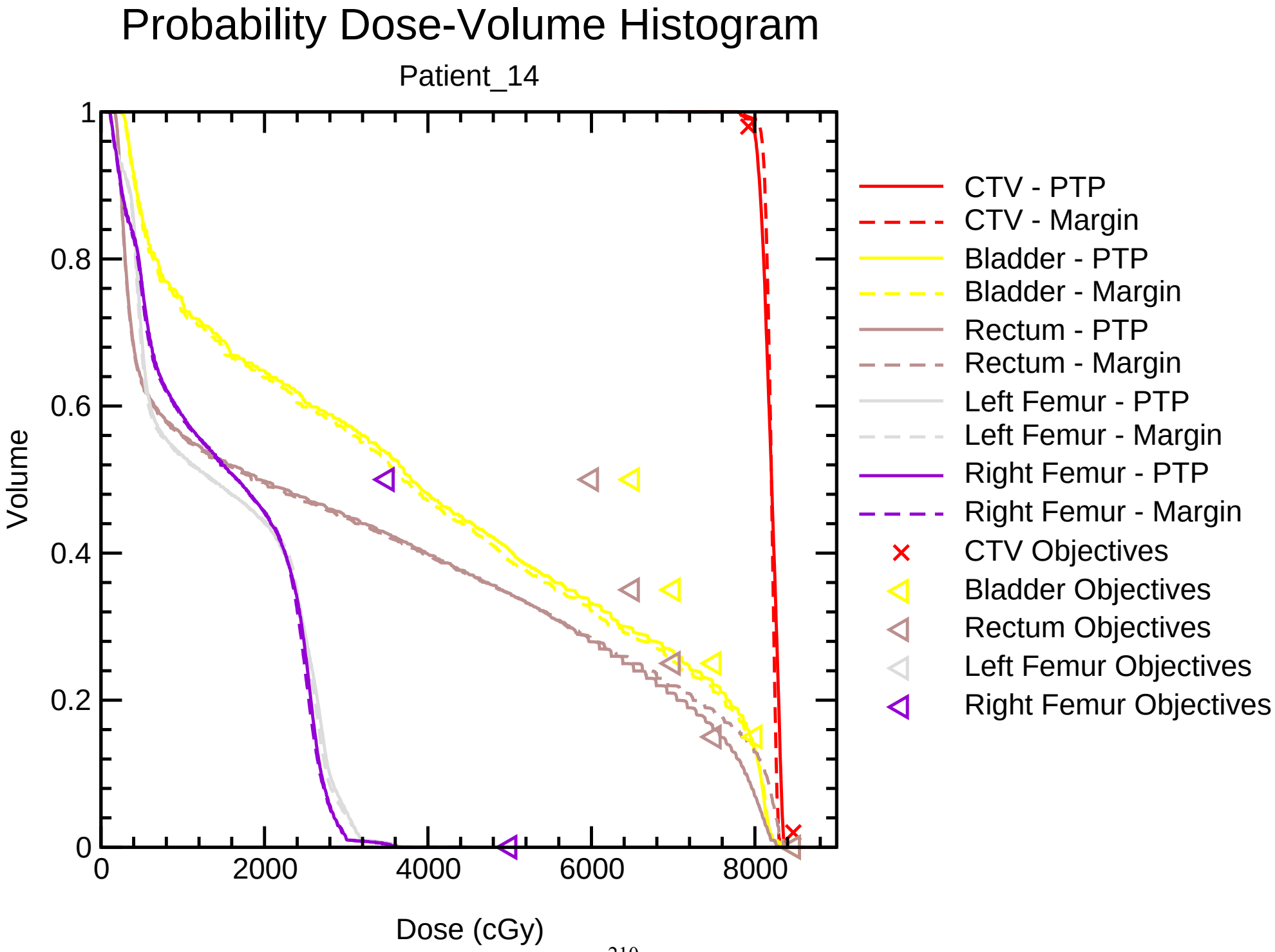
Probability Dose-Volume Histogram
Patient_14
Volume
Dose (cGy)
0
0.2
0.4
0.6
0.8
1
0
2000
4000
6000
8000
CTV - PTP
CTV - Margin
Bladder - PTP
Bladder - Margin
Rectum - PTP
Rectum - Margin
Left Femur - PTP
Left Femur - Margin
Right Femur - PTP
Right Femur - Margin
CTV Objectives
Bladder Objectives
Rectum Objectives
Left Femur Objectives
Right Femur Objectives

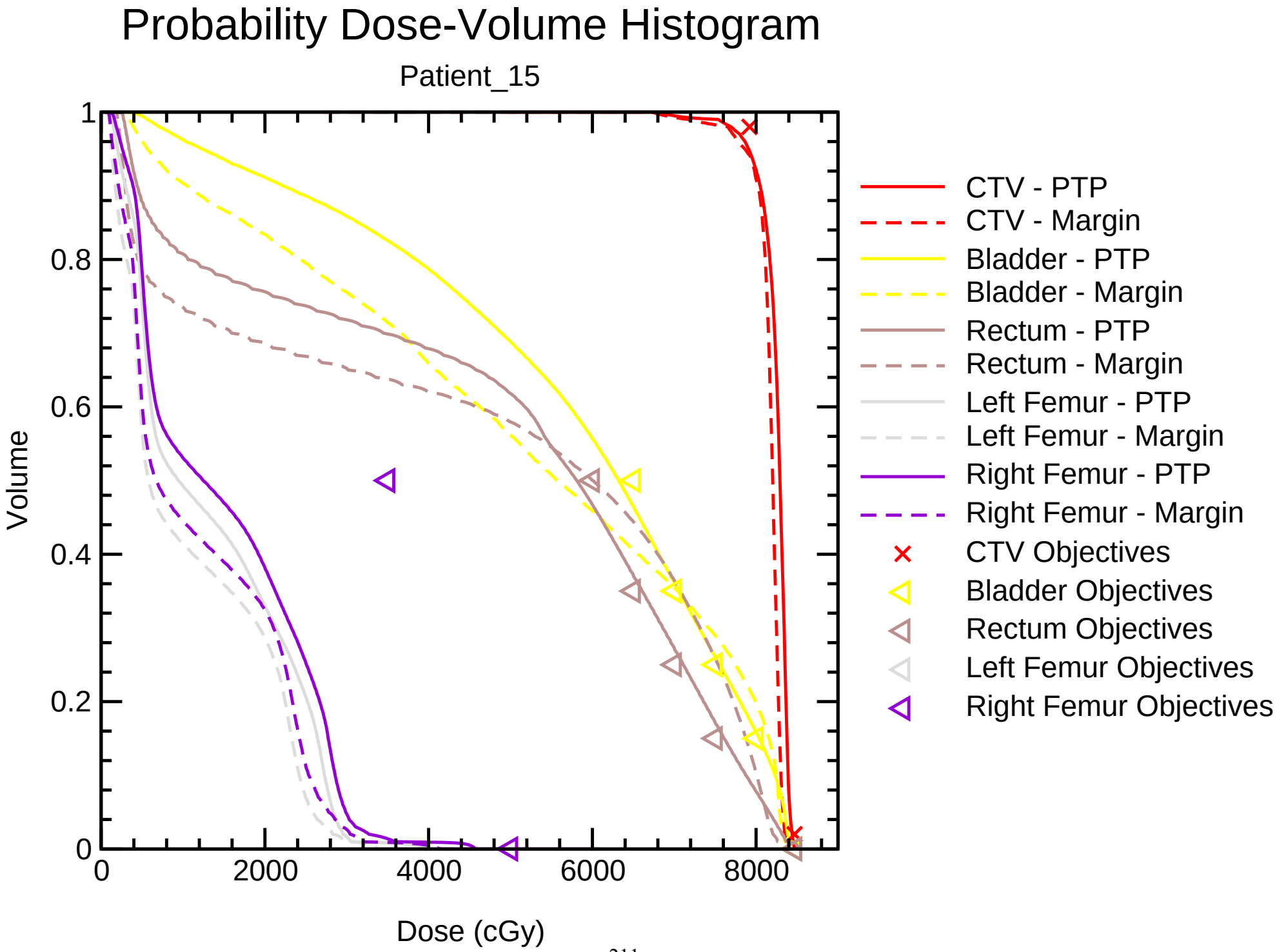
Probability Dose-Volume Histogram
Patient_15
Volume
Dose (cGy)
0
0.2
0.4
0.6
0.8
1
0
2000
4000
6000
8000
CTV - PTP
CTV - Margin
Bladder - PTP
Bladder - Margin
Rectum - PTP
Rectum - Margin
Left Femur - PTP
Left Femur - Margin
Right Femur - PTP
Right Femur - Margin
CTV Objectives
Bladder Objectives
Rectum Objectives
Left Femur Objectives
Right Femur Objectives

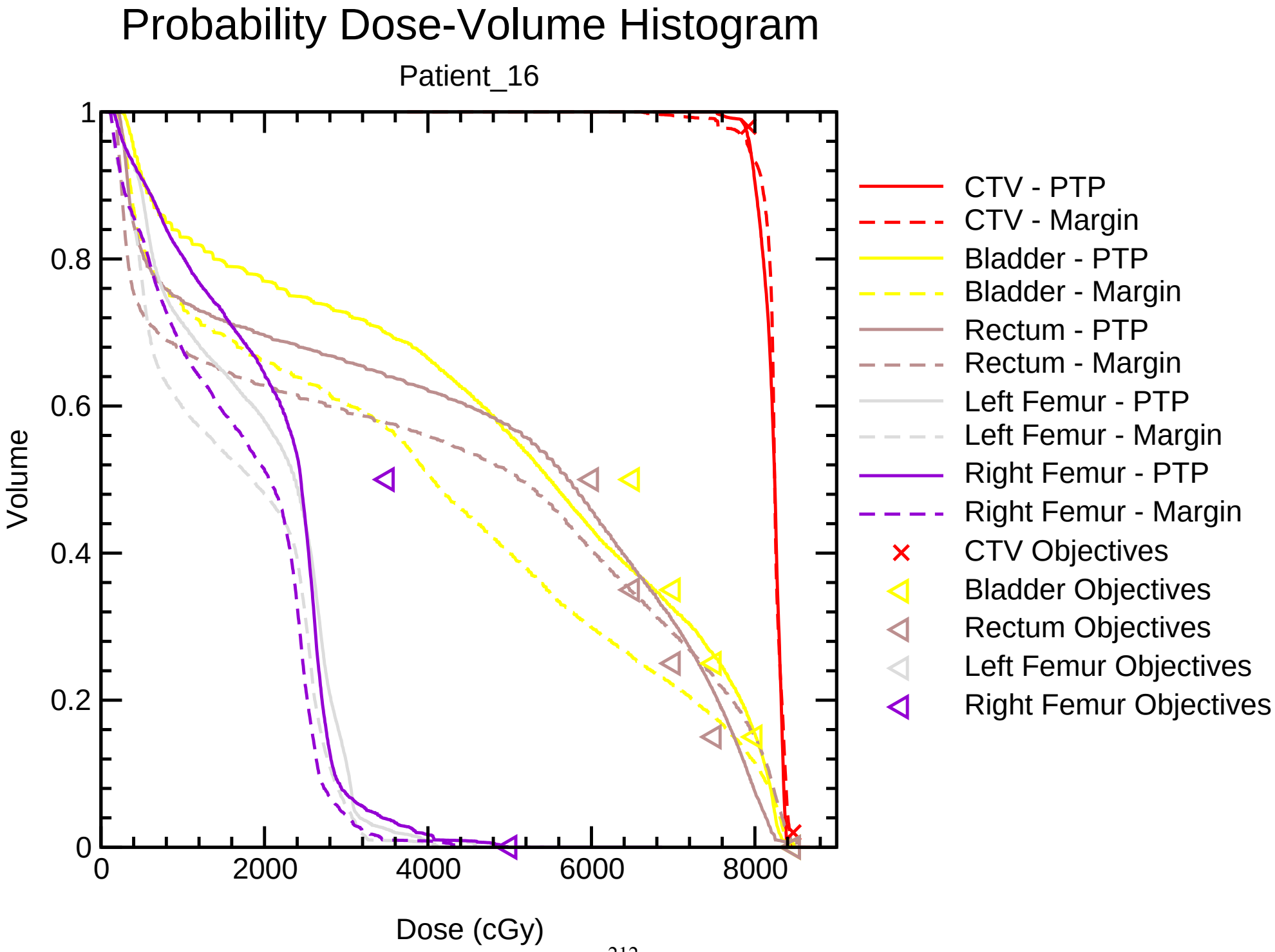
Probability Dose-Volume Histogram
Patient_16
Volume
Dose (cGy)
0
0.2
0.4
0.6
0.8
1
0
2000
4000
6000
8000
CTV - PTP
CTV - Margin
Bladder - PTP
Bladder - Margin
Rectum - PTP
Rectum - Margin
Left Femur - PTP
Left Femur - Margin
Right Femur - PTP
Right Femur - Margin
CTV Objectives
Bladder Objectives
Rectum Objectives
Left Femur Objectives
Right Femur Objectives

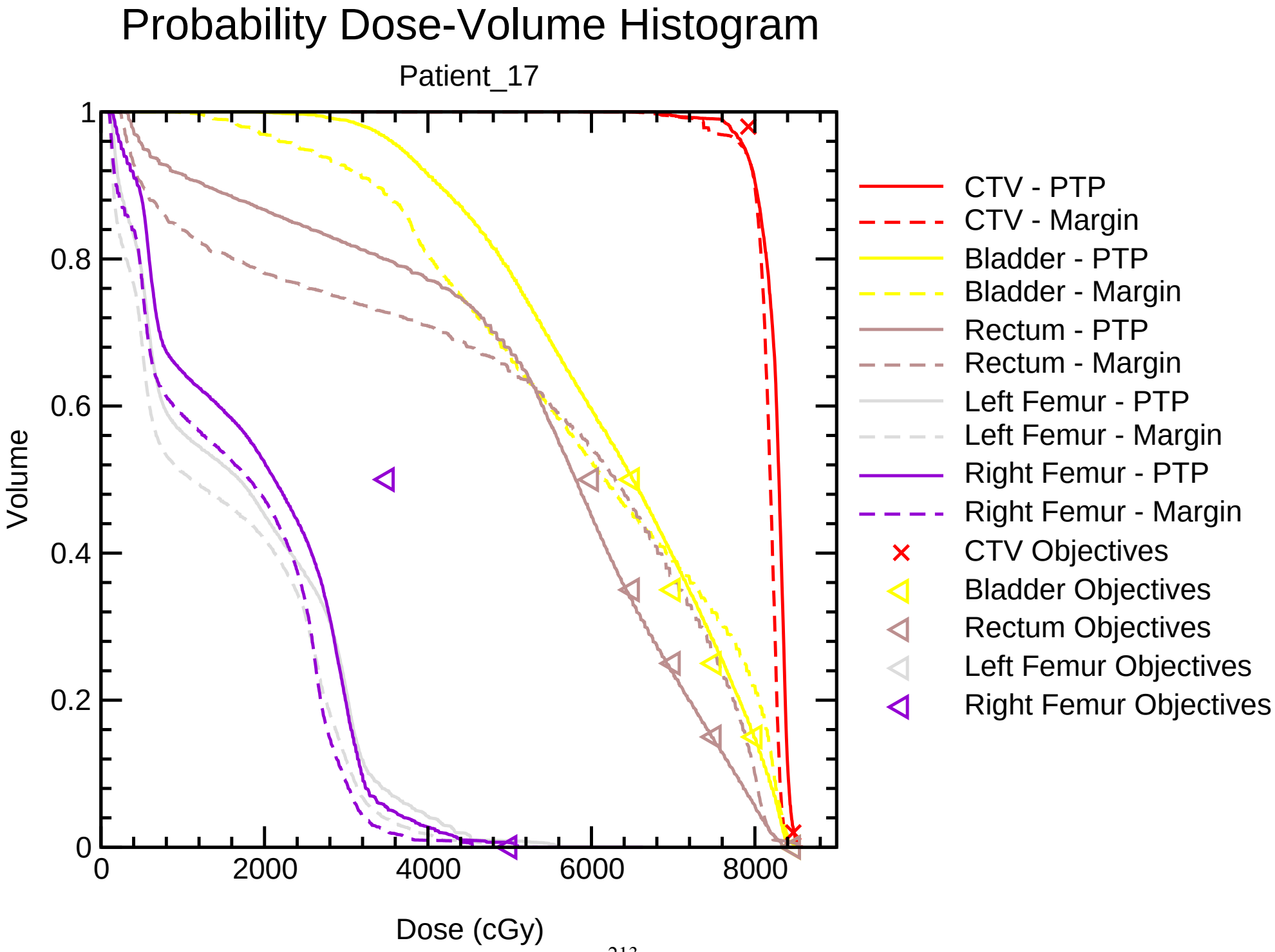
Probability Dose-Volume Histogram
Patient_17
Volume
Dose (cGy)
0
0.2
0.4
0.6
0.8
1
0
2000
4000
6000
8000
CTV - PTP
CTV - Margin
Bladder - PTP
Bladder - Margin
Rectum - PTP
Rectum - Margin
Left Femur - PTP
Left Femur - Margin
Right Femur - PTP
Right Femur - Margin
CTV Objectives
Bladder Objectives
Rectum Objectives
Left Femur Objectives
Right Femur Objectives

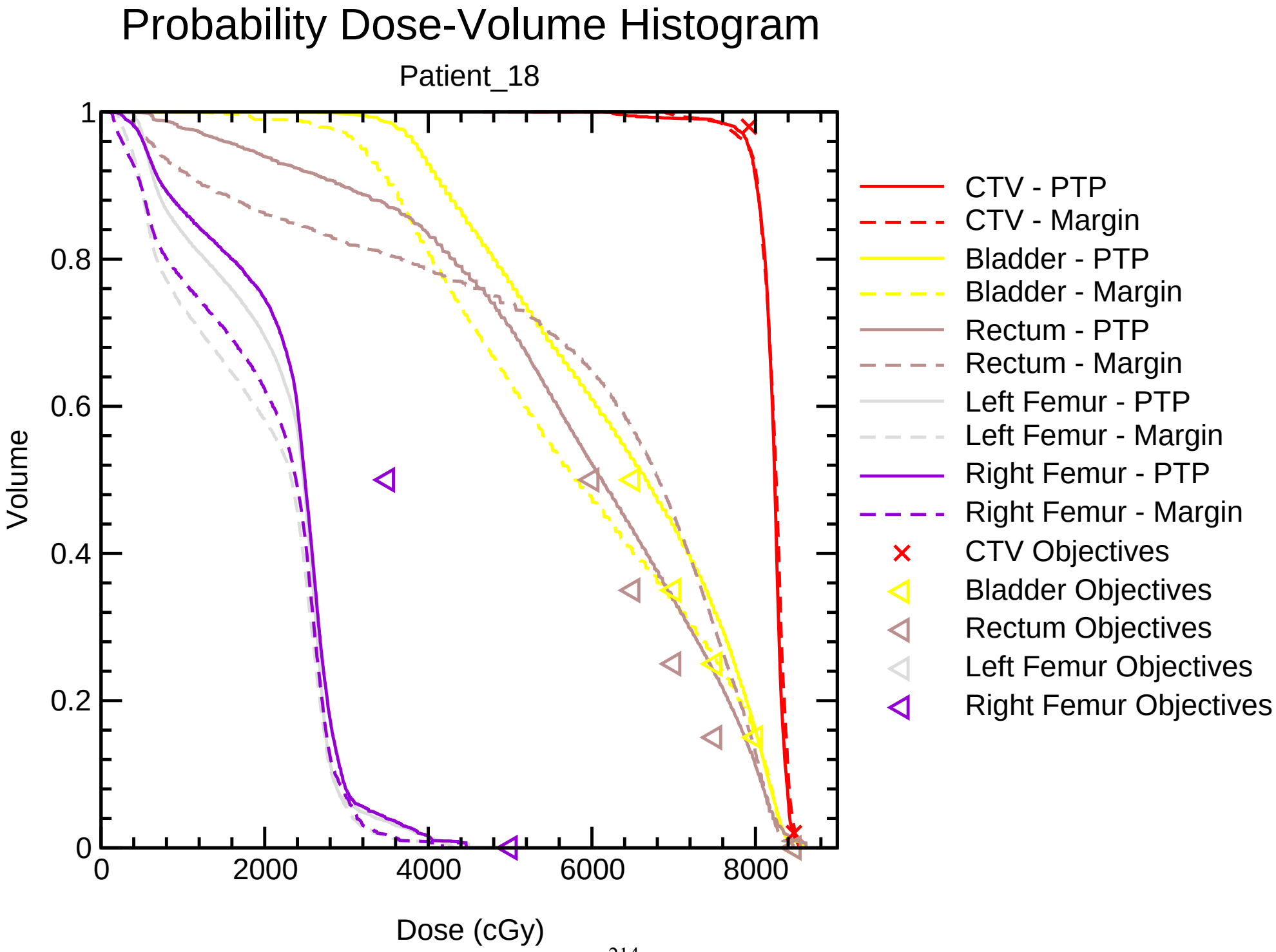
Probability Dose-Volume Histogram
Patient_18
Volume
Dose (cGy)
0
0.2
0.4
0.6
0.8
1
0
2000
4000
6000
8000
CTV - PTP
CTV - Margin
Bladder - PTP
Bladder - Margin
Rectum - PTP
Rectum - Margin
Left Femur - PTP
Left Femur - Margin
Right Femur - PTP
Right Femur - Margin
CTV Objectives
Bladder Objectives
Rectum Objectives
Left Femur Objectives
Right Femur Objectives

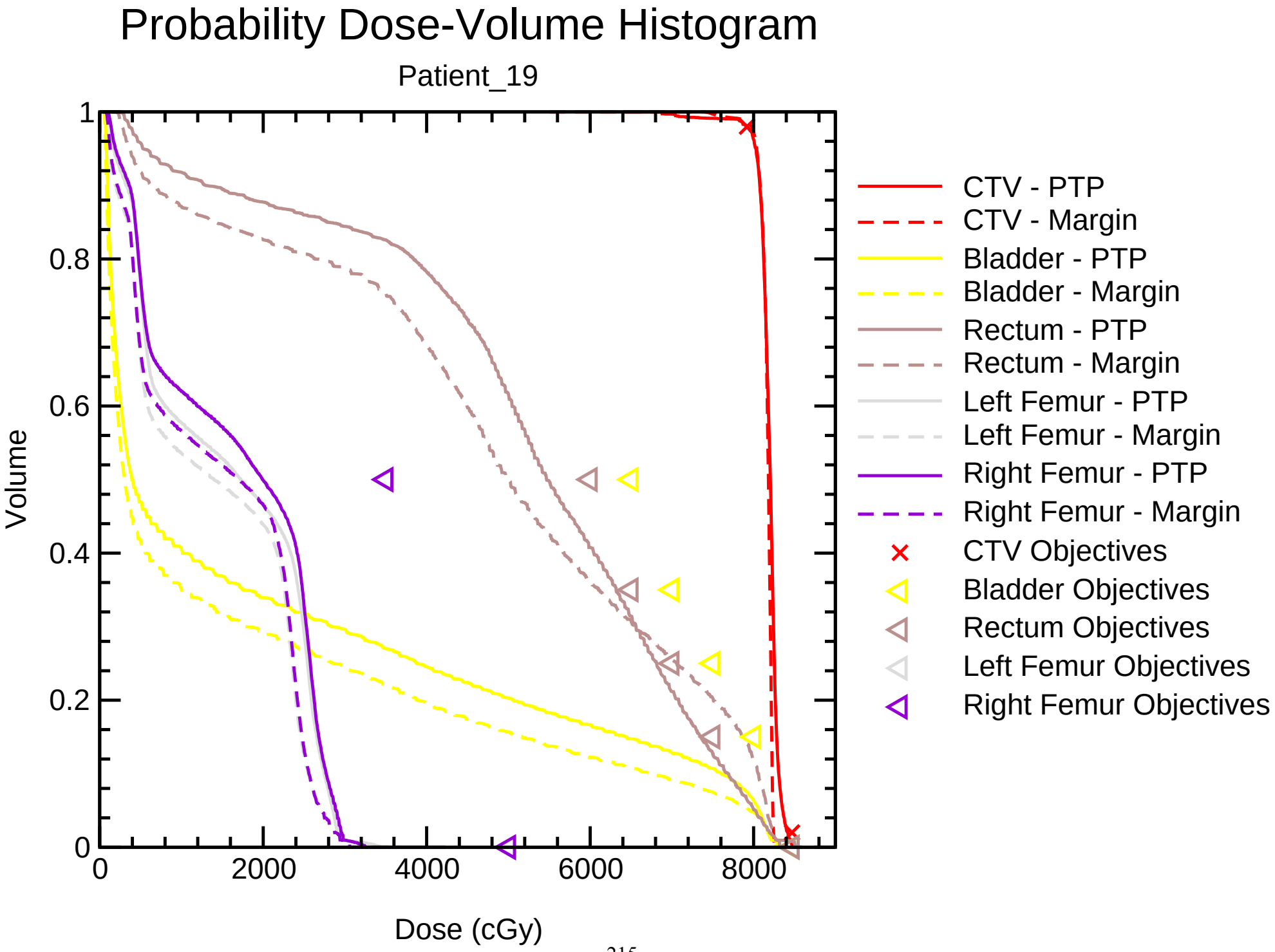
Probability Dose-Volume Histogram
Patient_19
Volume
Dose (cGy)
0
0.2
0.4
0.6
0.8
1
0
2000
4000
6000
8000
CTV - PTP
CTV - Margin
Bladder - PTP
Bladder - Margin
Rectum - PTP
Rectum - Margin
Left Femur - PTP
Left Femur - Margin
Right Femur - PTP
Right Femur - Margin
CTV Objectives
Bladder Objectives
Rectum Objectives
Left Femur Objectives
Right Femur Objectives

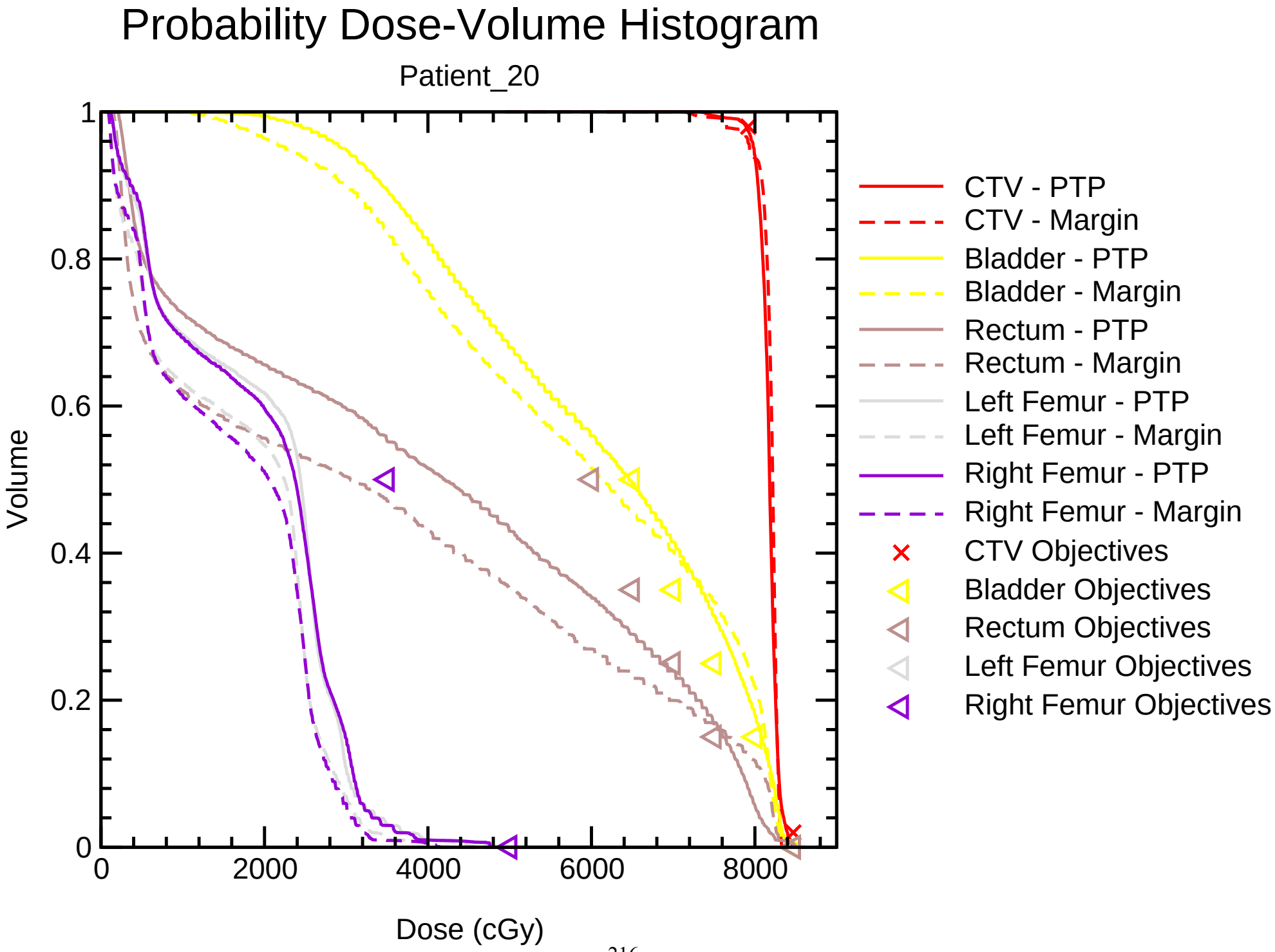
Probability Dose-Volume Histogram
Patient_20
Volume
Dose (cGy)
0
0.2
0.4
0.6
0.8
1
0
2000
4000
6000
8000
CTV - PTP
CTV - Margin
Bladder - PTP
Bladder - Margin
Rectum - PTP
Rectum - Margin
Left Femur - PTP
Left Femur - Margin
Right Femur - PTP
Right Femur - Margin
CTV Objectives
Bladder Objectives
Rectum Objectives
Left Femur Objectives
Right Femur Objectives

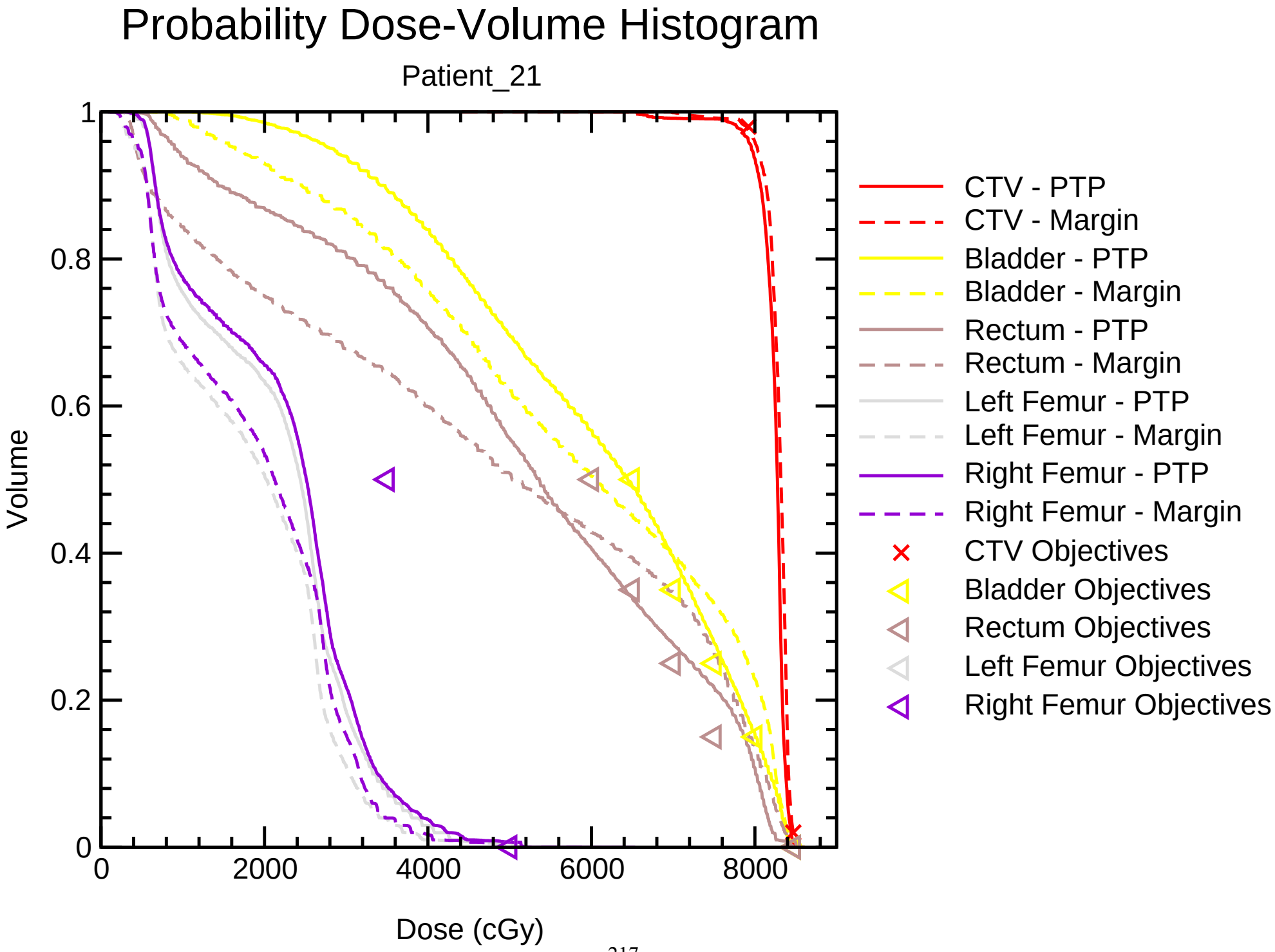
Probability Dose-Volume Histogram
Patient_21
Volume
Dose (cGy)
0
0.2
0.4
0.6
0.8
1
0
2000
4000
6000
8000
CTV - PTP
CTV - Margin
Bladder - PTP
Bladder - Margin
Rectum - PTP
Rectum - Margin
Left Femur - PTP
Left Femur - Margin
Right Femur - PTP
Right Femur - Margin
CTV Objectives
Bladder Objectives
Rectum Objectives
Left Femur Objectives
Right Femur Objectives

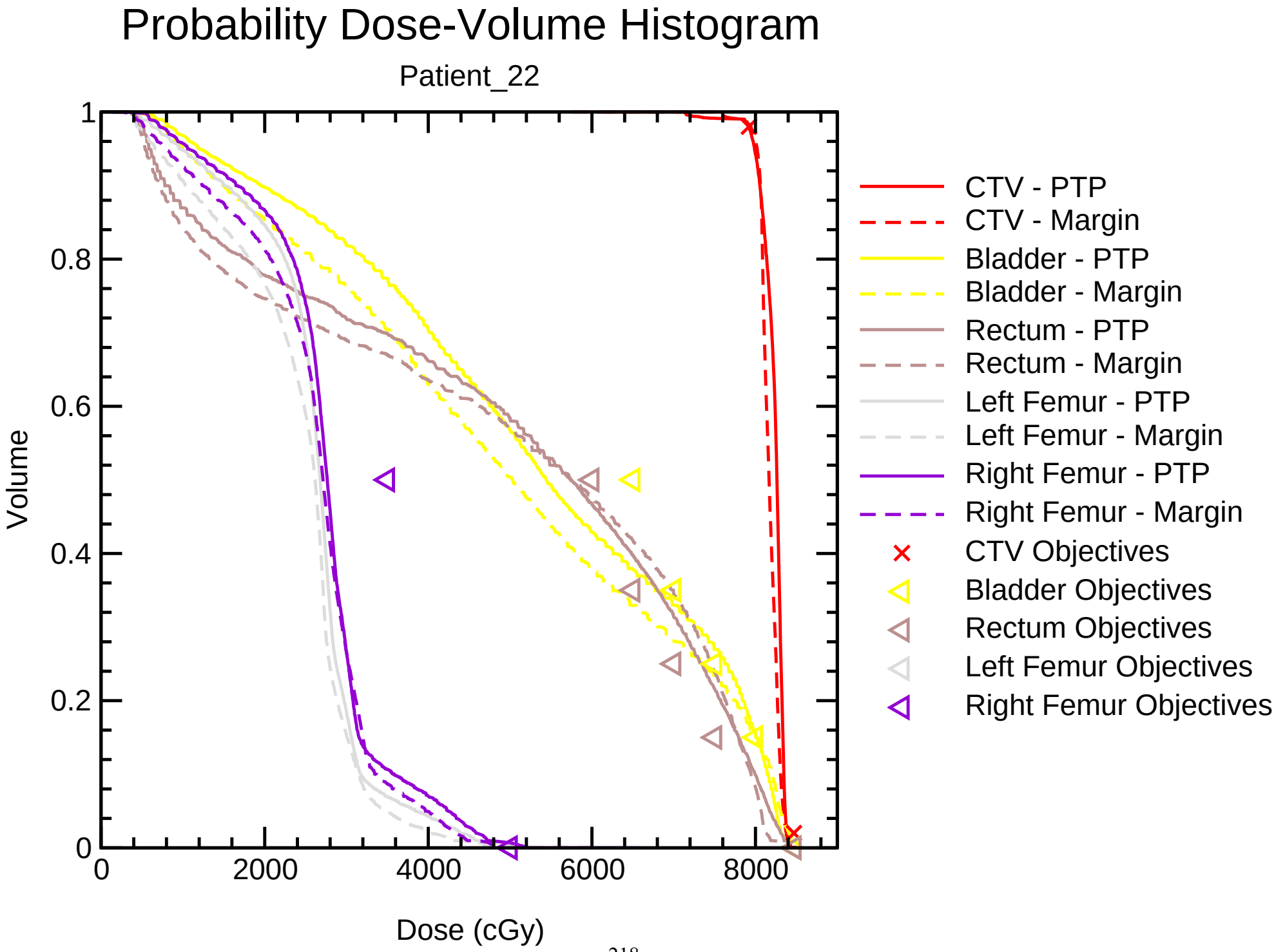
Probability Dose-Volume Histogram
Patient_22
Volume
Dose (cGy)
0
0.2
0.4
0.6
0.8
1
0
2000
4000
6000
8000
CTV - PTP
CTV - Margin
Bladder - PTP
Bladder - Margin
Rectum - PTP
Rectum - Margin
Left Femur - PTP
Left Femur - Margin
Right Femur - PTP
Right Femur - Margin
CTV Objectives
Bladder Objectives
Rectum Objectives
Left Femur Objectives
Right Femur Objectives

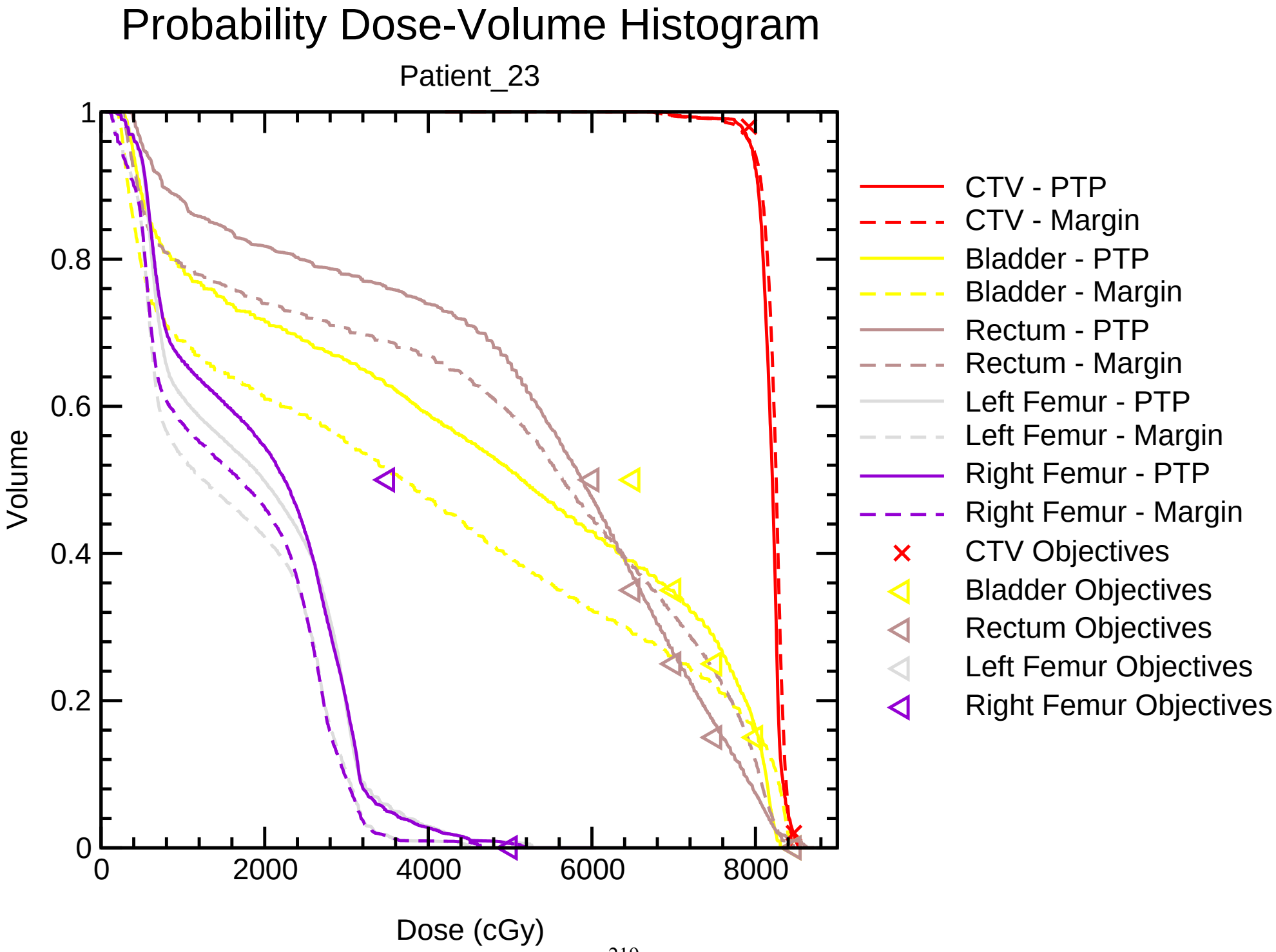
Probability Dose-Volume Histogram
Patient_23
Volume
Dose (cGy)
0
0.2
0.4
0.6
0.8
1
0
2000
4000
6000
8000
CTV - PTP
CTV - Margin
Bladder - PTP
Bladder - Margin
Rectum - PTP
Rectum - Margin
Left Femur - PTP
Left Femur - Margin
Right Femur - PTP
Right Femur - Margin
CTV Objectives
Bladder Objectives
Rectum Objectives
Left Femur Objectives
Right Femur Objectives

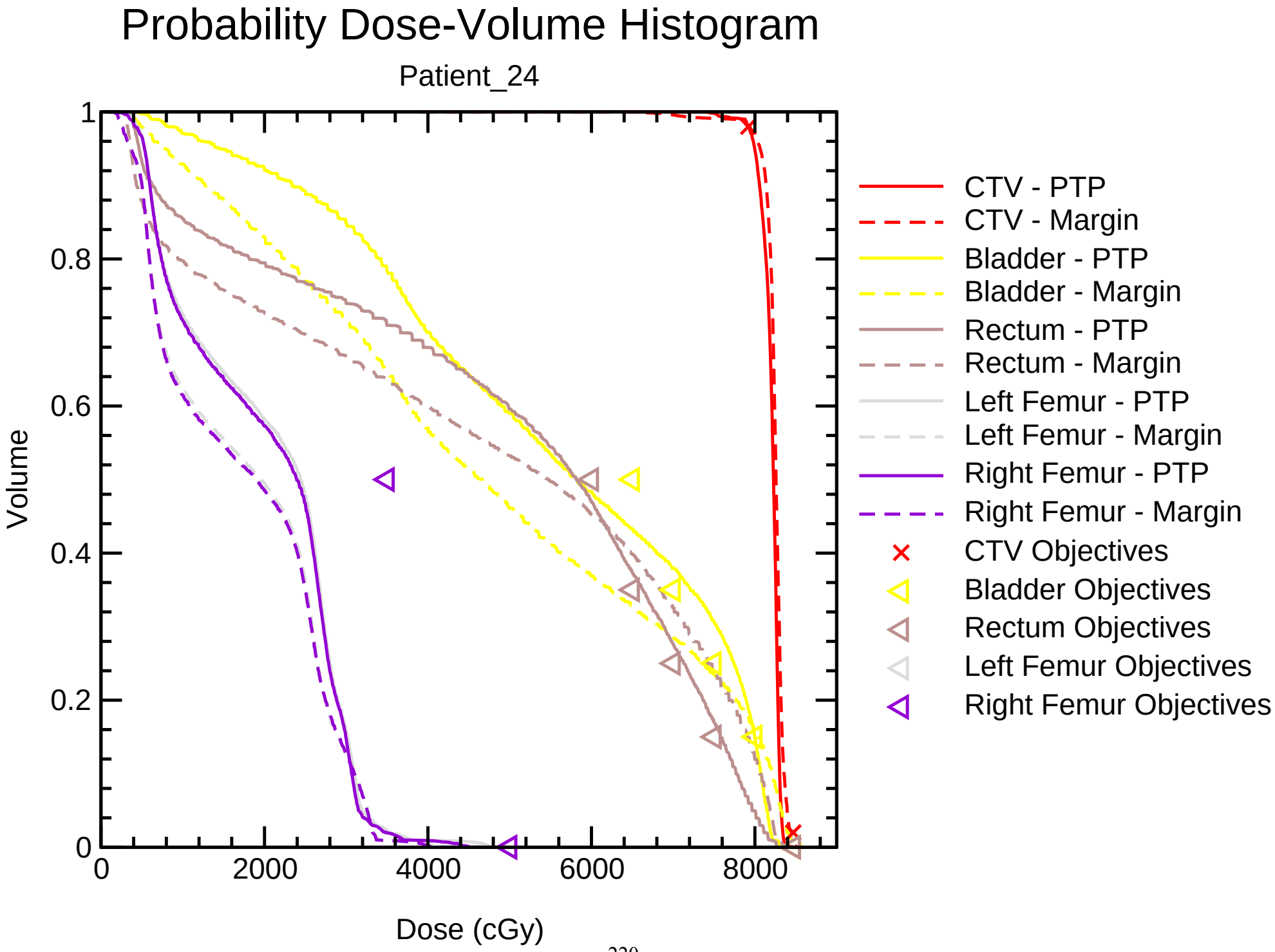
Probability Dose-Volume Histogram
Patient_24
Volume
Dose (cGy)
0
0.2
0.4
0.6
0.8
1
0
2000
4000
6000
8000
CTV - PTP
CTV - Margin
Bladder - PTP
Bladder - Margin
Rectum - PTP
Rectum - Margin
Left Femur - PTP
Left Femur - Margin
Right Femur - PTP
Right Femur - Margin
CTV Objectives
Bladder Objectives
Rectum Objectives
Left Femur Objectives
Right Femur Objectives

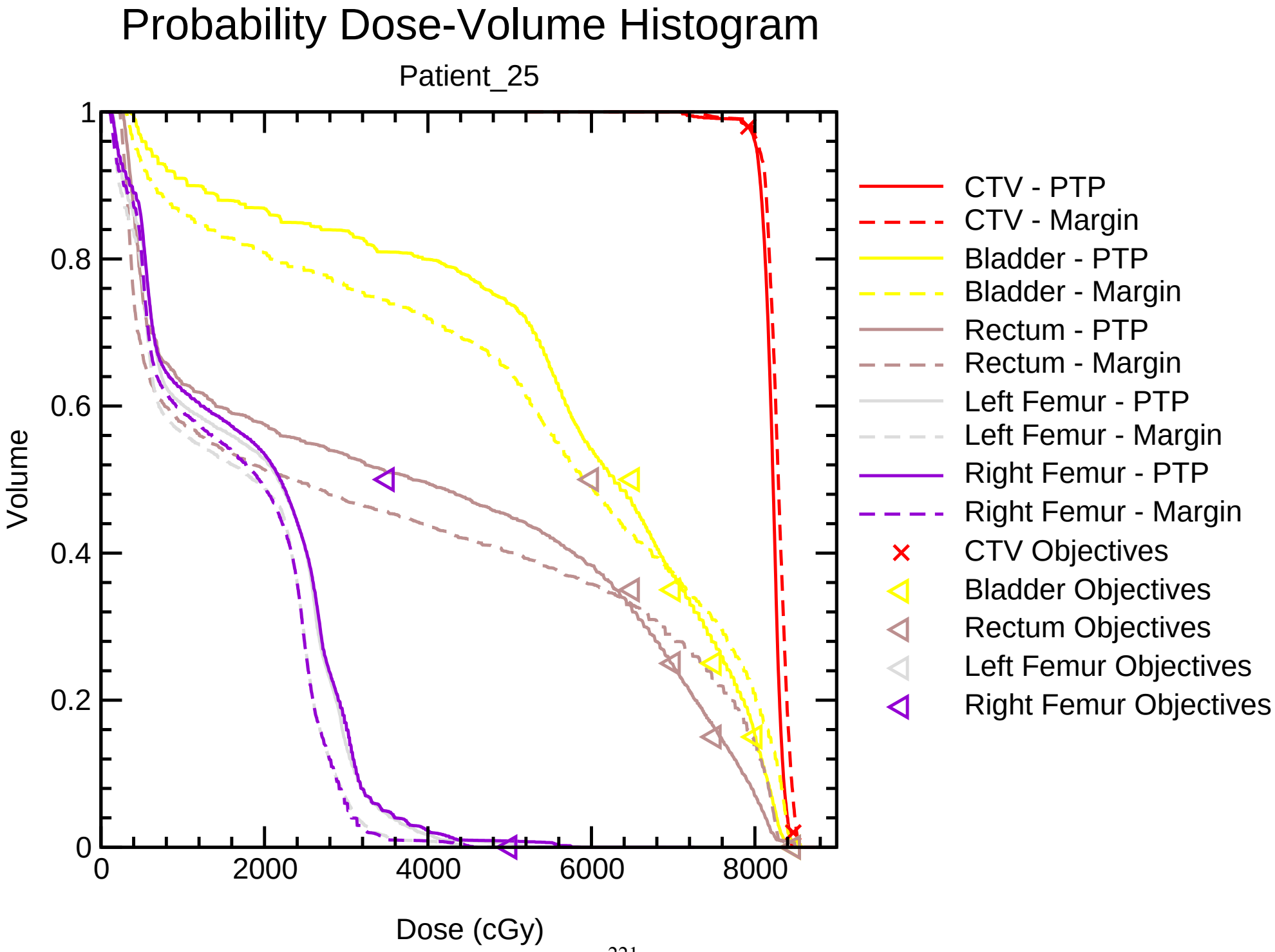
Probability Dose-Volume Histogram
Patient_25
Volume
Dose (cGy)
0
0.2
0.4
0.6
0.8
1
0
2000
4000
6000
8000
CTV - PTP
CTV - Margin
Bladder - PTP
Bladder - Margin
Rectum - PTP
Rectum - Margin
Left Femur - PTP
Left Femur - Margin
Right Femur - PTP
Right Femur - Margin
CTV Objectives
Bladder Objectives
Rectum Objectives
Left Femur Objectives
Right Femur Objectives

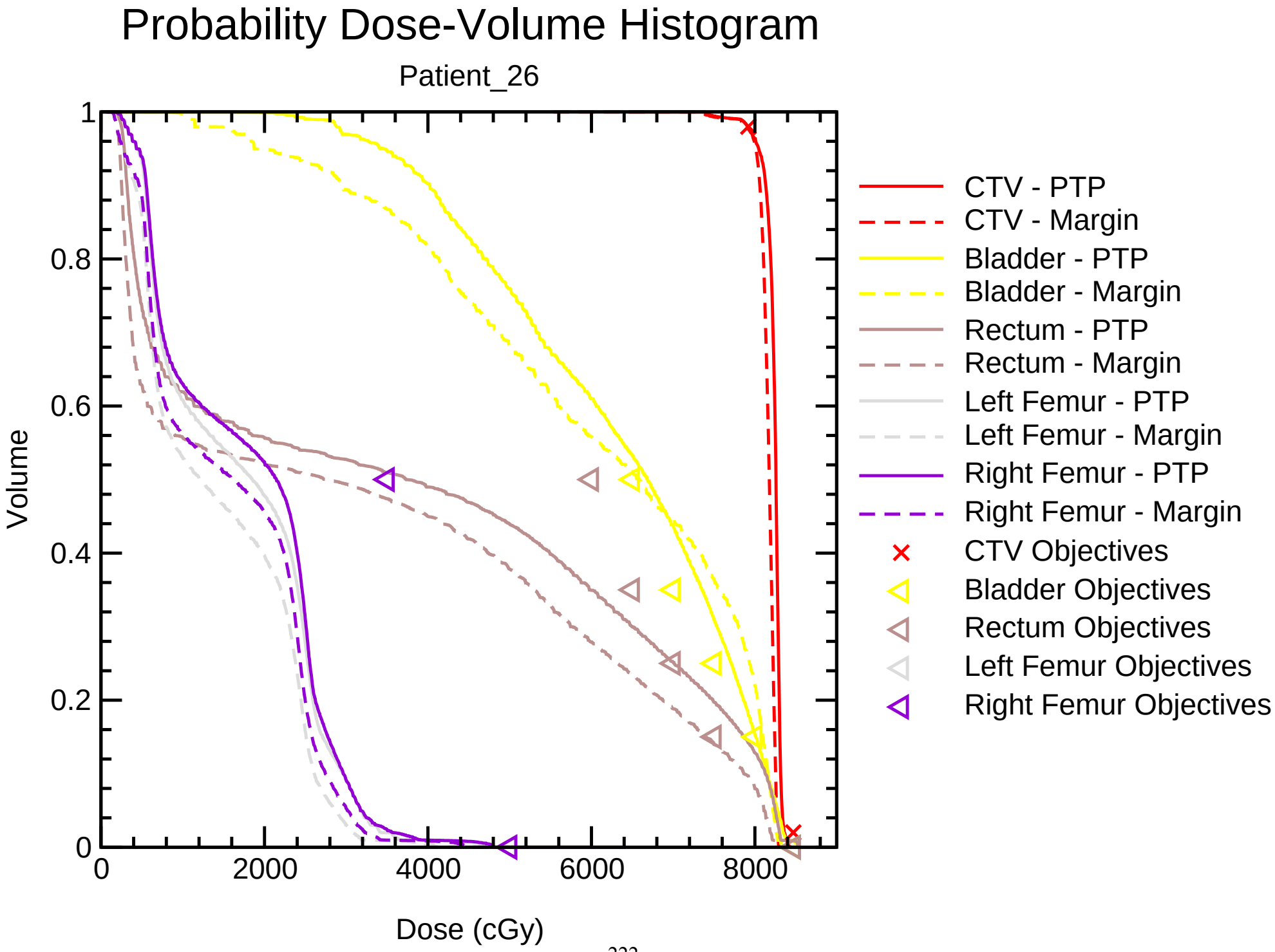
Probability Dose-Volume Histogram
Patient_26
Volume
Dose (cGy)
0
0.2
0.4
0.6
0.8
1
0
2000
4000
6000
8000
CTV - PTP
CTV - Margin
Bladder - PTP
Bladder - Margin
Rectum - PTP
Rectum - Margin
Left Femur - PTP
Left Femur - Margin
Right Femur - PTP
Right Femur - Margin
CTV Objectives
Bladder Objectives
Rectum Objectives
Left Femur Objectives
Right Femur Objectives

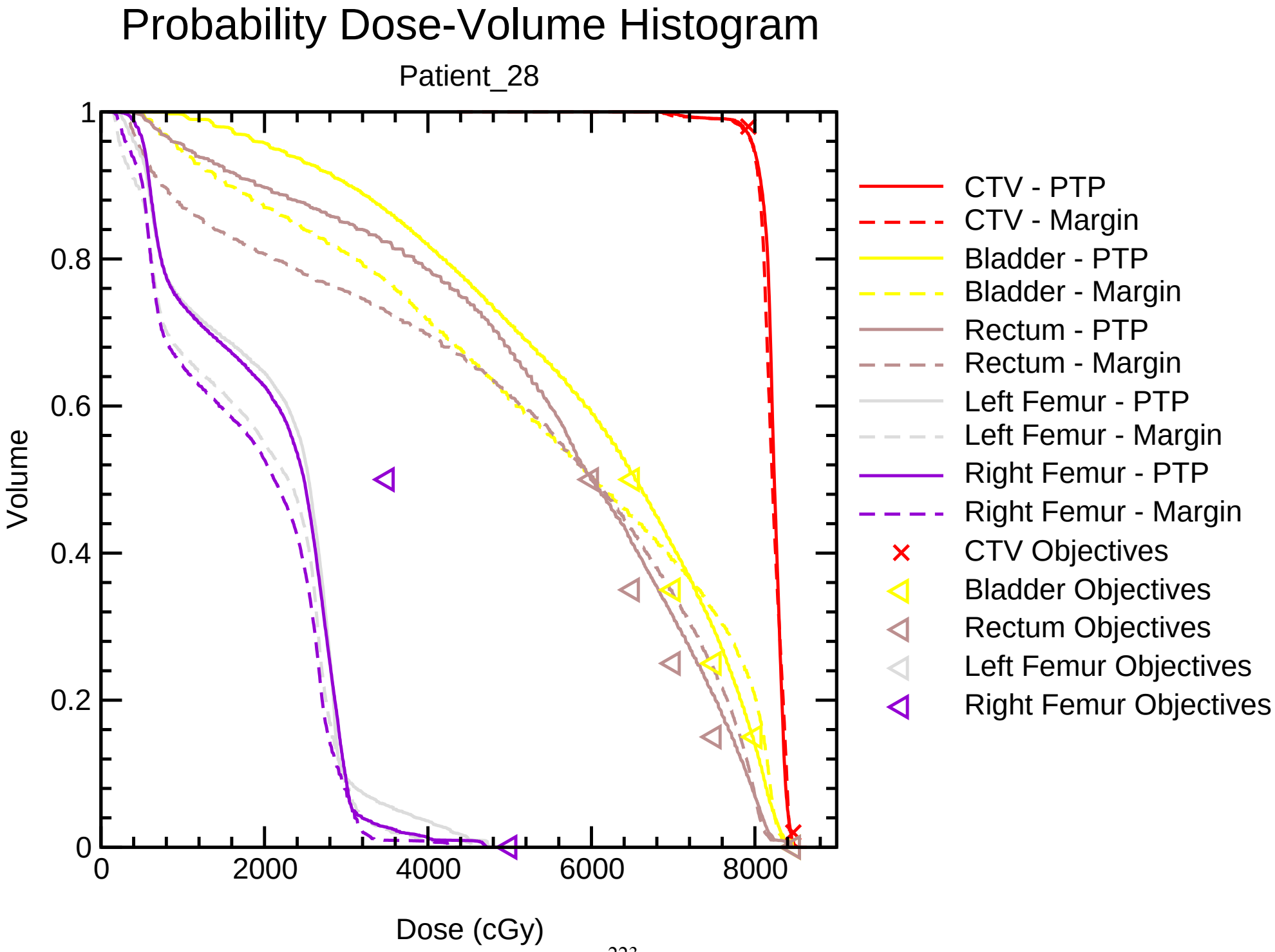
Probability Dose-Volume Histogram
Patient_28
Volume
Dose (cGy)
0
0.2
0.4
0.6
0.8
1
0
2000
4000
6000
8000
CTV - PTP
CTV - Margin
Bladder - PTP
Bladder - Margin
Rectum - PTP
Rectum - Margin
Left Femur - PTP
Left Femur - Margin
Right Femur - PTP
Right Femur - Margin
CTV Objectives
Bladder Objectives
Rectum Objectives
Left Femur Objectives
Right Femur Objectives

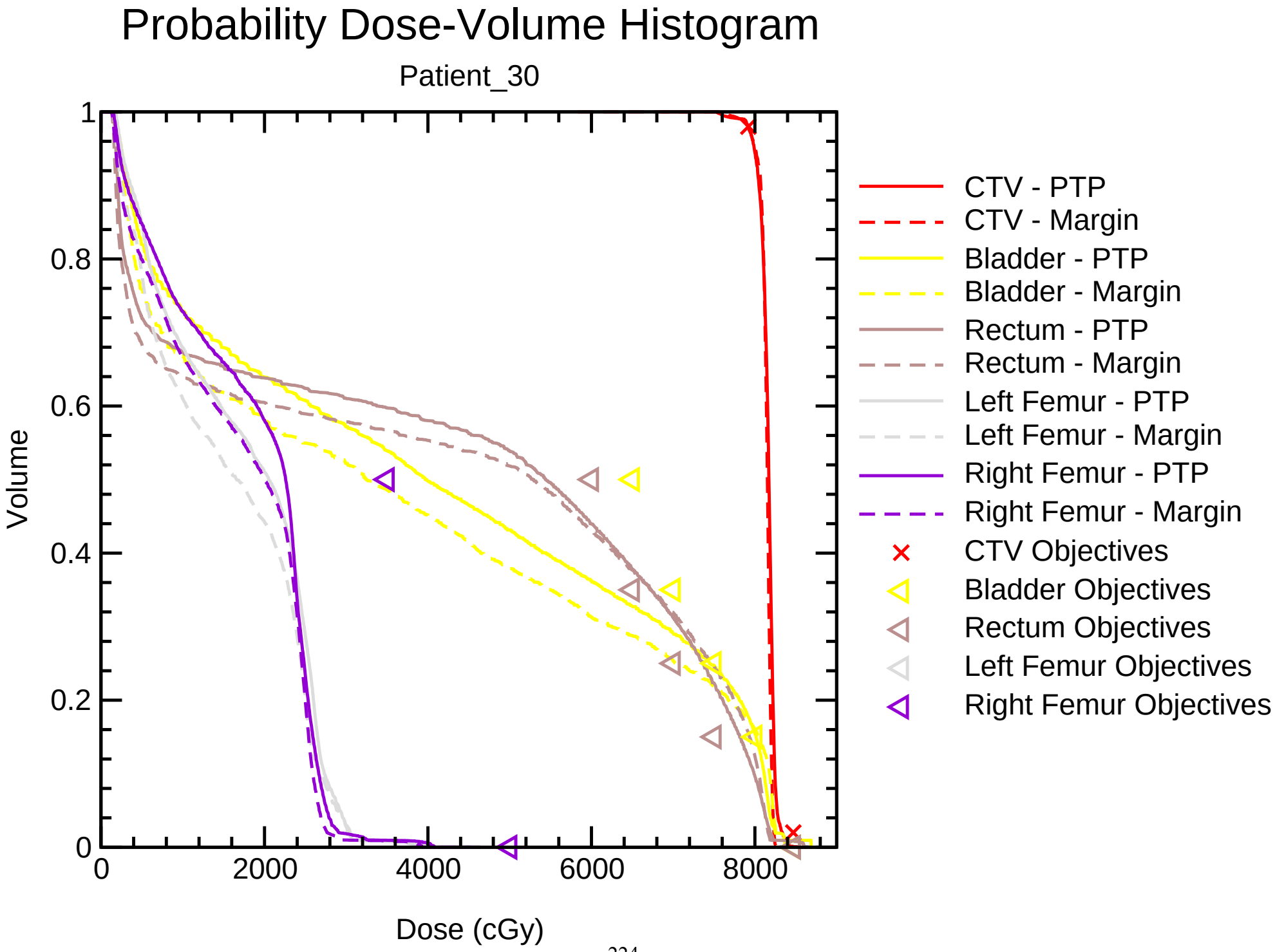
Probability Dose-Volume Histogram
Patient_30
Volume
Dose (cGy)
0
0.2
0.4
0.6
0.8
1
0
2000
4000
6000
8000
CTV - PTP
CTV - Margin
Bladder - PTP
Bladder - Margin
Rectum - PTP
Rectum - Margin
Left Femur - PTP
Left Femur - Margin
Right Femur - PTP
Right Femur - Margin
CTV Objectives
Bladder Objectives
Rectum Objectives
Left Femur Objectives
Right Femur Objectives

Vita

Joseph Andrew Moore was born on March 5th, 1983, in Richmond, Virginia. He graduated from Patrick Henry High School, Ashland, Virginia in 2000. He received a Bachelor of Science in Computer Science and a Bachelor of Science in Physics from Virginia Commonwealth University in 2003. He received a Master of Science in Applied Physics from Virginia Commonwealth University in 2004. He finally received a Doctor of Philosophy in Medical Physics from Virginia Commonwealth University in 2011.